INLAND WATERS BRANCH

DEPARTMENT OF THE ENVIRONMENT

Groundwater Inflow into Lake Ontario from the Canadian Side

C.J. HAEFELI

SCIENTIFIC SERIES NO.9

GROUNDWATER INFLOW INTO LAKE ONTARIO FROM THE CANADIAN SIDE

SCIENTIFIC SERIES NO.9

Groundwater Inflow into Lake Ontario from the Canadian Side

C.J. HAEFELI

INLAND WATERS BRANCH
DEPARTMENT OF THE ENVIRONMENT
OTTAWA, CANADA, 1972

Contents

Page

Contents (Cont'd)

Page

Illustrations

Illustrations (Cont'd)

Illustrations (Cont'd)

Illustrations (Cont'd)

Tables

Tables (Cont'd)

Preface

This report is concerned with groundwater movement on the Canadian side of Lake Ontario and comprises the major part of the author's project "Groundwater Inflow into Lake Ontario" (IHD Project GW 68-3) which is part of the International Field Year for the Great Lakes (IFYGL), a programmed period of concentrated co-operative hydrological investigation for the International Hydrological Decade (IHD). The Lake Ontario drainage basin has been selected as the type area on which all IFYGL work is carried out including studies of lake meteorology, energy balance, water movement and terrestrial water balance. The studies are performed simultaneously on the U.S. and Canadian sides and are led by a Steering Committee composed of scientists of both nations. The period of intensive data collection is scheduled to take place between April 1, 1971 and September 31, 1972.

The report deals with the contribution made by groundwater to terrestrial water balance, one of the four inter-disciplinary program areas which has as its overall objective the determination of the total inflow to and outflow from Lake Ontario. Although the investigations were terminated before the International Field Year began, it is believed that the year to year fluctuation of the groundwater movement does not significantly affect the results. Therefore, the investigations can be applied in studies of the terrestrial water balance of the IFYGL, keeping in mind, however, that the groundwater data on which the results are based are themselves only estimates.

Acknowledgments

I would like to express my gratitude and sincere thanks to: Dr. P. Meyboom and Dr. H. Ryckborst, for the enlightenment and guidance provided by many discussions of general and regional hydrogeological problems.

Dr. M. L. Parsons for his critical and competent review of the manuscript.

Messrs. K. Coombs, R. Crosby, J. Erxleben, D. French, P. Harker, L. Matthews, M. Oosterfeld, G. Westerby and D. Williams for their excellent assistance in the field and office.

Miss A. A. Fischer, for analyzing data by computer, and especially for her collaboration in developing the program FREQ.

Dr. E. Wojtek, who provided many travel time measurements of streams in the Lake Ontario basin.

Dr. R. K. Lane of the Canada Centre for Inland Waters (CCIW), who made the temperature survey along the shore possible.

Dr. C. F. M. Lewis, CCIW, for the core samples and the geological map of the bottom of Lake Ontario.

Mr. B. E. Russell and his staff of the Water Survey of Canada for the maintenance and operation of temporary stream gauging stations.

Messrs. G. D. Hobson, H. A. MacAulay and R. M. Gagné for their geophysical survey along the shore between Trenton and Toronto, and for their assistance in obtaining bedrock surface data of other areas.

Messrs. J. Kirk and D. Turnbull, Internation Water Supply Limited, Oakville, who provided much valuable pumping test data.

Mr. R. C. Ostry of the Ontario Water Resources Commission for the interesting discussions regarding the regional hydrogeology.

Dr. J. N. de Villiers of the National Research Council, who carried out the infrared survey along the shore of Lake Ontario.

Dr. Terasmae of Brock University, St. Catharines, who provided the logs of exploration wells at Dundas.

CHAPTER 1

Introduction

There were two major objectives of IHD Project GW 68-3: to determine the amount of groundwater flowing into Lake Ontario; and to investigate any major seepage across the basin boundary on the Canadian side. In a previous paper (Haefeli, 1970), the groundwater boundary between Lake Simcoe and Lake Ontario basin was investigated, leaving the Dundas Valley and the Niagara Peninsula as the only areas where the groundwater divide could be significantly different from the basin boundary.

The amount of groundwater discharging into the lake was computed in three different ways: 1) using the classic method after Darcy, 2) by a numerical approach, 3) by baseflow analysis. All three methods are based on Darcy's Law, which states that the flow through porous media is proportional to the head loss and inversely proportional to the length of the flow path. Henry Darcy reported in 1856 (as quoted by Todd, 1959):

> "I have attempted by precise experiments to determine the law of the flow of water through filters . . . The experiments demonstrate positively that the volume of water which passes through a bed of sand of a given nature is proportional to the thickness of the bed traversed; thus, in calling s the surface area of a filter, k a coefficient depending on the nature of the sand, e the thickness of the sand bed, $P - H_o$ the pressure below the filtering bed, $P + H$ the atmospheric pressure added to the depth of water on the filter; one has for the flow of this last condition $Q = (ks/e)\ (H + e + H_o)$, which reduces to $Q = (ks/e)\ (H + e)$ when $H_o = 0$, or when the pressure below the filter is equal to the weight of the atmosphere".

The original equation by Darcy is transformed for determining the groundwater flow through a cross-sectional area, to $Q = K\ I\ A$, where the hydraulic conductivity, K, replaces the permeability coefficient, k; $(H + e)/e$ is replaced by I (the hydraulic gradient); and s is replaced by A (the cross-sectional area). One of the main concerns of this study was consequently to derive the three hydraulic parameters controlling the discharge.

PHYSIOGRAPHY

Drainage and Climate

Lake Ontario, the smallest of the five Great Lakes, has a surface area of 7,540 square miles (19,800 Km^2) and a drainage area of 27,090 square miles (70,000 Km^2). With an average water level of 247 ft. (75 m) and a maximum depth of 800 ft. (244 m), Lake Ontario reaches far below sea level and is the third deepest of the Great Lakes, after Lakes Superior and Michigan. From west to east, the greatest length of the drainage basin is approximately 280 miles (450 Km) and the greatest width from north to south is about 240 miles (385 Km) (Fig. 1).

Most of the drainage basin lies below an elevation of 1000 ft. (305 m). The highest points, situated on its northern and southeastern edge, rise to 725 ft. near Bancroft in Ontario and 3744 ft. in the Adirondack Mountains of New York State. The general relief of the drainage basin looks relatively smooth on the Canadian side but is more accentuated in the United States (Fig. 2). As a result, the basin boundary is not well defined over large areas, especially in Ontario. On a small scale, however, the relief in some areas becomes very accentuated, for example, in the Adirondack Plateau, the Niagara Escarpment, or the bluffs along some parts of the shore. Powers (in Pincus, 1962) remarks, in general, that : "Outstanding features of the Great Lakes drainage basin are the obscure and ill-defined character of the boundary, the nearness of the divide to the lakes at several points, the absence of large tributary rivers . . . and the large extent to which the drainage pattern is controlled by such minor relief features as moraines and lacustrine beach ridges". In fact, the land surface and the drainage pattern reflect the bedrock surface below to only a limited extent; in most of the areas, the glacial deposits were of decisive influence.

The excess water of the upper Great Lakes flowing through the Niagara River into Lake Ontario is on the average 210,000 cubic feet per second (6000 m^3/sec.), leaving for the Lake Ontario drainage basin a net inflow of approximately 36,000 cubic feet per second (Morton and Rosenberg, 1959), (net inflow = inflow to the lake which is available for outflow). The net local water supply is composed of the surface and groundwater inflow plus the precipitation on the lake surface less the evaporation from the lake surface. The mean runoff from the drainage basin for the period 1935-64 was 16.0 inches (406 mm) (Pentland, 1968) and the mean basin evaporation for the same period as calculated by Morton (1966) was 18.7 inches (500 mm).

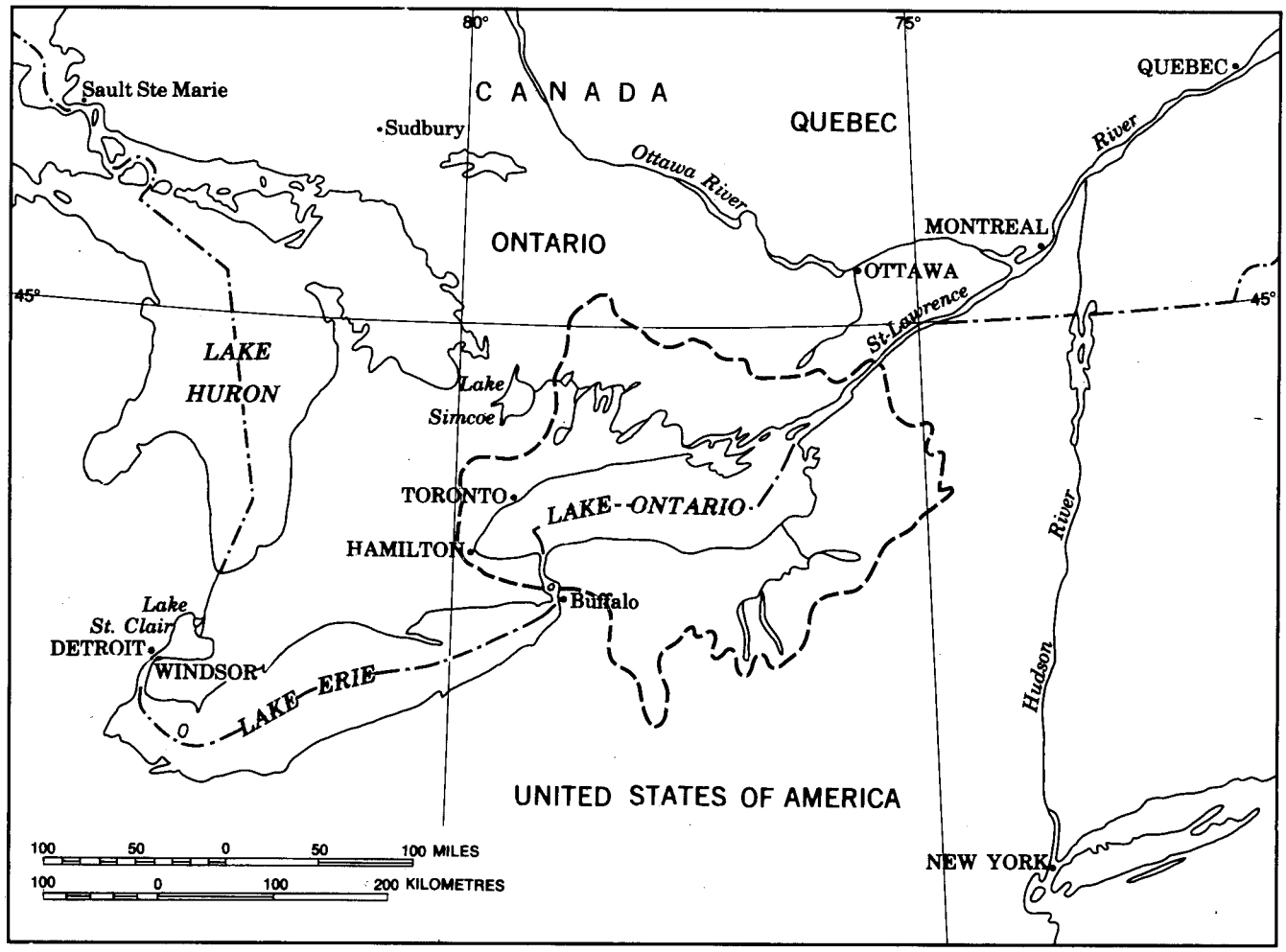

Figure 1. Index map of Lake Ontario.

For the whole drainage basin the annual precipitation since 1870 has varied from 25 to 43 inches with a mean of approximately 33 inches (840 mm). The precipitation and consequently the runoff are influenced orographically and by prevailing westerly winds. The winds pick up moisture during their sweep over Lake Ontario with the result that rain and especially large quantities of snow (up to 175 inches a year) are dropped on the hilly eastern part of the basin (Figs. 3 and 4). The average annual temperature is approximately 45°F (7°C) with extremes of 105°F (40.5°C) and -40°F(-40°C) (after Morton and Rosenberg, 1959).

In the subsequent paragraphs, only the Canadian side of the drainage basin will be dealt with.

Bedrock Geology

Precambrian rocks which form the Canadian shield underlie the drainage basin and outcrop in the northern part of it (Plate I). During the Paleozoic era, mainly limestones, shales, dolomites, and sandstones were being deposited on the eroded surface of the shield (Table 1). In the course of the sedimentation, certain areas were subsiding or lifting, causing a variable thickness of these strata. Later on, the originally horizontal deposits were very slightly pushed up in the north, which resulted in a southern inclination of less than half a degree over most of the basin. Some local undulations and dislocations have taken place which did not affect the general structure significantly, except in the Bay of Quinte and to some degree the Thousand Islands area (Frontenac Axis). However, no major faults have been observed in the basin.

Precambrian rocks consist of tightly folded metasedimentary- and metavolcanic rocks and acid- to basic intrusives. The structural trend is predominantly northeast, and faults and joints strike mainly ENE and SSE. Ridges of Precambrian rock commonly extend

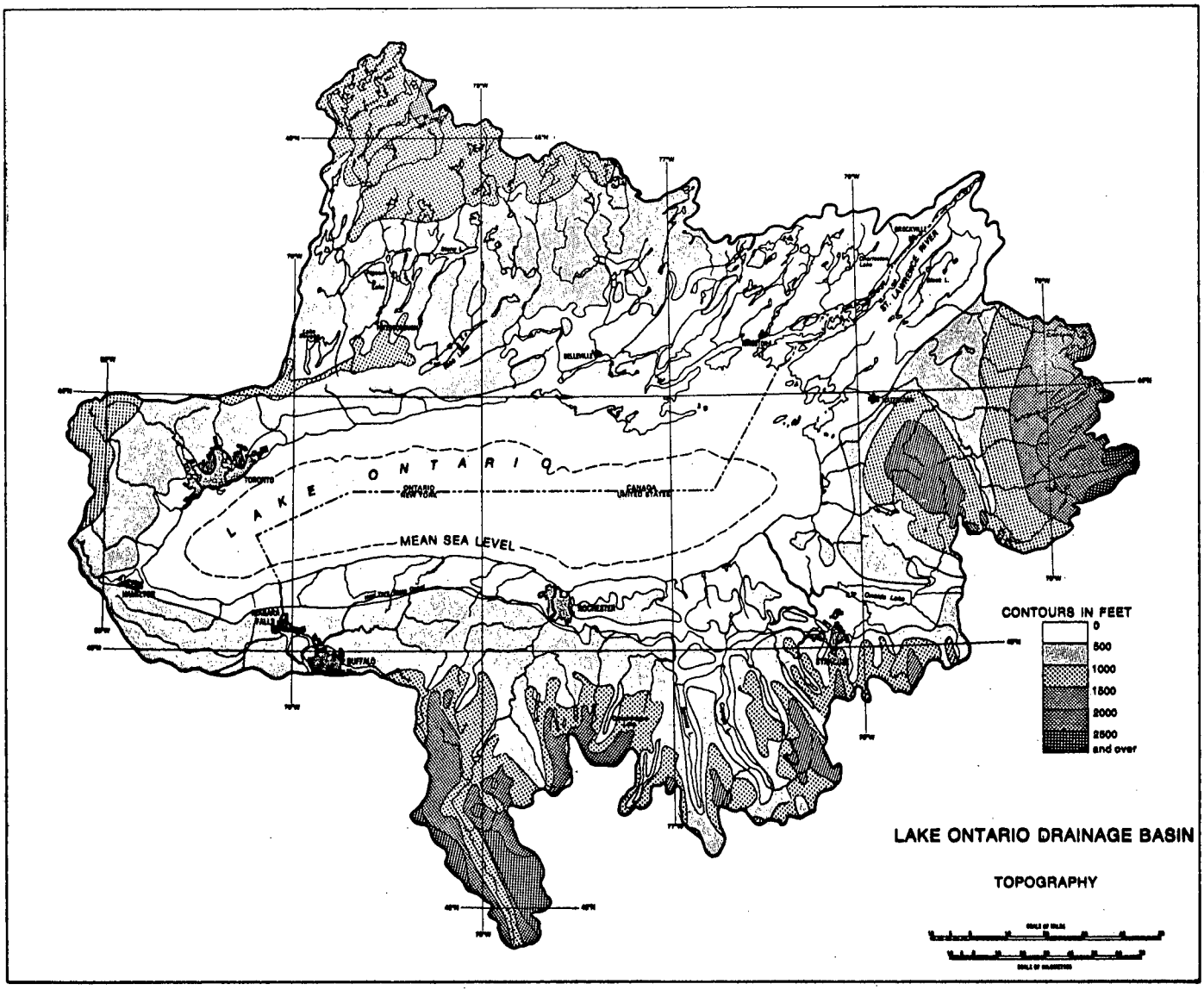

Figure 2. Topography of the Lake Ontario drainage basin.

southwest into the Paleozoic basin, and outliers are found up to 25 miles from the main Precambrian – Paleozoic contact.

The main contact extends ESE from Georgian Bay to the Kingston area. Paleozoic outliers commonly occur up to ten miles north of the contact. The Precambrian to the west of Kingston is normally overlain unconformably by red and green shale and arkose of the Middle Ordovician Shadow Lake formation, and in the Kingston area by conglomerate of the Upper Cambrian Nepean (Potsdam) formation. Basal Nepean conglomerate of the Ottawa – St. Lawrence sedimentary basin also occurs in the extreme northeastern part of the area. The lowest formations of the Paleozoic sequence are commonly missing in the vicinity of Precambrian outliers, and compaction of sedimentary rocks over outliers often produces dips up to 60° (Liberty, 1960a).

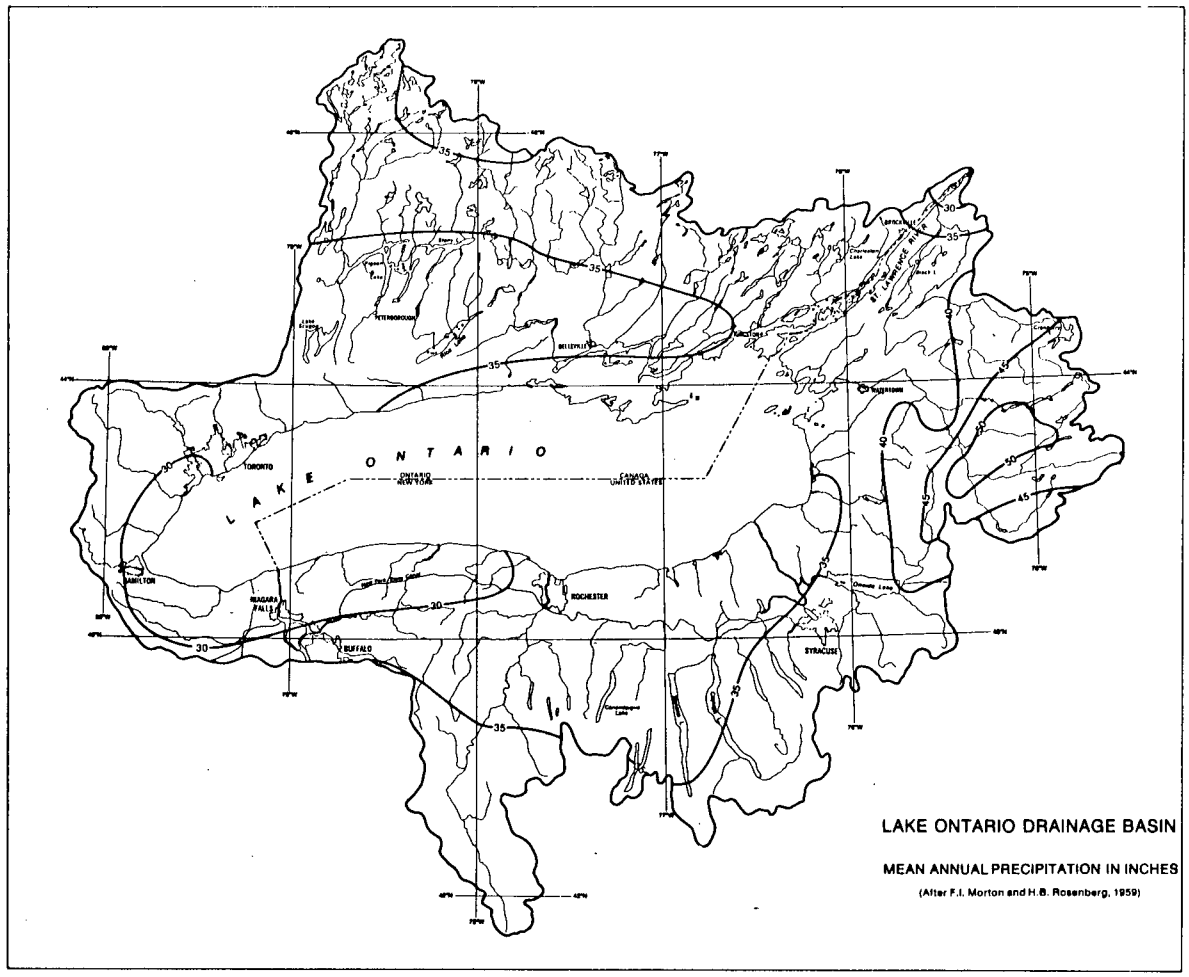

Figure 3. Mean annual precipitation on the Lake Ontario drainage basin (after Morton and Rosenberg, 1959).

The generalized Paleozoic sequence from the base upwards is as follows (Table 1): up to 150 feet of Upper Cambrian Nepean sandstone (northeastern part of the area only); up to 350 feet of Lower Ordovician Beekmantown dolomite (northeastern part of area only); 500 - 900 feet of Middle Ordovician limestone; 950 - 1850 feet of Upper Ordovician – Middle Silurian shale with some sandstone at the top; 450 - 750 feet of Middle-Upper Silurian dolomite; and 60 - 100 feet of Devonian limestone and dolomite. The total thickness of the Paleozoic rock in the southwestern part of the basin is approximately 3200 feet.

Disconformities occur at the base of the following formations: Bobcaygeon, Verulam, Collingwood, Cataract and Amabel. Regional strike of the bedding is east - west, and regional dip is 0.18° - 0.31° (16 - 28 ft./mile) to the south. East of the Lake Ontario drainage basin and to the northwest of a line running approximately from Barrie to Orangeville, regional strike changes to northwest – southeast. Main joint directions in the Paleozoic rocks are approximately 40°, 75°, 130° and 170°. The Paleozoic rocks of the basin are cut by normal and wrench faults of probable Late Carboniferous age, striking NNE and ESE. Three NNE fault zones known to occur in the central part of the area are: the Salmon River fault (Liberty, 1963), the Picton fault (Liberty, 1960b) and the Canoe Desert Lake fault (Jamieson, 1961). In all cases, the west side has been down-faulted. Reported displacements are about 100 feet for the Salmon River and Picton faults, and about 40 feet for the Canoe Desert Lake fault. The belt of faulting may extend across Lake Ontario; a fault

Table 1. Bedrock stratigraphy.

Era	Period	Epoch	Formation	Main Lithology	Thickness
Paleozoic	Devonian	Eifelian	Amherstburg	limestone, dolomite	75 - 120
		Emsian	Bois Blanc	limestone, dolomite, with sandstone	30 - 70
	Silurian	Ludlovian	Bertie	dolomite	35 - 85
			Salina	dolomite with shale	300 - 400
			Guelph	dolomite	80 - 120
		Wenlockian	Amabel	dolomite, shale	40 - 280
		Llandoverian	Cataract	sandstone, shale	120 - 240
	Upper Ordovician	Ashgillian	Queenston	red shale	160 - 750
			Meaford – Dundas	grey shale	400 - 570
		Caradocian	Blue Mountain	dark shale	
			Collingwood	black shale	165 - 290
	Middle Ordovician		Cobourg	limestone (Trenton group)	200 - 300
			Verulam	limestone (Trenton group)	200 - 350
			Bobcaygeon	limestone (Trenton group)	25 - 85
			Gull River	limestone (Black River group)	75 - 300
			Shadow Lake	shale with limestone (Black River group)	0 - 50
	Lower Ordovician	Arenigian	Beekmantown	dolomite with sandstone	0 - 350
	Cambrian		Nepean	sandstone, basal conglomerate	0 - 150
	Precambrian		Canadian Shield	crystalline rocks	

striking NNE from Batavia, New York, has been reported. Some Late Carboniferous (?) movements have occurred along faults active in Precambrian time, as demonstrated by Wynne-Edwards (1967) in the case of the Rideau Lake fault which strikes ENE to NE and forms a shear zone at least 1500 ft. wide. Several minor fault zones striking ESE occur in the area, from Burnt River in the west to Kingston in the east. At Madoc, displacement along the main Noyes – Perry wrench fault is at least 100 feet. Late faults of the Madoc area form important channels for the groundwater of the district (Wilson, 1929).

Gas-producing zones have been found in the south-western part of the drainage basin on the Niagara Peninsula and in the area of Acton, 30 miles west of Toronto. The production is obtained from the Black River Group, the Cataract Group, the lower Amabel Group and, to a minor degree, from the Trenton Group. Oil producing zones have been reported in the lower Cataract Group and below the Shadow Lake Formation (Caley, 1961; Sanford, 1961, 1970).

Pleistocene Geology

Through most of the Mesozoic and Cenozoic era, the bedrock surface was subjected to erosion. This resulted in the development of curved lowlands bounded inwardly by the Niagara escarpment (Chapman and Putnam, 1966). Today, its crest stands approximately 300 - 600 feet above the plains. Drainage from the upper Great Lakes passed through the Georgian Bay depression directly into the Lake Ontario basin. The many SSE directed, V-shaped valleys north of the lake, now covered by Pleistocene deposits, were rounded during glaciation. A link with the Lake Erie area may also have existed through the Dundas Valley at

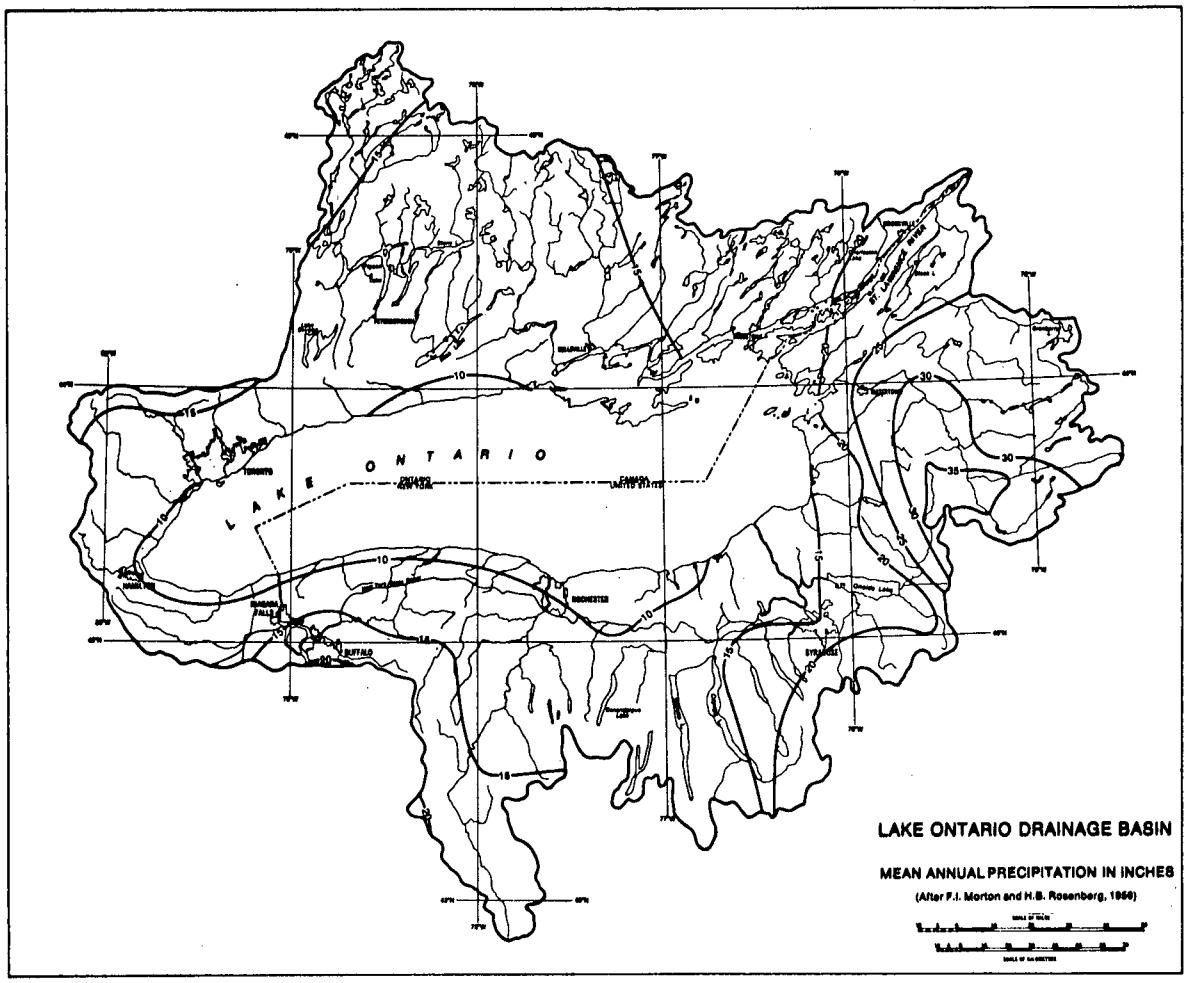

Figure 4. Mean annual runoff from the Lake Ontario drainage basin (after Morton and Rosenberg, 1959).

Hamilton; with a depth of over 200 feet below sea level, this is the deepest buried channel in the Lake Ontario basin.

During the earlier part of the Pleistocene, the whole area was covered by the Wisconsin glacier, which extended during its maximum stage to southern Ohio. The glacier, retreating with readvancements in several stages, left behind extensive ground moraine, drumlins and eskers, and basin-dividing lateral, frontal and particularly interlobate moraines. An excellent description of the recession of the Wisconsin glacier in Southern Ontario is provided by Chapman and Putnam (1949, 1966). At the stage of Lake Warren, the Oak Ridges interlobate moraine was shaped, forming the accentuated basin divide between Lake Ontario and Lake Simcoe (Fig. 5). During subsequent stages, the general outline of the remaining rather indistinct basin boundary was defined. Between Trenton and the Niagara River, Lake Iroquois, a forerunner of Lake Ontario, left shorecliffs and beaches two to eight miles from today's shoreline, except for the Scarborough bluffs which coincide with the present shore (Fig. 6). The Champlain Sea, which followed the stage of Lake Iroquois, covered only the most eastern part of the basin and left no distinct shores in this area. The final shape of the landscape after glaciation was produced mainly by the erosional force of streams and to a lesser extent by stream depositions and eolian erosion.

For the distribution of the main Pleistocene deposits in the Lake Ontario basin, the reader is referred to Figure 7. The map shows the features and deposits which appear at

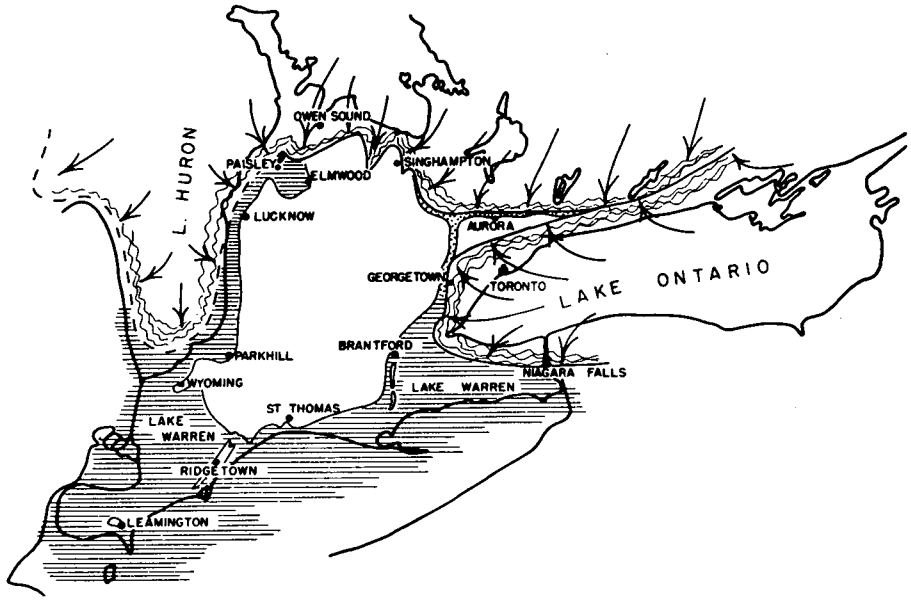

Figure 5. Stage during the life of Lake Warren (after Chapman and Putnam, 1949).

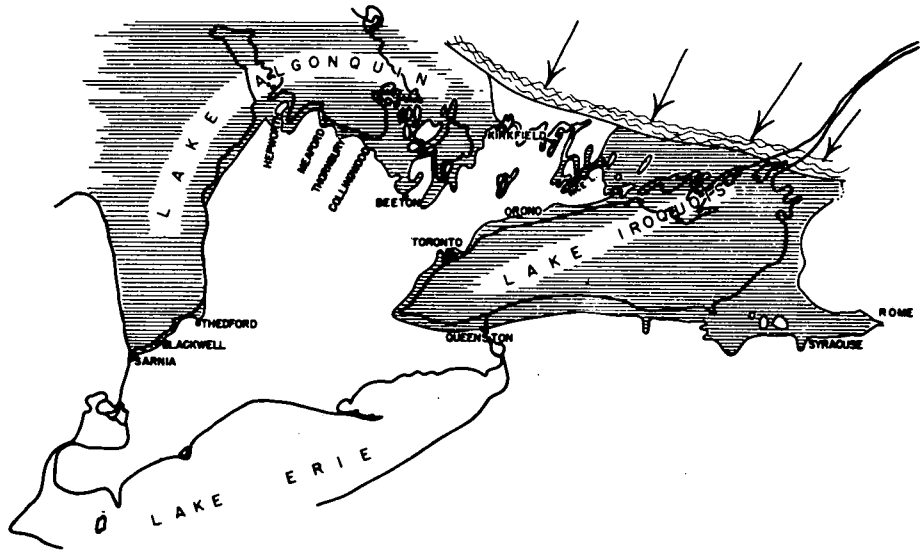

Figure 6. Stage at the times of Lakes Algonquin and Iroquois (after Chapman and Putnam, 1949).

the surface. Large areas are covered by till and clay sediments; to a large extent the same material is also underlying the sand plains and kame moraines. The entire overburden consists, therefore, of less permeable material than appears at first glance. In detail the deposits are composed of a large variety of glacial, fluvio-glacial and lacustro-glacial deposits, the latter ones being extended almost over the entire lake bottom (Fig. 33). The drift thickness varies considerably. East of Trenton and between Port Credit and Burlington, it is generally less than ten feet thick. In the area of the deeper buried channels north of Toronto, however, the overburden attains a thickness of up to 700 feet. Exploitable groundwater is found in lenticular sand and gravel layers. Extensive, high producing aquifers

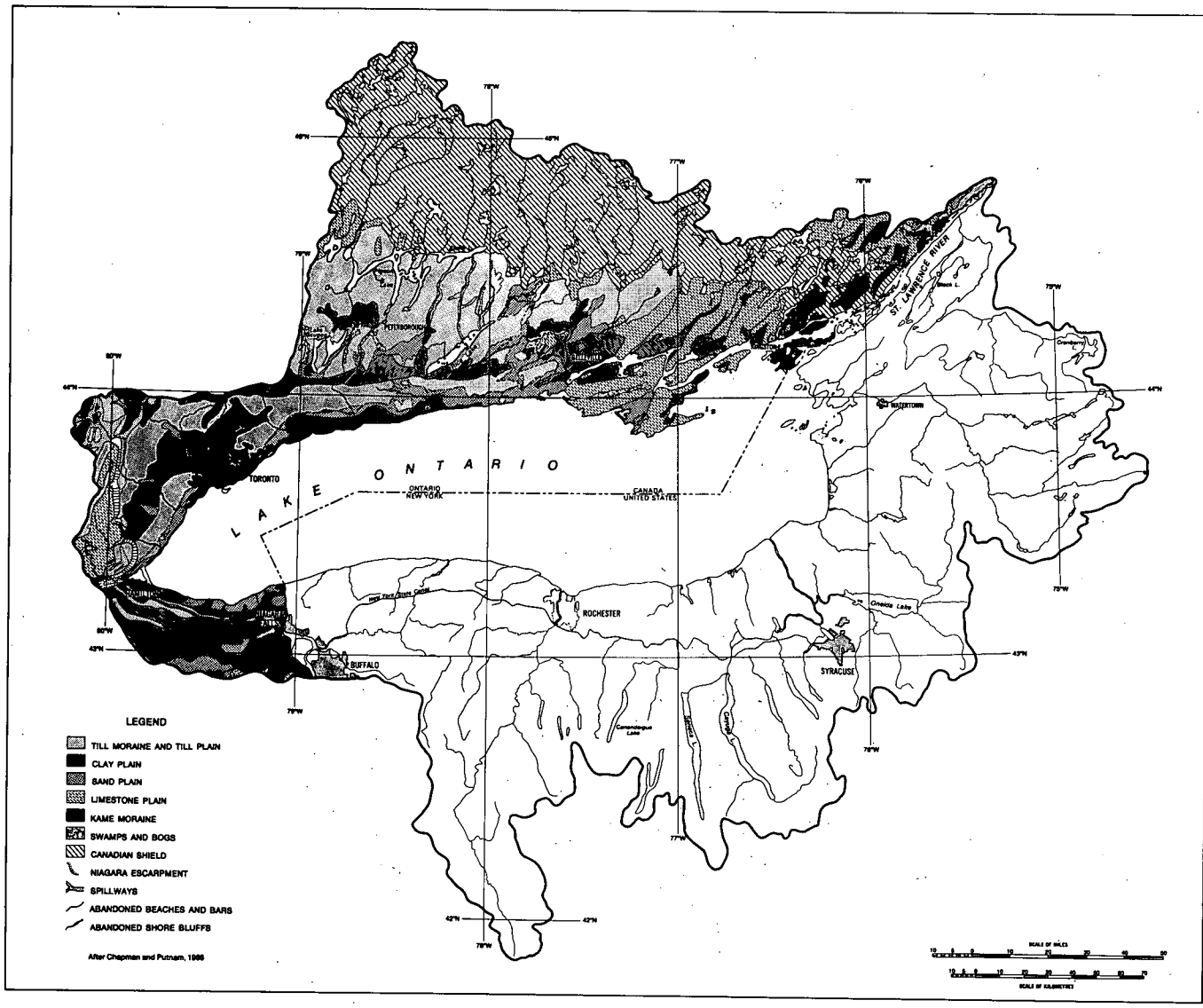

Figure 7. Pleistocene map of the Lake Ontario drainage basin (Canadian side).

occur rather seldom and are not related to the occurrence of buried valleys (Haefeli, 1970).

Since the soil is considered to be one of the most decisive factors controlling the groundwater recharge, a general map showing the major soil associations was included in the report (Figure 8). Four soil groups dominating the basin are: fine to very fine textured soil of low permeability in the southwestern region; medium textured soil of moderate permeability in the area bounded by Toronto, Peterborough and Belleville; mostly shallow, coarse textured soil on Precambrian rock and limestone in the northern and eastern part of the basin; and medium to coarse textured soil on till, sand and gravel, with moderate to high permeability distributed in patches over the entire area but occurring mainly in the northeastern part.

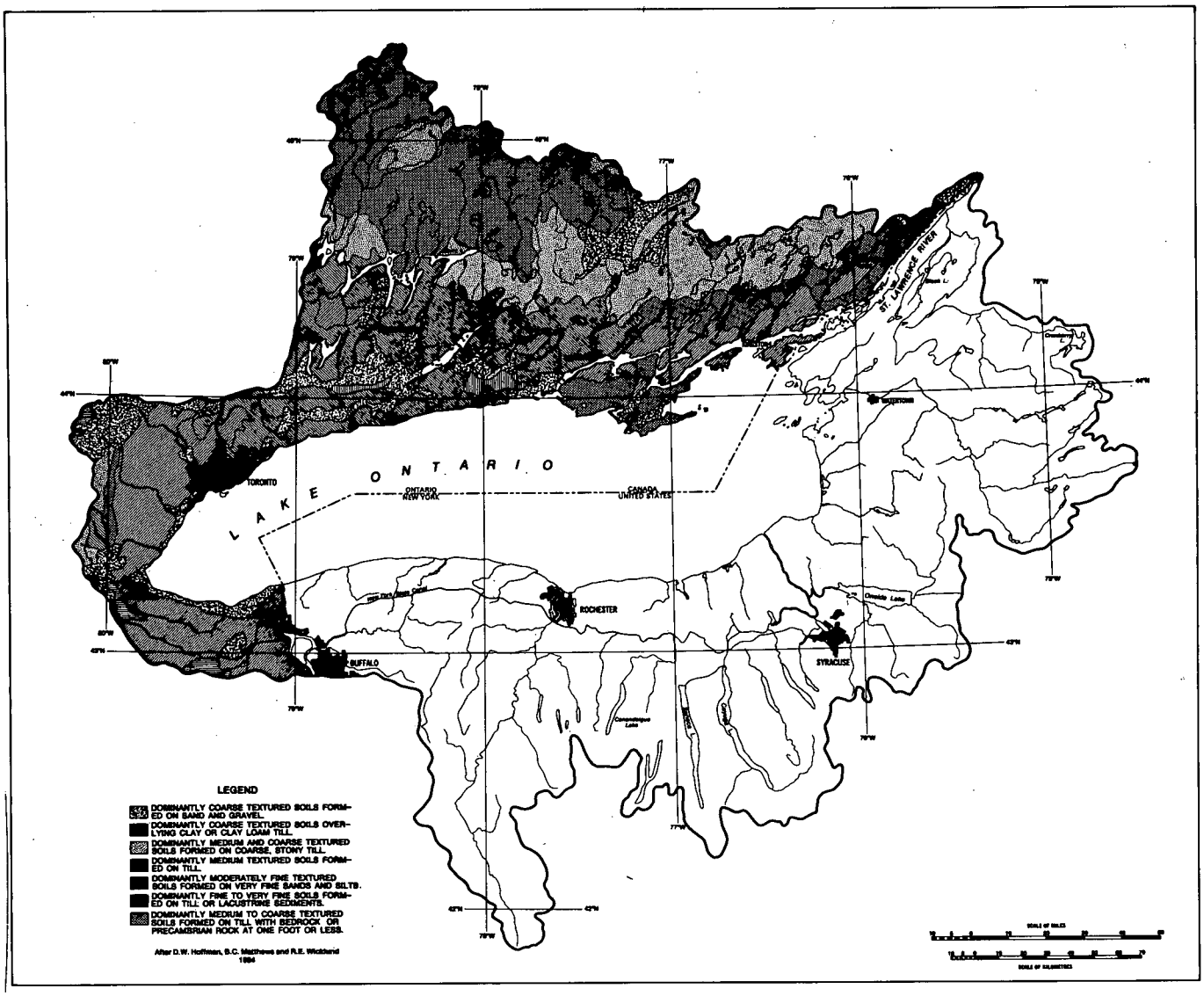

Figure 8. Soil map of the Lake Ontario drainage basin (Canadian side).

CHAPTER 2

Classic Method

PERMEABILITY

Analysis of specific capacity data

Method

The specific capacity, *Q/s*, of a well is defined as the yield of the well in imperial gallons per minute per foot of drawdown (Igpm/ft.) for a stated pumping period and rate. The specific capacity of wells is used in this study as a basis for estimating the hydraulic properties of the strata penetrated by them.

To analyze the average specific capacity of a formation, the hydrogeological relationships have to be considered and the man-made factors eliminated. Most of the wells are multi-strata wells. They penetrate more than one potential water producing formation. The specific capacity of a multi-strata well is the numerical sum of the specific capacities of the individual units (Csallany and Walton, 1963). However, since most of the formations are not homogeneous, the result obtained from a single well is only valid for that particular well location. Therefore, to get representative values of a formation, a large number of wells have to be analyzed. Furthermore, if necessary, the influence of the stratification and the change of fracture porosity with depth has to be taken into consideration. To obtain comparable data, the specific capacity per foot of penetration should be calculated.

The elimination of man-made factors is problematic and generally based on common sense. It is believed that the normal way for obtaining a water well is as follows: the owner requires a specified amount of water; the well is drilled until the required quantity is found; if the driller is not successful within a specified depth, the well is abandoned and one or more other wells are constructed. This means that not only wells going into the formation have to be considered for the evaluation of the average specific capacity, but also the ones going through it and, of course, all the dry ones.

From the foregoing, it is evident that the groundwater productivity of zone A of the schematic example in Figure 9 cannot be computed from the wells producing solely from zone A. Because of the heterogeneity in the media, *Q/s* for an individual zone should not be computed by subtracting known values of *Q/s* from some values of *Q/s* determined collectively for the three zones. Depending on the data available and the assumptions considered to be correct, the average specific capacity can be calculated in various ways. For example, the average specific capacity per foot of penetration is computed for zone A using different assumptions: Example (Fig. 9): Well 1 and 2 struck water in zone A, well 3 is dry and well 4 is reported having struck water in zone A and B.

Assumption I – All wells which went deeper than zone A did not strike water there, or the amount was negligible.

$$\text{mean } Q/s \text{ for A per ft.} = \frac{Q/s_{(1)} + Q/s_{(2)}}{x + y + 2a}$$

Assumption II – Well 4 hit the average amount of water produced by zone A.

$$\text{mean } Q/s \text{ for A per ft.} = \frac{Q/s_{(1)} + Q/s_{(2)} + \frac{Q/s_{(1)} + Q/s_{(2)}}{2}}{x + y + 2a}$$

Assumption III – Well 4 got half of its specific capacity in zone A.

$$\text{mean } Q/s \text{ for A per ft.} = \frac{Q/s_{(1)} + Q/s_{(2)} + \frac{Q/s_{(4)}}{2}}{x + y + 2a}$$

Assumption IV – Although it is not reported that well 4 struck water in C, it is believed that drilling of the well was continued until sufficient water was found.

$$\text{mean } Q/s \text{ for A per ft.} = \frac{Q/s_{(1)} + Q/s_{(2)} + \frac{Q/s_{(4)}}{3}}{x + y + 2a}$$

For the cased, overburden wells where multiple screens are very seldom used, Assumption I should prove correct. For the bedrock wells constructed as open holes through the bedrock all four assumptions might come true. Assumption I favours the lower zones, Assumption II the upper ones. They represent extreme cases. It is believed, therefore, that cases III and IV would be more appropriate. As an example, 182 wells of the Bobcaygeon, Gull River and Shadow Lake formation (limestone) grouped into six

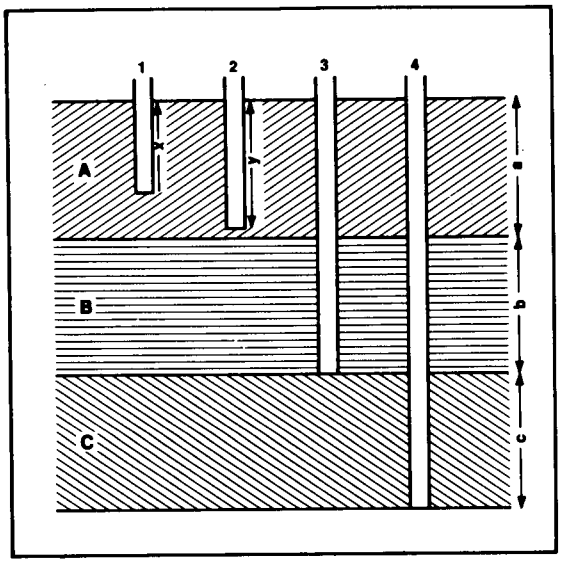

Figure 9. Schematic section showing wells penetrating different zones.

depth zones were analyzed according to Assumption I, II and IV (Fig. 10). In all cases, the main trend remained almost the same. For the present study, Assumption IV was considered the most suitable to analyze the specific capacity versus depth for bedrock wells.

Overburden Wells

The groundwater outflow through the overburden into the lake is controlled by a rather narrow strip along the shoreline, and as such is a function of the permeability and the hydraulic gradient in this area. The average specific capacity is therefore computed from the same shorebelt as the hydraulic gradient. To avoid the Niagara Escarpment and to obtain a sufficient number of wells, a 2.5-mile wide area was chosen rather arbitrarily. According to the bedrock types underlaying the Quarternary deposits, the shorebelt was divided into four different areas (Fig. 11).

The overburden in area A is covering the Queenston – Formation (shale); in area B, the Meaford – Dundas, Blue Mountain and Collingwood Formations (shale); and in area C the Cobourg Formation (limestone). Because of the very shallow drift and consequently small number of

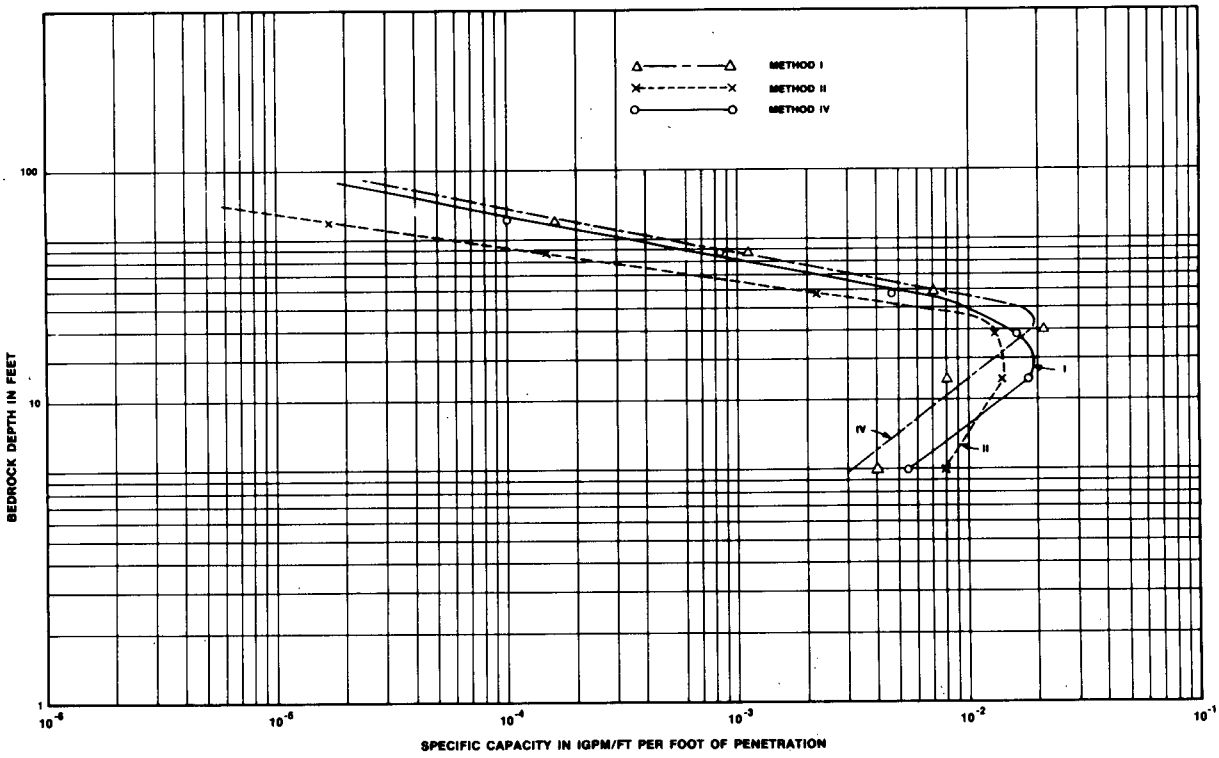

Figure 10. Relation of specific capacity to bedrock depth derived after different methods (example: Bobcaygeon, Gull River, Shadow Lake Formation).

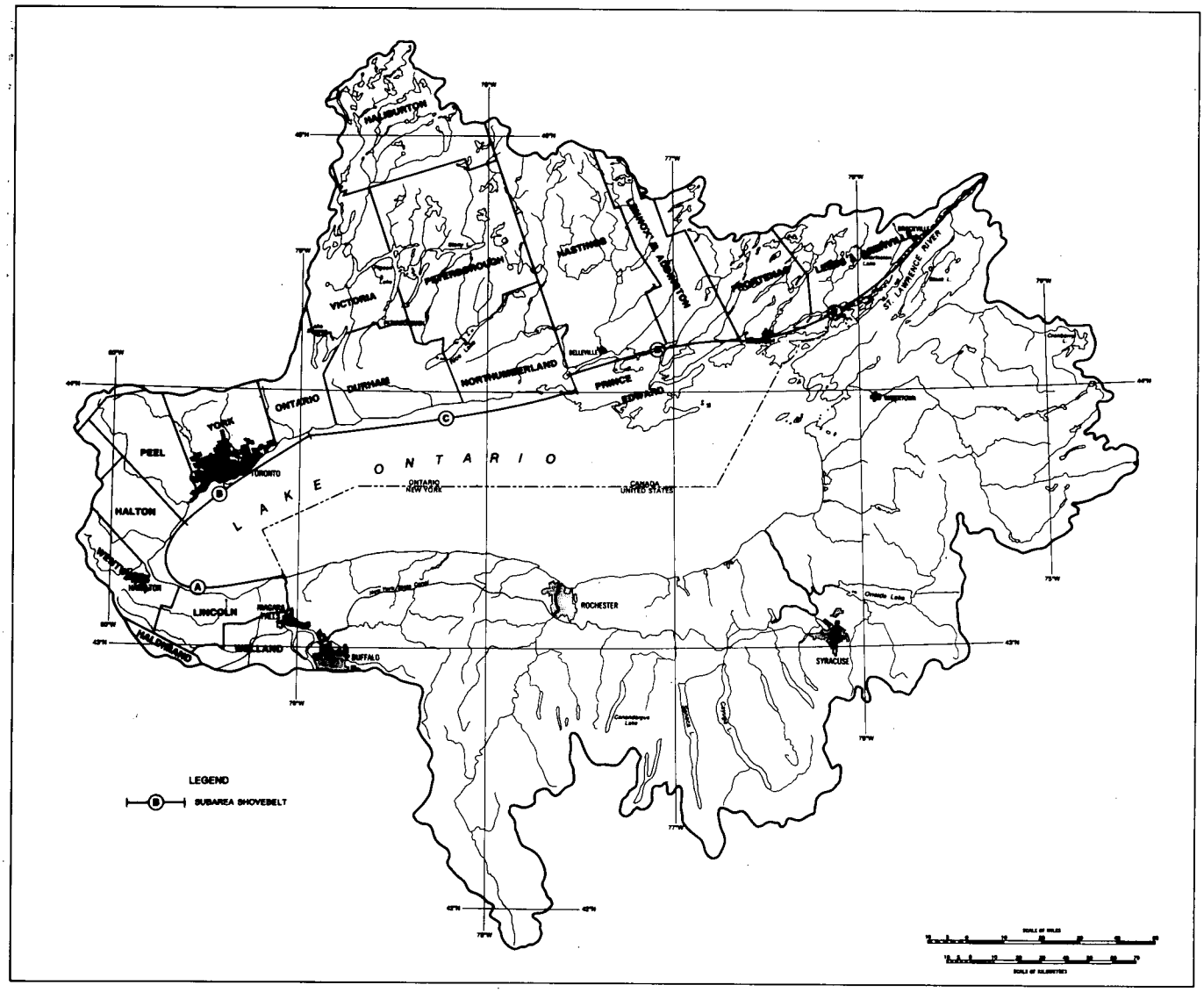

Figure 11. Division of shorebelt in area A, B, C, D and E.

overburden wells, area D comprising the lower members of the Trenton – Black River Group (limestone) and area E with bedrock consisting of crystalline rocks, sandstone and dolomite, were combined. The average specific capacity per foot of penetration for depth zones 0 - 50 ft. and > 50 ft. was computed after Assumption I in the last paragraph. The areas A, B, C and D were subdivided to obtain an equal distribution of wells. It is believed, therefore, that the values obtained are representative although the total number of wells is rather small (Table 2). The specific capacity of the deep overburden, which includes the buried valleys (depth > 50 ft.) is somewhat lower than that of the shallow overburden, as was observed in a previous survey (Figs. 27 and 28) (Haefeli, 1970). Therefore the difference in specific capacity between the upper and lower overburden reflects the lithology variation which would be expected. For comparison, the average specific capacity per foot of penetration versus the lithology was plotted, with the gravel content being taken as a measure of the permeability (Fig. 12).

Bedrock Wells

The permeability of the dense bedrock bordering Lake Ontario, mainly limestone and shale, is essentially a function of the opening and spacing of rock fractures rather than intergranular porosity. It has been observed in crystalline rocks and to a minor degree in sedimentary rocks that the fracture porosity decreases with depth. (Davis and Turk, 1964; Snow, 1968a, 1968b). Furthermore it is believed that the thickness of the low permeability overburden would affect the recharge of the bedrock and consequently reduce its specific yield.

Table 2 Mean specific capacities and hydraulic conductivities for different overburden depths and areas.

AREA	A		B		C		D & E
Depth Zone (ft.)	0 - 50	>50	0 - 50	>50	0 - 50	>50	0 - 60
Number of Wells	37	30	26	22	46	43	67
Q/s (Igpm/ft.)	0.55	0.42	0.17	0.20	0.43	0.26	1.16
Mean penetration (ft.)	29	20	31	42	31	53	30
$\frac{Q/s}{\text{ft.}}$ (Igpm/ft.)	0.019	0.021	0.0055	0.0048	0.014	0.0049	0.039
K (Igpd/ft.^{2})	30	33	8	7	22	7	65

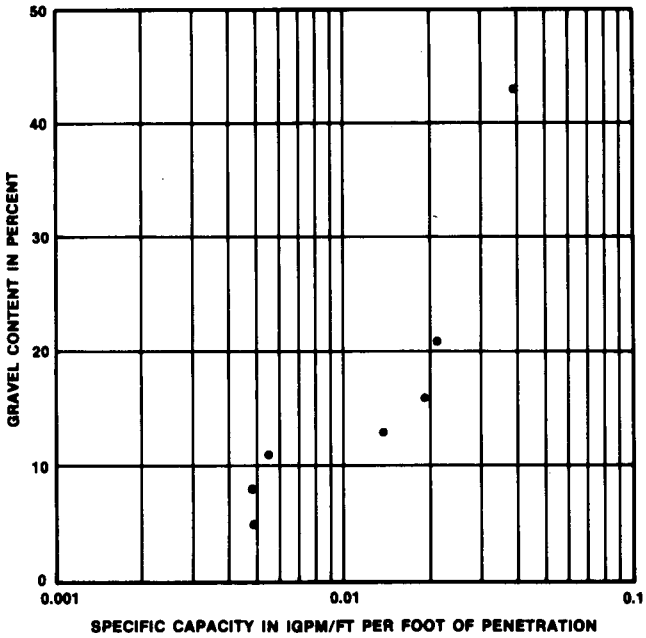

Figure 12. Specific capacity per foot of penetration versus gravel content in percent (after drillers log).

To obtain the tendency by which the specific capacity decreases with depth, the wells were grouped according to their depth of penetration into bedrock. According to the available number of wells the following depth zones in feet were chosen: 0 - 10, 11 - 20, 21 - 30, 31 - 50, 51 - 75, 76 - 100 >100 feet below bedrock surface. Each zone contained 12 to 50 wells. Although the analyzed limestone and shale formations are not uniform, for example, the microcrystalline Cobourg Formation contains interbeddings of calcarenite and shaly limestone, the lithological change should not significantly affect the fracture porosity within the formation. In fact it became evident that the trend between different lithostratigraphic units was very similar (Figs. 13 and 14).

Avoiding local high concentrations of wells, a total of 1123 bedrock wells within the 2.5-mile wide shorebelt and its vicinity were analyzed. The average specific capacities are presented in Tables 3 and 4. In Figures 13 and 14, the average specific capacity per foot of penetration versus depth was plotted logarithmically. Two relations are remarkable. The maximum specific capacity at depths 15 to 40 feet is seen to have a decreasing trend to the bedrock surface; at greater depths, it has a linear decrease with depth showing only a small variation between similar lithologic units. A similar decrease in the well yield with depth was observed in crystalline rocks by Davis and Turk (1964).

Usually, it is expected that the weathering of bedrock increases its porosity. In coarse-grained rock, a relatively high permeability may result from the weathered zone. In very fine-grained or relatively soft rocks which are covered by glacial deposits, the conditions seem to be different. The decreasing permeability trend towards the surface of the limestone and shale formations may have resulted from plugged fractures which are clogged by argillaceous material originating from overlaying till deposits. That trend may also be slightly influenced by the manner of sampling. Davis and Turk (1964) and Snow (1968a) noted that the distribution of specific capacities in fractured rock is always skewed to the right. The mean is larger than the median so, for a large number of wells, a greater capacity can be expected than for a single well. Snow (1968a) conducted studies to assess the effect of sample size. The reason for the increasing permeability with increasing size of sample or

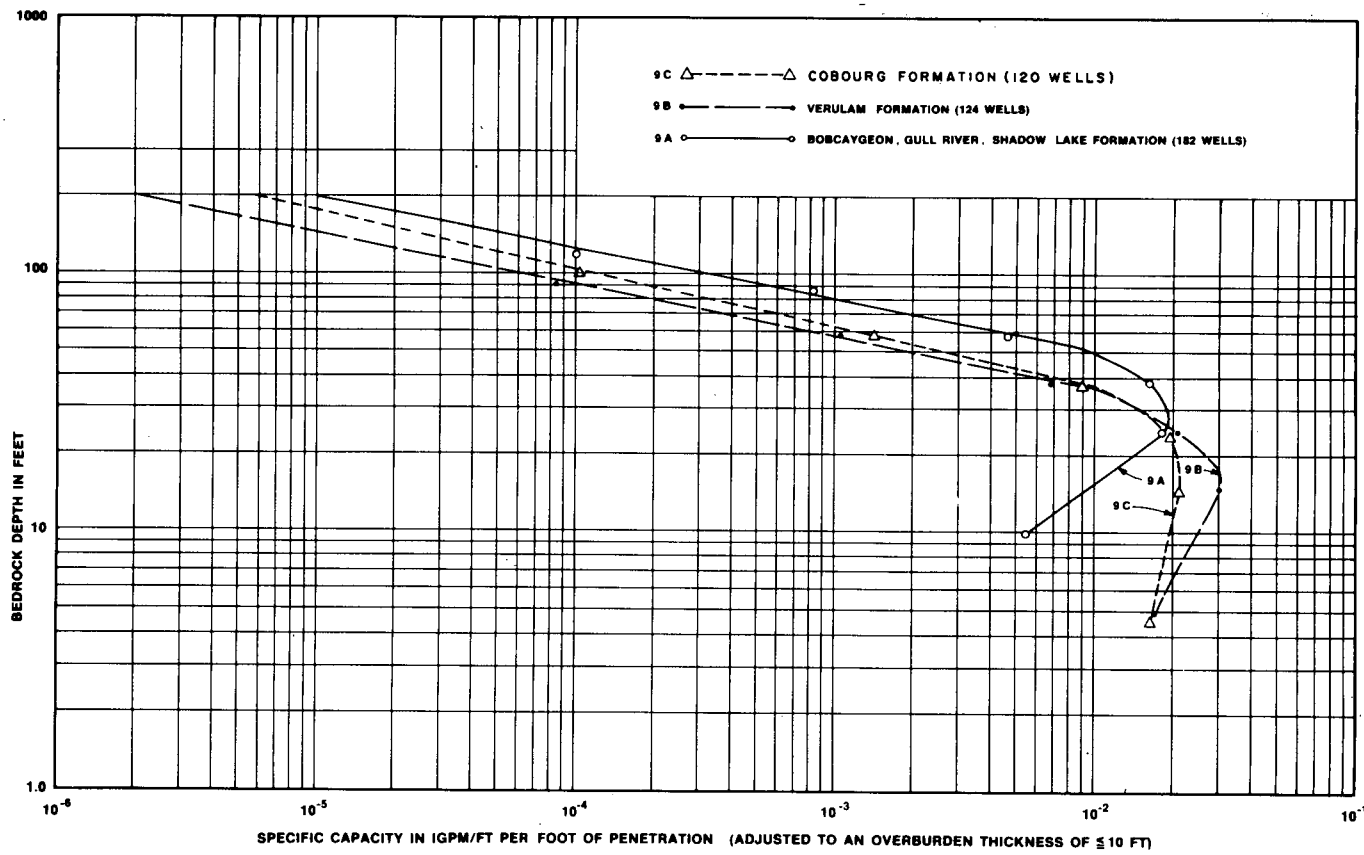

Figure 13. Relation between specific capacity and bedrock depth of the Trenton – Black River Group (limestone).

Table 3. Adjusted mean specific capacities for different bedrock depths of the Trenton – Black River Group (limestone).

FORMATION	COBOURG			VERULAM			BOBCAYGEON, GULL RIVER, SHADOW LAKE		
Total No. of Wells	120			124			182		
Depth Zone (ft.)	*Q/s* (Igpm/ft)	Mean penetration (ft)	*Q/s* per foot (Igpm/ft^2)	*Q/s* (Igpm/ft)	Mean penetration (ft)	*Q/s* per foot (Igpm/ft^2)	*Q/s* (Igpm/ft)	Mean penetration (ft)	*Q/s* per foot (Igpm/ft^2)
0 - 10	0.15	9.1	0.016	9.6	9.6	0.017	0.11	19.6	0.0054
11 - 20	0.18	8.9	0.020	0.27	9.3	0.030			
21 - 30	0.17	9.1	0.019	0.17	8.6	0.021	0.15	8.7	0.018
31 - 50	0.15	17	0.0088	0.11	15.9	0.0067	0.25	15.3	0.016
51 - 75	0.023	16.5	0.0014	0.019	16.8	0.0011	0.08	17.2	0.0046
75 - 100	0.0051	49.2	0.0001	0.002	36.9	0.00008	0.016	20.6	0.0008
>100							0.004	36.3	0.001

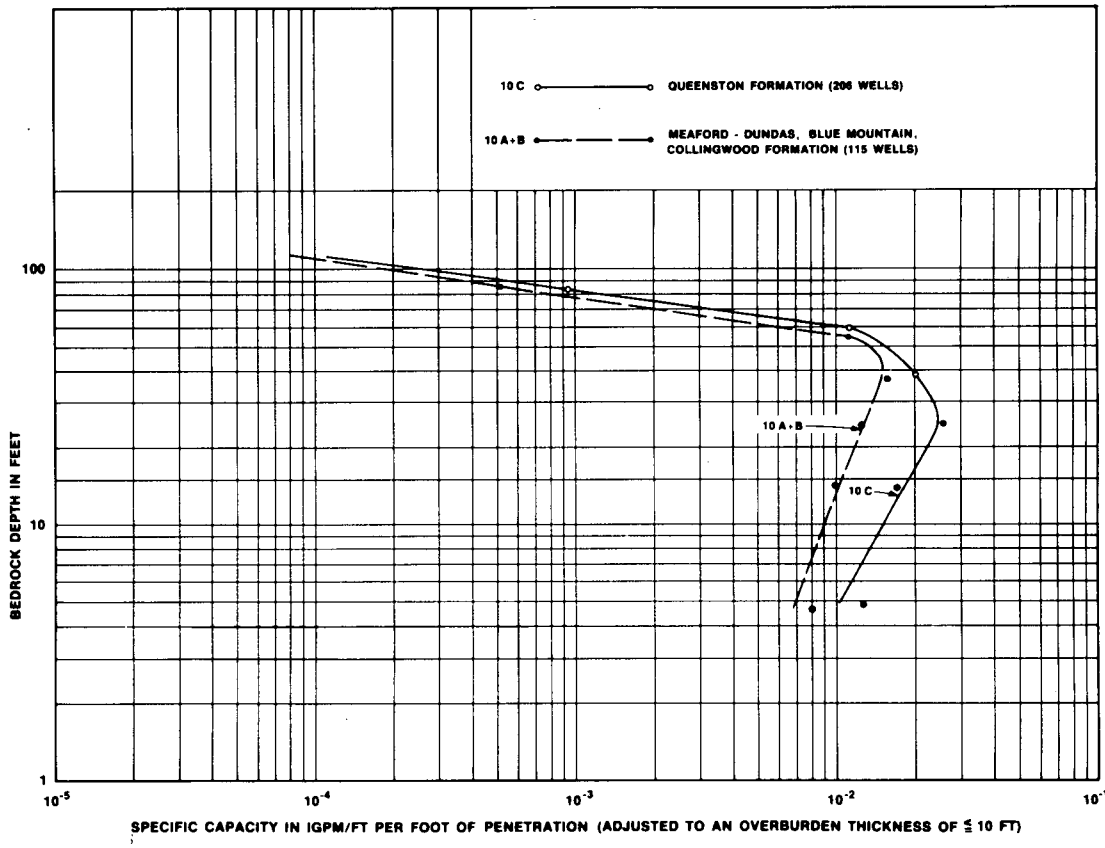

Figure 14. Relation between specific capacity and bedrock depth of the Upper Ordovician shale.

for an increasing number of wells is the fact that the fracture apertures are not all alike. The distribution of apertures is probably skewed to the right. In the present study where the sample size varies from 12 to 59, the largest number of samples is in the group 31 to 50 ft. deep, which coincides in some cases with the depth of the highest permeability (Figs. 13 and 14). Still another influence of the trend might result from cased wells through the weathered zone. This would, however, indicate a low water production in the upper part of bedrock.

Table 4. Adjusted mean specific capacities for different bedrock depths of the Upper Ordovician (shale).

FORMATION	QUEENSTON			MEAFORD, DUNDAS, BLUE MOUNTAIN, COLLINGWOOD		
Total Number of Wells	206			115		
Depth Zone (ft.)	*Q/s* (Igpm/ft)	Mean Penetration (ft.)	*Q/s* per foot (Igpm/ft.^{2})	*Q/s* (Igpm/ft)	Mean Penetration (ft.)	*Q/s* per foot (Igpm/ft.^{2})
0 - 10	0.12	9.6	0.013	0.075	9.5	0.0079
11 - 20	0.15	8.7	0.017	0.094	9.5	0.0098
21 - 30	0.23	8.4	0.027	0.11	9.0	0.013
31 - 50	0.27	13.8	0.020	0.21	13.7	0.015
51 - 75	0.15	14.3	0.011	0.15	12.8	0.011
>75	0.014	15.1	0.00093	0.011	26.3	0.00042

Because of the lack of data, only the average specific capacity for a depth range of 0 - 75 feet was computed for the formations bordering the comparatively shallow St. Lawrence River (Table 5). The widening of the fractures in the limestone due to dissolution

$$CaCO_3 + CO_2 + H_2O \rightarrow Ca(HCO_3)_2$$

seems not to be important in the shorebelt area. The results do not show any evidence. This may be because the low permeability of the glacial deposits reduces the recharge and the low hydraulic gradient causes a very slow groundwater flow. In fact, an aerial photographic survey showed almost no karstic phenomena occurring at the surface. Only two resurgences in the Lake Ontario basin are known to the author, one at Warsaw, northeast of Peterborough and the other at Collins Bay, west of Kingston.

All of the given Q/s values have been adjusted if necessary to an overburden depth of $\leq$ 10 feet. The effect of the thickness of overburden on the specific capacity of the bedrock was analyzed for different overburden depths by computing it for 243 wells penetrating 0 - 30 feet into the bedrock. The mean specific capacity of each overburden depth zone versus the mean depth of the zone was plotted (Figs. 15 and 16). Only three different formations had sufficient overburden thickness to allow an analysis. Both shale formations show a similar trend suggesting a linear log Q/s versus overburden depth relationship whereas the limestone formation seems to show an exponential trend. The rather low sample number does not provide a more definite relationship. A statistical analysis of the ungrouped data produced no significant correlation, indicating that more than 50 percent of variations from the best fit line are due to chance. This may be partly due to the strong skewness of the specific capacity data.

Table 5. Mean specific capacity Q/s per foot of penetration and permeability, K, for 0 - 75 ft. bedrock depth of the Beekmantown Group, Nepean Formation and Canadian Shield.

Number of Wells	Unit	Time	Rock	Q/s per foot (Igpm/ ft.^{2})	K (Igpd/ ft.^{2})
61	Beekmantown Group	Lower Ordovician	Dolomite, sandstone	0.07	100
73	Nepean (Potsdam) Formation	Upper Cambrian	Sandstone	0.03	40
122	Canadian Shield	Precambrian	Crystalline rocks	0.02	25

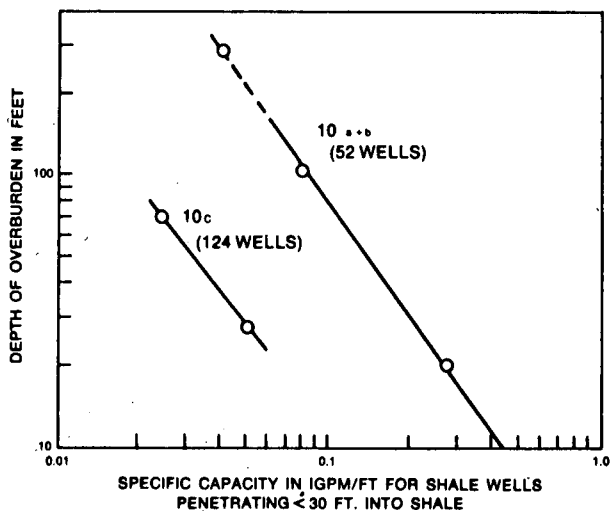

Figure 15. Relation between specific capacity of shale wells and thickness of overlaying Quaternary deposits.

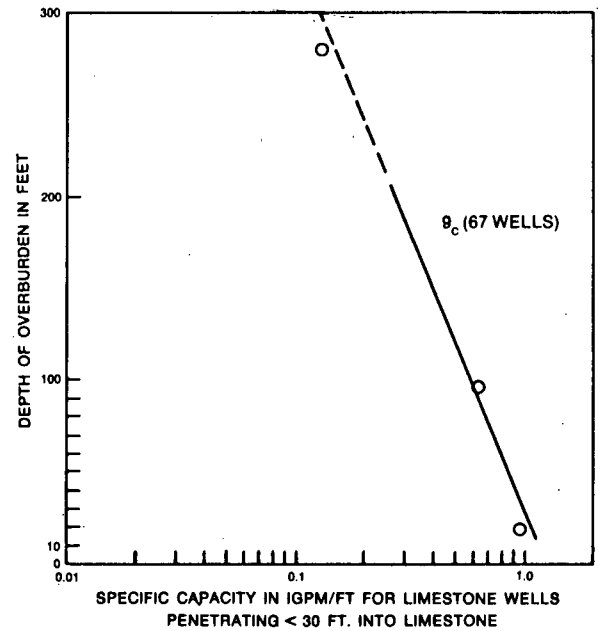

Figure 16. Relation between specific capacity of limestone wells and thickness of overlaying Quaternary deposits.

Estimating Transmissibility From Specific Capacity

Relation between Specific Capacity and Transmissibility

To estimate the coefficient of transmissibility from specific capacity, the following basic data have to be known: type of aquifer, storage coefficient, well diameter, pumping time, geological conditions and man-made factors affecting the well yield. High specific capacities generally indicate a high coefficient of transmissibility, T; low specific capacities indicate a low coefficient of transmissibility. T is defined as the rate of flow of water in imperial gallons per day through a vertical strip of the aquifer one-foot wide extending the full saturated height of the aquifer under a hydraulic gradient of 100 percent (1 foot per foot) and at the prevailing temperature of water.

Since the yield of a well per foot of drawdown is also a function of other factors (such as partial penetration, well loss, and geohydrological boundaries) the specific capacity cannot be an exact criterion of the coefficient of transmissibility. However to quote Theis and Brown (1963, p. 331) "... estimates of T that are based on the specific capacities of wells should be reasonably reliable and could be made without the elaborate tests necessary for precise determination".

The theoretical relation between the specific capacity and the transmissibility of a well discharging at a constant rate in a homogeneous, isotropic, artesian aquifer infinite in areal extent, is from the nonequilibrium formula (Theis, 1935) given by the following equation (Wenzel, 1942):

$$\frac{Q}{s} = \frac{T}{114.6 \cdot W(u)} \qquad (1)$$

where: $u = \dfrac{2242\ r_w^2\ S}{Tt}$ (2)

or can be written as follows (Theis, 1963):

$$T = \frac{114.6\ Q}{s}\left[-0.577 - \log_e\left(\frac{2242\ r_w^2\ S}{Tt}\right)\right] \qquad (3)$$

or by rearranging the terms and modifying equation (3):

$$\frac{Q}{s} = \frac{T}{264 \log \dfrac{Tt}{2242\ r_w^2\ S} - 65.5} \qquad (4)$$

where: Q is the discharge of a pumped well, in imperial gallons per minute

s is the drawdown, in feet

T is the coefficient of transmissibility, in imperial gallons per day per foot

S is the coefficient of storage

r_w is the nominal radius of well, in feet

t is the time after pumping started, in minutes

$W(u)$ is the well function for nonleaky artesian aquifer (Wenzel, 1942).

The equations assume that the well completely penetrates the aquifer, the well loss is negligible, and the effective radius of the well has not been affected by the drilling and development of the well and is equal to the nominal radius of the well.

Type of Aquifer

To obtain an indication of how much the specific capacity data computed from the water well records were affected by water table conditions, the depth where the well struck water was compared with the static water level or piezometric head. Over 95 percent of the bedrock wells and over 90 percent of the overburden wells showed confined conditions. With regard to the till character of the overburden and the location of the wells in the shorebelt, representing a distinct discharge area, this result could be expected. However, it is believed that for many wells, water table conditions became effective during pumping.

Storage Coefficient

The storage coefficient, S, is defined as the volume of water the aquifer releases or takes into storage per unit surface area of the aquifer per unit change in the component of head normal to that surface.

As mentioned before, most of the aquifers tapped by the surveyed wells are confined. Under artesian conditions the storage coefficient is a function of the elasticity or compressibility of the water and of the aquifer skeleton, as expressed in the following equation (Jacob, 1950):

$$S = \frac{\rho\ \gamma\ m\ \beta}{144}\left(1 + \frac{\phi}{\rho\beta}\right) \qquad (5)$$

where: ρ is the porosity fraction

m is the saturated thickness of aquifer, in feet.

β is the reciprocal of the bulk modulus of elasticity of water, or bulk modulus of compression, or compressibility of water; approximate value for average groundwater temperature is $3.3 \cdot 10^{-6}$ sq. in./lb.

Table 6. Coefficients for confined overburden aquifers evaluated from pumping tests.

Location	Q (Igpm)	S	T (Igpd/ft)	m (ft.)	K_h (Igpd/ft.^{2})	General lithology of Aquifer (after driller's log)
Markham	1012	$3.2 \cdot 10^{-4}$	110000	57	2470	sand and gravel
Milton	1010	$1.5 \cdot 10^{-3}$	116000	45	2570	sand and gravel.
1) Richmond Hill	750	$1.6 \cdot 10^{-10}$	83000	50	1680	sand and gravel with boulders.
1)*Vaughan Twp.	550	$1.0 \cdot 10^{-5}$	63000	100	630	sand with some clay.
Bolton		$1.1 \cdot 10^{-5}$	43300	20	2350	gravel and sand.
2) Oak Ridges	325	$1.5 \cdot 10^{-5}$	45000	28	1610	sand and gravel.
2)*Elmvale	357	$1.1 \cdot 10^{-5}$	41000	65	630	sand, gravel and silt.
1)*Bradford	400	$1.6 \cdot 10^{-4}$	40700	50	830	sand and gravel with some silt and clay.
Agincourt	600	$8.5 \cdot 10^{-5}$	38900	18	2160	sand and gravel.
Uxbridge	220	$2.2 \cdot 10^{-3}$	38100	56	700	sand and gravel with some silt.
2) Bradford	410	$4.8 \cdot 10^{-4}$	31300	19	1650	sand with some gravel.
*Ancaster	700	$4.6 \cdot 10^{-3}$	26700	77	350	sand and gravel with considerable silt and some clay.
*Toronto	12.5	$2.7 \cdot 10^{-4}$	22000	38	580	gravel, sand and clay with boulders.
Preston	135	$5.3 \cdot 10^{-5}$	16200	16	1100	gravel and sand with boulders.
Stayner	419	$1.3 \cdot 10^{-4}$	11100	27	410	sand and gravel with some clay.
Orono	26	$3.9 \cdot 10^{-5}$	11000	12	920	gravel with some clay.
*Thornburg	15	$3.8 \cdot 10^{-3}$	7170	51	140	sand, gravel and boulders.

* considerable partial penetrating effect on T and K_h
1) after C.J. Haefeli (1970)
2) after A.K. Watt (1963)

ϕ is the reciprocal of the bulk modulus of elasticity of aquifer skeleton or bulk modulus of compression, or vertical compressibility of aquifer skeleton, in lb/cu. ft.

γ is the specific weight of water, in lb./cu. ft.; the approximate value for average groundwater temperature is 62.4 lb./cu. ft.

The porosity, ρ, and especially the bulk modulus of compression, ϕ, are very seldom known. S has therefore to be derived most of the time from pumping tests. For example, by rearranging equation 2 and substituting r for r_w

$$S = \frac{T u t}{2242 r^2} \qquad (6)$$

where r is the distance of the observation well from the pumped well. Because the nominal radius, r_w, of the pumped well does not correspond exactly with the effective well radius, small errors in r_w would result in large errors of S. The storage coefficient has, therefore, to be computed from drawdown data of observation wells.

After Todd (1959, p. 31), the storage coefficient in most confined aquifers falls in the range of $5 \cdot 10^{-5} \leqq S \leqq 5 \cdot 10^{-3}$ and according to Ferris et al (1962, p. 76), in the range $1 \cdot 10^{-5} \leqq S \leqq 1 \cdot 10^{-3}$. The median storage coefficient of confined overburden aquifers computed from 17 pumping tests carried out in the Lake Ontario basin and vicinity was approximately $2.5 \cdot 10^{-4}$ (Table 6, Fig. 17). Since most pumping tests of bedrock aquifers are performed without observation wells, only a few data were available to compute S. Therefore, for comparison, values of a brief, random literature review were included in Table 7. Despite the different nature of rocks, the storage coefficient does not show a large variation. Only one out of 19 values exceeds the range of $2 \cdot 10^{-5} \leqq S \leqq 2 \cdot 10^{-3}$. From Figure 18 it can be seen that large errors in estimated coefficients of storage result in comparatively small errors in coefficients of transmissibility estimated using specific capacity data, because the specific capacity varies with log $1/S$. For example, by changing S by factor 10 , a change in T of less than 20 percent results. Therefore, the estimated median storage coefficient of $2 \cdot 10^{-4}$ for confined bedrock aquifers and $2 \cdot 5^{-4}$ for confined overburden aquifers does not appear critical with respect to estimated transmissibilities.

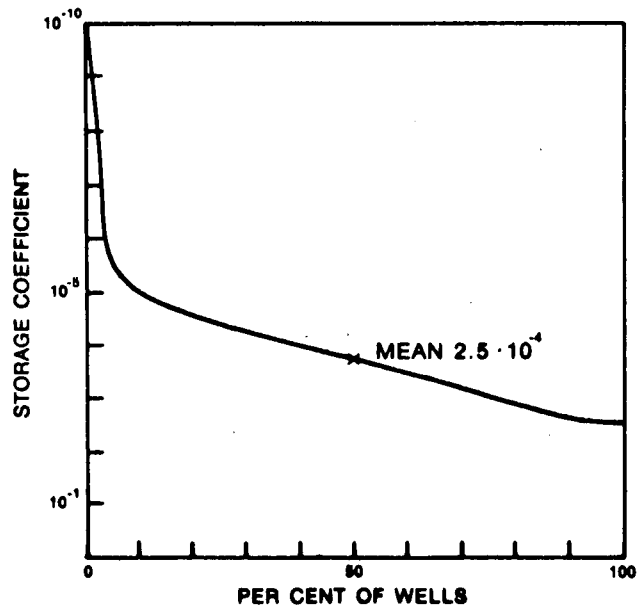

Figure 17. Approximate frequency curve for the storage coefficient of overburden wells.

Table 7. Storage coefficients of confined bedrock aquifers (from Lake Ontario Basin and random literature review).

Type of Bedrock	Stratigraphy	Location	S
Dolomite	Lucas Form., Devonian	St. Mary's Ont.	$2.0 \cdot 10^{-4}$
	Guelph Form., Silurian	Guelph, Ontario	$1.5 \cdot 10^{-3}$
	Guelph Form., Silurian	Preston, Ont.	$9.3 \cdot 10^{-4}$
	Guelph Form., Silurian	Preston, Ont.	$1.2 \cdot 10^{-3}$ (1)
	Silurian	Wheaton, Ill.	$3.5 \cdot 10^{-4}$ (2)
	Silurian	Argone, Ill.	$9.0 \cdot 10^{-5}$ (2)
Limestone	Dundee Form., Devonian	St. Mary's, Ont.	$2.5 \cdot 10^{-4}$
	Trenton-Black River, Ordovician	Winchester, Ont.	$2.3 \cdot 10^{-5}$ (1)
	Trenton-Black River, Ordovician	Chesterville, Ont.	$6.6 \cdot 10^{-6}$ (1)
		Burton, South Car.	$1.0 \cdot 10^{-4}$ (3)
	Tertiary	Jasper, South Car.	$5.0 \cdot 10^{-4}$ (3)
		Savannah, S. Car.	$3.0 \cdot 10^{-4}$ (3)
Shale	Trias	Flemington, N.J.	$2.5 \cdot 10^{-4}$ (4)
Clay and Siltstone	Pennsylvanian	Moncton, N.B.	$4.0 \cdot 10^{-4}$ (5)
		Moncton, N.B.	$2.2 \cdot 10^{-3}$ (5)
Sandstone	Pennsylvanian	Moncton, N.B.	$6.3 \cdot 10^{-4}$ (5)
		Moncton, N.B.	$1.8 \cdot 10^{-4}$ (5)
		Moncton, N.B.	$4.0 \cdot 10^{-3}$ (5)
	Cambrian-Ordovician	Northern Illinois	$3.5 \cdot 10^{-4}$ (6)

1) After Watt 1963
2) After Zeizel and others 1962
3) After Siple 1967
4) After Vecchioli 1967
5) After Carr 1968
6) After Walton and Csallany 1962

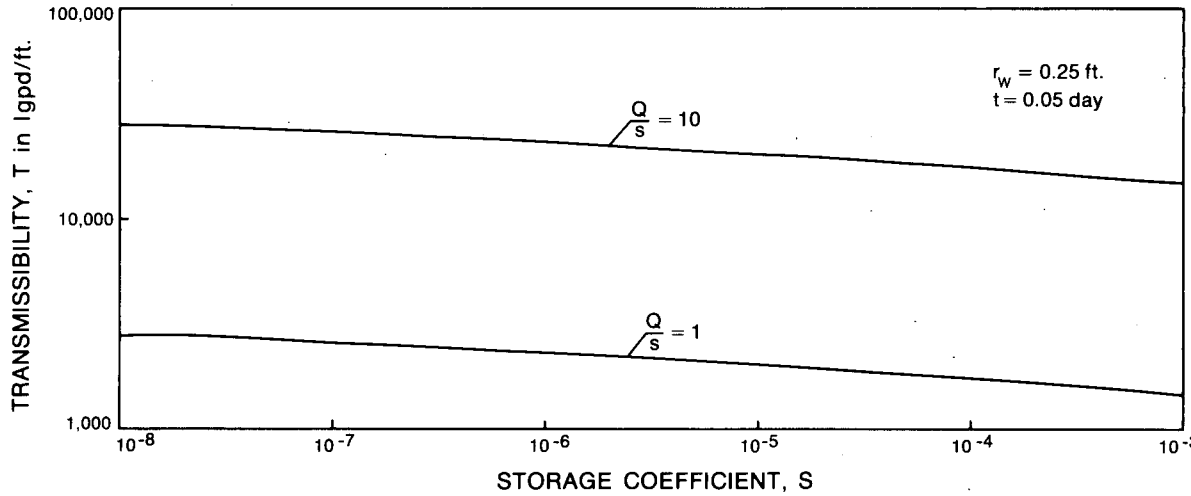

Figure 18. Theoretical relation between storage coefficient and coefficient of transmissibility.

Well Diameter and Pumping Time

The computed median well diameter, considered more representative than the average, was 6.25 inches for the overburdened wells and 5.95 inches for the bedrock wells (Figs. 19 and 20). The median pumping time for the overburden wells was 69 minutes (0.048 day), and for the bedrock wells, 72 minutes (0.050 day) (Figs. 21 and 22). The well radius and the pumping period in relation to the theoretical specific capacity are shown in Figures 23 and 24. Since the theoretical specific capacity is directly proportional to log r_w^2, and inversely proportional to log t, a large change in the radius of the well or the pumping period is accompanied by a comparatively small increase or decrease in specific capacity (Figs. 23 and 24). Since the specific capacity data cannot be compared unless they are adjusted to a common radius and pumping-period base, a well radius of 0.25 foot and a pumping period of 0.05 day or 72 minutes were used for all computations. In either case, the resulting errors amounted to less than 10 percent for 95 percent of the overburden and bedrock wells.

Partial Penetration, Well Loss, Geohydrologic Boundaries

Partial penetration, well loss and geohydrologic boundaries adversely affect the specific capacity. It is believed that the drawdown of most of the wells is particularly influenced by man-made factors. Domestic

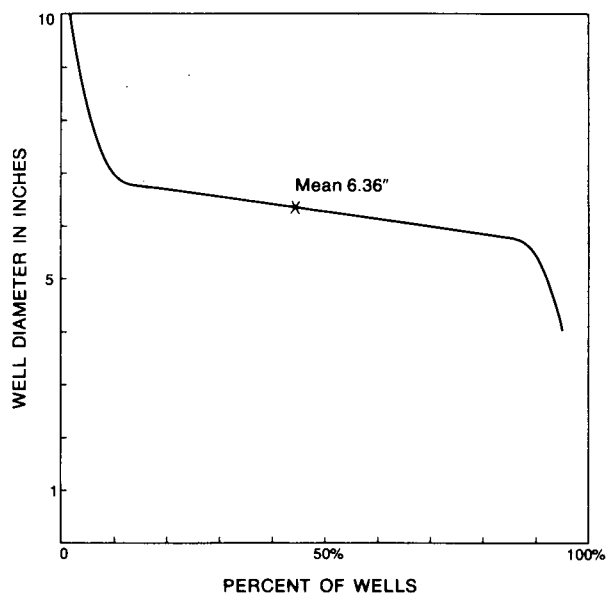

Figure 19. Frequency curve for the well diameter of overburden wells.

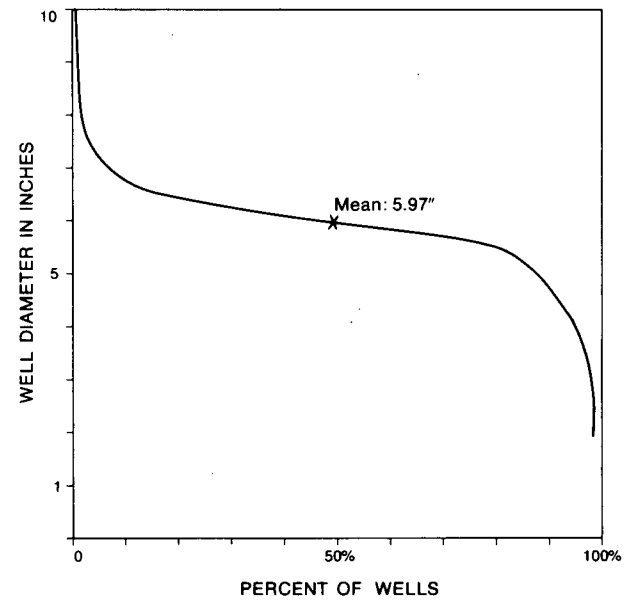

Figure 20. Frequency curve for the well diameter of bedrock wells.

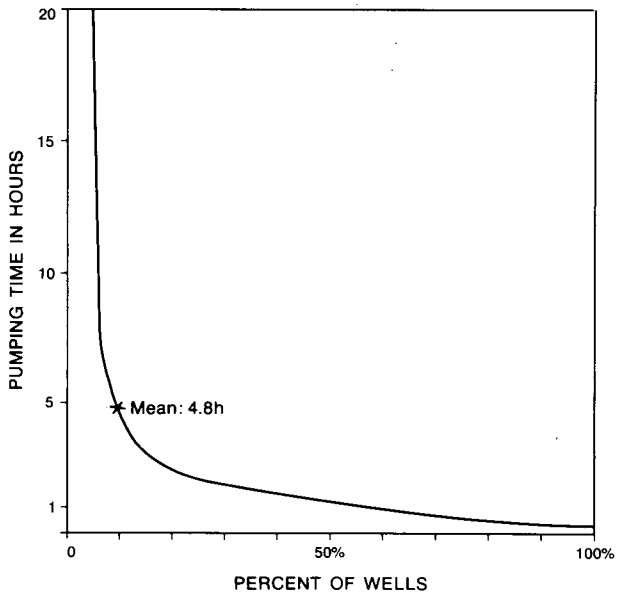

Figure 21. Frequency curve for the pumping time of overburden wells.

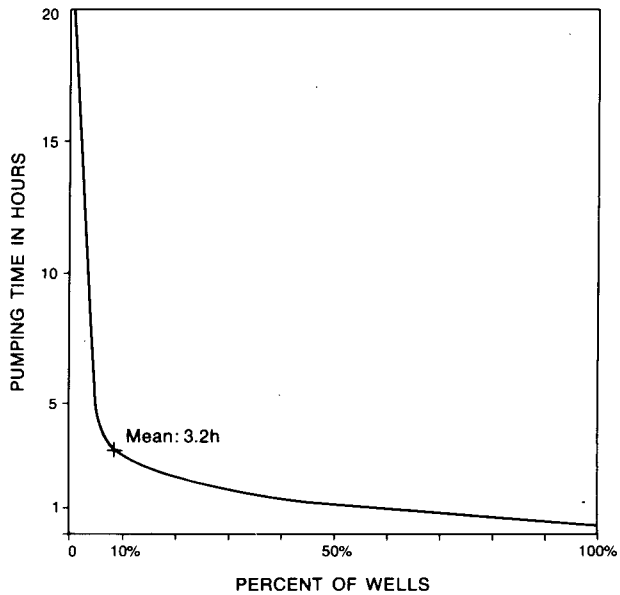

Figure 22. Frequency curve for the pumping time of bedrock wells.

water wells, which are represented for the most part, are usually drilled until sufficient water has been found without penetrating the full thickness of the aquifer. Well loss due to turbulent flow of the water entering the well might occur in industrial and municipal wells. Far more important, however, is the increased drawdown due to insufficient development, particularly in small wells. Based on the relation that the theoretical specific capacity does not change with the pumping rate, the approximate well loss may be computed by using the following equation (Jacob, 1946):

$$S_w = CQ^2 \qquad (7)$$

where S_w is the loss, in feet.
C is the well loss constant, in sec.^{2}/ft.^{5}
Q is the discharge, in cfs (the exponent for turbulent flow stands as square).

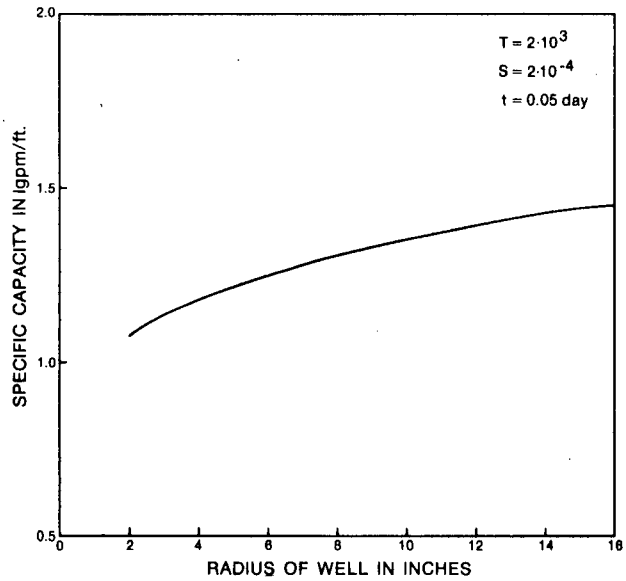

Figure 23. Theoretical relation between the specific capacity and the well radius.

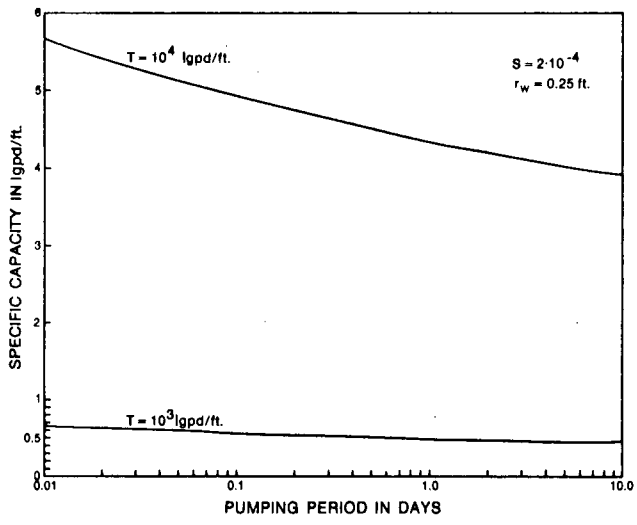

Figure 24. Theoretical relation between the specific capacity and the pumping period.

C is computed from a step-drawdown test after the following equation:

$$C = \frac{\left(\Delta s_n/\Delta Q_n\right) - \left(\Delta s_{n-1}/\Delta Q_{n-1}\right)}{\Delta Q_{n-1} + \Delta Q_n} \qquad (8)$$

where Δs is the increment of drawdown in the pumped well in feet produced by the increasing pumping rate ΔQ. Steps of any length of time may be used but must be the same for each Δs.

ΔQ is the increased pumping rate in cfs (1 cfs = 374 Igpm).

For illustration, the well losses of 12 municipal and industrial water wells in the Lake Ontario basin were computed. The values, which averaged 19 percent, ranged between 0 and over 100 percent.

Since most of the aquifers in the Lake Ontario basin are lenticular and bounded by till, geohydrological boundaries or interferences from other nearby wells often affect the yield, particularly of heavily pumped wells (Haefeli, 1970). On the other hand, it is known that drillers of domestic water wells are rather optimistic about the well production or, in some instances, do not report dry wells. For example, a survey conducted in Colorado (Snow, 1968a) revealed that the number of actual dry wells was a few times higher than reported and that the discharge rates were exaggerated for low capacity wells.

Since neither of the negative or positive factors can be ascertained, no adjustment of the specific capacity data was considered; however, a substantial error has to be taken into account.

Computation Method

Because of the mathematical difficulties encountered in applying the Theis equation when computing the coefficient of transmissibility from specific capacity data, several graphic solutions have been proposed, including that by Zeizel et al (1962), Theis and Brown (1963), Ogden (1965) and Hurr (1966). The method applied by Zeizel et al (1962) as well as Csallany and Walton (1963) was used to estimate the transmissibility of confined bedrock aquifers and was considered to be the most convenient one for this study. By assuming values for the pumping period, well radius and storage coefficient, the specific capacity is computed for different coefficients of transmissibility after equations (1) and (2) or (4). The calculated Q/s values versus T are plotted on log - log paper. From the resulting curve, T is estimated for various specific capacity data (Fig. 25). The following values were used to estimate T for all formations:

storage coefficent, $S = 2 \cdot 10^{-4}$
well radius, r_w = 0.25 foot
pumping period, t = 0.05 day or 72 minutes.

Estimating Permeability

Method

The coefficient of permeability of the aquifer (used synonymously with hydraulic conductivity), K, is defined as the rate of flow, Q, in imperial gallons per day passing through a cross-sectional area, A, of 1 square foot under a hydraulic gradient, I, of 1 foot per foot at the prevailing temperature of the water, which is Darcy's Law:

$$K = \frac{Q\,I}{A} \qquad (9)$$

For the sake of convenience, the term permeability is used thoughout this report rather than coefficient of permeability. The relation between the transmissibility and permeability is by definition:

$$K = \frac{T}{m} \qquad (10)$$

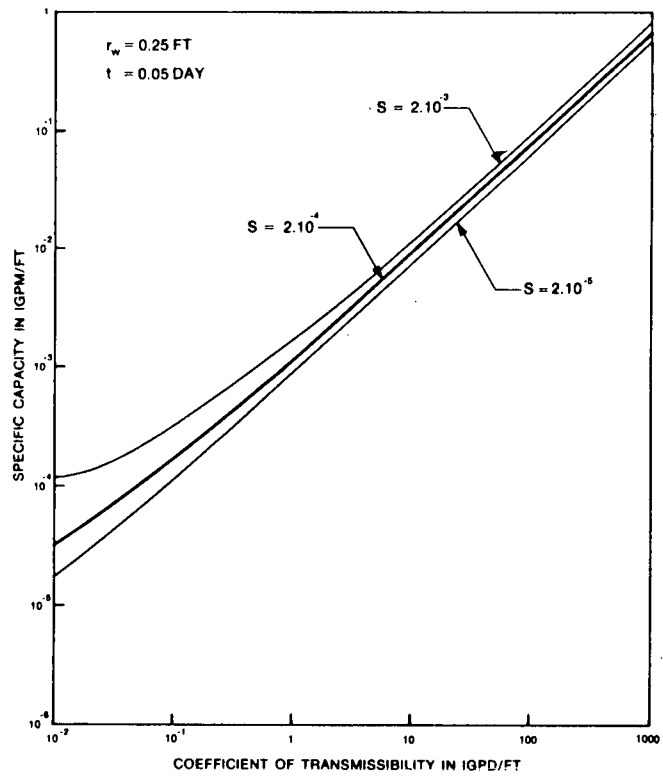

Figure 25. Theoretical relation between specific capacity and coefficient of transmissibility.

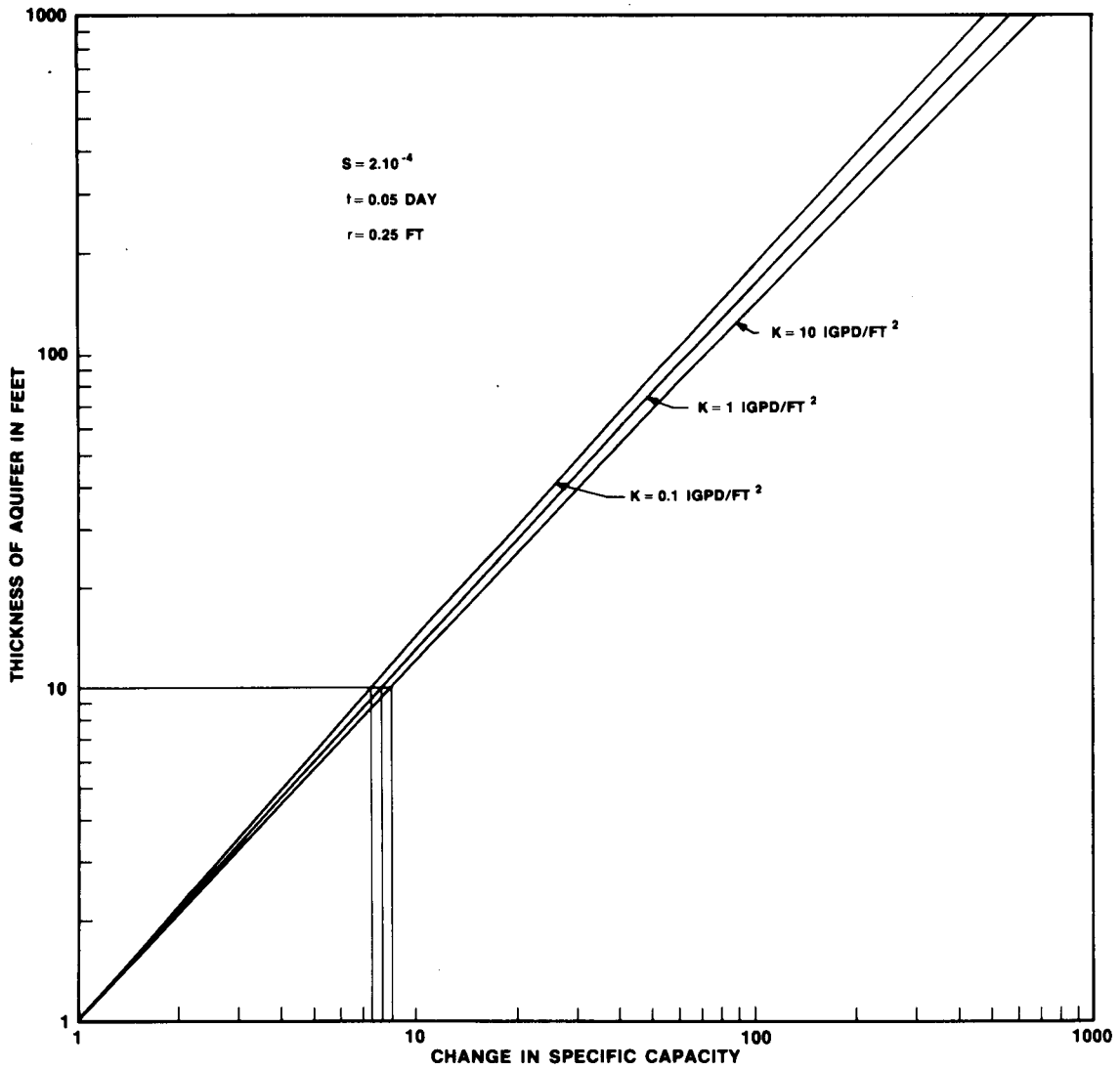

Figure 26. Theoretical relation between aquifer thickness and specific capacity.

where m is the thickness of the aquifer, in feet. For the numerical approach of this study and to compute the outflow, Q, through the bedrock, K is required rather than T.

The Dupuit or Thiem formula

$$K = \frac{Q \log_e r_2/r_1}{\pi(h_2^2 - h_1^2)} \qquad (11)$$

where r_1, r_2 are the distances of the observation wells from the pumped well,

h_1, h_2 are the drawdowns in the observation wells,

the only basic equation giving directly the coefficient of permeability from a pumping test, cannot be applied to our data because it requires steady state conditions and observation wells. T obtained from the Theis formula has therefore to be converted into K by dividing it by the aquifer thickness, m. However, there exists not only a groundwater flow through exploitable waterbearing formations or aquifers, but also through any strata of any permeability. Therefore, to obtain an average coefficient of permeability of an entire formation, the whole waterbearing section (and not only its most permeable part) has to be considered for the thickness, m. K, obtained by dividing T by the average well length (below static water level or piezometric surface) may be rather on the low side for the unconsolidated rock, because only the most permeable layers are screened and exploited; the results should be more accurate for the bedrock wells since they usually are constructed as open holes. However, since the permeability of the fractured bedrock is a function of bedrock depth (Figs. 13 and 14), it is more appropriate to

divide the bedrock into depth zones and to consider m as the average well length in each zone.

Overburden

The average permeabilities computed from specific capacity data are given in Table 2. The average hydraulic conductivity ranges from 7 to 65 Igpd/ft.^{2}. For comparison they are related to a permeability scale established by Todd (1959) and Castany (1967) (Fig. 35).

The permeability of the overburden is related to the bedrock geology. Although the Quaternary deposits of area A are overlaying the Queenston shale, which when weathered produces mainly argillaceous deposits, the permeability of the overburden remains rather high (Fig. 27). The reason for this phenomenon is the proximity of the Niagara Escarpment, where the exposed dolomite, limestone and sandstone formations are subject to continuous erosion. For area B, however, the fluvioglacial erosion of the Meaford-Dundas, Blue Moutain and Collingwood shale is manifested in the low permeability of the Quaternary deposits. In area C, most of the deep drift wells are situated in the western part of the area: erosion of the Collingwood formation to the north is still responsible for the low permeability of the drift below 50 feet in area C (Fig. 28). Moving east, the Quaternary deposits overlying limestone, crystalline rocks, sandstone, and dolomite between Trenton and Iroquois show a higher permeability, especially where they become very shallow.

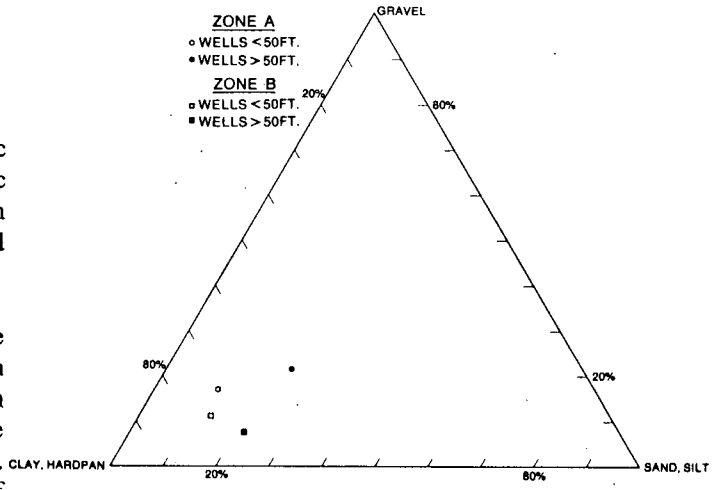

Figure 27. Lithology of overburden for the shorebelt area A and B (after drillers log).

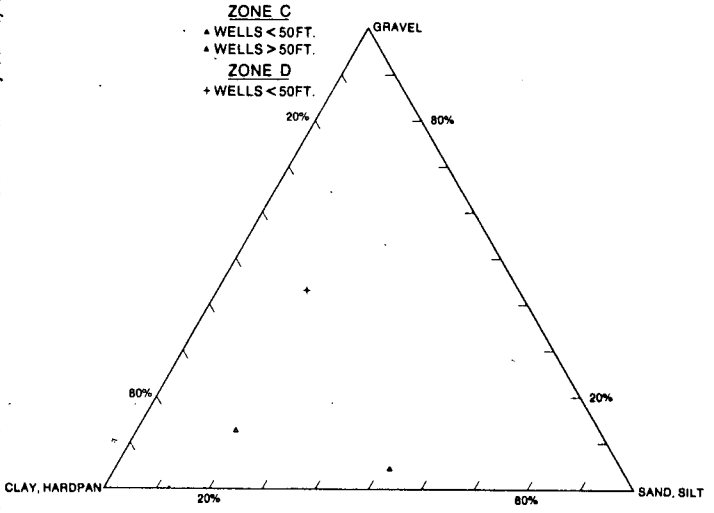

Figure 28. Lithology of overburden for the shorebelt area C and D (after drillers log).

Bedrock

The drawdown of wells drilled in fractured media may be affected by the heterogeneity of the rock. Since the open joints and fractures are not always interconnected, the flow to the pumped well may decrease sharply after the water of the surrounding fracture system is exploited, causing a boundary condition effect. Pumping tests conducted in crystalline rocks (Lewis and Burgy, 1964) indicate that well-flow equations derived for homogeneous, isotropic, granular media do not necessarily characterize the movement of water in fractured and jointed rock. However, if a pumping test is adapted to the hydraulic conditions of the rock by pumping an amount not exceeding the recharge capacity of the fracture system, the established pumping test equations may still be applicable. For example, several pumping tests conducted in limestone and dolomite aquifers in the Lake Ontario basin and vicinity were analyzed, some of them under leaky artesian conditions; the tests produced good drawdown curves (Appendix A), but it is very likely that many of the bedrock wells used for computation in this study were overpumped, thus giving erroneous drawdown data. Aware of these shortcomings, it is probable that the mean permeabilities obtained for the bedrock formations should nevertheless be of the right order of magnitude.

The plotting of the mean permeability versus the mean penetrated depth of each depth zone obviously produces the same kind of curve as for the specific capacity versus bedrock depth (Figs. 29 and 30). For comparison the part below 40 feet with the linear relationship is shown in Figure 31 for the different limestone and shale formations. Their means (Fig. 32) are compared with the permeability/-depth relationship of crystalline rocks of Colorado (Snow, 1968a). The equations of best fit for K in Igpd/ft.^{2} are:

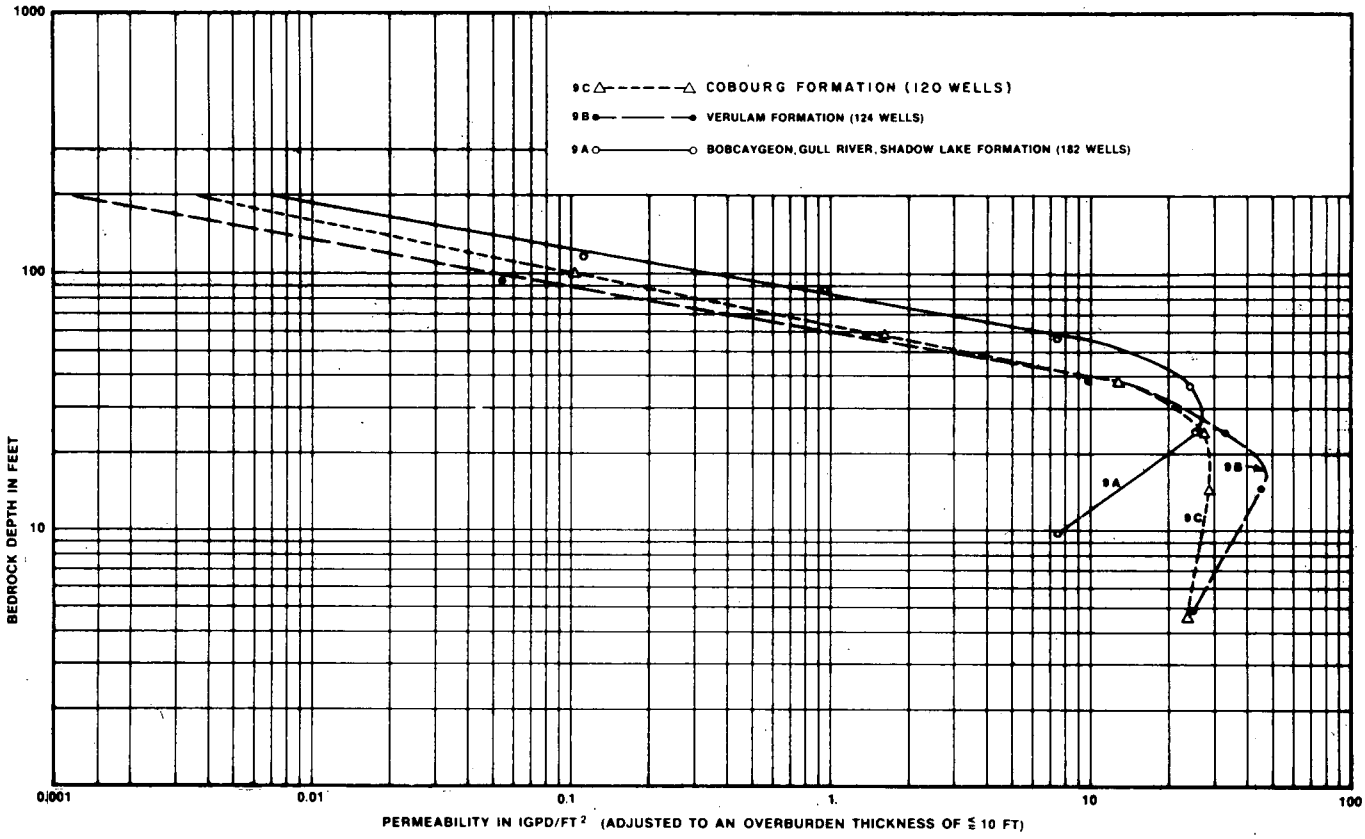

Figure 29. Average permeability in each depth zone versus the mean penetrated depth of each zone of the Trenton – Black River Group, Middle Ordovician (limestone).

Shale $\log K = -8.3 \log d + 14.90$

Limestone $\log K = -5.6 \log d + 10.08$

Crystalline rocks $\log K = -1.67 \log d + 3.28$

Of interest are the slopes of the curves for the different rock types. The rocks with low strength tend to close their fractures quicker with depth and rapidly become less permeable. This relationship was also observed by Davis and Turk (1964) by comparing low-grade metamorphic rocks with other crystalline rocks.

Permeability of Glacio-Lacustrine Lake Bottom Sediments

The major part of the bottom of Lake Ontario is covered as shown in Figure 33 with glacio-lacustrine clay. Since this material has a very low permeability, it controls the groundwater inflow in areas where the bedrock permeability exceeds that of the clay. Cores of the lake bottom taken under the direction of C.T.M. Lewis, Geol. Surv. of Canada, were obtained from the Canada Centre for Inland Waters. The four $2^1/_4$-inch ϕ cores originated from the four major subbasins of the lake (Table 8). The soft to semi-firm laminated glacio-lacustrine clay was covered in all four sampling areas with post-glacial, soft silt and clay.

The permeability of the samples was determined by means of consolidation tests. There is a range of permeabilities for each sample depending on the load applied to the sample (Fig. 34). This, of course, is because the permeability decreases as the soil becomes increasingly consolidated under higher loads. The most appropriate value of permeability for each particular sample is that corresponding most closely to the overburden pressure on the sample in its in-situ position (Fig. 34). Since the glacio-lacustrine clay generally has a thickness varying from 30 to 70 feet (C.T.M. Lewis, personal communication) and since more recent overlying sediments are of variable thickness, the overburden pressure at the bottom of the clay may generally be greater than two tons per square foot, thus giving a permeability of less than $1.7 \cdot 10^{-3}$ Igpd/ft.^{2} (10^{-7} cm/sec). Where the glacio-lacustrine clay is outcropping and wedging-out due to erosion, its maximum permeability would be in the order of $1.7 \cdot 10^{-1}$ to $1.7 \cdot 10^{-2}$ Igpd/ft.^{2} (10^{-5} to 10^{-6} cm/sec). As shown in Figure 34, the permeability decreases rapidly with increasing load up to 1 ton/sq. ft., which corresponds

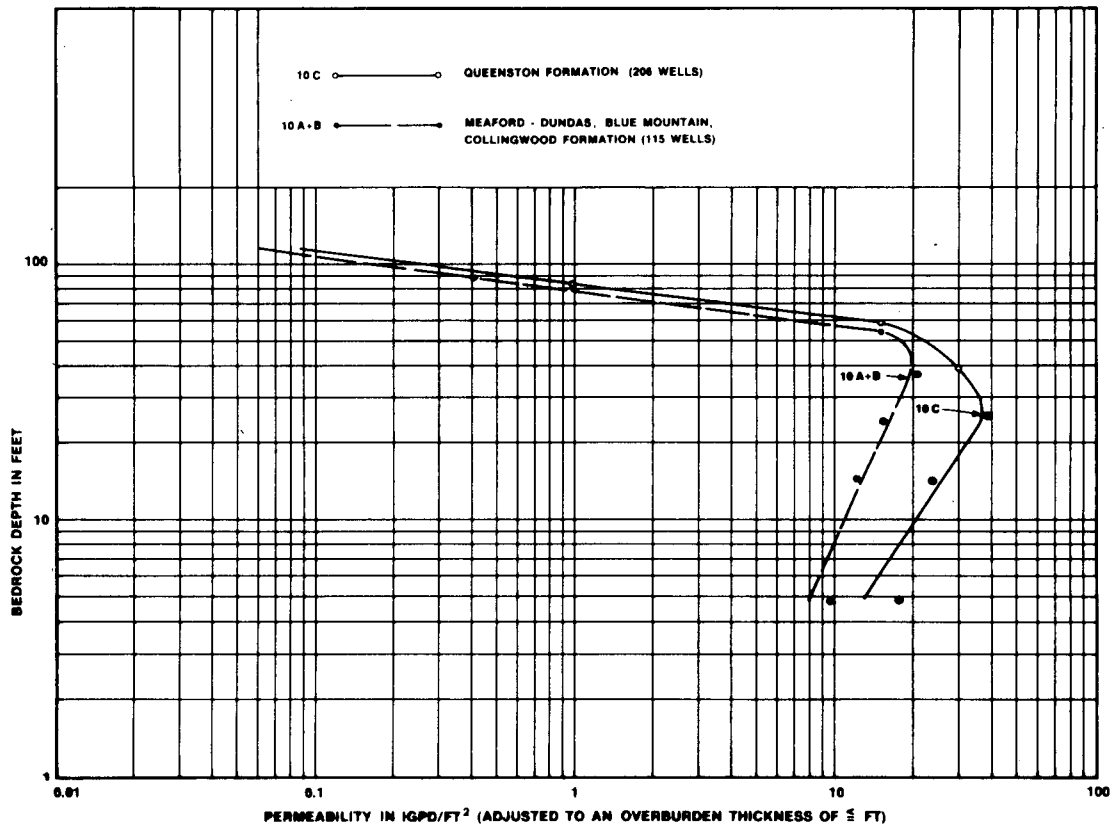

Figure 30. Average permeability in each depth zone versus the mean penetrated depth of each zone of the Upper Ordovician shale.

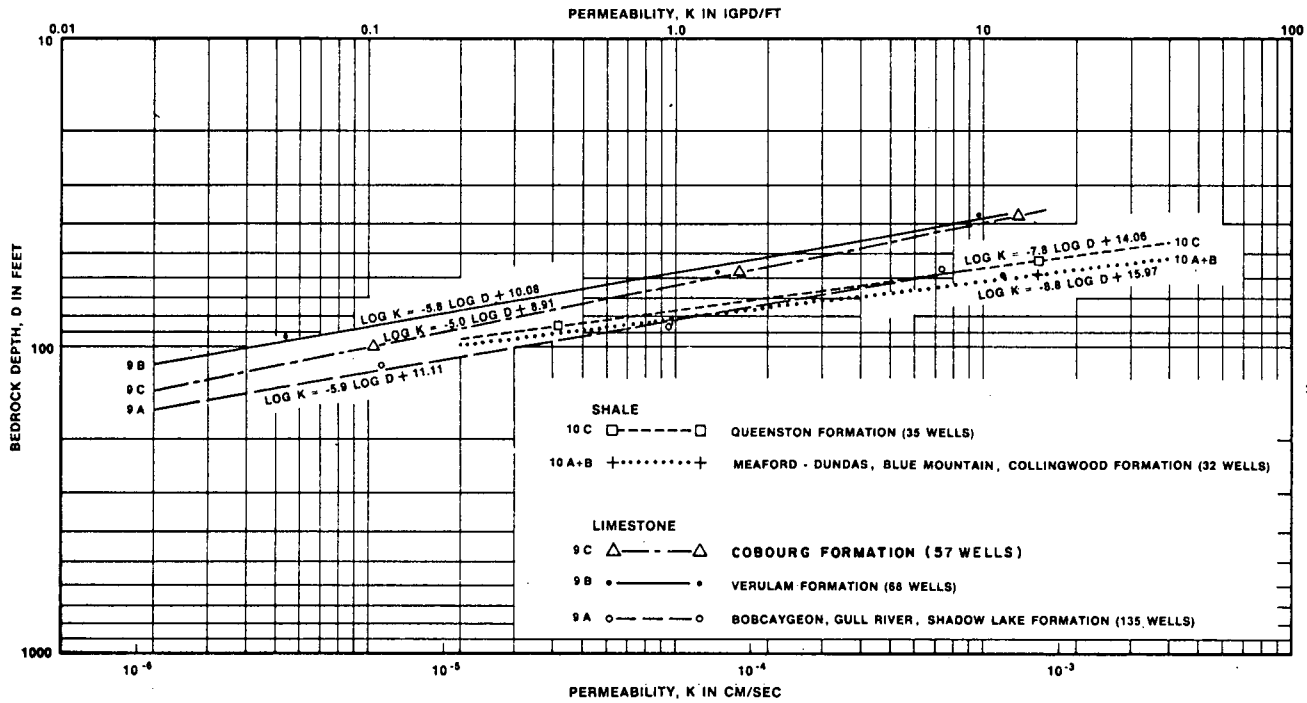

Figure 31. Mean permeability in each depth zone below 40 feet versus the mean penetrated depth of each zone of the bedrock formations bordering Lake Ontario (equations for K in Igpd/ft.²).

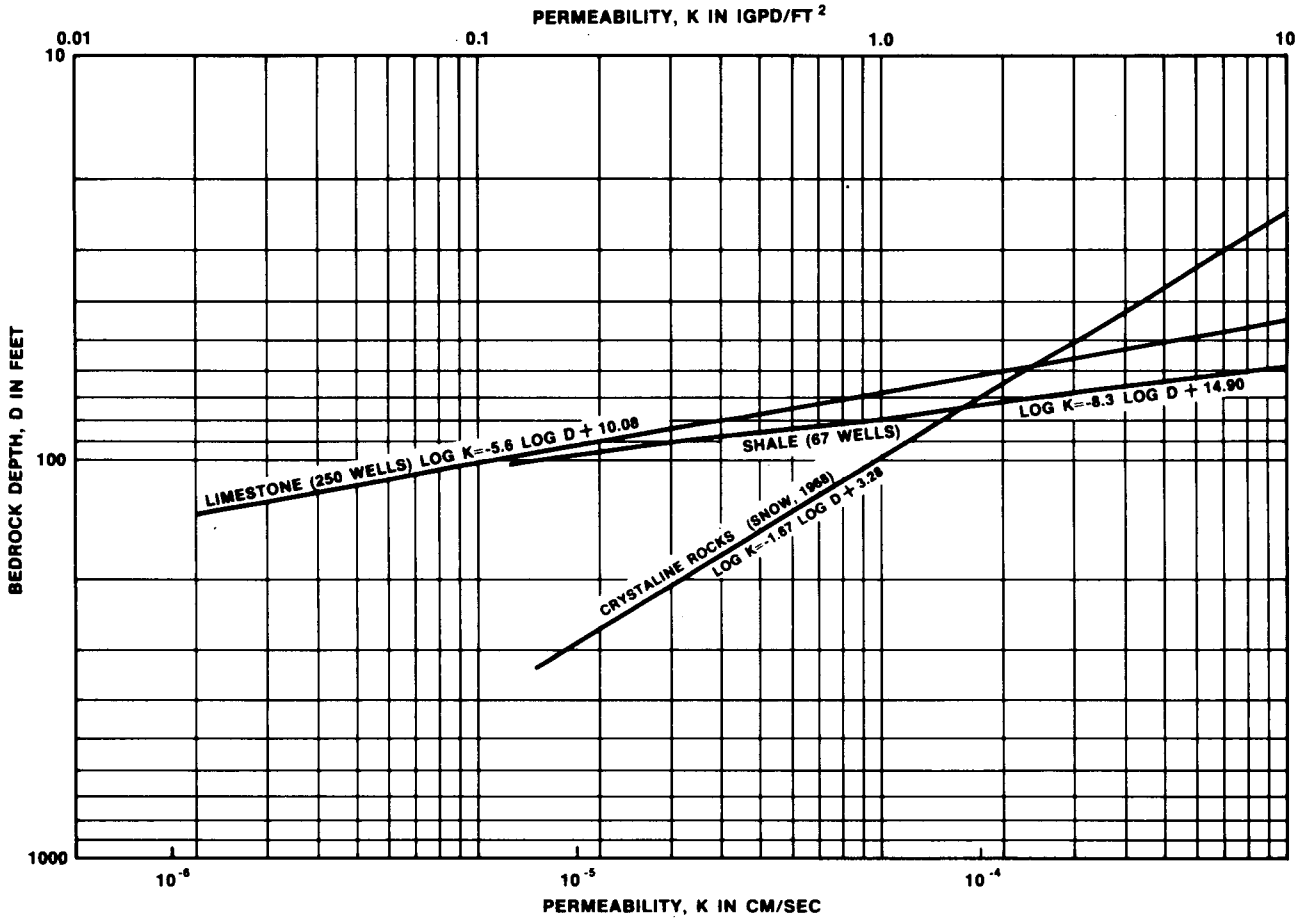

Figure 32. Bedrock depth versus mean permeability of shale and limestone bordering Lake Ontario (computed from pumping test data) compared with the permeability/depth relationship of crystalline rocks of Colorado (after D.T. Snow, 1968, computed from injection tests) (equations for K in Igpd/ft.²).

approximately to 20 feet of overburden (density: 1.6); from there it decreases more slowly and becomes probably not lower than 1.7 10^{-4} Igpd/ft.² (10^{-8} cm/sec). Figure 35 shows the general relationship between the main deposits and rocks, and the permeability in the Lake Ontario basin.

Vertical Permeability

Due to the predominantly horizontal groundwater flow during pumping tests, the permeabilities estimated from specific capacity data are considered to be horizontal permeabilities, K_h. Several analyses of aquifer tests under leaky artesian conditions were made to estimate the vertical permeability, K_v, of the Quaternary deposits. To determine K_v and the leakage coefficient, K_v/m', the equation developed by Hantush and Jacob (1955a) and described by Walton (1960) was used:

$$T = \frac{114.6 \cdot Q \cdot W(u_1 r/B)}{s} \qquad (12)$$

where: $$u = \frac{2242\, r^2\, S}{Tt} \qquad (13)$$

and $$\frac{r}{B} = \frac{r}{\sqrt{T/(K_v m')'}} \qquad (14)$$

or $$K_v = \frac{T\, m' \left(\frac{r}{B}\right)^2}{r^2} \qquad (15)$$

where s is the drawdown in observation well, in feet
r is the distance from the pumped well to the observation well, in feet
Q is the discharge, in Igpm
t is the time after pumping started, in minutes
T is the coefficient of transmissibility, in Igpd/ft.
S is the coefficient of storage of aquifer
K_v is the coefficient of vertical permeability of confining bed, in Igpd/ft.²
m' is the thickness of confining bed through which leakage occurs, in feet.

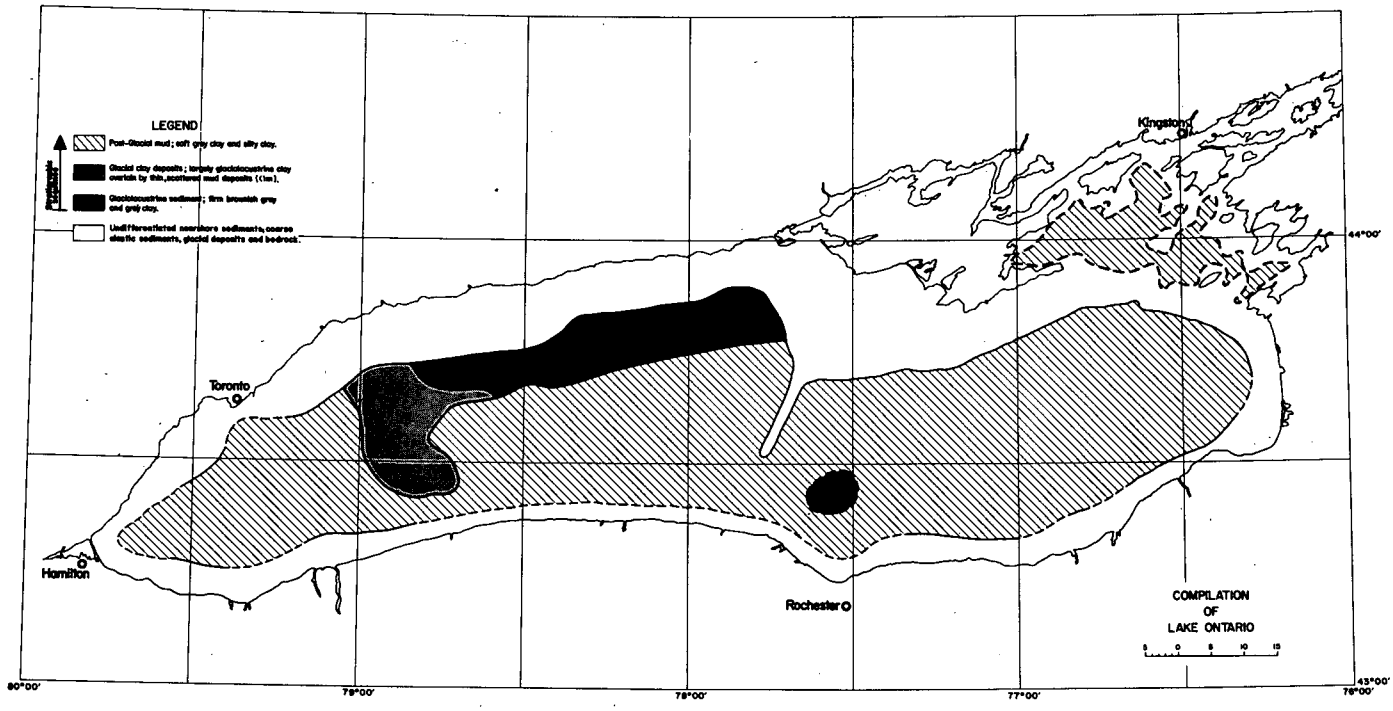

Figure 33. Stratigraphy of Quaternary lake bottom sediments (after C.T.M. Lewis, Geological Survey of Canada, personal communication).

Table 8. Data of the Lake Ontario Glacio-Lacustrine Sediment Core Samples (From C.F.M. Lewis, Geol. Surv. of Canada, 1970, personal communication).

CORE DESIGNATION Cruise	Station	Core No.	LOCATION Area	Latitude	Longitude	Water Depth (Echo Sounder)	Sampling Date	Total Core Length (cm)	Position of Sample below Top of Core (cm)	Material of Sample
68 - 0 - 17	1	2	Western Lake Ontario, Niagara Basin	43°24.0′N	79°28.6′W	322	Sept. 1968	1412	734 - 769	Soft to semi-firm laminated glacio-lacustrine clay.
68 - 0 - 17	7 =	1	Central Lake Ontario, Mississauga Basin	43°40.0′N	78°22.3′W	470	Sept. 1968	1113	1060 - 1095	
69 - 0 - 16	E30	PC1	Eastern Lake Ontario, Rochester Basin	43°30.4′N	76°54.0′W	666	Oct. 1969	1258	1211 - 1236	
69 - 0 - 16	PC1	1	Northeastern Lake Ontario Kingston Basin	43°59′45″N	76°51′03″W	106	Oct. 1969	N600	509 - 539	

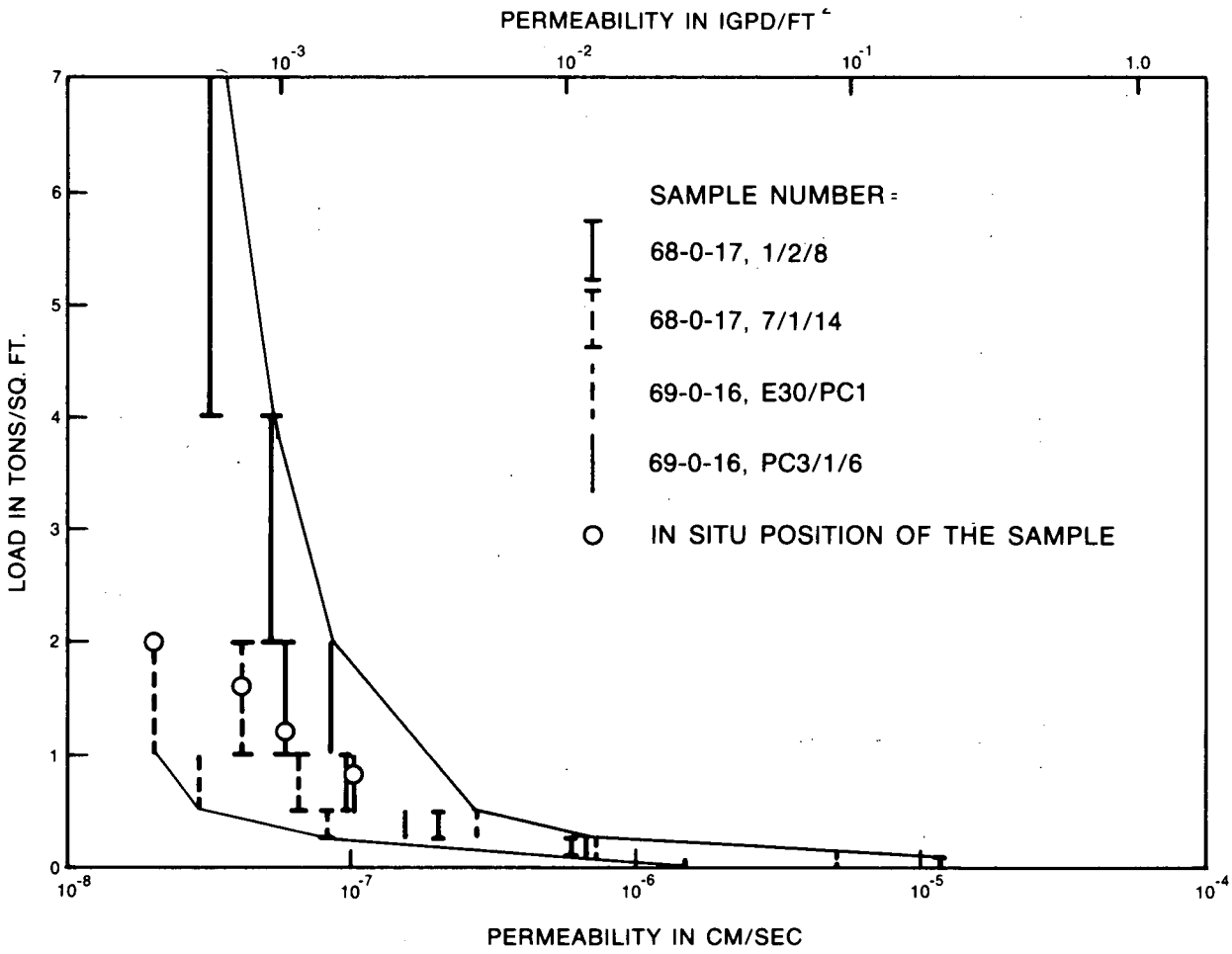

Figure 34. Permeability of glacio-lacustrine clay of the lake bottom determined by means of consolidation tests for various loads.

$W(u_1\ r/B)$ is the well function for leaky artesian aquifers [values may be obtained from tables by Hantush (1956) or Walton (1962)].

The data were computed from pumping tests carried out between 1954 and 1969 in the Lake Ontario basin and its western vicinity. The drift or bedrock (dolomite, limestone) aquifers were overlain in all cases by rather low permeable Quaternary deposits through which leakage from shallow aquifers or surface water occurred. The drawdown curves of the observation wells with the computed hydraulic parameters are enclosed in Appendix A. The coefficients of leakage and vertical permeability are listed in Table 9. The vertical permeability, varying between 0.041 and 6.9 Igpd/ft.^{2}, shows a rather good correspondence with the lithology of the confining bed. However, in this connection, it should be pointed out that the permeability is very sensitive to the content of clay minerals. The presence of two percent of illite in an otherwise clean sand can lower the permeability by two orders of magnitude and the presence of two percent montmorillomite by four orders of magnitude (after Freeze, 1969b), from Lovas (1963). Nevertheless, the relationship between the amount of clay and silt (after drillers logs) and the vertical permeability (Fig. 36) was used to estimate K_v of the glacial deposits along Lake Ontario. The resulting approximate coefficients of vertical permeability and permeability ratios are presented in Table 14.

For comparison, values of vertical hydraulic conductivity for till deposits in Ohio, Illinois and South Dakota (Norris, 1962) and in Illinois (Walton, 1965) are given in Figure 37 and Table 10. They are of the same order of magnitude but slightly lower than those values obtained for the till of

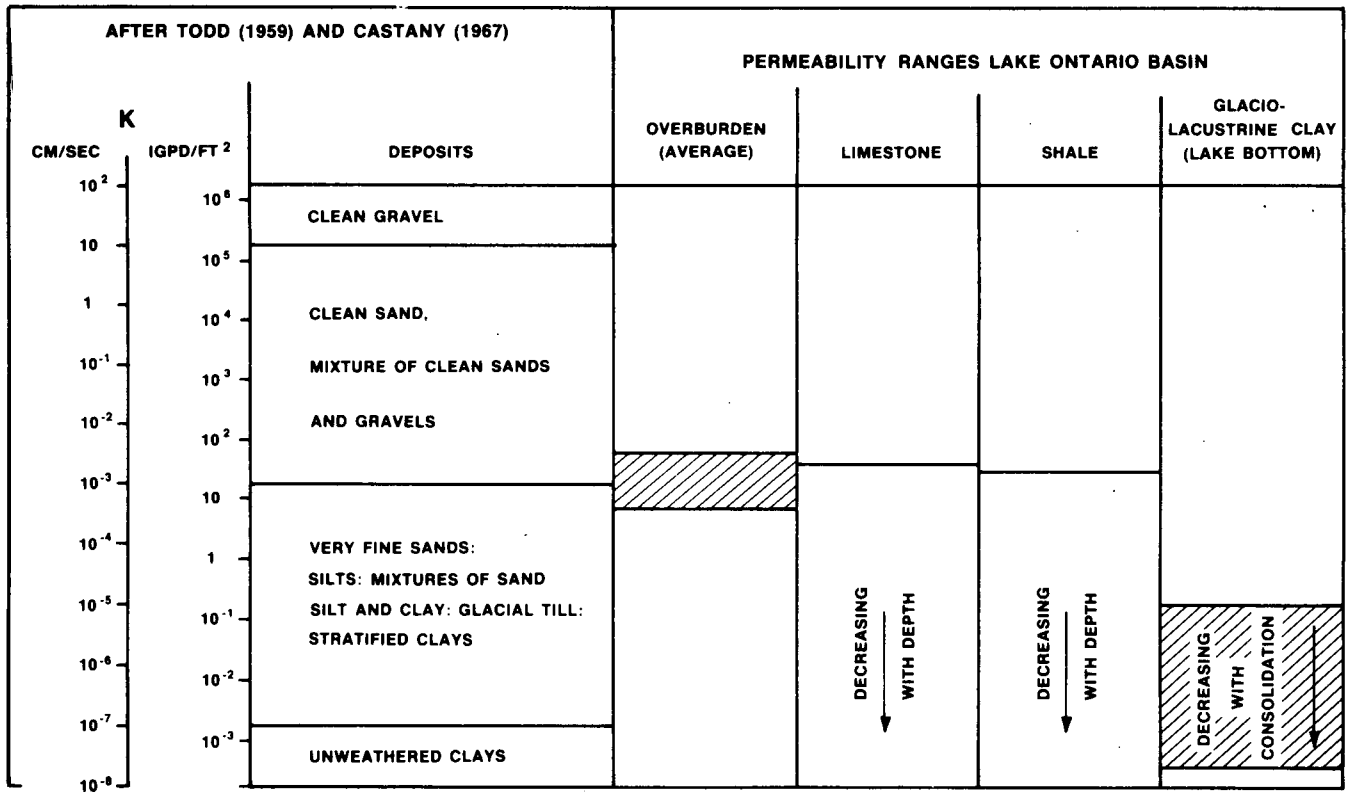

Figure 35. General relation between the main soil and rock types and the permeability.

Table 9. Coefficients of leakage and vertical permeability.

Location	K_v (Igpd/ft.^{2})	m'	K_v/m' (Igpd/ft.^{3})	General Lithology of confining layers (after driller's log)
Markham	5.3	60	$8.8 \cdot 10^{-2}$	sand and gravel with silt and clay.
Milton	3.7	44	$8.4 \cdot 10^{-2}$	sand and gravel with considerable clay and some silt.
Uxbridge	2.4	130	$1.8 \cdot 10^{-2}$	sand with considerable clay and gravel and some silt.
Stayner	1.39 (mean)	76	$1.8 \cdot 10^{-3}$	clay and gravel with considerable sand and silt.
Orono	0.17	30	$5.7 \cdot 10^{-3}$	clay with considerable gravel.
St. Mary's	0.21	15	$1.4 \cdot 10^{-2}$	clay with considerable gravel.
Preston	0.11	62	$1.8 \cdot 10^{-3}$	clay and silt with sand and some gravel.
Guelph	0.074	17	$4.3 \cdot 10^{-3}$	clay with silt, sand and gravel.
Agincourt	0.041	50	$8.2 \cdot 10^{-4}$	clay with silt, sand and gravel.

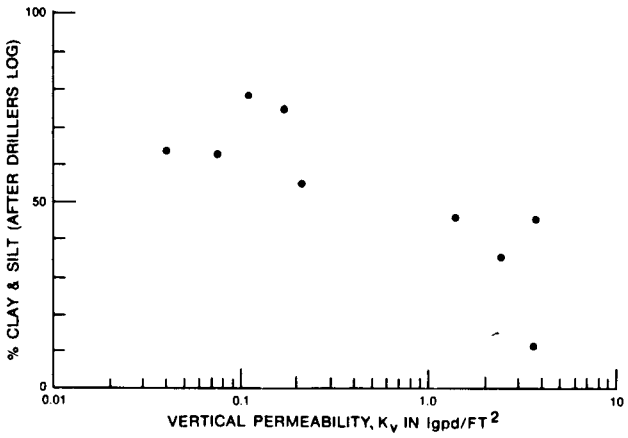

Figure 36. Vertical permeability versus clay and silt content (after drillers log) of confining bed.

southern Ontario. R.A. Freeze (1969c) used the same method to calculate K_v values of 4.1 and 1.2 Igpd/ft.^{2} for confining till beds in Gravelbourg, Saskatchewan. For the numerical analysis of the groundwater flow of the same area, a K_h/K_v ratio of 100:1 used on a trial and error approach, produced a potential pattern almost identical to the field results (Freeze, 1969a).

Unless the direction, aperture, and spacing of the bedrock fractures are measured and carefully analysed, the K_h/K_v anisotropy for fractured bedrock is very difficult to estimate on a regional scale. The analysis of a pumping test carried out at St. Marys, Ontario, (Appendix A Fig. 82) produced a vertical permeability of $2.6 \cdot 10^{-2}$ Igpd/ft.^{2} for a confining limestone bed. For comparison, Walton (1965) obtained for a dolomite shale in Illinois a vertical permeability of $5 \cdot 10^{-5}$ USgpd/ft.^{2}. Since the fracture

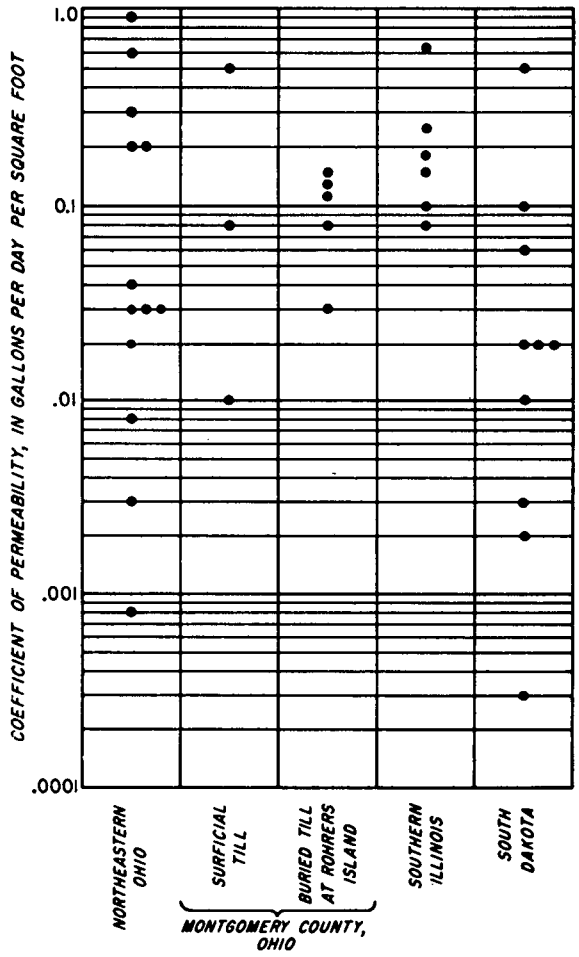

Figure 37. Coefficient of permeability per square foot for till deposits in Ohio, Illinois and South Dakota (from Norris, 1962).

Table 10. Coefficients of leakage and vertical permeability of till deposits in Illinois (from Walton, 1965).

Lithology	K_v/m' (USgpd/cu. ft.) Range	K_v (USgpd/sq. ft.) Range	Average
Drift, sand and gravel, some clay and silt	$3.4 \cdot 10^{-2}$ - $2.3 \cdot 10^{-1}$	1.02 - 1.60	1.31
Drift, clay and silt with considerable sand and gravel	$6.1 \cdot 10^{-3}$ - $5.2 \cdot 10^{-2}$	0.10 - 0.63	0.25
Drift, clay and silt with some sand and gravel	$8.3 \cdot 10^{-5}$ - $5.0 \cdot 10^{-3}$	0.01 - 0.08	0.03
Drift, clay and silt with some sand and gravel and dolomite	$4.5 \cdot 10^{-5}$ - $3.2 \cdot 10^{-4}$	0.005 - 0.011	0.008
Drift, clay and silt with some sand and gravel and shaly dolomite	$5.0 \cdot 10^{-5}$	0.005	0.005

system is changing with area and depth, these data are certainly not representative. Because of the lack of data, it was assumed, therefore, that the near-vertical fracture system and horizontal bedding equally control the groundwater flow in the bedrock, thus giving $K_h = K_v$.

CROSS-SECTIONAL AREA

According to Darcy's Law (equation 9) the amount of groundwater seeping through the lake bottom was evaluated by introducing a cross-sectional area, A, along the shoreline. A geological profile of approximately 300 miles was constructed along the Canadian shore of Lake Ontario, from the outlet of the Niagara River to Iroquois. The bottom of the profile varied between 200 feet below and 150 feet above sea level depending on the depths of such features as the lake, the St. Lawrence River, the buried bedrock channels, and the extension of glacio-lacustrine clay of the lake bottom. The boundaries of the bedrock formations were mainly constructed after various publications of Sanford, Liberty and Caley (reference list) as well as Wynne-Edwards (1962, 1963) and Wilson (1942). Since the structure of the bedrock is very uniform and monotonous (Chapter 2) the determination of the geological boundaries did not cause any problems, except for small parts between Kingston and Brockville where the irregular surface of the Precambrian causes a patchy distribution of various sedimentary formations. However, since the profile did not exceed a depth of 100 feet in this particular area, boundaries were extrapolated from bedrock surface maps without large errors.

Much attention was given to the determination of the bedrock surface along the shore, particularly in the central part where buried channels were expected. A reconnaissance field survey of the geology and examination of detailed geological and pedeological maps and water well records did not show any remarkable buried bedrock valleys east of Trenton except for three wells, 50 to 70 feet deep, west of Kingston, at Cataraqui, Parrot Bay, and 2 miles west of Cardinal. In fact, the bedrock to Iroquois is outcropping almost continuously along the shore or is covered by only a few feet of soil. The largest buried bedrock surface relief is encountered between Brighton and Port Credit. An excellent bedrock contour map of the Metropolitan Toronto area by Rogers, Ostry and Karrow (1961) based on bedrock wells and a geophysical survey along the Scarborough Bluffs by Hobson (1970) revealed bedrock valleys exceeding a depth of 150 feet below lake level (Plate III). Since water wells also indicated an irregular drift thickness of considerable depth east of Scarborough, an extensive hammer seismic survey extending approximately 75 miles to Trenton and involving some 700 locations along the shore, was performed during the summer of 1969 by the Geological Survey of Canada under the direction of G.D. Hobson, with the assistance of H. MacAulay and R. Gagné. Being of multipurpose value, especially for the development of groundwater resources, the profile shows a very irregular bedrock surface with few valleys deeper than 100 feet below lake level (Plates IV and V). Bedrock shallower than 30 feet below lake level was found for about 75 percent of the profile. Generally, the overburden in the direction of Toronto becomes thicker and the channels more frequent and deeper. They tend to be narrow, commonly between $^1/_4$- and $^3/_4$-mile wide. Because the shore was not accessible in a few areas, some measurements had to be extrapolated from inland. To verify that the bedrock surface along the shore did not merely represent the shelf below cliffs of the early Lake Ontario or Lake Iroquois, some seismic profiles were laid perpendicular to the shore or parallel, further inland. They revealed that, towards the lake, the bedrock surface decreases in elevation by a slope of approximately 0.008 - 0.01, which corresponds to the inclination of the land surface. Moving inland for more than two miles, the Quaternary deposits became generally thicker as indicated by water wells. Bedrock surface maps by Karrow (1962) and water wells show no sign of any significant valleys between Port Credit and Burlington except for the recent channels of the Credit River, Oakville and Bronte Creek. The shale is mostly outcropping, or is covered by shallow soil. The Dundas buried valley, exceeding 200 feet below sea level and representing the deepest depression in the bedrock, runs WSW through Hamilton Harbour. Its deepest point has not yet been revealed (Chapter 6). The Quaternary deposits between Hamilton and the Fifty Mile Point are generally between 20- and 60-feet thick; from Fifty Mile Point to Beamsville, the drift is shallower and outcrops are found in the area west of Grimsby. East of Vineland, as far as Niagara-on-the-Lake, the bedrock topography again seems to be more accentuated. Water wells and geophysical surveys (Hobson and Terasmae, 1969; Hobson, personal communication) furnish evidence of a wide, buried valley approximately 80- to 100-feet deep at Jordan Harbour and narrow channels 60- to 80-feet deep at St. Catharines (Lakeside Park) in the vicinity of Four Mile Point and west of Niagara-on-the-Lake (Mississauga Beach).

HYDRAULIC GRADIENT

The difference in hydraulic head, h, divided by the distance, l, along the flow path is the hydraulic gradient:

$$I = \frac{\Delta h}{\Delta l} \qquad (16)$$

The slope of the water table or piezometric surface can be assumed to be a measure of the hydraulic gradient under which groundwater movement takes place.

Since the quantity of groundwater flow is a function of the permeability and the hydraulic gradient, both parameters had to be determined from the same area, as was indicated previously. The shorebelt, four kilometers wide, was divided into ten different areas according to the morphology and geology (Fig. 11), (Table 11), and the mean hydraulic gradient was computed in each of them using a total of some 1500 water wells.

The slope of the water table (piezometric surface) near the shore is probably parabolic (Castany, 1967, p. 425), and to avoid this local anomaly, the water-table head, between one and three kilometers from shore, was used to estimate the horizontal hydraulic gradient of the shorebelt (Fig. 38).

Note the similarity between the groundwater levels and the surface elevations. The mean depth below the land surface for all the wells located 2 to 4 km. from the shore is 13.7 feet, and for the wells located 0 to 2 km. from the shore is 14.8 feet. The hydraulic gradient in the ten areas varied between 0.0056 and 0.0154, or 18.2 ft./km. and 50.6 ft./km. (Table 11).

Having estimated values for K and I, the velocity can be estimated by Darcy's Law, namely:

$$V = K \cdot I \qquad (17)$$

Where V is the groundwater velocity.

Table 11. Hydraulic gradient of the Shorebelt Area

Area	County	Mean Water Level below Surface at		Mean Surface Elevation at		Difference in Elevation per Km		Hydraulic Gradient
		1 Km	3 Km	1 Km	3 Km			
		(feet)	(feet)	(feet)	(feet)	(feet)	(Meters)	
A1	Wentworth, Lincoln	14.27	14.17	262.10	298.56	18.23	5.6	0.0056
A2	Halton	11.30	11.30	293.45	378.21	42.38	12.9	0.012
B1	Peel, Toronto W	10.33	10.90	269.69	240.06	35.19	10.7	0.0107
B2	Toronto E, Ontario W	16.14	15.77	286.48	399.22	36.37	11.1	0.0111
B3	Ontario E	17.27	16.53	253.75	303.49	24.87	7.6	0.0076
C1	Durham	16.19	17.94	303.00	404.12	50.56	15.4	0.0154
C2	Northumberland	13.84	11.88	280.13	399.26	59.57	18.2	0.0182
D	Hastings, Lennox & Addington, Frontenac	14.39	13.27	257.74	297.98	20.12	6.5	0.0065
E1	Leeds	19.6	16.2	283.1	326.4	23.35	7.1	0.0071
E2	Grenville	17.13	14.44	282.9	329.5	24.60	7.5	0.0075

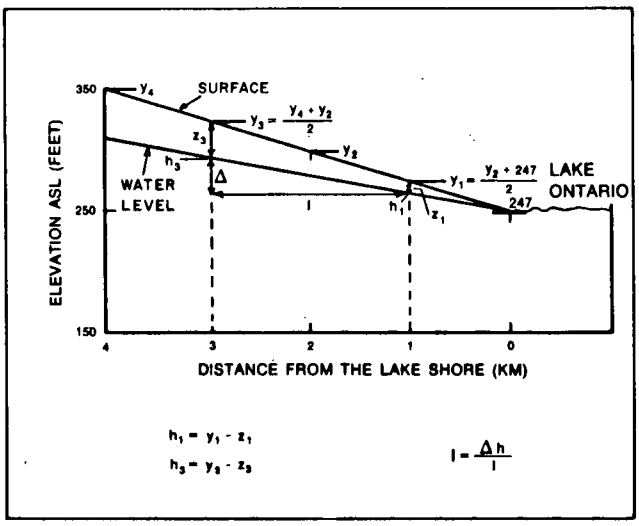

Figure 38. Computation of the mean hydraulic gradient in the shorebelt.

Rather low velocity values ranging between 0.1 and 0.01 ft./day in the drift and less than 0.1 ft./day in the bedrock have been determined by this method.

GROUNDWATER INFLOW

According to the different hydraulic gradients, and the permeability values depending on overburden thickness and bedrock depth, the cross-sectional area was divided into small units (Fig. 39). The sub-areas were calculated with an integrating planimeter and the groundwater flow through each sub-area was computed using Darcy's equation:

$$Q = K I A \qquad (18)$$

The sum was computed separately for the overburden and bedrock for various depths for every hydraulic gradient area and was listed in Table 12. Due to the rapidly decreasing permeability of the bedrock with depth, it soon became

Table 12. Groundwater inflow into Lake Ontario by Counties,computed using the Classic Method.

County	Units ft.	Overburden ⩽50	Overburden >50	Overburden Total	Bedrock 0 - 50	Bedrock 50 - 100	Bedrock 100 - 150	Bedrock Total	Totals
Lincoln Wentworth	Area $ft.^2$	$6.547 \cdot 10^6$	$1.717 \cdot 10^6$	$8.264 \cdot 10^6$	$9.806 \cdot 10^6$	$7.578 \cdot 10^6$	$4.865 \cdot 10^6$	$22.249 \cdot 10^6$	$30.513 \cdot 10^6$
	Q Igpd	$3.031 \cdot 10^6$	$5.30 \cdot 10^6$	$3.612 \cdot 10^6$	$1.011 \cdot 10^6$	$1.59 \cdot 10^6$	$1.3 \cdot 10^6$	$1.170 \cdot 10^6$	$4.783 \cdot 10^6$
	Q c.f.s.	5.6346	1.0787	7.7133	1.8795	0.2943	0.0024	2.1762	9.8895
Halton	Area $ft.^2$	$7.30 \cdot 10^4$		$7.30 \cdot 10^4$	$3.832 \cdot 10^6$	$3.400 \cdot 10^6$	$3.340 \cdot 10^6$	$10.572 \cdot 10^6$	$10.645 \cdot 10^6$
	Q Igpd	$2.82 \cdot 10^4$		$2.82 \cdot 10^4$	$1.063 \cdot 10^6$	$1.911 \cdot 10^5$	$2.22 \cdot 10^3$	$1.256 \cdot 10^6$	$1.284 \cdot 10^6$
	Q c.f.s.	$5.23 \cdot 10^{-2}$		$5.23 \cdot 10^{-2}$	1.9682	0.3540	$4.1 \cdot 10^{-3}$	2.3263	2.3786
Peel	Area ft^2	$2.58 \cdot 10^5$	$1.158 \cdot 10^6$	$1.416 \cdot 10^6$	$5.600 \cdot 10^6$	$5.600 \cdot 10^6$	$5.600 \cdot 10^6$	$16.800 \cdot 10^6$	$18.216 \cdot 10^6$
	Q Igpd	$1.94 \cdot 10^4$	$9.91 \cdot 10^4$	$1.185 \cdot 10^5$	$8.210 \cdot 10^5$	$2.138 \cdot 10^5$	$2.66 \cdot 10^3$	$1.037 \cdot 10^6$	$1.156 \cdot 10^6$
	Q c.f.s.	0.0358	0.1836	0.2194	1.5204	0.3959	0.0049	1.9212	2.1406
York & Ontario west of Frenchman Bay	Area $ft.^2$	$3.911 \cdot 10^6$	$9.38 \cdot 10^5$	$4.849 \cdot 10^6$	$4.753 \cdot 10^6$	$4.753 \cdot 10^6$	$4.753 \cdot 10^6$	$14.259 \cdot 10^6$	$19.108 \cdot 10^6$
	Q Igpd	$2.52 \cdot 10^5$	$4.99 \cdot 10^4$	$3.02 \cdot 10^5$	$2.56 \cdot 10^5$	$5.98 \cdot 10^4$	$8.2 \cdot 10^2$	$3.17 \cdot 10^5$	$6.18 \cdot 10^5$
	Q c.f.s.	0.4664	0.0924	0.5588	0.4740	0.1107	0.0015	0.5862	1.1450
Ontario east of Frenchman Bay	Area $ft.^2$	$3.208 \cdot 10^6$	$7.20 \cdot 10^5$	$3.928 \cdot 10^6$	$4.125 \cdot 10^6$	$4.125 \cdot 10^6$	$4.125 \cdot 10^6$	$12.375 \cdot 10^6$	$16.303 \cdot 10^6$
	Q Igpd	$1.95 \cdot 10^5$	$3.83 \cdot 10^4$	$2.33 \cdot 10^5$	$4.63 \cdot 10^5$	$3.87 \cdot 10^4$	$1.1 \cdot 10^3$	$5.02 \cdot 10^5$	$7.36 \cdot 10^5$
	Q c.f.s.	0.3613	0.0709	0.4322	0.8568	0.0717	0.0020	0.9305	1.3627
Durham	Area $ft.^2$	$4.231 \cdot 10^6$	$4.69 \cdot 10^5$	$4.700 \cdot 10^6$	$7.076 \cdot 10^6$	$7.076 \cdot 10^6$	$7.076 \cdot 10^6$	$21.228 \cdot 10^6$	$25.428 \cdot 10^6$
	Q Igpd	$1.427 \cdot 10^6$	$5.01 \cdot 10^4$	$1.478 \cdot 10^6$	$2.006 \cdot 10^6$	$6.59 \cdot 10^4$	$3.3 \cdot 10^3$	$2.075 \cdot 10^6$	$3.553 \cdot 10^6$
	Q c.f.s.	2.6435	0.0927	2.7362	3.7145	0.1221	0.0061	3.8427	6.5789
Northumberland	Area $ft.^2$	$2.025 \cdot 10^6$		$2.025 \cdot 10^6$	$8.828 \cdot 10^6$	$6.037 \cdot 10^6$	$7.502 \cdot 10^6$	$22.367 \cdot 10^6$	$24.392 \cdot 10^6$
	Q Igpd	$8.48 \cdot 10^5$		$8.48 \cdot 10^5$	$2.780 \cdot 10^6$	$2.88 \cdot 10^4$	$2.4 \cdot 10^3$	$2.811 \cdot 10^6$	$3.658 \cdot 10^6$
	Q c.f.s.	1.5696		1.5696	5.1473	0.0534	0.0045	5.2052	6.7748

Table 12. Groundwater inflow into Lake Ontario by Counties computed using the Classic Method. (Cont'd)

County	Units ft.	Overburden <50	Overburden >50	Overburden Total	Bedrock 0-50	Bedrock 50-100	Bedrock 100-150	Bedrock Total	Totals
Hastings, Lennox & Addington	Area $ft.^2$	$1.437 \cdot 10^6$		$1.437 \cdot 10^6$	$4.283 \cdot 10^6$			$4.283 \cdot 10^6$	$5.720 \cdot 10^6$
	Q Igpd	$6.07 \cdot 10^5$		$6.07 \cdot 10^5$	$8.95 \cdot 10^5$			$8.95 \cdot 10^5$	$1.503 \cdot 10^6$
	Q c.f.s.	1.1245		1.1245	1.6579			1.6579	2.7824
Frontenac & Leeds as far east as Rockport	Area ft^2	$1.350 \cdot 10^6$		$1.350 \cdot 10^6$	$10.685 \cdot 10^6$	$3.506 \cdot 10^6$	$.082 \cdot 10^6$	$14.273 \cdot 10^6$	$15.623 \cdot 10^6$
	Q Igpd	$5.96 \cdot 10^5$		$5.96 \cdot 10^5$	$2.406 \cdot 10^6$	$1.62 \cdot 10^5$	$4.3 \cdot 10^3$	$2.572 \cdot 10^6$	$3.168 \cdot 10^6$
	Q c.f.s.	1.1043		1.1043	4.4548	0.3001	0.0080	4.7629	5.8672
Leeds east of Rockport, Grenville, & Dundas west of Iroquois	Area $ft.^2$	$2.205 \cdot 10^6$		$2.205 \cdot 10^6$	$13.429 \cdot 10^6$			$13.429 \cdot 10^6$	$15.634 \cdot 10^6$
	Q Igpd	$1.088 \cdot 10^6$		$1.088 \cdot 10^6$	$5.803 \cdot 10^6$			$5.803 \cdot 10^6$	$6.891 \cdot 10^6$
	Q c.f.s.	1.9556		1.9556	10.7495			10.7495	12.7051

apparent that the quantity of flow below bedrock depth (150 feet) was negligible, being less than 0.1 percent of the flow in the overlaying rocks. The glacio-lacustrine clay of the lake bottom had to be taken into consideration where it

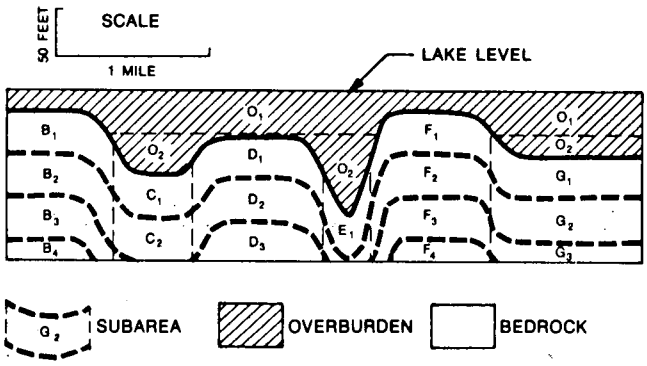

Figure 39. Schematic division of cross-section along the shore for computation of subareas.

was controlling the groundwater inflow, that is, where its assumed permeability of 10^{-3} Igpd/$ft.^2$ was less than that of the bedrock. This was the case east of Hamilton, southwest of Trenton and south of Kingston where the clay is encountered at a depth less than 200 feet below lake level (Fig. 33). The grand total of the groundwater inflow is estimated by this method to be $27.35 \cdot 10^6$ Igpd, or 51.62 cfs, as listed in Table 13.

Table 13. Total groundwater inflow computed using Classic Method

Units	Overburden	Bedrock	Totals
Area ($ft.^2$)	$30.25 \cdot 10^6$	$151.83 \cdot 10^6$	$182.08 \cdot 10^6$
Q (I g p d)	$8.91 \cdot 10^6$	$18.44 \cdot 10^6$	$27.35 \cdot 10^6$
Q (c.f.s.)	17.46	34.15	51.62

Numerical Solution

The groundwater inflow may also be computed in sections orthogonal to the shoreline by means of mathematical models. The numerical method developed by Freeze and Witherspoon (1966, 1967, 1968) and Freeze (1969a) is equally well suited to qualitative (Haefeli, 1970) and quantitative problems, (Freeze, 1969b) and has been applied. Only a brief description of the technique is included here.

QUANTITATIVE FLOW NET ANALYSIS (METHOD)

The first significant graphical analyses of flow patterns were developed by Forchheimer (1930) and Casagrande (1937). More recently, good descriptions and examples of two-dimensional profiles have been given by Harr (1962) and Bennett (1962) and especially by Freeze (1969a).

In nonhomogeneous media, the flow lines and equipotential lines are refracted at a permeability interface according to the tangent law:

$$\frac{K_1}{K_2} = \frac{\tan \theta_1}{\tan \theta_2} \qquad (19)$$

The flow lines and equipotential lines form a quantitative flow net of curvilinear squares or rectangles. In the latter ones, the ratio of the length of the sides is proportional to the permeability ratio of the adjacent formations (Fig. 40):

$$\frac{K_1}{K_2} = \frac{\Delta m_2}{\Delta s_2} \qquad (20)$$

In anisotropic media, the flow lines generally do not intersect the equipotential lines at right angles (Fig. 41c). Therefore, considerable care must be exercised in the construction of quantitative flow nets in nonhomogeneous and anisotropic profiles.

Two dimensional quantitative flow nets of anisotropic, nonhomogeneous media using computer generated equipotential lines (Fig. 41a) may be constructed as follows: the plot is transformed so that all layers become isotropic. By

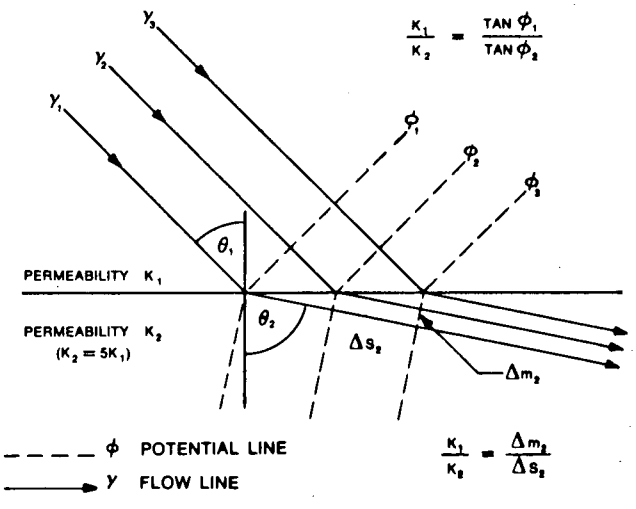

Figure 40. Refraction of flow lines across a boundary between media of different permeabilities (after Todd, 1959).

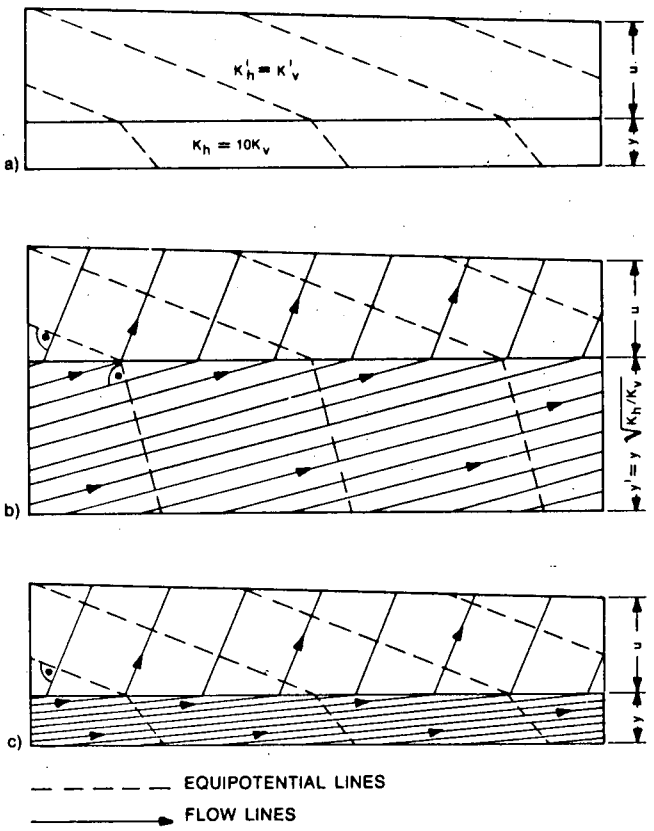

Figure 41. Construction of flow lines in a non-homogeneous anisotropic profile.

keeping the horizontal scale constant, the vertical scale for each layer becomes $y' = \sqrt{\frac{K_h}{K_v}}$ (Fig. 41b). The flow lines are drawn perpendicular to the equipotential lines on the transformed net so that they form curvilinear squares or rectangles with the equipotential lines. For example, if the network of a layer with a permeability $K_1 = 1$ is formed by curvilinear squares, the network of the adjacent layer with $K_2 = 10$ will consist of curvilinear rectangles with a flow path, Δs, ten times as long as the width, Δm. Then the flowlines are transferred back to the original computer plot (Fig. 41c).

The discharge in each flow channel bounded by flow lines (Fig.42) is computed by Darcy's Law written as:

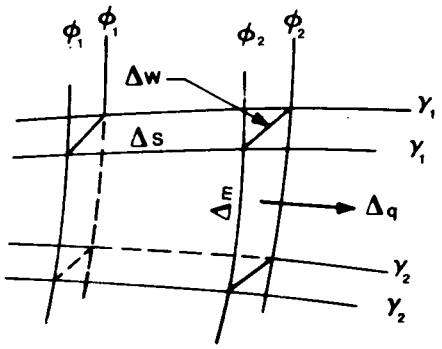

Figure 42. Discharge through one flow channel.

$$\Delta q = K \frac{\Delta\phi}{\Delta s} \cdot \Delta m \cdot \Delta s \qquad (21)$$

where Δq is the discharge through a segment of flow net
K is the permeability
ϕ is the drop in hydraulic head between equipotential surfaces
Δs is the length of flow path in the segment of flow net
Δm is the width of the segment
Δw is the thickness of the flow system.

In a homogeneous medium where the quantitative flow net is formed by curvilinear squares, the length of the flow path is equal to the width of the segment, and the flow through a channel becomes:

$$\Delta q = K \cdot \Delta\phi \cdot \Delta w \qquad (22)$$

If the medium is nonhomogeneous and the section consists of several layers with different permeabilities, only one layer will possess a flow net of curvilinear squares. However, according to equation (20), $\Delta m/\Delta s$ is a function of the permeability ratios and, therefore, the quantity of flow remains constant through all rectangle- and square-shaped channels in the whole profile.

The total discharge through the section is obtained by multiplying the number of flow channels by the amount of flow through one curvilinear square obtained after equation (21). Freeze (1969a) provides an excellent example of the computation of discharge in quantitative flow nets. However, for the present study, the wide range of permeability made it more convenient to compute the flow for various channels separately (Plate VI).

RESULTS

Ten profiles, each approximately 3 miles long and perpendicular to the shore, were chosen to be representative of sub-areas (Fig. 11). The groundwater flow through these profiles was analyzed. According to the rapidly decreasing permeability with bedrock depth, the bottom of the profile was set at 300 feet below lake level. Any groundwater flow beyond this depth was considered to be negligible (Chapter 3). The same permeability values were used as in the classic method.

In many places, the land surface and the groundwater table become steeper towards the shore, and the overburden thickness decreases rapidly as a result of slope retreat along the shoreline. Therefore, the hydraulic gradient and the groundwater velocity become higher, and the flow through a unit area of the overburden increases proportionally. The groundwater inflow through the Quaternary deposits computed by the classic method, using the cross-sectional area along the shoreline and an average hydraulic gradient through the shorebelt, is therefore too small, especially in areas where high bluffs occur.

The flow pattern obtained by the numerical method in profiles perpendicular to the shore makes it possible to compute the groundwater flow through any cross-sectional area parallel to the shore. A cross-section was selected near the shoreline in order to account for the recharge which occurs near the lake and because the configuration of the bedrock near the lake is known. A cross-section was chosen where the direction of flow lines is horizontal to allow use of only K_h in the calculation of total flow.

The discharge was computed as described previously. The construction of an entire quantitative flow net was not necessary because only one segment of flow lines from the top to the bottom of the profile was required. The decreasing permeability with depth of the bedrock was accounted for by using 50-foot wide flow channels with different isotropic permeabilities, thus obtaining a different flow through each channel. An example of a representative profile is given in Plate VI.

Table 14. Approximate mean horizontal and vertical hydraulic conductivities for the shorebelt area.

Area Shorebelt	Approximate Hydraulic Conductivity in Igpd/ft.^{2}		Approximate mean Ratio
	K_h	K_v	K_h/K_v
A	30	0.2	150:1
B	8	0.05	150:1
C	13	0.5	25:1
D	60	2.0	30:1

The total discharge through the bedrock (Table 14) compares favourably with the flow obtained with the classic method (Table 13). For the overburden, however, the inflow determined numerically is considerably higher than that obtained by the classic method (Table 15). The numerical method for the overburden is probably more accurate since it simulates more accurately the near-shore conditions.

Table 15. Total groundwater discharge obtained using the Numerical Method

Units	Overburden	Bedrock	Total
Igpd	$14.14 \cdot 10^6$	$20.18 \cdot 10^6$	$34.32 \cdot 10^6$
c.f.s.	26.28	37.52	63.80

CHAPTER 4

Baseflow Analysis

GROUNDWATER FLOW SYSTEMS

Based on his theory of groundwater motion, Hubbert (1940) gave some classic examples of the theoretical distribution of flow and equipotential lines in a groundwater body and the adjacent media. Figure 43 shows an idealized flow pattern between two valleys, and Figure 44 represents the flow of groundwater into a lake. A more complicated model corresponding to topography with sinusoidal "highs" and "lows" was developed by Tóth (1963). Depending on the potential distribution, different types of flow systems may occupy a basin (Fig. 45). He distinguished between (a) a local groundwater flow system with a recharge area at a topographic high and a discharge area at an adjacent topographic low, (b) an intermediate system with one or more topographic highs between the recharge and the discharge area, and (c) a regional system where the recharge area occupies the basin water divide and the discharge area lies at the bottom of the basin. Freeze (1969a) and Parsons (1970) provide excellent numerical and observed flow patterns, which basically verify Tóth's theory.

The greatest flow line densities are found at shallow depths of local flow systems (Fig. 45). The density of flow decreases rapidly with depth and with the transition from the local to the intermediate region, and reaches its minimum in the regional system. This tendency is valid for a homogeneous, isotropic medium and becomes generally more accentuated in reality because the horizontal permeability is usually predominant in unconsolidated rocks and the bedrock fracture porosity decreases rapidly with depth (Chapter 3). Generally, the higher the relief, the

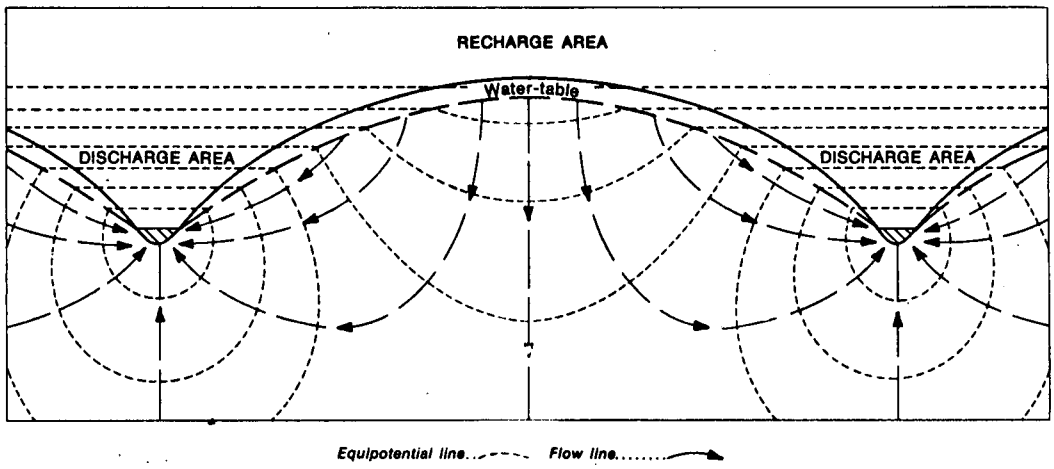

Figure 43. Schematic flow pattern in uniformly permeable material between two effluent streams (after Hubbert, 1940).

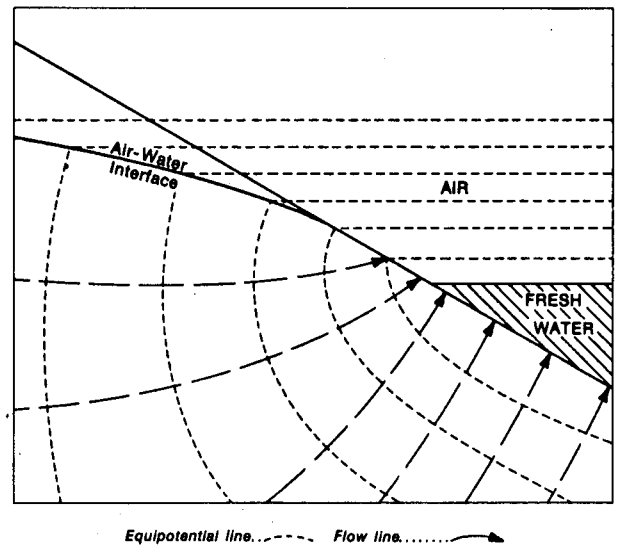

Figure 44. Schematic flow pattern in uniformly permeable material at a lake (after Hubbert, 1940).

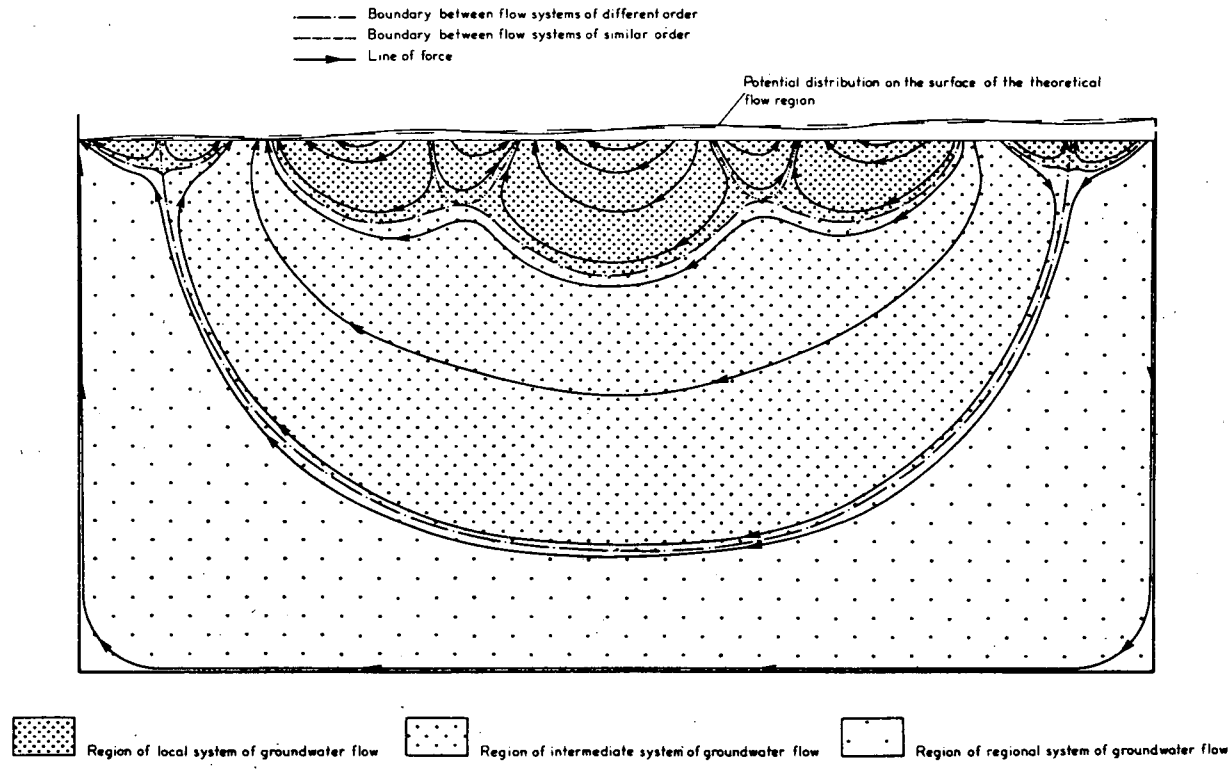

Figure 45. Theoretical flow pattern in a small drainage basin underlain by an impermeable boundary (after Tóth, 1962).

stronger and deeper are the local flow systems. The groundwater flow occurs, therefore, mainly in the local system and is intercepted by the surface drainage within the same watershed. In cases where deep layers of high permeability exist , a strong intermediate, or regional flow system may result. Depending on the hydrogeological situation, it is possible to estimate the groundwater flow of a watershed by analyzing its streamflow. The prevailing conditions in the Lake Ontario basin are well suited for this type of analysis.

METHOD

Depending on the path by which the water reaches the stream channel, stream runoff may consist of different components. Barnes (1939) and Meyer (1940) introduced the classic concept of three constituents: overland flow or surface run off; interflow, which consists of water flowing underground without reaching the saturated zone; and baseflow or groundwater flow. Several methods have since been developed to analyze the three components and to separate them on stream hydrographs. Many of them have neglected the interflow or taken it as a part of the groundwater flow. It is believed that interflow occurs only where low permeable layers above the groundwater table exist or where the land surface has an extremely strong relief. Ferris (14th Midwest Groundwater Conference, Lexington, 1969) pointed out that the interflow is, in general, a very minor, negligible component which cannot be separated from stream hydrographs. In the present study, stream hydrographs were only separated into surface flow and groundwater flow.

The analysis of stream hydrographs is carried out in two steps. First, the baseflow recession constant, a measure of the depletion of the stream runoff during dry weather, is computed. Second, with the help of a standard recession curve described by the recession constant, the hydrograph is separated into its components. The first fundamental equations to compute recession slopes were developed independently by Horton (1935) and Maillet (1903). They observed that the recession curve of a streamflow hydrograph during a period of drought has the characteristic equation:

$$Q_t = Q_o \cdot e^{-ct} \qquad (23)$$

where Q_o is the flow at any time
Q_t is the flow occurring after time t
t is the time interval between Q_o and Q_t
c is the recession constant.

Barnes (1939) introduced the equation:

$$Q_t = Q_o \cdot K^{rt} \qquad (24)$$

where $Kr = e^{-c}$

or $c = \log_e Kr$

Butler (1957) developed the formula:

$$Q_t = \frac{K_1}{10^{t/K_2}} \qquad (25)$$

where K_1 is equivalent to Q_o

K_2 is the recession constant which is the time for a log cycle change in discharge

or $K_2 = \frac{1}{\log K}$

where t is the time interval between K_1 and Q_t.

After the surface runoff has ceased, the recession constant can be calculated from the stream hydrograph by any of the equations above. Most convenient is Butler's formula which is rearranged to

$$K_2 = \frac{t}{\log K_1 - \log Q_t} \qquad (26)$$

where K_2 is obtained by counting the days for a log-cycle change of discharge.

Often, however, the depletion curve is irregular and either varies from one recession to another or is not of sufficient duration. Three main methods have been proposed to solve these problems: The envelope curve by Langbein (1940) on which Q_t versus Q_{t-1} during recession periods is analyzed (Fig. 46a); the composite curve by Linsley, Kohler and Paulhus (1958) who have pieced together tails of recession curves (Fig. 46c), and the minimum discharge curve described by Meyboom (1961) who has connected the points of minimum discharge during a seasonal depletion (Fig. 46b). The composite and envelope curve methods produce standard recessions which are generally too slow and consequently K_2 values which are too large, and the minimum discharge method is very dependable on daily and seasonal precipitations. For comparison, the recession constant was computed for the Spencer Creek watershed by the envelope (Fig. 47) and the composite method (Fig. 48).

The values for K_2 by these methods have a considerable variation, from 20 to 52 days. In addition, a large number of methods have been proposed to separate baseflow from surface runoff on the stream hydrograph. A good description of the ten main procedures is provided by Dickinson (1963). Many of the procedures depend on individual judgement, and overemphasize the surface runoff. Kraijenhoff van der Leur (1958) observed in this respect that, in flat regions with deep Quaternary deposits, the drainage system can be attributed almost exclusively to groundwater. No method accounts for the various conditions in a drainage basin, especially the influence of

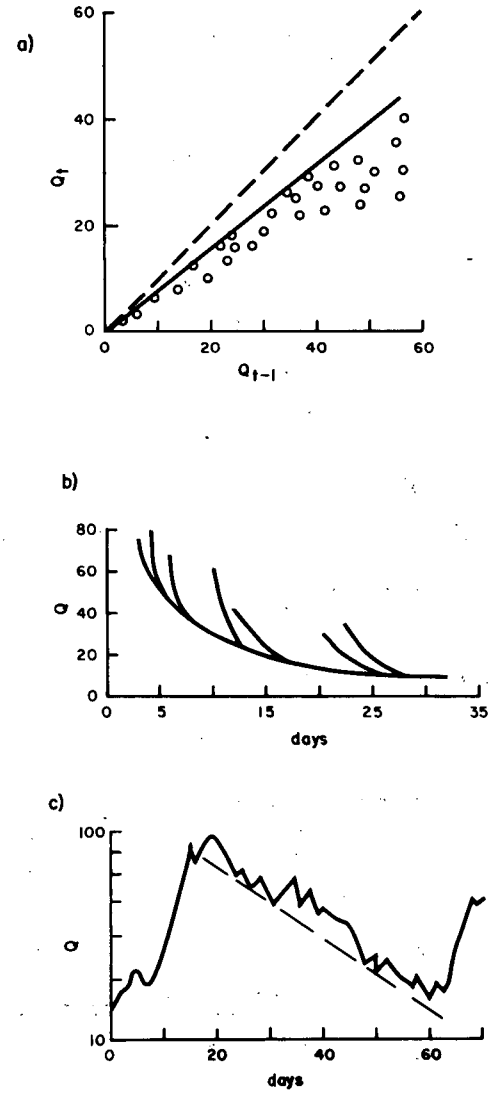

Figure 46. Methods to compute the baseflow recession constant: (a) envelope curve, (b) composite curve, (c) minimum discharge curve.

temperature and different permeabilities. In general the relations are as follows:

high permeability → slow recession

high temperature → high evapotranspiration → fast recession.

The recession will therefore be slower or faster depending on the season and the area in the drainage basin (soil, rock) over which a storm occurs. An average method which considers these variations to some extent was developed for this study. The average baseflow recession was obtained as follows:

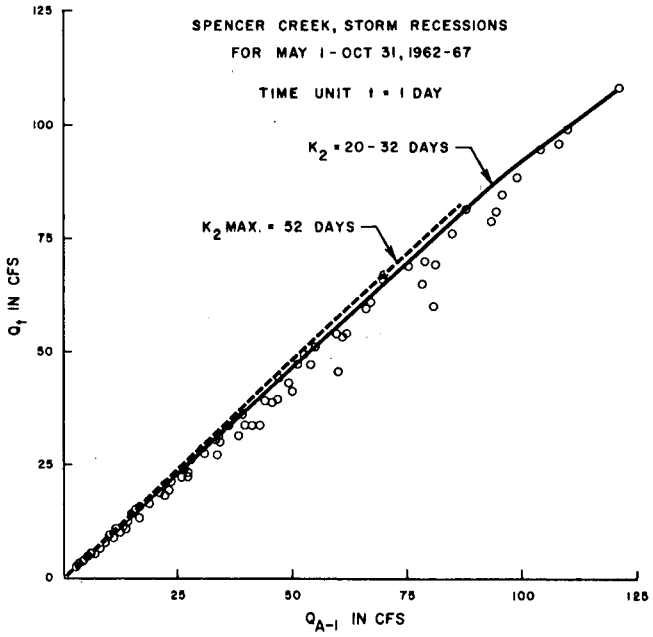

Figure 47. Envelope recession curve for Spencer Creek watershed.

(a) The hydrograph of a streamflow gauging station was plotted on semi-log paper using daily means. An investigation period of several years, if possible not less than four, should be chosen.

(b) Thiessen polygons of precipitation stations covering the entire drainage basin were constructed. Dry periods common to all precipitation stations and exceeding the estimated maximum travel time of the main stream were marked on the hydrograph. The travel time may be estimated by analyzing well-defined single storms which are succeeded by dry periods on the hydrograph (Fig. 49). However, a better way is to measure the travel time in the field by means of dye tracers.

(c) To compute the recession slope of the baseflow, well-defined recessions during dry periods were chosen. The estimated maximum travel time was added to the time where the peak of the hydrograph occurred. The remaining recession slope was considered to be characteristic of the baseflow (Fig. 50).

(d) The recession constant was computed by Butler's method for each suitable recession, and the average constant was calculated for the whole investigation period.

Before describing the separation procedure of the stream hydrograph, some consideration should be given to the mechanism of water movement below the surface. Although the water moves rather slowly underground, in the order of a foot/day or a fraction of it, its reaction toward recharge is much faster. Precipitation reaching the surface induces an almost instantaneous propagation of pressure through the unsaturated zone. Soil water, retained

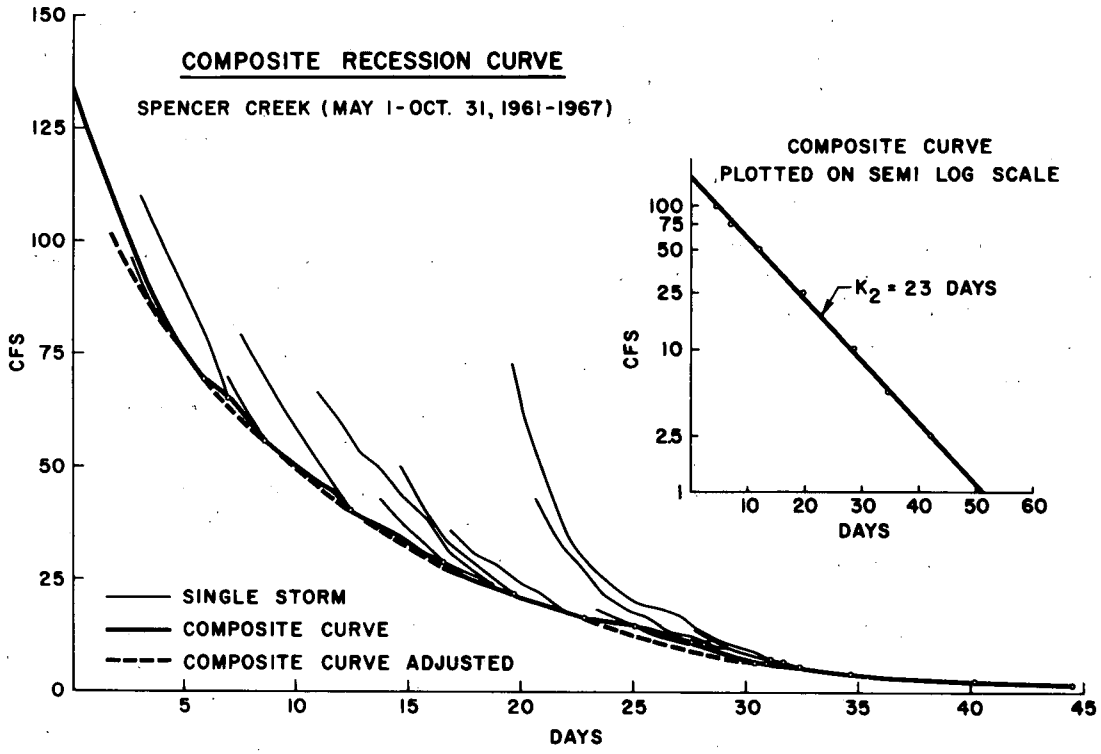

Figure 48. Composite recession curve for Spencer Creek watershed.

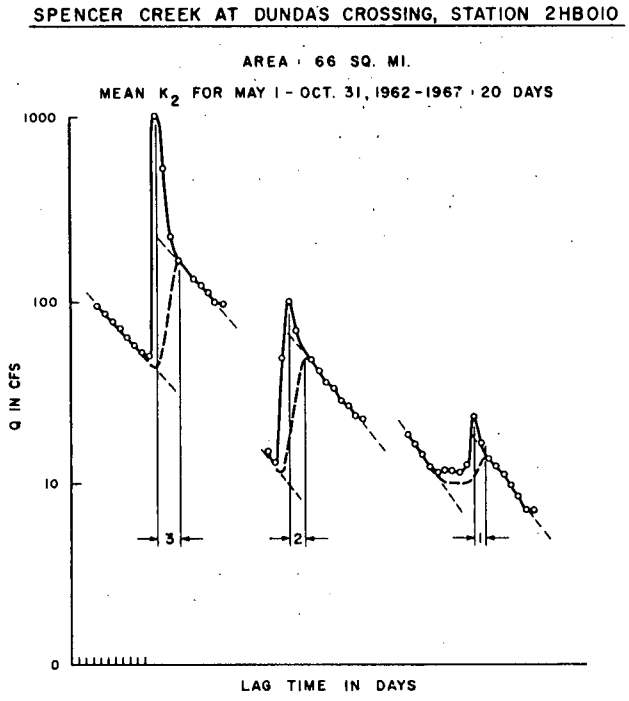

Figure 49. Hydrograph seperation for single storms of Spencer Creek watershed.

against gravity, is displaced downwards by water infiltrating the surface (Horton and Hawkins, 1965; Rubin and Steinhardt, 1963, 1964) and recharges the saturated zone. The increase in head in the recharge area may induce a fairly quick response in the flow system resulting in an increase in discharge. Propagation speeds of pressure waves of up to 800 meters/day in fractured basalt have been observed by Barraclough et al (1967) and over 1000 meters/day in sand and gravel deposits by Hofbauer (1968). Although the time lag between the hydrograph rise and increase in groundwater discharge cannot be computed, it apparently ranges between a few hours and a few days, depending on the nature of soil and rock and the drainage density. For this study a time lag of one day was assumed.

The hydrograph was separated according to the following method: the standard recession slope described by the average recession constant was plotted as a tangent to every depletion period lasting beyond surface runoff (Fig. 50). The beginning or highest point of the baseflow recession slope was assumed to be given by the maximum travel time (time lag after the peak). For small storms covering only a part of the drainage basin, a shorter time lag seems to be more appropriate (Fig. 49).

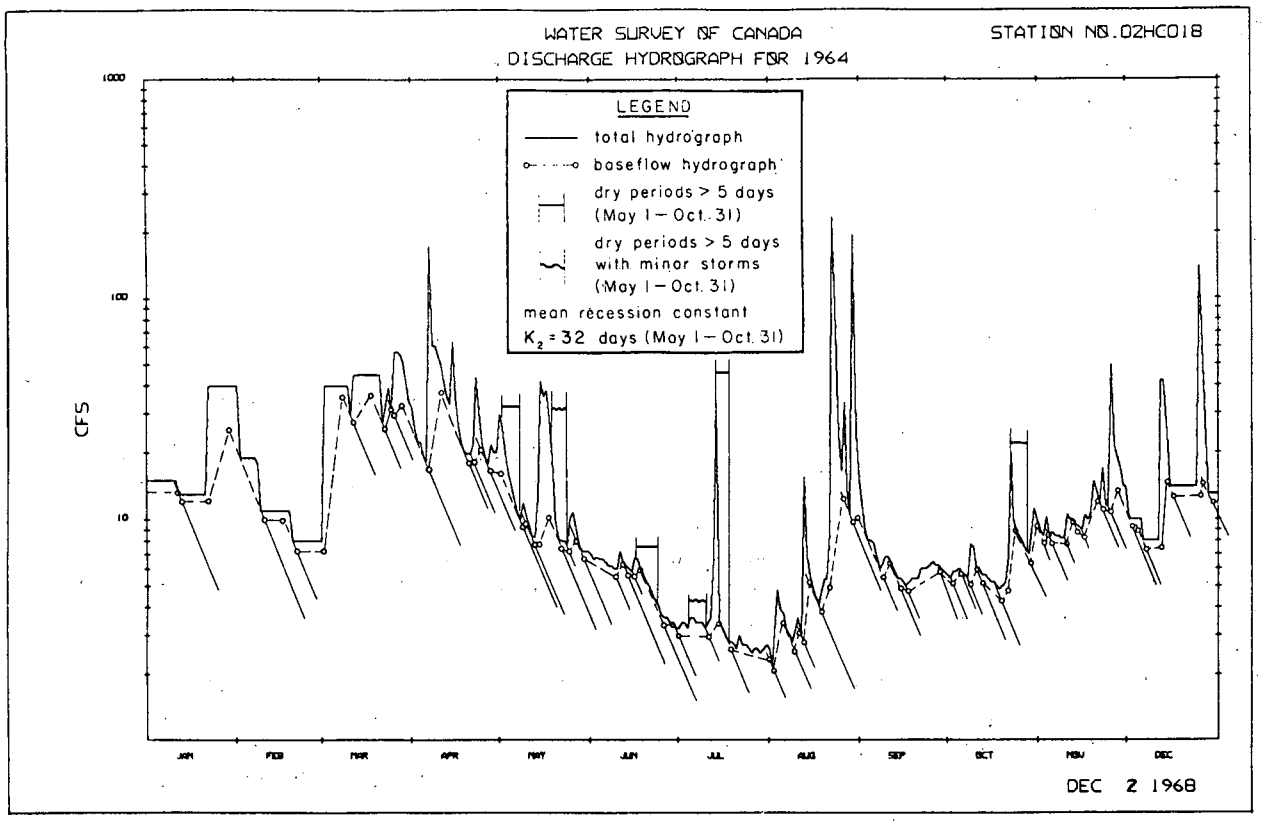

Figure 50. Example of discharge hydrograph (computer plot) with baseflow separation.

With regard to the beginning of the baseflow recession, it should be emphasized that the groundwater discharge could have reached its peak before the surface runoff ceased. Therefore, the method described provides a rather minimum baseflow. However, the selection of the beginning and ending of the recession is not too critical with respect to the computation of the groundwater discharge. For example, a shift of one day at the beginning and ending points of the recessions over a six-year period in the Rouge and Credit Rivers watersheds (Table 16) resulted in a variation in groundwater discharge of only 6.4 percent of the baseflow.

Table 16. Variation of baseflow for different beginnings (high points) and endings (low points) of the baseflow recession over a six-year period for the Rouge and Credit Rivers.

Watershed	Rouge	Credit
Station No.	2HC22	2HB2
Drainage Area (sq. mi.)	72	320
Average total runoff (c.f.s.)	32.9	231.4
Average baseflow (c.f.s.)	14.9	139.0
Baseflow recession constant K_2 (days)	29	46
Hydrograph separations (baseflow in %)		
Normal high point (n.h.p.) and low point (n.l.p.)	100.0	100.0
n.h.p. + 1 day and n.l.p. + 1 day	95.0	94.0
n.h.p. + 1 day and n.l.p.	95.7	94.8
n.h.p. and n.l.p. + 1 day	96.4	97.7
n.h.p. and n.l.p. − 1 day	102.0	103.7
n.h.p. − 1 day and n.l.p. − 1 day	106.4	104.5

The storage on the mean baseflow may be computed after the equation of Horton (1935) and Maillet (1903):

$$S_t = \int_t^{\infty} Q_t \, dt = \frac{Q_t}{c} \qquad (27)$$

or after any formula developed by Barnes (1939), Butler (1957) and Meyboom (1961). However, since the hydrograph of one year generally consists of over twenty small recessions, each single recession would involve a calculation and also, the baseflow during recharge periods would have to be computed. To overcome these difficulties, Searcy (1959) proposed using a frequency or flow duration curve. The ordinates representing the amount of baseflow are added together and the average is computed from:

$$Q_{mean} = \frac{sum\ of\ ordinates}{number\ of\ ordinates}$$

However, the mean was obtained more conveniently by integrating the area below the curve with a planimeter (Fig. 51). For comparison, the mean baseflow for the Rouge River for the year 1963 was computed by Searcy's method and by the integrating planimeter method. By taking 40 ordinates, the mean was 13.25 cfs; with 80 ordinates it was 12.77 cfs. The integrating planimeter method produced a mean of 12.50 cfs.

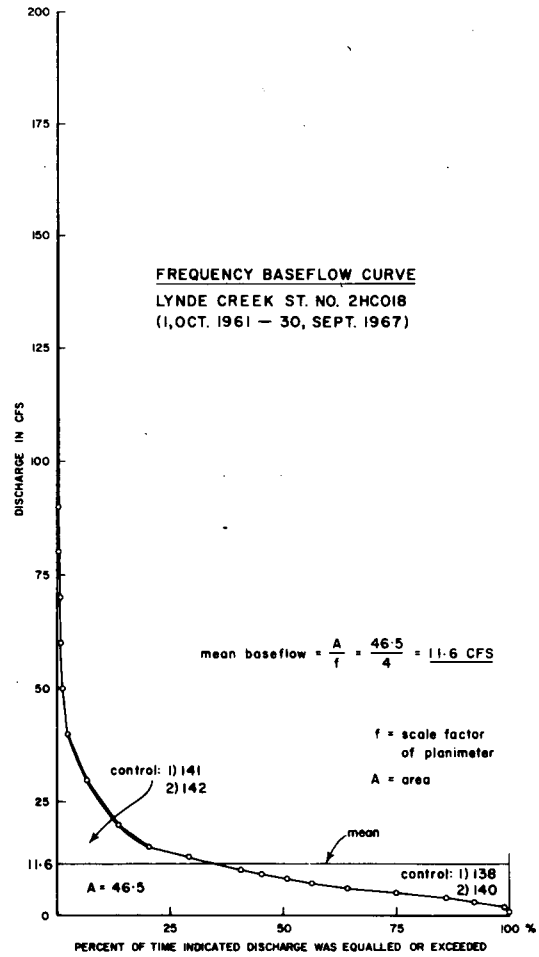

Figure 51. Computation of mean baseflow from a frequency curve by means of planimeter.

COMPUTATION AND DISCUSSION OF BASEFLOW AND RELATED PARAMETERS

Twenty watersheds were selected around Lake Ontario to obtain representative baseflow data for the different physiographic and geological areas (Fig. 52). In the three watersheds, Little Creek, Blessington Creek and Millhaven Creek, automatic stream gauging recorders were temporarily installed and operated during the summers of 1968 and 1969. All gauging stations were maintained by the

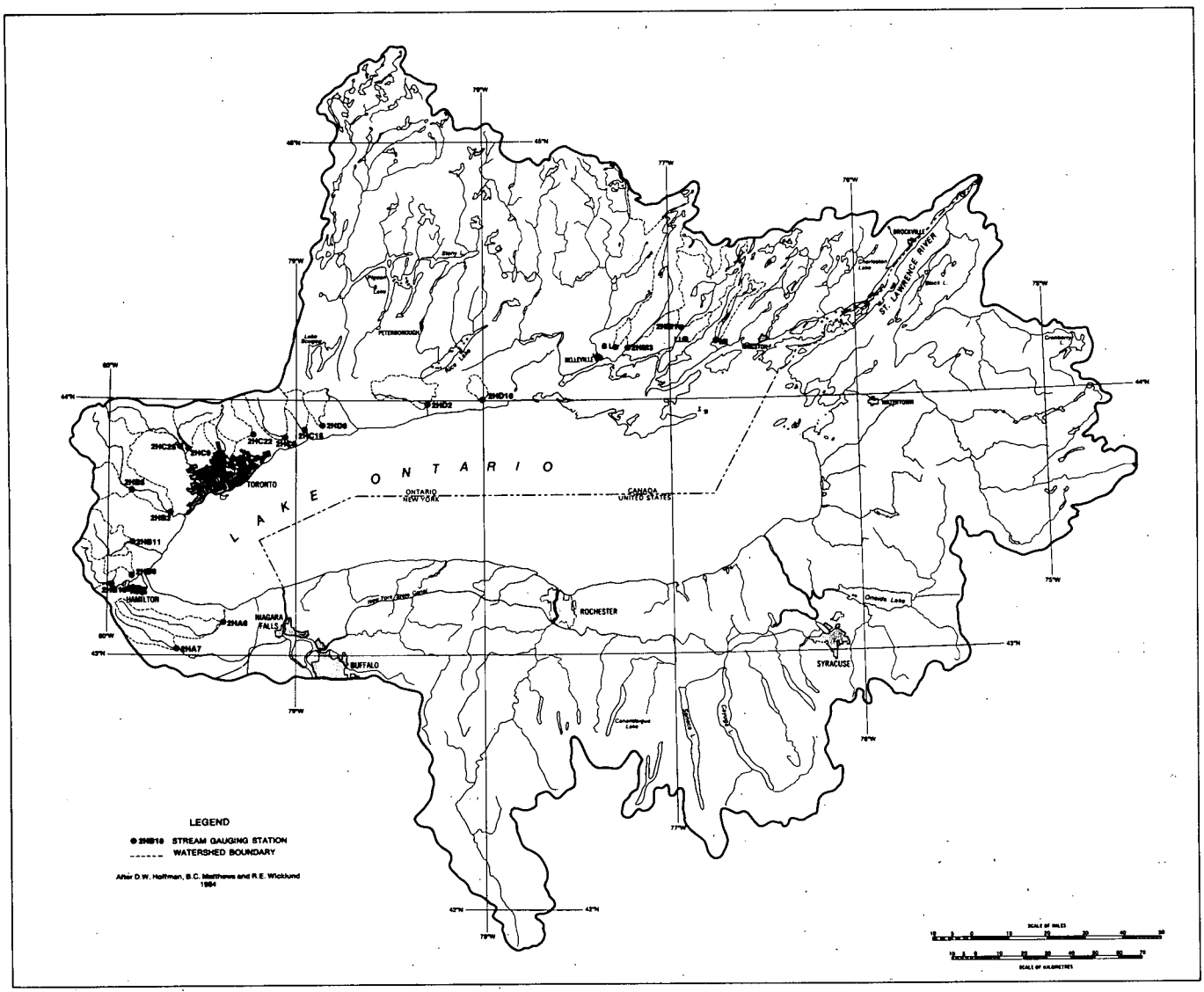

Figure 52. Location of analyzed watersheds and gauging stations.

Water Survey of Canada. The extent of the investigation was determined by the scarce distribution of the gauging stations prior to 1960 and the increasing regulation of streams in recent years. A six-year period starting October 1, 1961, was analyzed. Watersheds with too many or too large lakes had to be avoided because of their dampening effect on streamflow. The temporarily gauged streams as well as the Welland River and Twenty Mile Creek were used only for comparative purposes.

A total of 102 years of streamflow hydrographs was analyzed. Computer plots of these on a semi-logarithmic scale were obtained through the Water Survey of Canada. An example is shown in Figure 50. The calculation of the recession constants, the hydrograph separation and the computation of the mean baseflow for the entire year and the summer period were carried out according to the methods described previously. Since the measurement of the stream runoff during the winter is greatly affected by prevailing ice conditions, the summer period was considered more important and, therefore, analyzed separately. A list of the recession constants is presented in Table 17.

To obtain an estimate of the maximum duration of the surface runoff, the travel time of several streams was measured during the spring of 1969 and during the spring and early summer of 1970. Rhodamine B dye was injected as high upstream as possible in one of the main watercourses. Samples were taken at the gauging station and analyzed by a fluorometer. The travel time, which is a function mainly of the discharge and channel slope, but

also of other factors such as tortuosity and roughness of the channels, varied considerably for the five selected streams (Fig. 53). Depending on the location of the injection point,

Table 17. Recession constants.

Station No.	Watershed	Recession constant K_2	K_r	c
2HA7	Welland	11	0.811	0.209
2HA6	Twenty-Mile	10	0.794	0.230
2HB10	Spencer	20	0.891	0.115
2HB6	Grindstone	21	0.896	0.109
2HB11	Bronte	26	0.915	0.088
2HB8	Rogers	51	0.955	0.045
2HB2	Credit	46	0.951	0.050
2HC25	Humber	36	0.938	0.063
2HC9	East Humber	28	0.921	0.082
2HC4	Little Don	27	0.918	0.085
2HC22	Rouge	29	0.923	0.079
2HC6	Duffin	25	0.912	0.092
2HC18	Lynde	32	0.930	0.071
2HD8	Oshawa	26	0.915	0.088
2HD2	Ganaraska	43	0.947	0.053
2HM3	Salmon	28	0.921	0.082
2HM1	Napanee	29	0.923	0.079
	Blessington	12	0.825	0.191
	Little Creek	11	0.811	0.209
	Millhaven	18	0.879	0.127

the measured travel time might represent approximately 4/5 of the maximum duration of surface runoff, except for Spencer Creek where only a short reach was measured representing about 1/3 of the total stream length. The results showed that in small to medium sized watersheds (20 - 100 sq. mi.) in the Lake Ontario basin, the surface runoff ceases after a maximum of 3 days. In larger watersheds (e.g., Credit, Napanee) the longest duration may not exceed 4 to 5 days.

Depending on the watershed, the baseflow varies between 21 and 78 percent of the total runoff for the whole six-year period and between 17 and 90 percent for the summer periods (Tables 18 and 19). Similarly, the baseflow varies between 6.5 and 29.8 percent of precipitation in the six-year period and between 2.6 and 45.0 percent for the summer periods (Tables 20 and 21). To find the main reasons for these variations and to prove the validity of the baseflow data, the groundwater discharge was compared with flow duration analyses, surficial geology and water balance parameters.

The Q_{90}, which is the discharge of a stream equalled or exceeded 90 percent of the time, is a very useful flow-duration parameter to characterize dry weather streamflow. At this point it can be assumed that almost the entire flow comes from groundwater sources. Cross (1949)

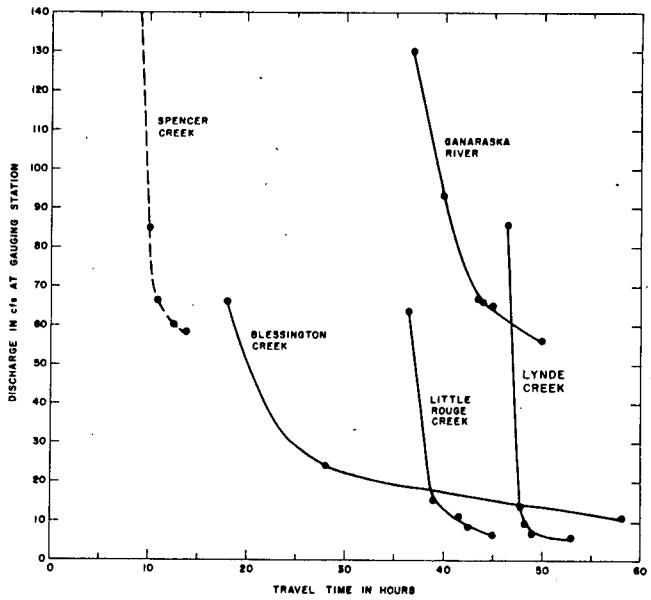

Figure 53. Discharge versus travel time of various streams of the Lake Ontario basin.

demonstrated a distinct relation between the shape of the lower end of the duration curve and the groundwater geology of the watersheds. High permeability deposits produce a high flat end of the duration curve and consequently a high Q_{90}. Steep low tails with a low Q_{90} reflect a groundwater body of low permeability. Ayers and Ding (1967) obtained a definite relationship between the surficial geology, baseflow and Q_{90} in eight selected watersheds of Southern Ontario. Since the preparation of flow frequency curves on a daily mean basis is very time-consuming, a computer program was developed. The frequency analyses carried out by the program FREQ (Appendix B) first reads daily discharges (computer format compatible with the Water Survey of Canada system), classifies them into ranges (maximum 50), outputs the percentage of data which falls in each range, and calculates the mean flow. The second part of the program plots the discharge ranges versus the cumulative percentage on a semi-logarithmic scale. The values of Q_{90} are presented in Table 18 and the relation between Q_{90} and the baseflow is given in Figure 54. The watersheds of similar physiographic areas show a close grouping between Port Credit and Port Hope; the catchments with predominantly deep glacial deposits lie almost in one line and accentuate the close relationship between the baseflow and Q_{90}.

The nature of the soil, especially its texture, determines primarily how much precipitation will infiltrate and significantly influences the ratio between surface and groundwater runoff. Based on the soil map of Southern Ontario (Hoffman, Matthews and Wicklund, 1964), Hoffman (personal communication) has rated the soils into

Table 18. Mean flows for the period May 1, 1961 – April 30, 1967.

Station No.	Watershed	Mean flow cfs/sq. mi. Total	Surface	Baseflow	Baseflow in % of Total Flow	Q_{90} cfs/sq. mile
2HA7	Welland	0.69	0.54	0.15	21.7	0.0
2HA6	Twenty-Mile	0.67	0.49	0.18	26.8	0.0
2HB10	Spencer	0.83	0.29	0.54	71.4	0.07
2HB6	Grindstone	0.78	0.27	0.51	65.4	0.13
2HB11	Bronte	0.90	0.26	0.64	71.1	0.12
2HB8	Rogers	0.70	0.30	0.40	57.1	0.24
2HB2	Credit	0.72	0.29	0.43	59.7	0.27
2HC25	Humber	0.57	0.20	0.37	64.9	0.27
2HC9	East Humber	0.33	0.15	0.18	54.5	0.09
2HC4	Little Don	0.62	0.24	0.38	61.2	0.27
2HC22	Rouge	0.46	0.25	0.21	45.7	0.10
2HC6	Duffin	0.65	0.24	0.41	63.1	0.29
2HC18	Lynde	0.57	0.29	0.28	49.1	0.14
2HD18	Oshawa	0.78	0.30	0.48	61.5	0.38
2HD2	Ganaraska	1.03	0.34	0.69	67.0	0.56
2HM3	Salmon	0.82	0.18	0.64	78.0	0.04
2HM1	Napanee	0.93	0.31	0.62	67.0	0.08

infiltration categories. The rate of infiltration is presumed to be that which might be measured for the third hour of a wet run by the tube method. It is comparable to the rating of Free, Browning and Musgrave (1940) for soils in the United States. The average infiltration rate for each watershed was computed from the soil map and Hoffman's infiltration categories by means of an integrating planimeter. Since the amount of baseflow depends not only on the infiltration through the uppermost few feet of soil, the infiltration rate cannot be an exact criterion of the baseflow. However, Figure 55 illustrates a fairly well defined relationship between mean infiltration rate and baseflow in the Lake Ontario drainage basin.

Table 19. Mean flows for the summer periods (May 1 – September 30, 1961 – 1967).

Station No.	Watershed	Mean flow cfs/sq. mi. Total	Surface	Baseflow	Baseflow in % of Total Flow
2HA7	Welland	0.17	0.14	0.03	17.6
2HA6	Twenty-Mile	0.16	0.10	0.06	37.5
2HB10	Spencer	0.39	0.11	0.28	71.8
2HB6	Grindstone	0.30	0.07	0.23	76.6
2HB11	Bronte	0.41	0.09	0.32	78.0
2HB8	Rogers	0.42	0.11	0.31	73.7
2HB2	Credit	0.42	0.11	0.31	76.2
2HC25	Humber	0.38	0.11	0.29	73.7
2HC9	East Humber	0.16	0.05	0.11	68.6
2HC4	Little Don	0.39	0.10	0.29	74.2
HC22	Rouge	0.23	0.11	0.12	52.2
2HC6	Duffin	0.43	0.10	0.33	77.4
2HC18	Lynde	0.27	0.11	0.16	59.1
2HD8	Oshawa	0.55	0.16	0.39	71.0
2HD2	Ganaraska	0.70	0.14	0.56	79.9
2HM3	Salmon	0.32	0.04	0.28	87.5
2HM1	Napanee	0.29	0.03	0.26	89.8

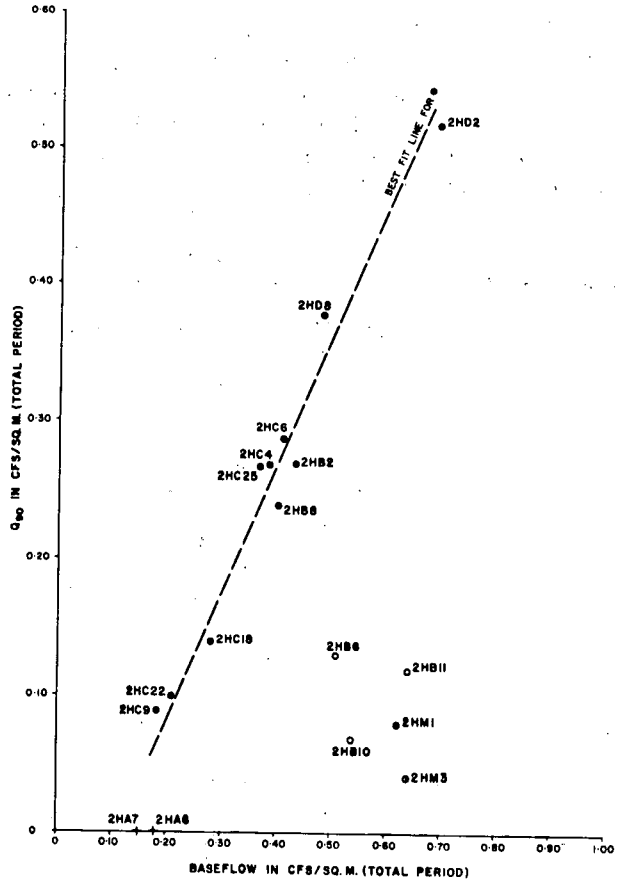

Figure 54. Relation between baseflow and Q_{90} (gauging stations)

Table 20. Water balance for the period May 1, 1961 – April 30, 1967.

(1)	(2)	(3)	(4)	(5)	(6)		(7)	
				Runoff				
Station No.	Watershed	Precipitation (inches)	Total (inches)	Surface (inches)	Baseflow (inches)	% of (3)	Loss (inches)	% of (3)
2HA7	Welland	30.60	9.36	7.33	2.04	6.5	21.23	69.0
2HA6	Twenty-Mile	31.81	9.08	6.63	2.44	7.7	22.73	71.5
2HB10	Spencer	31.51	11.26	3.93	7.33	23.2	20.74	64.3
2HB6	Grindstone	32.11	10.58	3.67	6.91	21.5	21.52	67.0
2HB11	Bronte	31.21	12.22	3.53	8.69	27.8	18.99	61.0
2HB8	Rogers	30.11	9.50	4.07	5.43	18.2	20.60	68.3
2HB2	Credit	29.80	9.77	3.93	5.83	19.5	20.02	67.4
2HC25	Humber	28.49	7.73	2.71	5.02	17.6	20.75	73.1
2HC9	East Humber	29.36	4.47	2.03	2.44	8.3	24.88	85.0
2HC4	Little Don	28.91	8.41	3.28	5.14	17.8	20.49	71.0
2HC22	Rouge	29.84	6.24	3.39	2.85	10.0	23.59	79.0
2HC6	Duffin	28.98	8.82	3.25	5.56	19.2	20.15	69.5
2HC18	Lynde	28.07	7.73	3.93	3.80	13.6	20.33	72.5
2HD8	Oshawa	29.28	10.58	4.07	6.51	22.2	18.69	63.7
2HD2	Ganaraska	31.50	14.10	4.73	9.36	29.8	17.40	55.3
2HM3	Salmon	30.54	11.13	2.44	8.68	28.4	19.40	63.5
2HM1	Napanee	29.94	12.59	4.17	8.41	28.2	17.35	57.8

Monthly means for 46 precipitation stations were used in the calculation of the mean precipitation for each watershed. The average for each catchment was obtained by the Thiessen polygon method (Tables 20 and 21). Figure 56 presents an inverse relationship between baseflow and loss (precipitation minus total runoff).

The relationship is influenced by evapotranspiration (which is inversely related to slope) and by deep groundwater flow which may occur in basins of high relief. For example, Twenty Mile Creek (2HA6) and Welland River (2HA7) have high losses and a low baseflow which may be related to the Niagara Escarpment, inducing a deep groundwater flow system to the adjacent lowland. On the contrary the Oshawa (2HD8) and Ganaraska Rivers have low losses and high baseflows which are probably related to steep slopes (Table 22), deep coarse-textured soil and a possible gain from Lake Scugog and Rice Lake.

Table 21. Water balance for the summer periods (May 1 – September 30, 1961 – 1967).

(1)	(2)	(3)	(4)	(5)	(6)		(7)	
				Runoff				
Station No.	Watershed	Precipitation (Inches)	Total (Inches)	Surface (Inches)	Baseflow (Inches)	% of (3)	Loss (Inches)	% of (3)
2HA7	Welland	15.78	2.31	1.90	0.41	2.6	13.47	85.3
2HA6	Twenty-Mile	16.64	2.17	1.36	0.81	4.8	14.47	86.9
2HB10	Spencer	16.05	5.29	1.49	3.80	23.6	10.76	67.0
2HB6	Grindstone	16.47	4.07	0.95	3.12	18.9	12.40	75.2
2HB11	Bronte	16.14	5.57	1.23	4.34	26.8	10.57	65.4
2HB8	Rogers	15.65	5.71	1.50	4.21	26.9	9.94	63.5
2HB2	Credit	15.76	5.71	1.50	4.21	26.7	10.05	63.7
2HC25	Humber	15.21	5.16	1.22	3.94	25.9	10.05	66.0
2HC9	East Humber	15.69	2.17	0.68	1.49	9.5	13.52	86.1
2HC4	Little Don	15.33	5.29	1.35	3.94	25.70	10.04	65.4
2HC22	Rouge	15.90	3.13	1.64	1.49	9.3	13.77	86.6
2HC6	Duffin	16.26	5.84	1.36	4.48	27.5	10.42	64.0
2HC18	Lynde	15.73	3.67	1.50	2.17	13.8	13.06	83.0
2HD8	Oshawa	15.67	7.47	2.18	5.29	33.7	8.20	52.3
2HD2	Ganaraska	16.89	9.50	1.90	7.60	45.0	7.39	43.7
2HM3	Salmon	15.08	4.34	0.54	3.80	25.2	10.64	70.5
2HM1	Napanee	14.94	5.01	2.01	3.00	20.0	9.93	66.4

Table 22. Drainage characteristics.

Station No.	Watershed	Drainage Area (sq. mi.)	Stream Length (feet)	Average Landslope (ft./ft.)
2HA7	Welland	87	$7.61 \cdot 10^5$	0.014
2HA6	Twenty-Mile	113	$6.46 \cdot 10^5$	0.011
2HB10	Spencer	66	$3.48 \cdot 10^5$	0.021
2HB6	Grindstone	28	$1.90 \cdot 10^5$	0.018
2HB11	Bronte	93	$5.29 \cdot 10^5$	0.026
2HB8	Rogers	49	$2.53 \cdot 10^5$	0.028
2HB2	Credit	271	$1.67 \cdot 10^6$	0.031
2HC25	Humber	117	$7.21 \cdot 10^5$	0.038
2HC9	East Humber	76	$4.48 \cdot 10^5$	0.036
2HC4	Little Don	50	$2.75 \cdot 10^5$	0.031
2HC22	Rouge	72	$4.41 \cdot 10^5$	0.025
2HC6	Duffin	110	$7.05 \cdot 10^5$	0.039
2HC18	Lynde	41	$2.51 \cdot 10^5$	0.036
2HD8	Oshawa	43	$2.33 \cdot 10^5$	0.040
2HD2	Ganaraska	94	$4.17 \cdot 10^5$	0.045
2HM3	Salmon	344	$1.76 \cdot 10^6$	0.038
2HM1	Napanee	233	$1.66 \cdot 10^6$	0.024

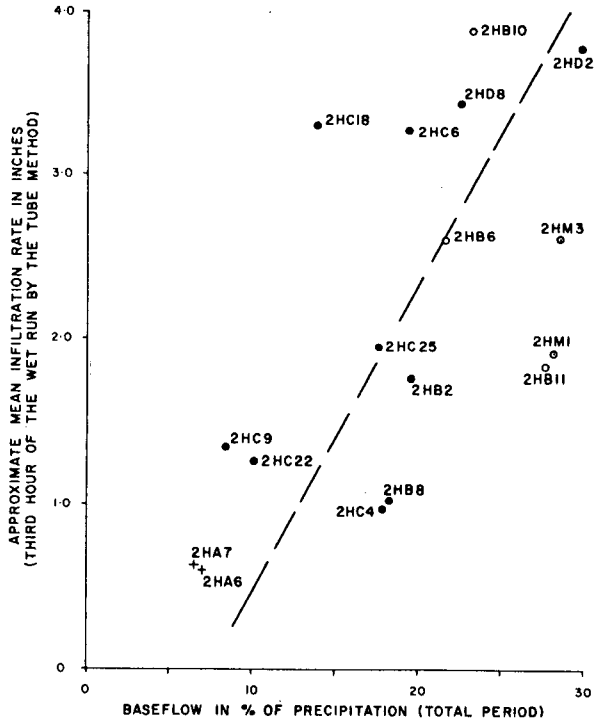

Figure 55. Relation between baseflow and approximate mean infiltration rate through the uppermost feet of soil (gauging stations).

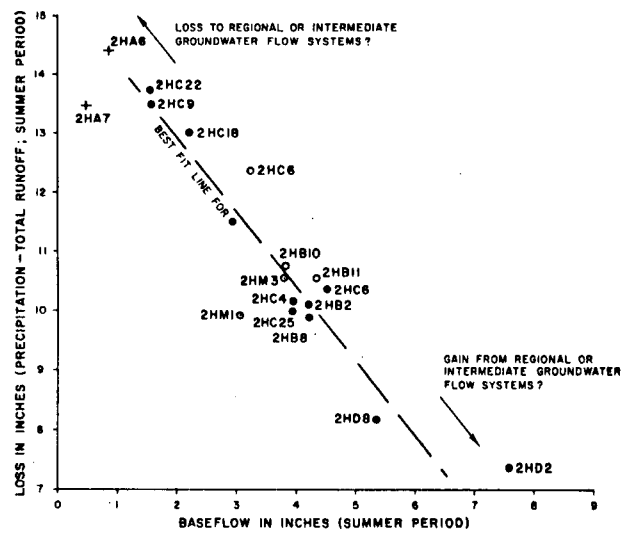

Figure 56. Relation between baseflow and loss (precipitation – total runoff) (gauging stations).

ESTIMATION OF GROUNDWATER DISCHARGE INTO LAKE ONTARIO

For purposes of this study, it is probable that most of the groundwater is intercepted by streams before reaching Lake Ontario. Under the assumption that deep groundwater flow systems and evaporation from groundwater do not significantly affect the magnitude of baseflow, a rough estimate of the groundwater discharge into Lake Ontario based on baseflow data is feasible.

Method A

An area along the shore is discharging its groundwater directly into the lake. By knowing the boundary of this catchment and the baseflow produced per unit area, it is possible to compute the groundwater discharge. In this

catchment a large number of small watercourses exist, which are only active during storms and drain only surface water. They should be considered in defining the drainage area. The catchment was, therefore, outlined during a field survey in July and August 1969 after dry periods of more than four consecutive days. Due to the fluctuation of the groundwater level, however, the drainage area may vary considerably and be much smaller during the winter half year. A rise of the groundwater level of a few feet may activate many of the small watercourses and diminish the direct groundwater flow into the lake and the catchment area, particularly in flat regions. The outlined catchment from Niagara-on-the-Lake to Kingston, consisting of 72 drainage areas with a total area of 390 square miles, was considered to represent only summer conditions.

The baseflow per square mile from the watersheds around the lake was applied to the shore catchment. Because of lack of data, the area east of Kingston and the islands could not be included in the computations. The author is aware that the hydrogeological conditions of the watersheds do not always correspond entirely with the conditions along the shore. This is especially true along the Niagara Peninsula where the baseflow per square mile in the Spencer, Grindstone and Bronte watersheds was applied to the shore area. Table 23 presents the direct local groundwater runoff of the shore catchment computed with summer baseflow data.

Table 23. Estimates of groundwater discharge from the shore catchment (Niagara-on-the-Lake to Kingston, computed from summer period data) after method A

Area (County)	Shore Catchment (sq. mi.)	Extrapolated Baseflow per sq. mi. (cfs)	Groundwater Discharge (cfs)
Lincoln	43	0.28	12.0
Wentworth	15	0.28	4.2
Halton	30	0.28	8.4
Peel	29	0.24	7.0
Ontario	49	0.24	11.8
Durham	34	0.43	14.6
Northumberland	56	0.43	24.1
Hastings	39	0.27	10.5
Lennox & Addington	91	0.27	24.5
Frontenac (W of Kingston)	4	0.27	1.1
TOTAL	390		118.2

Method B

The second method is based on Darcy's Law and estimates the transmissibility according to the equation:

$$T = \frac{Q_b}{I(2L)} \qquad (28)$$

where Q_b *is the baseflow*

I *is the average water table slope*

L *is the stream length*

This method was used successfully by Olmsted and Hely (1962) to compute the average T in a small representative basin. However, in the present study, the terms I and particularly L, cannot be computed accurately and consequently T will be only a rough estimate. The mean water table slope was assumed to be equivalent to the land slope, an assumption which is justified by the results in Chapter 3. The average landslope was obtained by establishing an orthogonal grid over the topographic map of the watershed (Linsley, Kohler, Paulhus, 1949), measuring the length of each grid line within the basin boundary, and counting contour crossings for tangents to each line. The landslope Δs in a north-south or east-west direction is then

$$\Delta s = \frac{N \Delta Z}{\Sigma l} \qquad (29)$$

and the mean slope

$$\Delta s = \frac{\Delta s_{north} + \Delta s_{west}}{2} \qquad (30)$$

where: N is the total number of contour crossings in a given direction

Σl is the total number of lines in that direction, in feet

ΔZ is the contour interval, in feet.

The stream length was measured from topographic maps by using streams printed in blue (the so-called blue-print method). Morisawa (1957) observed a significant difference between the stream length measured in the field and on maps in the United States. In the Lake Ontario basin, it was observed that printing of the stream network even varies considerably between some map editions. Prints after 1964 sometimes show a network which is much too dense. The stream length, L, was therefore computed for all watersheds from earlier editions. On the basis of a field survey, it is believed that the measured stream length is still on the high side and, therefore, the computed T represents a minimum value. The total mean baseflow over the six-year period was used for Q_b.

The computed transmissibilities largely represent the overburden in which exist shallow local groundwater flow systems, especially for the region west of Trenton (Table 24). A plot of K values from the shorebelt versus T values from the river watersheds (Figure 57) for regions A, B and C illustrates a linear relationship. This suggests that both methods of analysis consider the same aquifer materials,

Table 24. Estimated mean watershed transmissibilities from baseflow data.

Station No.	Watershed	Transmissibility (Igpd/ft.)
2HB10	Spencer	1312
2HB6	Grindstone	1123
2HB11	Bronte	1164
2HB8	Rogers	744
2HB2	Credit	605
2HC25	Humber	425
2HC9	East Humber	228
2HC4	Little Don	599
2HC22	Rouge	369
2HC6	Duffin	441
2HC18	Lynde	342
2HD8	Oshawa	595
2HD2	Ganaraska	929
2HM3	Salmon	885
2HM1	Napanee	925

namely the shallow overburden. If it is assumed that the aquifer thickness is constant for the three regions, then the permeability values obtained by the two methods are in fair agreement.

The groundwater discharge directly into the lake is obtained by multiplying T by the flow system width, which is the shoreline length, and the hydraulic gradient obtained from water well data (Table 11):

$$Q = T I W \qquad (31)$$

Because of the lack of baseflow data, the area east of Kingston was not included in the computations. The results

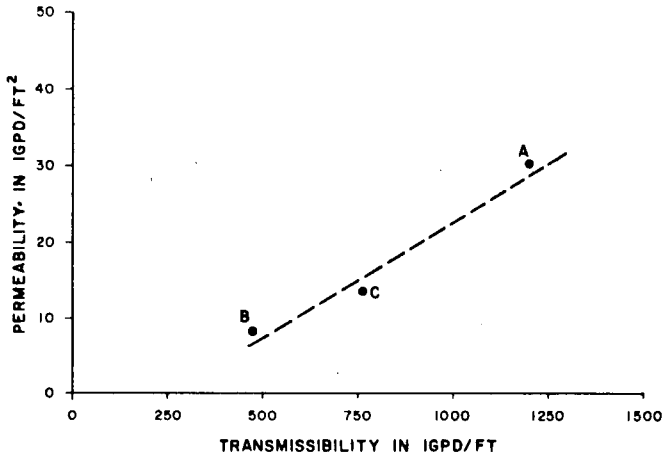

Figure 57. Relation between the coefficient of transmissibility computed from baseflow data and the coefficient of permeability computed from specific capacity data for the shorebelt areas A, B and C.

Table 25. Estimated discharge into Lake Ontario (Niagara-on-the-Lake to Kingston) from baseflow data.

Region	Discharge	
	Igpd	cfs
A	$2.94 \cdot 10^6$	5.46
B	$1.40 \cdot 10^6$	2.61
C	$4.41 \cdot 10^6$	8.19
D	$2.97 \cdot 10^6$	5.52

which are presented in Table 25 represent a conservative estimate of the minimum discharge because T was estimated conservatively.

CHAPTER 5

Buried Valleys

TORONTO AREA

A large number of bedrock channels, most of which are less than 100 feet deep, empty into Lake Ontario between Trenton and Port Credit (Plates II, III, IV, V). Most of them are situated in the area of Toronto, for which Hobson (1970) has given an excellent compilation of the bedrock surface. Since data for deep water wells are very scarce or nonexistent in the Metropolitan Toronto area (Fig. 58), especially in the vicinity of the shore, additional information was sought in the summer of 1969 by drilling seven exploration wells. Although the entire area is almost built over, it was possible to drill three wells in the Humber Valley, two in the Don Valley and one each in the buried channels at Scarborough and West Rouge. The main objectives of the drilling program were:

(a) to delineate bedrock channels and determine the depth of the bedrock,

(b) to determine the hydrogeological conditions in the overburden,

(c) to define the boundary between the Cobourg and Collingwood Formations,

(d) to determine to some extent the hydrogeological conditions in the bedrock,

(e) to obtain water samples from the Cobourg Formation in order to determine the groundwater velocity by means of Radiocarbon (C^{14}) analysis.

Table 26 gives a general review of the achieved goals mentioned above. A summary of the test well data and the

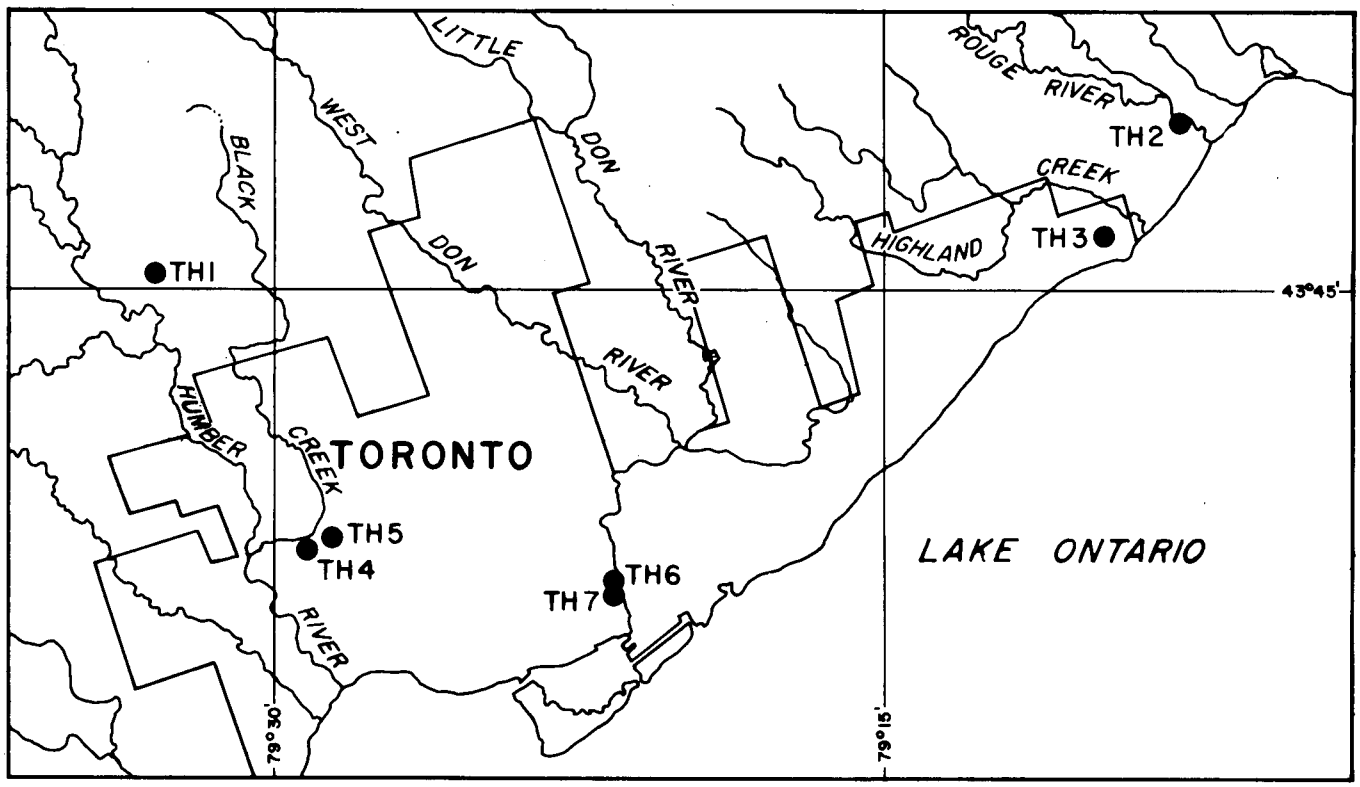

Figure 58. Location of exploration wells TH-1 to TH-7.

Table 26. Achieved objectives of test wells TH1 - TH7.

Achieved Objectives:	a)	b)	c)	d)	e)
TH 1	yes	no	yes	partial	no
TH 2	partial	no	yes	partial	no
TH 3	yes	yes	yes	partial	no
TH 4	yes	yes	N/A	N/A	N/A
TH 5	yes	yes	N/A	N/A	N/A
TH 6	yes	yes	N/A	N/A	N/A
TH 7	yes	yes	N/A	N/A	N/A

detailed borehole logs are presented in Appendix C. All wells have hit the channels intended except TH 2/69 in the Rouge River Valley where, despite geophysical assistance, a very narrow twisted channel close to the stream was missed. Extensive coarse deposits were not encountered near the bottom of the channels. Generally, the overburden does not become more permeable with depth, an observation which corresponds to the result of a previous survey conducted between Toronto and Lake Simcoe (Haefeli, 1970). The data from short pumping tests carried out in TH5 and TH7 are given in Figures 85 and 86 (Appendix C) and a summary is shown in Table 27. These results indicate that, in general, the overburden in the bedrock valleys of the Toronto area probably does not yield more groundwater than the drift to the north and east. Therefore, the bedrock channels have not been treated separately for groundwater discharge computations (Chapter 3). Since the channels were eroded in shale, a source of rather fine sediments, the lack of coarse sediments in channels is not surprising; on the other hand, large quantities of coarse material found in lenticular layers throughout the overburden may have been transported from limestone layers farther north.

The Cobourg Formation and deeper limestone members form reservoir rock from which gas is produced southwest of Toronto. It seems reasonable to assume that for several reasons no significant amount of groundwater flows into Lake Ontario where the Trenton Group is overlain by shale layers. Firstly, no water could be recovered from the Cobourg Formation, even with the use of explosives to induce groundwater flow from the limestone. Also the entrapment of gas near the subcrop of the south dipping Trenton Group (Plate I), suggests the lack of groundwater movement.

The bedrock holes TH1, TH2 and TH3 disclosed some new aspects of the bedrock geology around Toronto (Fig. 59). The thickness of the lower and middle member of the Blue Mountain – Collingwood Formation is considered to be 120 feet at Toronto and wedges out to 30 feet near

Table 27. Summary of test well data.

Well No. GW68-3	Date Completion 1969	Location	Surface Elevation	Borehole ϕ (inch)	Borehole depth (ft.)	Casing ϕ od (inch)	Casing depth (ft.)	Bedrock elevation (ft.)	Drift thickness (ft.)	SWL Drift (ft.)	Pumping Test depth (ft.)	Pumping Test gal/min	Pumping Test drawdown (ft.)
1/69	Oct. 9	79°32'57"	490	$7^7/_8$ $6^1/_4$ 5	525 531 728	$5^1/_2$	531	79	411		bedrock		
2/69	Sept. 23	79°07'36" 43°47'54"	252	$9^7/_8$ $7^7/_8$ $6^1/_4$ 5	26 177 181 325	8 $5^1/_2$	26 181	229	23	4	bedrock	$^1/_8$	
3/69	Sept. 29	79°09'18" 43°45'57"	302	$7^7/_8$ $6^1/_4$ 5	188 193 392	$5^1/_2$	193	207	95	~40	bedrock 92	$^1/_5$ $^3/_4$	~30 after 1^h
4/69	Aug. 21	79°28'56" 43°40'28"	341	$9^7/_8$ $7^7/_8$ $6^1/_4$	9 26 152	8	9	194	147				
5/69	Sept. 6	79°28'40" 43°40'33"	393	$7^7/_8$ $6^1/_4$	232 271	4 screen	212 222	143	250	38.5	222	8.7	2.5 after $7^1/_2{}^h$
6/69	Sept. 15	79°21'51" 43°39'29"	258	$6^1/_4$	103	4 screen	78 83	165	93	9.0	83	5	11 after 3^h
7/69	Sept. 19	79°21'50" 43°39'28"	258	$6^1/_4$	111	4 screen	91 96	159	99	10.9	96	12.5	7.7 after 3^h

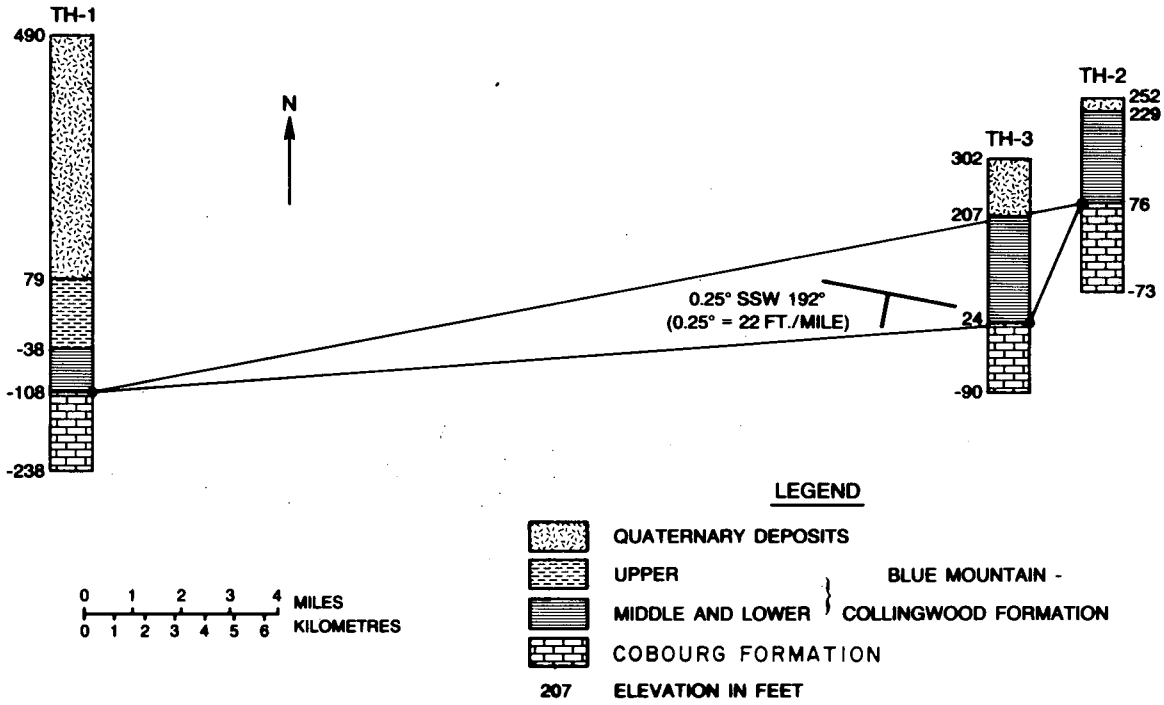

Figure 59. Stratigraphy of bedrock in the exploration boreholes TH-1, TH-2, and TH-3, and inclination of the surface of the Cobourg Formation.

Nottawasaga Bay (Liberty, 1969). This trend was verified by TH1 which penetrated a thickness of 70 feet, and by TH2 and TH3 which penetrated a thickness of greater than 183 feet (eroded top). The dip of the bedding was computed under the assumption that no remarkable disconformity exists between the Cobourg and Collingwood Formations. A computed dip of 22 ft./mile SSW 192° of the bedding corresponds approximately with descriptions by other authors. TH1, one of the deepest bedrock wells in the northern outskirts of Toronto struck the Upper Blue Mountain – Collingwood Formation instead of the anticipated Meaford-Dundas Formation at an unexpected depth of 79 feet a.s.l., thus adding important control to the assumed bedrock boundaries in this particular area (Haefeli, 1970).

DUNDAS VALLEY

The depth of the buried valley passing through Dundas into Hamilton Harbour has long been a subject of speculation and its greatest depth is still not known despite some exploration boreholes drilled in recent years. It has a width at the Burlington Sky Way of approximately 5 miles and a depth of over 450 feet below the lake level (Fig. 60). The valley begins northeast of Brantford, about 25 miles SSW of Hamilton Harbour (Karrow, 1963, 1964), and reaches its great depth due to a sharp drop of the bedrock surface west of Copetown (Plate VII). The Dundas Valley cuts across the Lake Ontario basin boundary, and therefore the amount of groundwater discharge along the valley into the lake is of interest, as is any possible groundwater seepage from outside of the basin.

The permeability values of the overburden from Halton and Wentworth Counties had to be used for the computation of the goundwater inflow into the lake (Fig. 11, Area A) since almost no water wells are situated at the inlet of the valley. The average drift lithology of five exploration wells situated east of Dundas (Plate VII) and of 35 water wells (for depth > 150 feet) further west (Plate VII) is shown in Figure 61. Clay is predominant and the amount of gravel is less than 8 percent. Using the lithologic composition of the overburden as a guide (Fig. 27), the permeability of the Dundas Valley deposits generally appears lower than overburden along the shorebelt of Halton and Wentworth Counties, thus agreeing with the predominant trend observed for the buried valleys on the north side of the lake. For illustration, the drillers log of the deepest exploration borehole is presented in Figure 62. It should be pointed out that the contours of the bedrock surface (Plate VII) were not altered according to new data from the exploration wells because the data are only now being analyzed by J. Terasmae (Brock University, St. Catharines). Because the glacial lacustrine clay of the lake

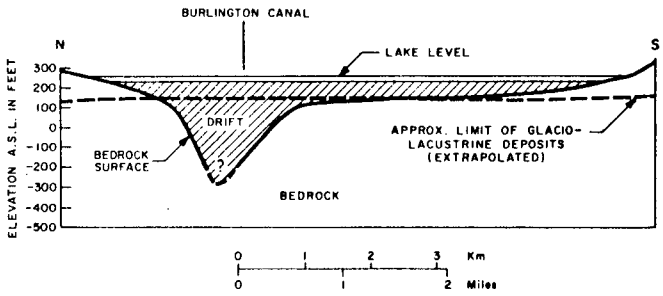

Figure 60. Cross-section through buried Dundas Valley at the Sky Way, Hamilton.

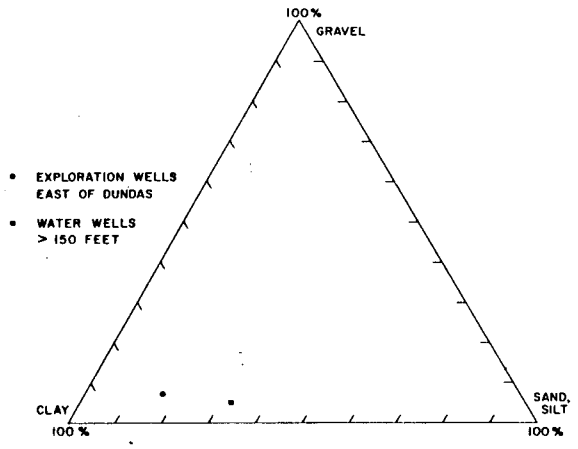

Figure 61. Lithology (after drillers log) of exploration and water wells in the buried Dundas Valley (locations on Plate VII).

bottom appearing below a depth of 100 - 120 feet is overlying the deeper part of the inlet of the buried valley (Fig. 60), the groundwater inflow through the buried valley is reduced substantially (Chapter 3). According to the surrounding Niagara escarpment, it is believed that the three main prevailing groundwater flow directions at the inlet of the valley are: NNE and SSE into Hamilton Harbour only; and ENE into Hamilton Harbour and Lake Ontario. Values for the hydraulic gradients, which are assumed to correspond to the mean slope of the land surface, range between 0.014 and 0.031. By computing the various cross-sectional areas perpendicular to three main flow directions, an approximate total inflow of 3.15 cubic feet per second through the overburden resulted. It is believed that this inflow might be rather large because the permeability was extrapolated from adjacent areas.

To obtain the boundary of the groundwater flow systems, the piezometric surface along the buried valley was determined and the flow pattern was analyzed after Freeze's numerical method. The piezometric surface

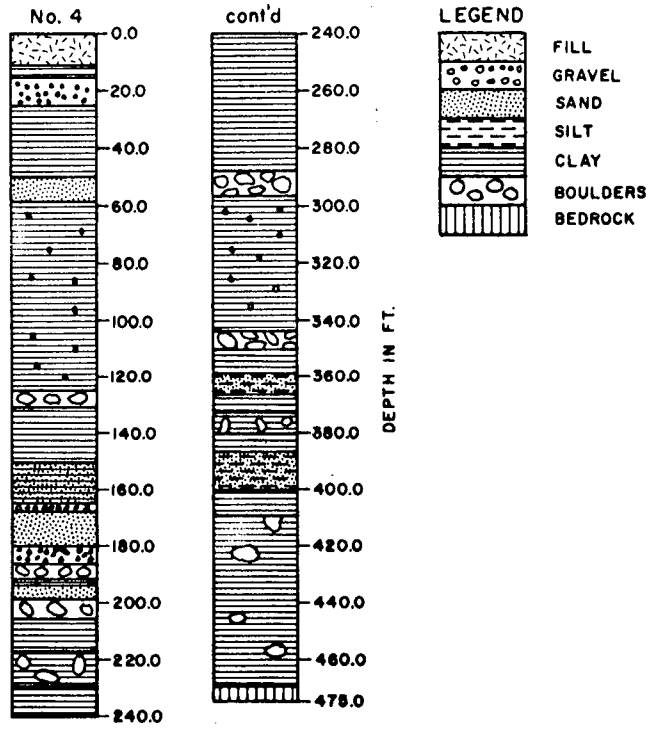

Figure 62. Drillers log of exploration borehole No. 4 in the buried Dundas Valley.

obtained by means of water well records (Ontario Water Resources Commission) and a field survey is presented in Plate VII. Only wells with depths greater than 150 feet were considered to indicate the distribution of the hydraulic head of deeper flow systems. The groundwater divide cannot be pinpointed from Plate VII, because it is situated within the 700-foot contour interval not more than 0.5 mile east and 2.5 miles west from the basin boundary. A more accurate picture is provided by a generalized profile (Plate VIII) along the deepest part of the valley showing the entire groundwater flow pattern. For the upper 200 feet of the overburden, the groundwater divide and the basin boundary coincide approximately. Due to the steep incline of the bedrock surface west of Copetown, however, the divide is shifted for up to two miles to the west in the lower drift and bedrock. This is mainly because the influence of the piezometric surface configuration (established mainly from wells between 150 and 250-feet deep) is diminishing and the influence of the steep bedrock surface is increasing (permeability boundary). The permeability values should be of the right order of magnitude and should at least represent the permeability relations between the different layers. It should also be pointed out that the land surface east of the basin boundary has been very generalized. According to these results, it seems probable that the buried Dundas Valley does not transmit a significant amount of groundwater from outside of the basin.

NIAGARA PENINSULA

Lake Erie, which is separated from Lake Ontario by the Niagara Peninsula has a surface elevation of 572 feet and lies 325 feet higher than Lake Ontario. The ill-defined basin divide with an altitude between 580 and 650 feet follows within one to six miles of the Lake Erie shore from Buffalo to Dunnville where it bends off and follows the Grand River in a NW direction. Since the basin boundary of Lake Ontario is not much higher than Lake Erie, only eight to fifteen feet between Morgans Point and Mohawk Point (Fig. 63), groundwater seepage into Lake Ontario appeared to be possible. Watershed boundaries farther inland, however, have an altitude of over 600 feet.

A general investigation carried out by R. Ostry, Ontario Water Resources Commission, indicated that there is no major groundwater flow through the bedrock or Quaternary deposits from Lake Erie into Lake Ontario (personal communication). However, a buried valley leading from Lowbanks over Welland and Fonthill to Jordan Harbour has a bedrock elevation of about 400 feet between Lake Erie and Fonthill, and was considered worthy of being examined in the field. Twenty-eight water wells with depths exceeding 50 feet were surveyed at the inlet of the channel in the vicinity of Morgans Point, Mohawk Point, and Wainfleet (Fig. 63). The elevations of the wells were determined within an accuracy of 2 feet and the water levels were obtained from the well records of the Ontario

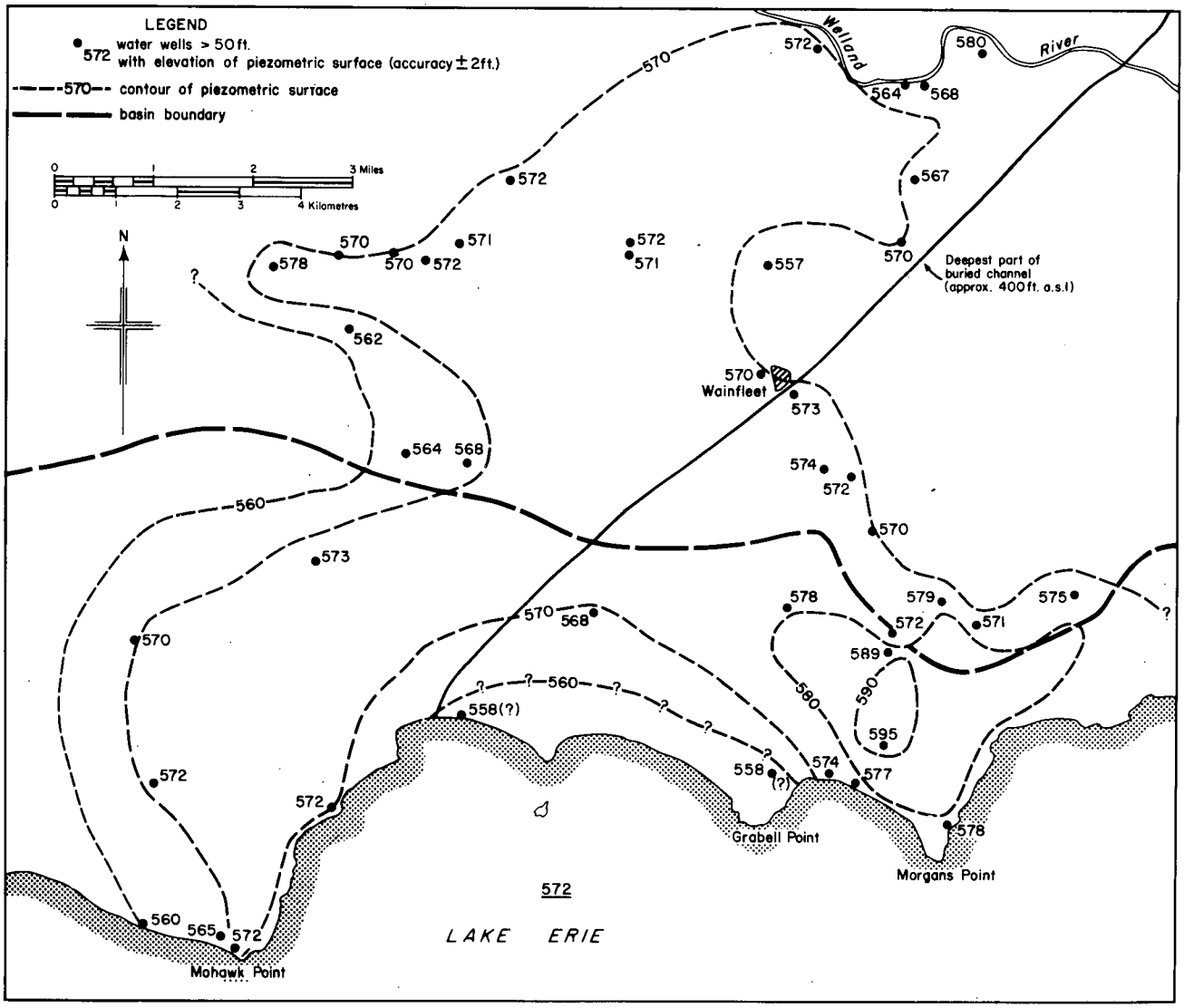

Figure 63. Contour map of piezometric surface between Welland River and Mohawk Point.

Water Resources Commission. Except for a small anomalous inclination of the groundwater level near Lake Erie for which no explanation is offered, the groundwater level remains almost horizontal up to the Welland River. The elevation of 570 ± 5 feet exists over a distance greater than 7 miles. With very low hydraulic gradient, the groundwater velocity must be extremely low. Along with an increased surface elevation in the Fonthill region farther north and the flat bedrock surface, seepage from Lake Erie through the buried channel fill appears to be impossible.

A representative profile (Plate VIII) was produced for the Niagara Peninsula, showing the general groundwater flow pattern between Grant Point and Grimsby. The shape of the groundwater table is considered to be given by the land surface, which has been very generalized. Only major elevation changes were taken into account. The profile shows a distinct local groundwater flow system with various recharge and discharge areas and a regional system showing one groundwater divide in the bedrock (Plate VIII). Due to the sharply declining groundwater level at the Niagara escarpment, the bedrock groundwater divide is situated over five miles north of the highest surface elevation and 13 miles away from the basin boundary. However, the difference in hydraulic head between the groundwater divide in the bedrock and Lake Erie remains significant. Although the bedrock groundwater divide on the Niagara Peninsula may generally be much closer to Lake Ontario than the basin boundary, seepage from Lake Erie through the bedrock seems to be very unlikely.

TEMPERATURE SURVEYS

An attempt was made to detect concentrated groundwater inflow along the shore by means of temperature surveys in Lake Ontario and by remote infrared scanning from an aircraft. The temperature of groundwater occurring at a depth of 30 to 60 feet generally exceeds the mean annual air temperature by 1 to 2°C. The annual range of the earth's temperature at this depth may be expected to be less than 1°C (Todd, 1959). At greater depths, the temperature increases approximately 1°C for each 100 feet. The average annual temperature is approximately 7°C in the Lake Ontario basin, while the temperature of the groundwater for the upper 100 feet varies from about 8° to 11°C (46° to 52°F). In comparison to the upper few feet of the lake water the groundwater is expected to be warmer during the winter months and colder during the summer and early fall (Fig. 64). Accordingly, it should be possible to detect groundwater discharge into the lake, particularly

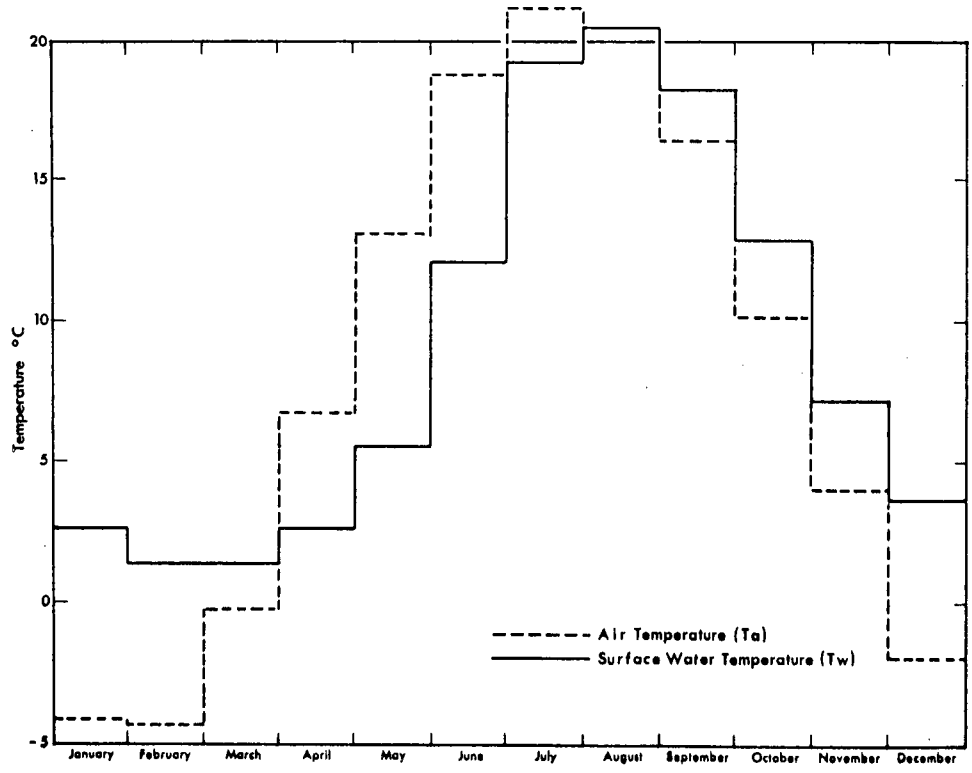

Figure 64. Mean surface water and air temperature of Lake Ontario (after Bruce and Rodgers in Pincus, 1962).

strong local discharges. If the average velocity of the groundwater inflow is less than 1 ft./day ($3.5 \cdot 10^{-4}$ cm/sec.) compared to current velocities of from 5 to 40 cm/sec. (Weiler, 1968) in Lake Ontario, any temperature difference between groundwater infiltrating the lake bottom and the lake water itself could be dissipated very quickly. To make detection possible, the velocity of the groundwater presumably has to be very large and its inflow should be concentrated locally. These requirements might be fulfilled by buried valleys containing highly permeable gravel deposits, or by large open bedrock fractures, or extremely high hydraulic gradients in moderately permeable material.

In cooperation with the Canada Centre for Inland Waters (CCIW) at Burlington, a temperature survey from a boat was performed in July 1969 along the shore from Niagara-on-the-Lake to Kingston. The launch was instrumented with a single channel recorder, a thermistor bridge with selector switch and three temperature sensors having an accuracy of ± 0.1°C and a time constant (response time) of approximately 0.2 second. One sensor was installed at the cooling water intake of the boat motor underneath the hull, approximately one foot below water level; another was towed beside the boat at a depth of about 3 feet; and the third sensor was used to perform vertical profiles. The survey was carried out at an approximate lake depth of 10 - 12 feet with the depth being controlled by a recording echo sounder. First, horizontal profiles along the shore were taken at a speed of 5 - 7 miles/hour. Then vertical profiling was attempted at locations where temperature anomalies were indicated. Although the vertical profiling was not completed due to mechanical difficulty, it became apparent that the influence of currents, winds, streams and man made factors (sewage, irrigation, cooling water, etc.) tends to mask effluent groundwater in certain areas. The masking effect appears strongest between Toronto and Hamilton and to a lesser degree between Port Dalhousie and Niagara-on-the-Lake. Cold anomalies for which none of the above mentioned factors could be related are considered to be questionable groundwater inflow spots and are marked as such in Figure 65. Cool anomalies do not appear to correspond to the locations of buried bedrock channels, which generally are filled with rather low permeable till deposits (Chapter 3). No remarkable anomalies were found east of Trenton where concentrated inflow through fractures or karstic hollow spaces could occur. However, along steep bluffs, erratic temperature changes were sometimes observed. Two different examples are shown in Figures 66 and 67.

In connection with infrared survey experiments in Canada, H.R.B. Singer Inc. carried out flights in October 1965 along the shore between Cobourg and Niagara-on-the-Lake. For the present study, additional flights over the same area were performed in March 1969 and 1970 by the

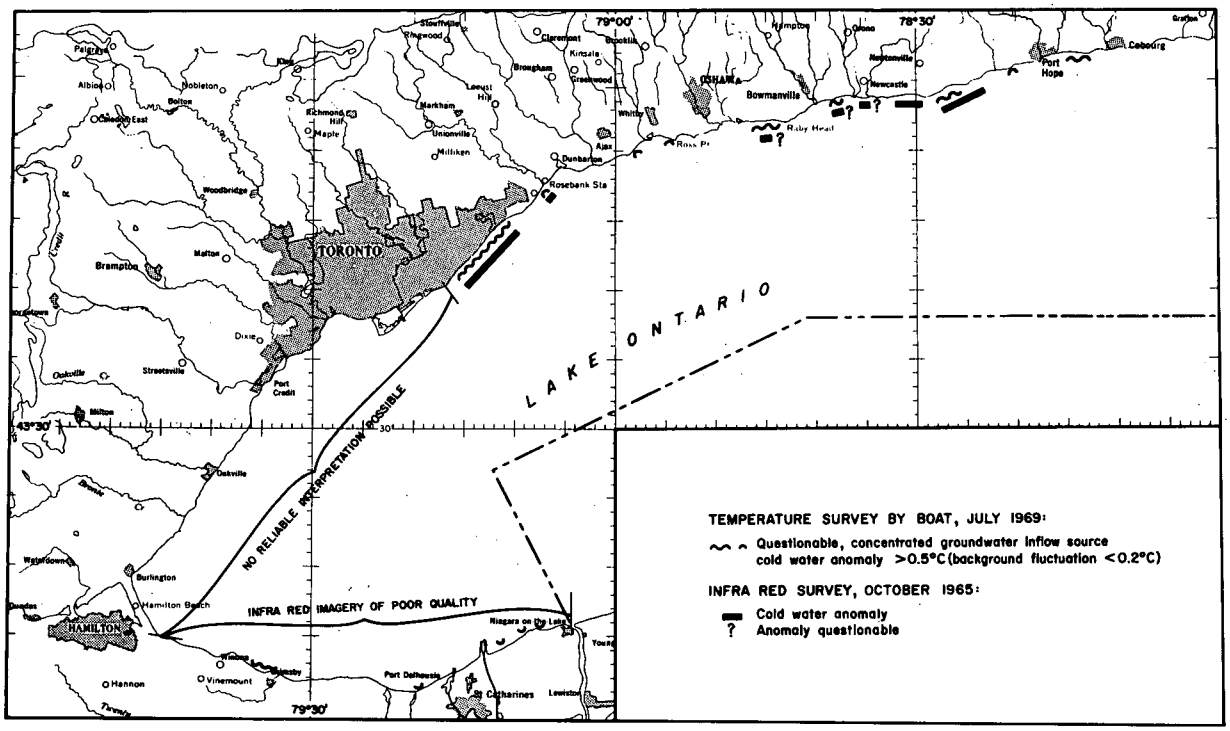

Figure 65. Locations of concentrated groundwater inflow sources detected by temperature and infrared surveys.

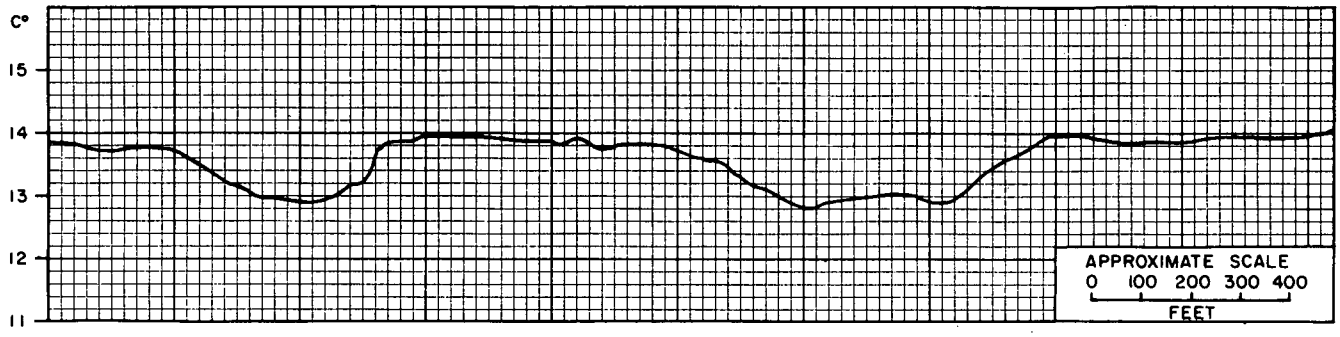

Figure 66. Chart of temperature survey by boat showing erratic anomalies at Birch Cliff (Scarborough).

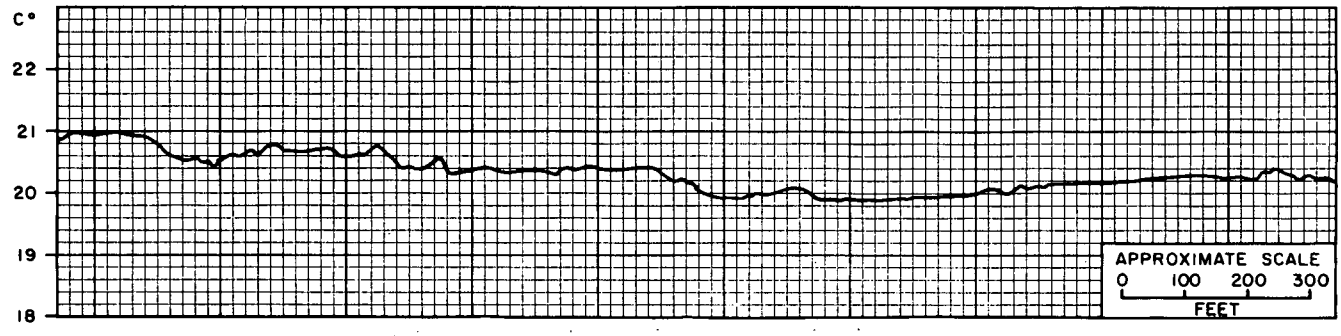

Figure 67. Chart of temperature survey by boat showing erratic anomalies along bluffs west of Grimsby.

National Research Council under the direction of N. de Villiers.

The IR imagery is well suited, as Slaney, Gross and Morley (1969) pointed out, for examining details of the temperature changes in water bodies. However, the IR scanner has no penetrating power; it measures and records on film only the radiation from the top few layers of molecules. Warmer temperature appears as light areas and cooler temperature as dark areas on the imagery. The thermal sensitivity of the equipment depends on the temperature range of the scan area on the ground; the smaller the temperature range, the better the accuracy. The smallest temperature change the instrument is capable of detecting is about 0.01°C. Since most of the time the land surface has a much different temperature than the lake water, the accuracy of the method used at the present time along the shoreline is drastically reduced. This and the capability of recording only temperatures of the skin of the water appear to be the major shortcomings in the endeavor to pinpoint groundwater inlets. Nevertheless, positive results have been obtained in this field by Slaney, Gross and Morley (1969). Good descriptions of the principles of infrared scanning are provided by the same authors and by de Villiers (1969).

Probably because of the low turbulence in the lake, the best imagery was obtained in October 1965 from an altitude of 5000 feet. Aside from three questionable small spots, all anomalies were recorded along high bluffs between Cobourg and Toronto (Figure 65). Unfortunately, the quality of the IR imagery did not allow any interpretation for the area between Hamilton and Niagara-on-the-Lake. The relationship between high steep shores and cold water anomalies, observed also to a minor degree on the boat survey, seemed to be significant. It may be explained in terms of groundwater discharge along the bottom of the bluffs where the hydraulic gradient may be large. The groundwater level in the 4-kilometer wide shorebelt is 10 - 20 feet below the surface (Table 11) and it declines rapidly in the direction of the bluffs, which are up to 250 feet high. The hydraulic gradient (Table 11), and with it the groundwater velocity, may increase in these areas by two orders of magnitude or more, causing a concentrated shallow groundwater outflow close to the lake surface (Fig. 68). Figures 69 and 70 show two such temperature anomalies at Scarborough and east of Newcastle between Bouchette Point and Crysler Point.

Although the infrared surveys were rather limited, substantial anomalies other than those related to bluffs

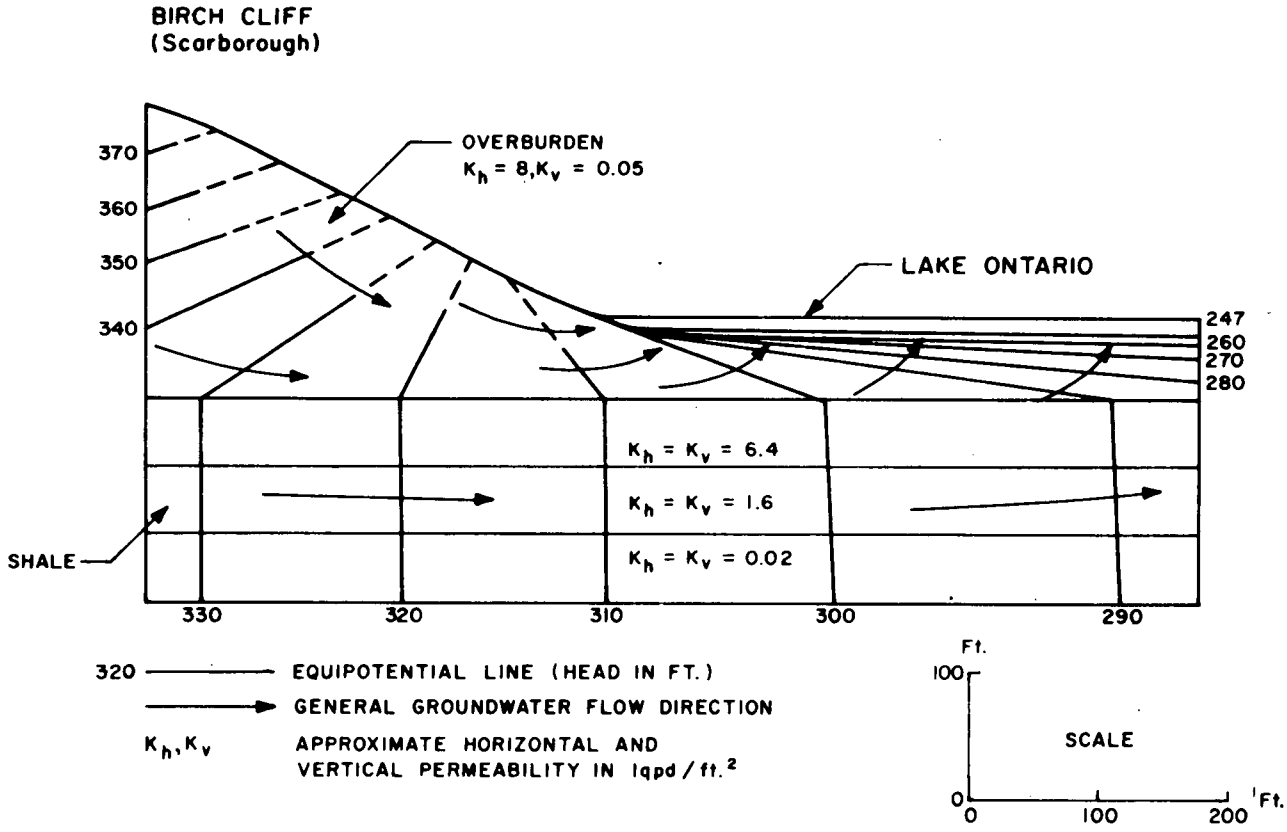

Figure 68. Distribution of equipotential lines and general groundwater flow direction at Birch Cliff (Scarborough).

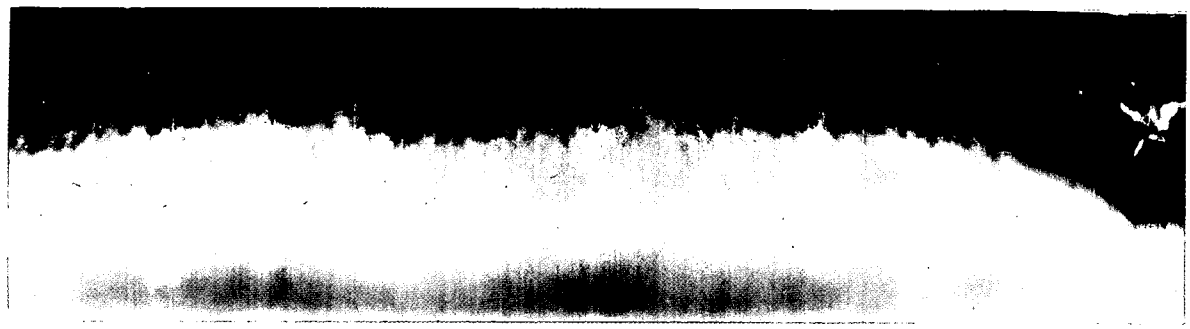

Figure 69. Infrared imagery at Birch Cliff, Scarborough (scale: 1 inch approximately 3600 ft.).

Figure 70. Infrared imagery between Bouchette Point and Crysler Point (west of Port Hope) (scale 1 inch approximately 3600 ft.).

were not detected. This may be interpreted as indicating the absence of local large groundwater discharge, or it may be taken as an indication that the low temperature effect of groundwater discharge is masked by other influences such as currents, wind and industrial and municipal waste disposal.

CHAPTER 6

Summary and Conclusions

1. A major part of this study was based on data from some 2000 bedrock and overburden water wells which were mainly situated within a 2.5-mile wide shorebelt area between Niagara-on-the-Lake and Iroquois. The majority of them (over 90 percent) showed confined aquifer conditions. Their median well diameter was approximately 6 inches and their median pumping time, only 1.2 hours. A median storage coefficient of $2 \cdot 10^{-4}$ was determined for the confined overburden aquifers and $2.5 \cdot 10^{-4}$ was assumed for the confined bedrock aquifers. The permeability of the different formations was computed from specific capacity data using a modified version of the Theis nonequilibrium formula.

2. The overburden, consisting mainly of till deposits (essentially clay and silt), seems to influence the water yielding capacity of the underlying bedrock. The specific capacity of bedrock water wells decreases with increasing overburden thickness. Because of the lack of well data and the strong skewness of the specific capacity figures, no exact relationship between these two parameters could be established.

3. The specific capacity and the permeability decrease sharply with bedrock depth, presumably due to decreasing fracture opening and frequency. Rocks with low strength tend to close their fractures quicker with depth and rapidly become less permeable. The following relationship was found (K is the permeability, d is the bedrock depth):
for shale, $\log K = -8.3 \log d + 14.9$
for limestone, $\log K = -5.6 \log d + 10.08$
The trend corresponds with the equation found for crystalline rocks in a different area: $\log K = -1.67 \log d + 3.28$.

4. The permeability of the glacio-lacustrine clay which covers the major part of the lake bottom was determined by consolidation tests from core samples. Depending on the overburden pressure, the permeability varied between 0.17 and $1.7 \cdot 10^{-3}$ Igpd/ft.^{2} (10^{-5} to 10^{-7} cm/sec.). The glacio-lacustrine clay controls the groundwater inflow in areas where the permeability of the bedrock exceeds that of the clay.

5. The vertical permeability, K_v, of the overburden was determined by analyzing pumping tests carried out under leaky artesian conditions after the equations by Hantush and Jacob. According to the nature of the confining bed, K_v varied between 0.041 and 5.3 Igpd/ft^2 and the coefficient of leakage varied between $8.2 \cdot 10^{-4}$ and $8.8 \cdot 10^{-2}$.

6. The mean groundwater level of the shorebelt follows very closely the land surface. For the area within 0 - 1.25 miles from shore, the mean groundwater level was 13.7 feet below land surface, and for the area situated 1.25 to 2.5 miles from shore, 14.8 feet. The mean hydraulic gradient determined county-wise varied between 0.0056 and 0.0154 in the 2.5 mile wide shorebelt. The average groundwater velocity is less than 0.1 foot /day for the overburden as well as for the bedrock.

7. The vertical profile along the lakeshore from Niagara-on-the-Lake to Iroquois shows the overburden to have a total cross-sectional area of $1.82 \cdot 10^8$ ft^2 (6.55 sq. miles). The bedrock is generally very close to the surface or outcropping between Iroquois and Trenton. From there it declines gradually towards the Toronto area, forming buried valleys with a maximum depth of 170 feet below lake level. The average southern inclination of the bedrock surface in this area is 0.008 to 0.01 (ft./ft.). No major buried channels exist between Port Credit and Burlington. The Dundas buried valley, with a depth exceeding 450 feet below lake level, by far the largest one, has its inlet at Hamilton Harbour. The drift thickness between Hamilton and Niagara-on-the-Lake is between 20 and 60 feet, with a few exceptions; the bedrock is outcropping near Grimsby while between Jordan Harbour and Niagara-on-the-Lake, three buried valleys have depths of less than 100 feet.

8. The baseflow of 20 watersheds situated around the Canadian side of Lake Ontario was analyzed for the period May 1, 1961 to April 30, 1967. The recession constant, K_2, obtained from Butler's equation, varied between 10 and 51 days. The mean baseflow in cfs/sq. mile, computed from a reproduceable, average method ranged for the total period between 0.15 and 0.69 (6.5 and 29.8 percent of precipitation) and between 0.03 and 0.56 for the summer half year. Q_{90}, the discharge of streams equaled or exceeded 90 percent of time, varied between 0.0 and 0.56 cfs/sq. mile. To obtain Q_{90} most conveniently from streamflow

records, the computer program FREQ was developed. There exists a definite relationship between the baseflow and Q_{90} as well as between the average infiltration rates of soils and the total loss (precipitation minus total runoff).

9. The groundwater inflow into the Canadian side of Lake Ontario was computed in three different ways: (a) after the classic method (Darcy) using permeability values converted from specific capacity data of water wells situated in the shore belt area, the average hydraulic gradient of this region and the cross-sectional area along the shore; (b) after a numerical method developed by Freeze, and based on Laplace's equation, using ten representative profiles perpendicular to the shore, computing for each of them, the distribution of the hydraulic potential and by means of a quantitative flow net, the groundwater flow; (c) after two methods, Methods A and B, using baseflow data but ignoring deep groundwater flow systems; method A extrapolates the baseflow per unit area of the watersheds around the lake to the shore catchment discharging directly into Lake Ontario; method B uses the transmissibility values, T, computed from baseflow, the average water table slope and stream length of the various watersheds. T is extrapolated to the shore area and used with the shore length and the hydraulic gradient (from the classic method) to derive the groundwater inflow.

The results of the various methods are listed in the following table:

10. The effect of buried, bedrock valleys on the groundwater divide of the Lake Ontario basin was studied according to their presence in three different areas: between Toronto and Lake Simcoe; in the Hamilton area; and on the Niagara Peninsula. A previous study (Haefeli, 1970) showed that the groundwater divide coincides generally with the basin boundary south of Lake Simcoe. The same was found for the buried Dundas Valley at Hamilton. No groundwater is seeping from Lake Erie into Lake Ontario; however, the groundwater divide in the bedrock seems to be farther north than the basin boundary and, thus, groundwater is drained from the Lake Ontario basin.

11. In buried valleys where exploration holes were bored (Dundas, Humber, Don) the overburden was generally less permeable than the surrounding Quaternary deposits. In particular, no extensive gravel layers were found at the valley bottoms. The boreholes also revealed that the Cobourg Formation and other limestone members below, being gas-producing zones in southwestern Ontario, still carry enough gas in the Toronto area to prevent any significant groundwater flow.

12. The detection of concentrated groundwater inflow along the shore, in particular through buried valleys, was attempted by temperature surveys using a conventional method by boat and by remote infrared sensing. No temperature anomalies could be attributed with certainty

Table 28. Comparison of total discharge computed using various methods.

Method	Total Inflow (cfs.)	Adjustments	Remarks
Classic	51.6	+approx. 9 cfs. for flow through overburden (Hydraulic gradient).	Values rather on the low side, probably too much emphasis on overburden thickness in relation to bedrock permeability.
Numerical	63.7	None	
Baseflow A	118.2	+approx. 20 percent for the area between Kingston and Iroquois	rough estimation.
Baseflow B	21.8		probably too low (stream length %)

Due mainly to the many non-controllable factors associated with the determination of the permeability, it is believed that the error for any of the computed discharge data could exceed 100 percent. Compared with the stream runoff which might be approximately two orders of magnitude higher, the groundwater inflow becomes almost a negligible factor for the terrestrial water balance of the Lake Ontario basin.

to buried valleys or large open bedrock fractures, either because the velocity of the inflowing groundwater was too low in comparison with lake currents or because the velocities were non-existent. However, a positive relationship was found between high steep shores and temperature anomalies which may be due to the rapidly increasing hydraulic gradient and groundwater velocity towards the bottom of the bluffs.

References

American Association of Petroleum Geologists, and The Society of Economic Paleontologists and Mineralogists, 1964. Guide Book, Geology of Central Ontario.

Ayers, H.D., and J.Y.H. Ding, 1967. Effects of Surficial Geology on Streamflow Distribution in Southern Ontario, Canadian Journal of Earth Sciences, Vol. 4, 1967, pp. 187-197.

Barnes, B.S. 1939. The Structure of Discharge-Recession Curves, Trans. Amer. Geophys. Union, 1939, Part IV, pp. 221-225.

Barroclough, J.T., W.E. Teasdale, J.B. Robertson, and R.G. Jensen, 1967. Hydrology of the National Reactor Testing Station, Idaho. Report TID-45, USGS open file.

Bennett, R.R. 1962. Flow Net Analysis. *in* Theory of Aquifer Tests by J.G. Ferris, et al., United States Geological Survey Water-Supply Paper 1536-E, pp. 139-168.

Bental, R. 1963. Methods of Determining Permeability, Transmissibility, and Drawdown. United States Geological Survey Water-Supply Paper 1536-I.

Brown, D.M., G.A. McKay, and L.J. Chapman, 1968. The Climate of Southern Ontario. Department of Transport, Meteorological Branch. Climatological Studies Number 5.

Bruce, J.P., and G.K. Rodgers, 1962. Water Balance of the Great Lakes System, in Great Lakes Basin. Publication No. 71 of the American Association for the Advancement of Science.

Butler, S.S. 1957. Engineering Hydrology, Prentice-Hall, Inc., Englewood Cliffs, N.J.

Caley, J.F. 1941. Paleozoic Geology of the Brantford Area, Ontario, Geological Survey of Canada, Memoir 226.

Caley, J.F. 1961. Paleozoic Geology of the Toronto-Hamilton Area, Ontario, Geological Survey of Canada, Memoir 224.

Canadian National Committee for the International Hydrological Decade, 1967. Groundwater Streamflow Systems.

Carr. P.A. 1968. Hydrogeology of the Moncton Map Area, New Brunswick. Department of Energy, Mines and Resources, Inland Waters Branch, Scientific Series No. 1.

Casagrande, A. 1937. Seepage Through Dams, Harvard Graduate School, Engineering Publication 209.

Castany, G. 1967. Traité Pratique des Eaux Souterraines, Dunod, Paris.

Chapman, L.J., and D.F. Putnam, 1943. The Moraines of Southern Ontario, Trans. Royal Society of Canada, Section IV, 1943, pp. 33-41.

Chapman, L.J., and D.F. Putnam, 1943. The Physiography of Southwestern Ontario, Reprinted from Scientific Agriculture, Vol. 24, No. 3, Nov. 1943, pp. 101-125.

Chapman, L.J., and D.F. Putnam, 1949. The Recession of the Wisconsin Glacier in Southern Ontario, Trans. Royal Society of Canada, Volume XLIII, Series III, June 1949, Section IV, pp. 23-52.

Chapman, L.J., and D.F. Putnam, 1966. The Physiography of Southern Ontario, Second Edition, University of Toronto Press.

Cross, W.P. 1949. The Relation of Geology to Dry Weather Stream Flow in Ohio, Trans. Amer. Geophys. Union, Vol. 30, No. 4, Aug. 1949, pp. 563-566.

Croxton, F.E., and D.J. Cowden, 1939. Applied General Statistics, Prentice-Hall, Inc., New York.

Csallany, S., and W.C. Walton, 1963. Yields of Shallow Dolomite Wells in Northern Illinois, Illinois State Water Survey, Report of Investigation 46.

Davis, S.N., and L.J. Turk, 1964. Optimum Depth of Wells in Crystalline Rocks, Groundwater, Vol. 2, No. 2, April 1964, pp. 6-11.

Deane, R.E. 1950. Pleistocene Geology of the Lake Simcoe District, Ontario, Geological Survey of Canada, Memoir 256.

Department of Energy, Mines and Resources, Inland Waters Branch, Water Survey of Canada, 1970. Description of Card and Tape Formats for Supplying Streamflow Data, Data Control Section, Ottawa.

Department of Public Works, Testing Laboratories, 1968. Hamilton-Dundas, Ontario. Stratigraphic Drilling.

Dickinson, W.T. 1963. Unit Hydrograph Characteristics of Selected Ontario Watersheds, M.Sc. thesis in Agriculture, Toronto.

Ferris, J.G., et al, 1962. Theory of Aquifer Tests, United States Geological Survey Water-Supply Paper 1536-6.

Forchheimer, 1930. Hydraulik, 3d ed., Leipzig and Berlin, Teubner.

Free, G.R., G.M. Browning, and G.W. Musgrave, 1940. Relative Infiltration and Related Physical Characteristics of Certain Soils, United States Department of Agriculture, Tech. Bull. No. 729.

Freeze, R.A. 1969a . Theoretical Analysis of Regional Groundwater Flow, Department of Energy, Mines and Resources, Inland Waters Branch, Scientific Series No. 3.

Freeze, R.A. 1969b . Regional Groundwater Flow – Old Wives Lake Drainage Basin, Saskatchewan. Department of Energy, Mines and Resources, Inland Waters Branch, Scientific Series No. 5.

Freeze, R.A. 1969c . Hydrogeology and Groundwater Resources of the Gravelbourg Aquifer, Saskatchewan. Department of Energy, Mines and Resources, Inland Water Branch, Scientific Series No. 6.

Freeze, R.A., and P.A. Witherspoon, 1966. Theoretical Analysis of Regional Groundwater Flow-I. Analytical and Numerical Solutions to the Mathematical Model. Water Resources Research, Vol. 2, No. 4.

Freeze, R.A., and P.A. Witherspoon, 1967. Theoretical Analysis of Regional Groundwater Flow-II. Effect of Water-Table Configuration and Sub-Surface Permeability Variation, Water Resources Research, Vol. 3, No. 2.

Freeze, R.A., and P.A. Witherspoon, 1968. Theoretical Analysis of Regional Groundwater Flow-III. Quantitative Interpretations. Water Resources Research, Vol. 4, No. 3.

Geological Survey of Canada, 1967. Groundwater in Canada. Edited by I.C. Brown, Geological Survey of Canada, Economic Geology, Report No. 24.

Gravenor, C.P. 1957. Surficial Geology of the Lindsay-Peterborough Area: Ontario, Victoria, Peterborough, Durham, and Northumberland Counties, Ontario, Geological Survey of Canada, Memoir 288.

Haefeli, C.J. 1970. Regional Groundwater Flow Between Lake Simcoe and Lake Ontario, Department of Energy, Mines and Resources, Inland Waters Branch,Tech. Bull. No. 23.

Hantush, M.S. 1956. Analysis of Data From Pumping Tests in Leaky Aquifers, Trans. Amer. Geophys. Union, Vol. 36, No. 6.

Hantush, M.S. 1961. Drawdown Around a Partially Penetrating Well, Journal of the Hydraulics Division, American Society of Civil Engineers.

Hantush, M.S., and C.E. Jacob, 1955a. Non-Steady Radial Flow in an Infinite Leaky Aquifer, Trans. Amer. Geophys. Union, Vol. 36, No. 1.

– 1955b. Non-Steady Green's Functions for an Infinite Strip of Leaky Aquifers, Trans. Amer. Geophys. Union, Vol. 36, No. 1.

– 1955c. Steady Three-Dimensional Flow to a Well in a Two-Layer Aquifer, Trans. Amer. Geophys. Union, Vol. 36, No. 2.

Hantush M.S., and R.G. Thomas, 1966. A Method for Analyzing a Drawdown Test in Isotopic Aquifers, Water Resources Research, Vol. 2, No. 2, Second Quarter, 1966, pp. 281-285.

Harr, M.E. 1962. Groundwater and Seepage, McGraw-Hill, Inc., New York.

Hely, A.G., and F.H. Olmsted, 1963. Some Relations Between Streamflow Characteristics and the Environment in the Delaware River Region, United States Geological Survey, Professional Paper 417-B.

Hewitt, D.F. 1966. Geological Notes for Map 2117, Paleozoic Geology of Southern Ontario, Ontario Department of Mines, Geological Circular 15.

Hobson, G.D. 1970. Bedrock Topography of an Area North of and Including Metro Toronto, Geological Survey of Canada, Paper 70-25.

Hobson, G.D. and J. Terasmae, 1969. Pleistocene Geology of the buried St. Davids Gorge, Niagara Falls, Ontario, Geophysical and Palynological Studies, Geological Survey of Canada, Paper 68-67.

Hofbauer, J. 1968. Analysis of the Ground Water Hydrograph, International Association of Scientific Hydrology, Publication No. 77, pp. 219-224.

Hoffman, D.W., B.C. Matthews, and R.E. Wicklund, 1964. Soil Associations of Southern Ontario, Report No. 30 of the Ontario Soil Survey.

Horton, J.H., and R.H. Hawkins, 1965. Flow Path of Rain from the Soil Surface to the Water-Table, Soil Science, Vol. 100, No. 6, Dec. 1965, pp. 377-383.

Horton, R. 1935. Surface Runoff Phenomena, Part 1, Analysis of the Hydrograph, Horton Hydrological Laboratory, Publication 101, New York.

Hubbert, M.K. 1940. Theory of Groundwater Motion, Journal of Geology, Vol. 48, No. 8, Part 1, pp. 785-944.

Hurr, R.T. 1966. A New Approach for Estimating Transmissibility from Specific Capacity, Water Resources Research, Vol. 2, No. 4, Fourth Quarter, 1966.

Jacob, C.E. 1946. Effective Radius of Drawdown Test to Determine Artesian Well, Proceedings of American Society of Civil Engineers, Vol. 72, No. 5, May, 1946.

Jacob, C.E. 1950. Flow of Groundwater, *Chapter 5 in* Engineering Hydraulics. John Wiley and Sons, New York.

Jamieson, E.R. 1961. The Geology of the Paleozoic Rocks in an area south of Knowlton Lake, Frontenac County, Ontario, Unpublished B.Sc. thesis, Queen's University, Kingston, Ontario.

Johnston, W.A. 1916. The Trent Valley Outlet of Lake Algonquin and the Deformation of the Algonquin Water-Plane in the Lake Simcoe District, Ontario, Geological Survey of Canada, Museum Bulletin No. 23, Geological Series,No. 32.

Karrow, P.F. 1963. Bedrock Topography of the Galt Area, Southern Ontario, Ontario Department of Mines, Map 2030.

Karrow, P.F. 1963. Bedrock Topography of the Brantford Area, Southern Ontario, Ontario Department of Mines, Map 2035.

Karrow, P.F. 1964. Bedrock Topography of the Hamilton Area, Southern Ontario, Ontario Department of Mines, Map 2034.

Karrow, P.F., J.R. Clark, and J. Terasmae, 1961. The Age of Lake Iroquois and Lake Ontario, Journal of Geology, Vol. 69, No. 6, Nov. 1961, pp. 659-667.

Kraijenhoff, van de Leur, D.A., 1958. A Study of Non-Steady Groundwater Flow with Special Reference to a Reservoir Coefficient, Bouw-En Waterbouwkunde, Vol. 9, 1958.

Kraijenhoff, van de Leur, D.A. 1962. A Study of Non-Steady Groundwater Flow - II. Computation Methods for Flow to Drains, Bouw-En Waterbouwkunde, Vol. 23, 1962, pp. 285-291.

Kunkle, G.R. 1962. The Base-Flow Duration Curve, a Technique for the Study of Groundwater Discharge from a Drainage Basin, Journal of Geophysical Research, Vol. 67, No. 4, pp. 1543-1554.

Lane, R.K. 1968. Application of Remote Sensing to Pollution Studies, Department of Energy, Mines, and Resources, Inland Waters Branch, Reprint Series No. 36.

Langbein, W.B. 1940. Some Channel Storage and Unit Hydrograph Studies, Trans. Amer. Geophys. Union, Vol. 21, Part 2, pp. 620-627.

Lawson, D.W. 1968. Groundwater Flow Systems in the Crystalline Rocks of the Okanagan Highland, British Columbia, Canadian Journal of Earth Sciences, Vol. 5, 1968, pp. 813-824.

Lewis, D.C. and R.H. Burgy, 1964. Hydraulic Characteristic of Jointed Rock, Groundwater, Vol. 2, No. 3, July 1964, pp. 4-9.

Liberty, B.A. 1953. Alliston; Simcoe, York, and Dufferin Counties, Ontario, Geological Survey of Canada, Paper 53-9.

Liberty, B.A., 1953. Newmarket; Ontario and York Counties, Ontario, Geological Survey of Canada, Paper 53-2.

Liberty, B.A. 1953. Oshawa; Ontario and Durham Counties, Ontario, Geological Survey of Canada, Paper 53-18.

Liberty, B.A. 1953. Scugog; Durham, Ontario and Victoria Counties, Ontario, Geological Survey of Canada, Paper 53-19.

Liberty, B.A. 1960a). Rice Lake; Port Hope and Trenton Map-Areas, Ontario, Geological Survey of Canada, Paper 60-14.

Liberty, B.A. 1960b). Belleville and Wellington Map-Areas, Ontario, Geological Survey of Canada, Paper 60-31.

Liberty, B.A. 1963. Geology of Tweed, Kaladar, and Bannockburn Map-Areas, Ontario, Geological Survey of Canada, Paper 63-14.

Liberty, B.A. 1969. Paleozoic.Geology of the Lake Simcoe Area, Ontario, Geological Survey of Canada, Memoir 355.

Linsley, R.K. Jr., M.A. Kohler and J. Paulhus, 1949. Applied Hydrology, McGraw-Hill Book Company, Inc.

Linsley, R.K., M.A. Kohler, and J. Paulhus, 1958. Hydrology for Engineers. McGraw-Hill Book Company, Inc.

Lovas, L. 1963. The Effect of Clay Minerals on the Permeability of Sand Soils, International Association of Scientific Hydrology, Berkley Assembly, Publication 64, pp. 274-289.

Moasland, M. 1957. Soil Anisotropy and Land Drainage *in* Drainage of Agricultural Lands, edited by J.N. Luthin. American Society of Agronomy, pp. 216-285.

Maillet, E. 1903, Essai d'Hydraulique Fluviale, Hermann, Paris.

Meyboom. P. 1961. Estimating Groundwater Recharge from Stream Hydrographs, Journal of Geophysical Research, Vol. 66, No. 4. pp. 1203-1214.

Meyer, O.H. 1940. Analysis of Runoff Characteristics, Transaction American Society of Civil Engineers, Vol. 105, 1940, pp. 83-90.

Morisawa, M. 1957. Accuracy of Determination of Stream Lengths from Topographic Maps, Trans. American Geophysical Union, Vol. 38, 1957.

Morton, F.I., and H.B. Rosenberg, 1959. Hydrology of Lake Ontario, Journal of the Hydraulics Division, American Society of Civil Engineers, May 1959.

Morton, F.I. 1965. Potential Evaporation and River Basin Evaporation, Journal of the Hydraulics Division, American Soc. of Civil Engineers, November 1965.

Norris, S.E. Permeability of Glacial Till, U.S. Geological Survey Research, 1962.

Ogden, L. 1965. Estimating Transmissibility with one Drawdown, Groundwater, Vol. 3, No. 3, July 1965.

Olmsted, T.H., and A.G. Hely, 1962. Relation Between Groundwater and Surface Water in Brandywine Creek Basin, Pennsylvania. United States Geological Survey, Professional Paper 417-A.

Ontario Department of Mines, Ground Water Bulletins: No. 145 (1953) for 1948, 1949, 1950; No. 152 (1957) for 1951, 1952. Toronto.

Ontario Water Resources Commission, Groundwater Bulletins: No. 1 (1961) for 1953, 1954; No. 2 (1963) for 1955, 1956; No. 3 (1965) for 1957; No. 4 (1966) for 1958; No. 5 (1967) for 1959. Toronto.

Parsons, M.L. 1970. Groundwater Movement in a Glacial Complex, Cochrane District, Ontario, Canadian Journal of Earth Sciences, Vol. 7, No. 3.

Pentland, R.L. 1968. Runoff Characteristics in the Great Lakes Basin, Eleventh Conference on Great Lakes Research and Second Meeting of the International Association for Great Lakes Research in Great Lakes Basin, edited by Pinius.

Powers, W.E. 1962. Drainage and Climate in Great Lakes Basin, Publication No. 71 of the American Association for the Advancement of Science.

Rasmussen, W.C., and G.E. Andreasen, 1959. Hydrologic Budget of the Beaverdam Creek Basin, Maryland, United States Geological Survey Water-Supply Paper 1472.

Riggs, H.C. 1964. The Baseflow Recession Curve as an Indicator of Groundwater, World Meteorological Organization and the International Association of Scientific Hydrology, pp. 352-366.

Rogers, D.P., R.C. Ostry, and P.F. Karrow, 1961. Metropolitan Toronto Bedrock Contours, Preliminary Map 102, Ontario Department of Mines, Toronto.

Rubin, J, and R. Steinhardt, 1963. Soil Water Relations during Rain Infiltration: I, Theory, Soil Science Society of America, Proceedings, 1963. Vol. 27, No. 3, pp. 246-251.

Sanford, B.V. 1954. Haldimand County and part of Brent, Wentworth and Lincoln Counties, Ontario, Geological Survey of Canada, Paper 53-30.

Sanford, B.V. 1956. Welland County, Showing Drift Thickness and Bedrock Contours, Geological Survey of Canada, Paper 55-20.

Sanford, B.V. 1961. Subsurface Stratigraphy of Ordovician Rocks in Southwestern Ontario, Geological Survey of Canada, Paper 60-26.

Sanford, B.V. 1970. Geological Map of Toronto, Windsor Area, Geological Survey of Canada, Map 1263A.

Sanford, B.V., and R.G. Quillion, 1959. Subsurface Stratigraphy of Upper Cambrian Rocks in Southwestern Ontario, Geological Survey of Canada, Paper 58-12.

Schoeller, H. 1962. Les Eaux Souterraines, Masson & Cie, Editeurs, Paris.

Searcy, J.K., 1959. Manual of Hydrology: Part 2, Low Flow Techniques, United States Geological Survey Water-Supply Paper 1542-A.

Searcy, J.K. 1960. Graphical Correlation of Gaging Station Records, United States Geological Survey Water-Supply Paper 1541-C, pp. 67-100.

Siple, G.E. 1967. Salt-Water Encroachment of Tertiary Limestones along Coastal South Carolina, Proceedings of the Dubrovnik Symposium, October 1965, Hydrology of Fractured Rocks, Vol. 2, pp. 439-453.

Slaney V.R., H. Gross, and L.W. Morley, 1969. Airborne Infrared Scanning Survey along the Shoreline of the Lower Great Lakes.

Snow, D.T. 1968a . Hydraulic Characteristics of Fractured Metamorphic Rocks of Front Range and Implications to the Rocky Mountain Arsenal Well, Quarterly of the Colorado School of Mines, Vol. 63, No. 1, January 1968.

Snow, D.T. 1968b . Rock Fracture Spacings, Openings, and Porosity, Journal of the Soil Mechanics and Foundation Division, Proceedings of the American Society of Civil Engineers, Jan. 1968, pp. 73-91.

St. Morin, H. 1967. Relations entre les Facteurs d'ordre Géologique et les caractéristiques de l'Ecoulement, Décennie Hydrologique Internationale, Québec.

Theis, C.V. 1935. The Relation Between the Lowering of Piezometric Surface and the Rate and Duration of Discharge of a Well using Groundwater Storage, Trans. American Geophys. Union, 16th Annual Meeting, Part 2.

Theis, C.V. and R.H. Brown, 1963. Estimating the Transmissibility of a Water Table Aquifer from the Specific Capacity of a Well, *in* Methods of Determining Permeability, Transmissibility, and Drawdown, compiled by R. Bentall, United States Geological Survey Water-Supply Paper 1536-I.

Todd, D.K. 1959. Groundwater Hydrology, John Wiley and Sons.

Tóth, J. 1963. Theoretical Analysis of Groundwater Flow in Small Drainage Basins, Proceedings of Hydrology Symposium No. 3, Groundwater.

Vecchioli, J. 1967. Directional Hydraulic Behaviour of a Fractured Shale Aquifer in New Jersey. Proceedings of the Dubrovnick Symposium, October 1965, Hydrology of Fractured Rocks, Vol. 1, pp. 318-326.

de Villiers, N. 1969. Develop Infrared Scanner for Canadian Uses. Science Dimension, National Research Council of Canada, Vol. 1, No. 2, June 1969.

Walton, W.C. 1960. Leaky Artesian Aquifer Conditions in Illinois, Illinois State Water Survey, Report of Investigation 39.

Walton, W.C. 1962. Selected Analytical Methods for Well and Aquifer Evaluation, Illinois State Water Survey, Bulletin 49.

Walton, W.C. 1965. Groundwater Recharge and Runoff in Illinois, Illinois State Water Survey Report of Investigation 48.

Walton, W.C. 1970. Groundwater Resource Evaluation, McGraw-Hill Book Co.

Watt, A.K. 1955. Pleistocene Geology and Groundwater Resources of the Township of North York, York County, 64th Annual Report of the Ontario Department of Mines, Vol. LXIV, Part 7, 1955.

Watt, A.K. 1962. An Assessment of the Non-Equilibrium Equations in Various Aquifers, Proceedings of Hydrology Symposium No. 3, Groundwater.

Weeks, E.P. 1964. Field Methods for Determining Vertical Permeability and Aquifer Anisotropy, United States Geological Survey Professional Paper 501-D, pp. D193 - D198.

Weeks, E.P. 1969. Determining the Ratio of Horizontal to Vertical Permeability by Aquifer Test Analysis, Water Resources Research, Vol. 5, No. 1, February 1969, pp. 196-214.

Weiler, H.S. 1968. Current Measurements in Lake Ontario in 1967, Department of Energy, Mines and Resources, Inland Waters Branch, Reprint Series No. 46.

Wenzel, L.K. 1942. Methods for Determining Permeability of Water-Bearing Material, with Special Reference to Discharging Well Methods, United States Geological Survey Water-Supply Paper 887.

Wilson, A.E. 1942. Geological Map of the Ottawa – Cornwall Area, Geological Survey of Canada, Map 852A.

Wilson, M.E. 1929. Fluorspar Deposits of Canada, Geological Survey of Canada, Economic Geology Series No. 6.

Wojtek, E. 1970. Time-of-Travel Studies of Ganaraska River, Little Rouge Creek and Lynde Creek, Southern Ontario, Internal Report, Department of Energy, Mines and Resources, Inland Waters Branch, Groundwater Subdivision, Ontario.

Wright, J.F. 1963. Brockville – Mallorytown Map Area, Ontario, Geological Survey of Canada, Memoir 134, No. 115,Geological Series.

Wynne-Edwards, H.R. 1962. Geological Map of Gananoque, Ontario, Geological Survey of Canada, Map 27-1962.

Wynne-Edwards, H.R. 1963. Geological Map of Brockville – Mallorytown Area, Ontario. Geological Survey of Canada, Map 7, 1963.

Wynne-Edwards, H.R. 1967. Westport Map Area, Ontario, Geological Survey of Canada, Memoir 346.

Zeizel, A.J. et al, 1962. Groundwater Resources of Pupage County, Illinois. Cooperative Groundwater Report No. 2, Illinois State Water Survey and State Geological Survey.

EVALUATION OF PUMPING TEST DATA

APPENDIX A

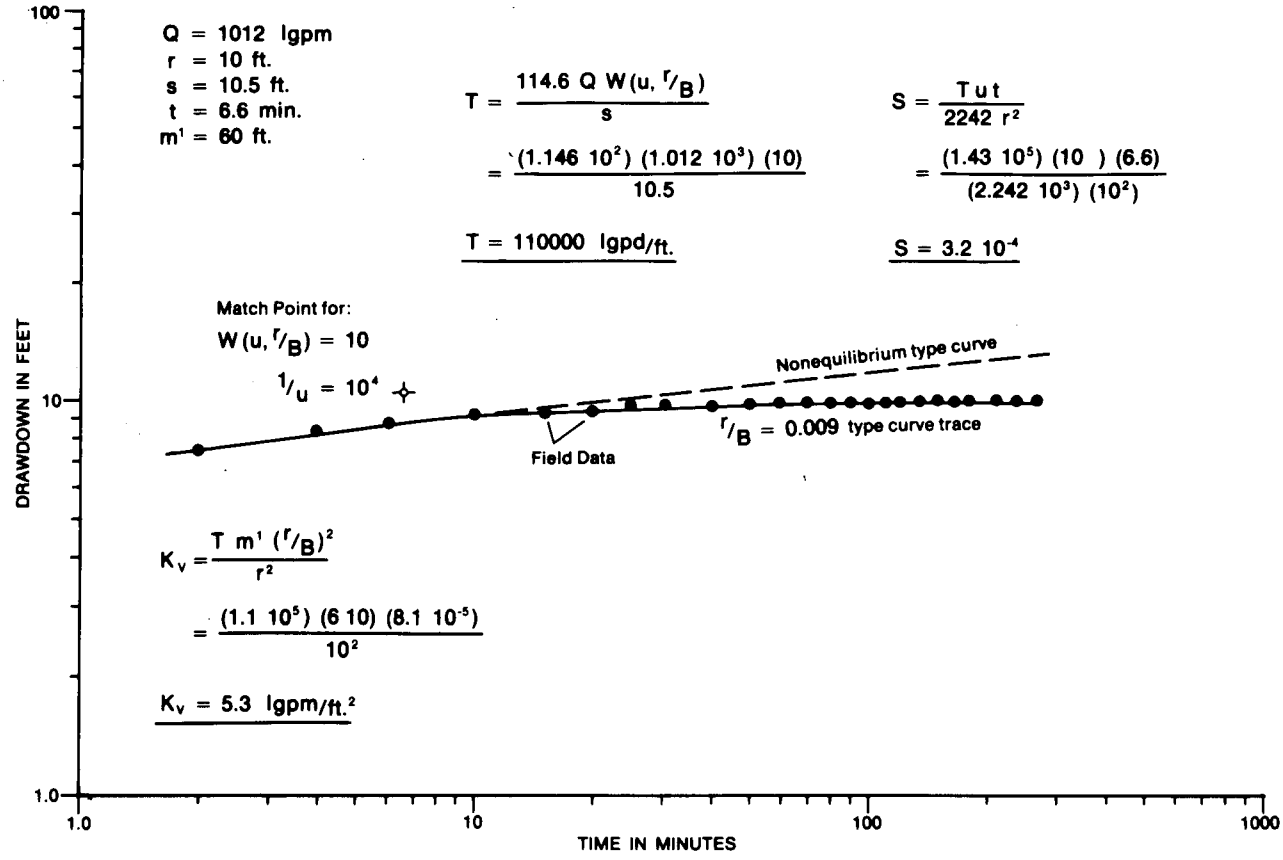

Figure 71. Time/drawdown curve of an observation well at Markham, June 1969.

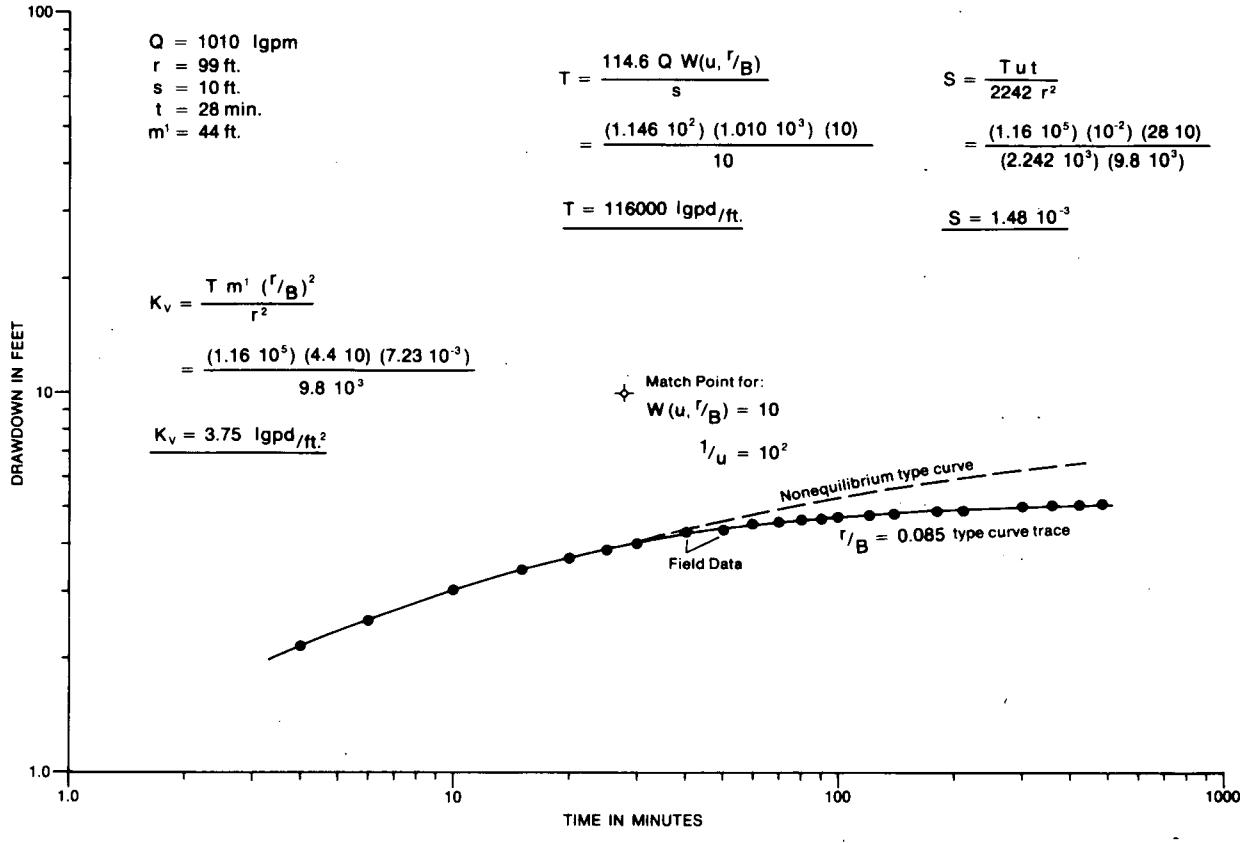

Figure 72. Time/drawdown curve of an observation well at Milton, June 1964.

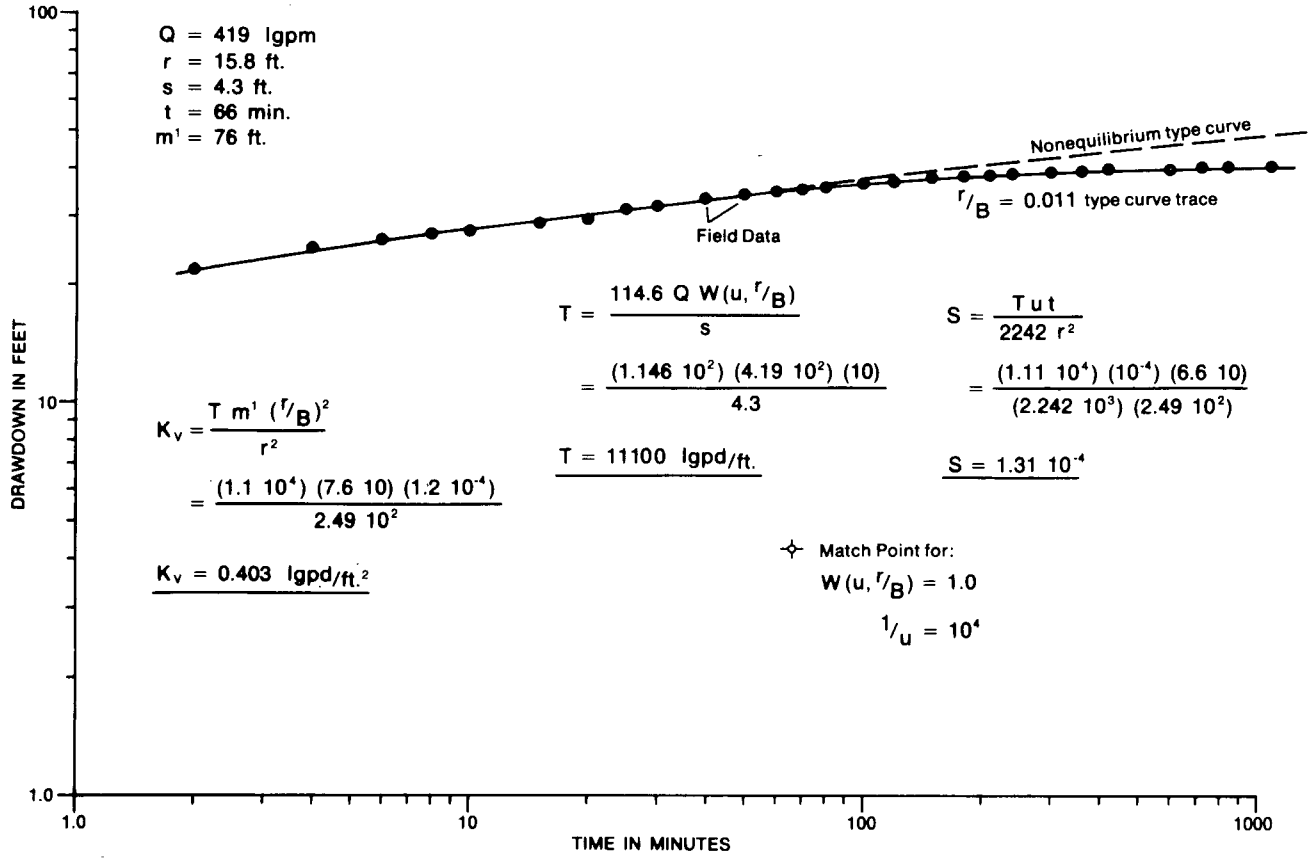

Figure 73. Time/drawdown curve of an observation well at Stayner, August 1968.

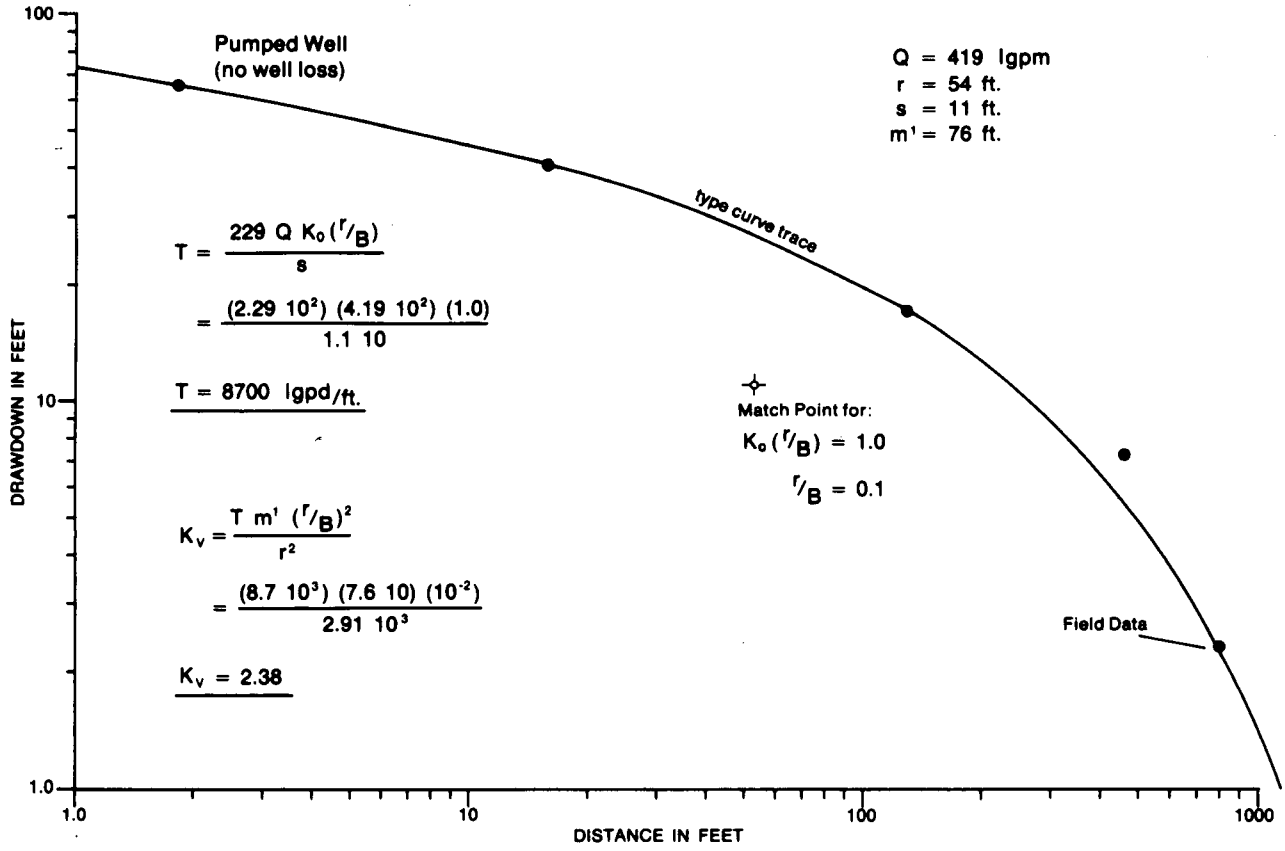

Figure 74. Distance/drawdown curve of an observation well at Stayner, August 1968.

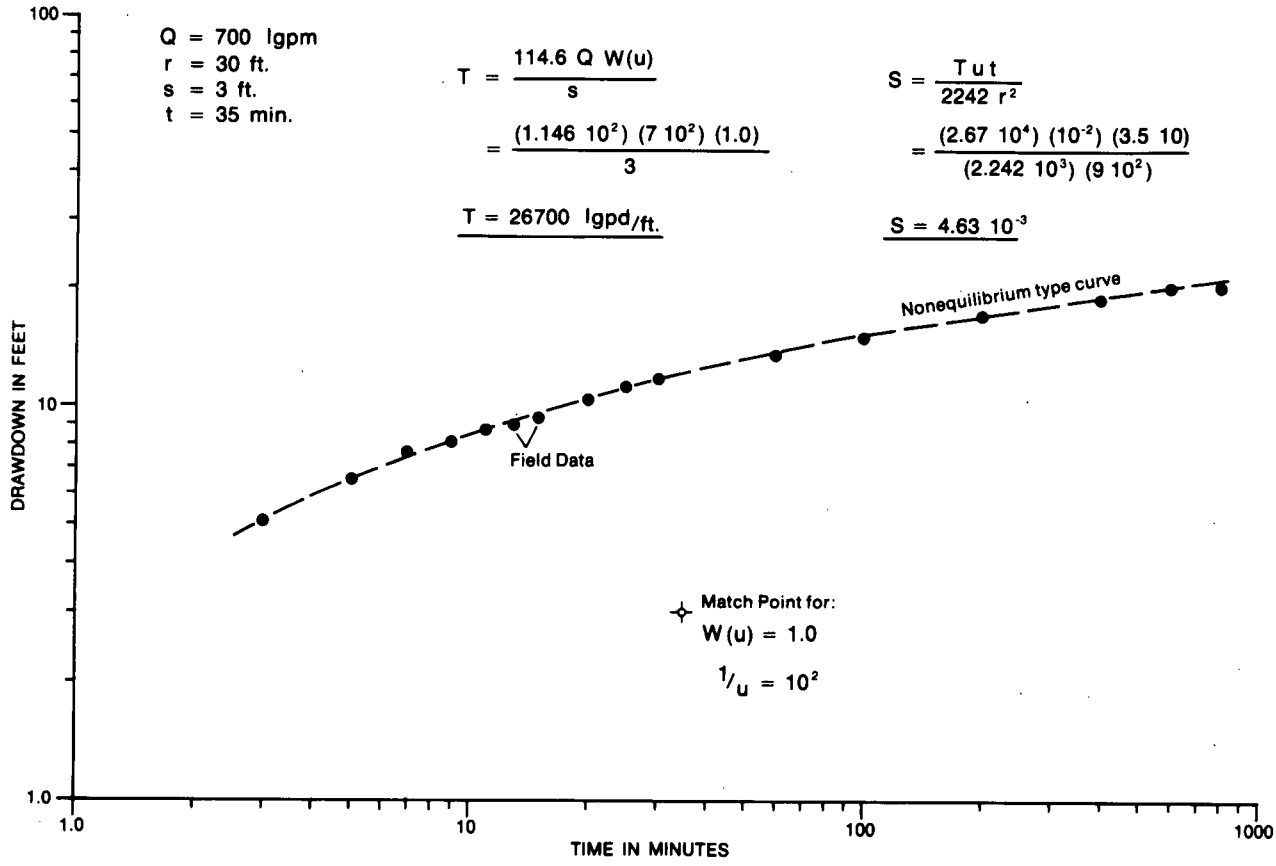

Figure 75. Time/drawdown curve of an observation well at Ancaster, April 1969.

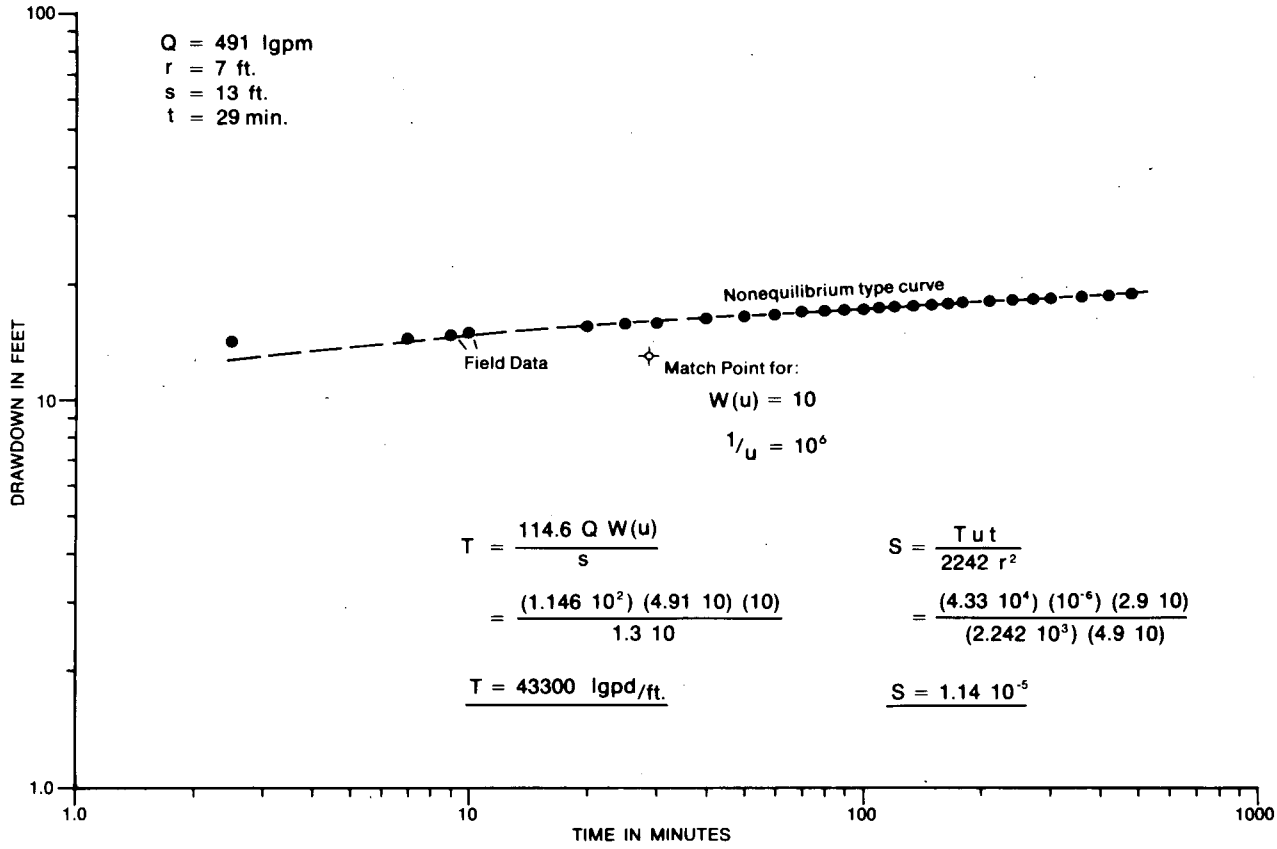

Figure 76. Time/drawdown curve of an observation well at Bolton, May 1954.

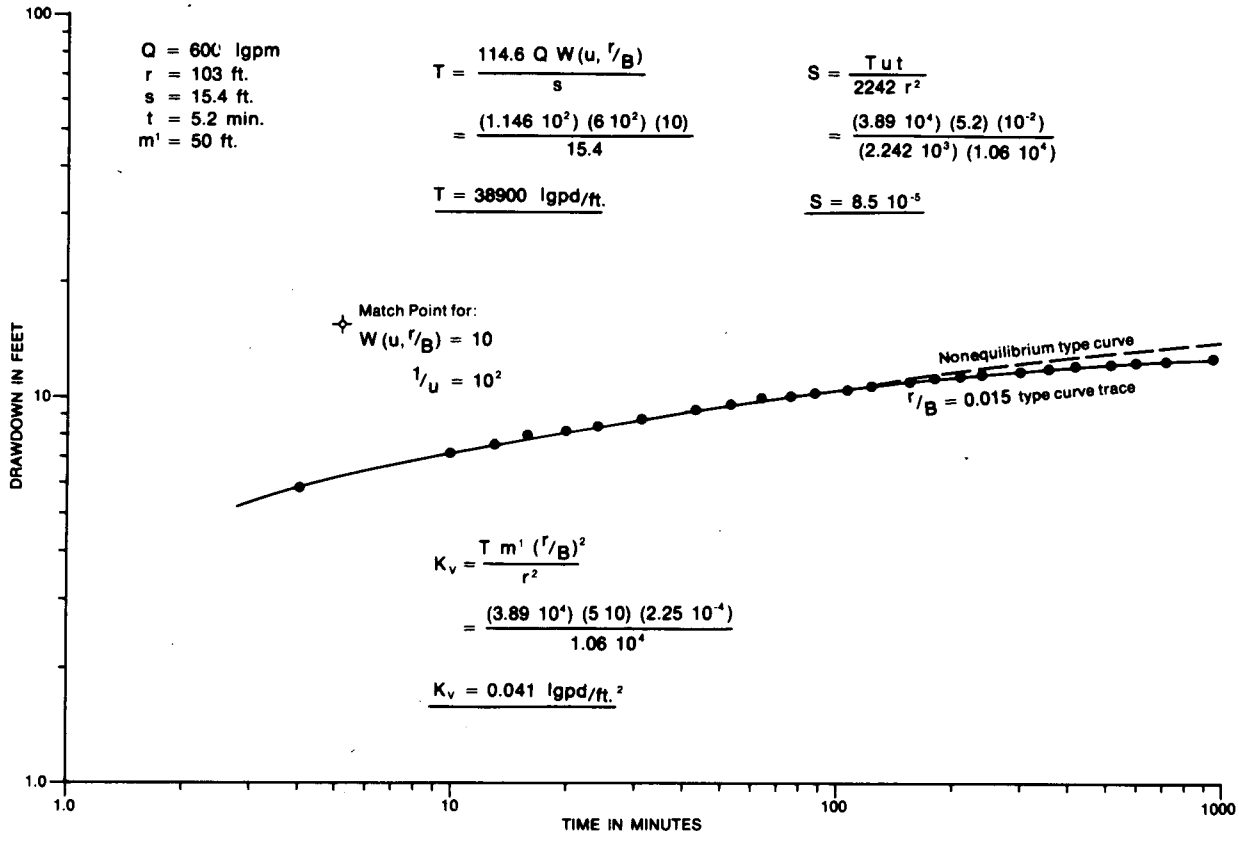

Figure 77. Time/drawdown curve of an observation well at Agincourt, March 1968.

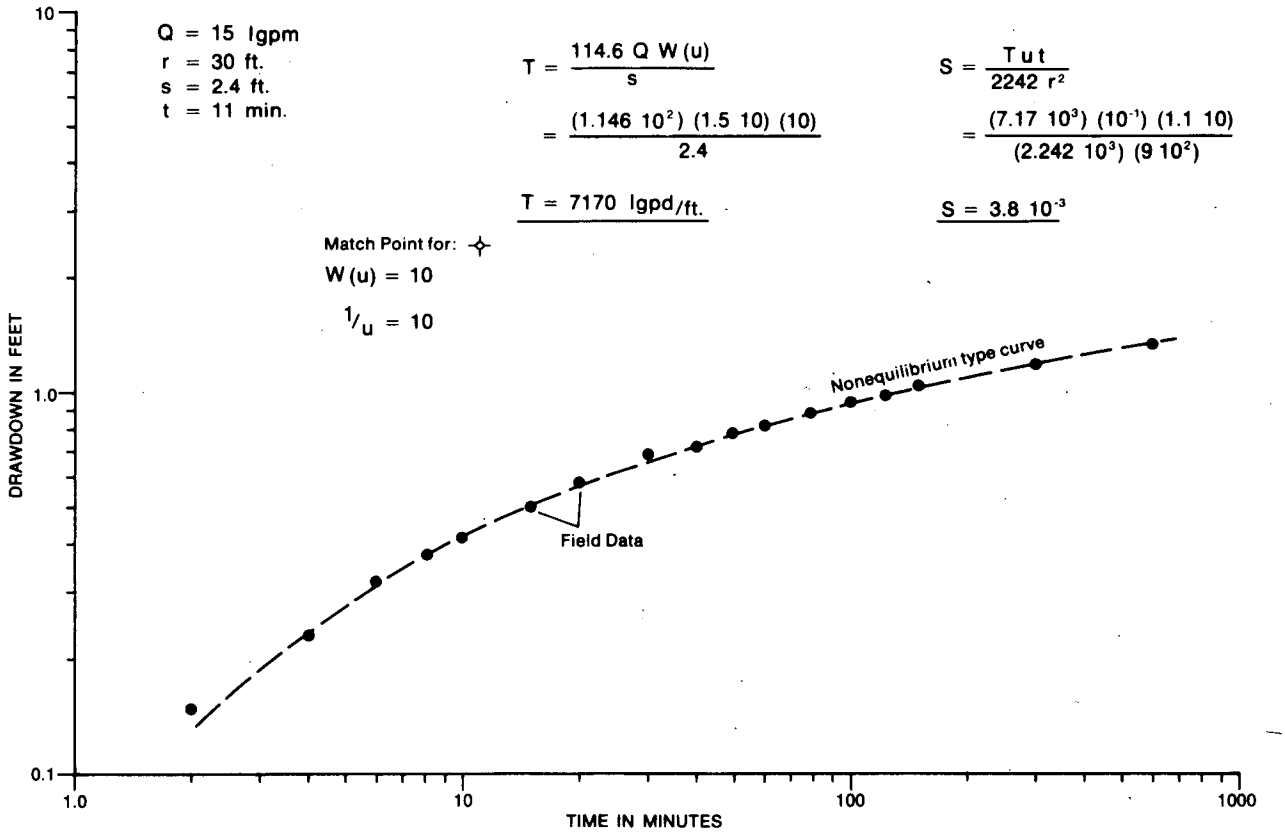

Figure 78. Time/drawdown curve of an observation well at Thornburg, May 1969.

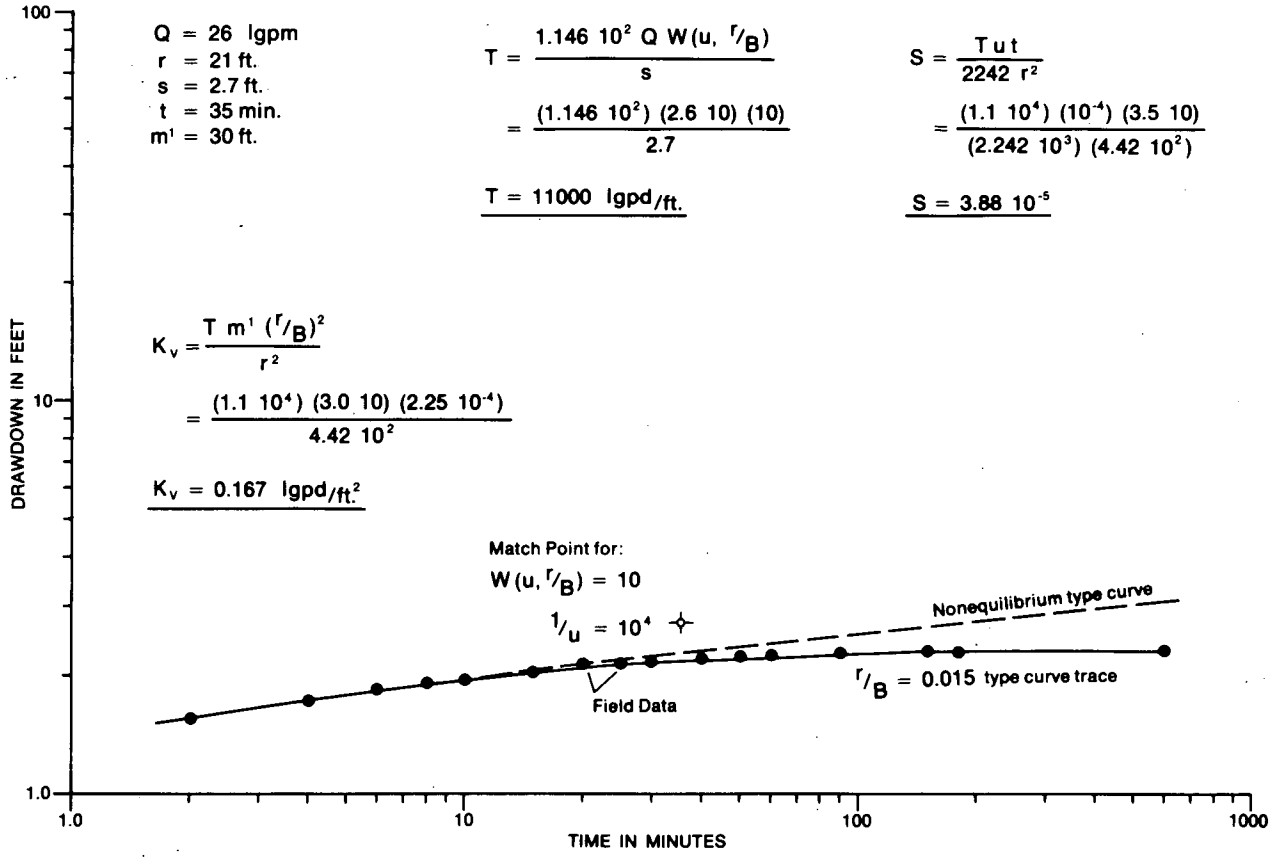

Figure 79. Time/drawdown curve of an observation well at Orono, May 1960.

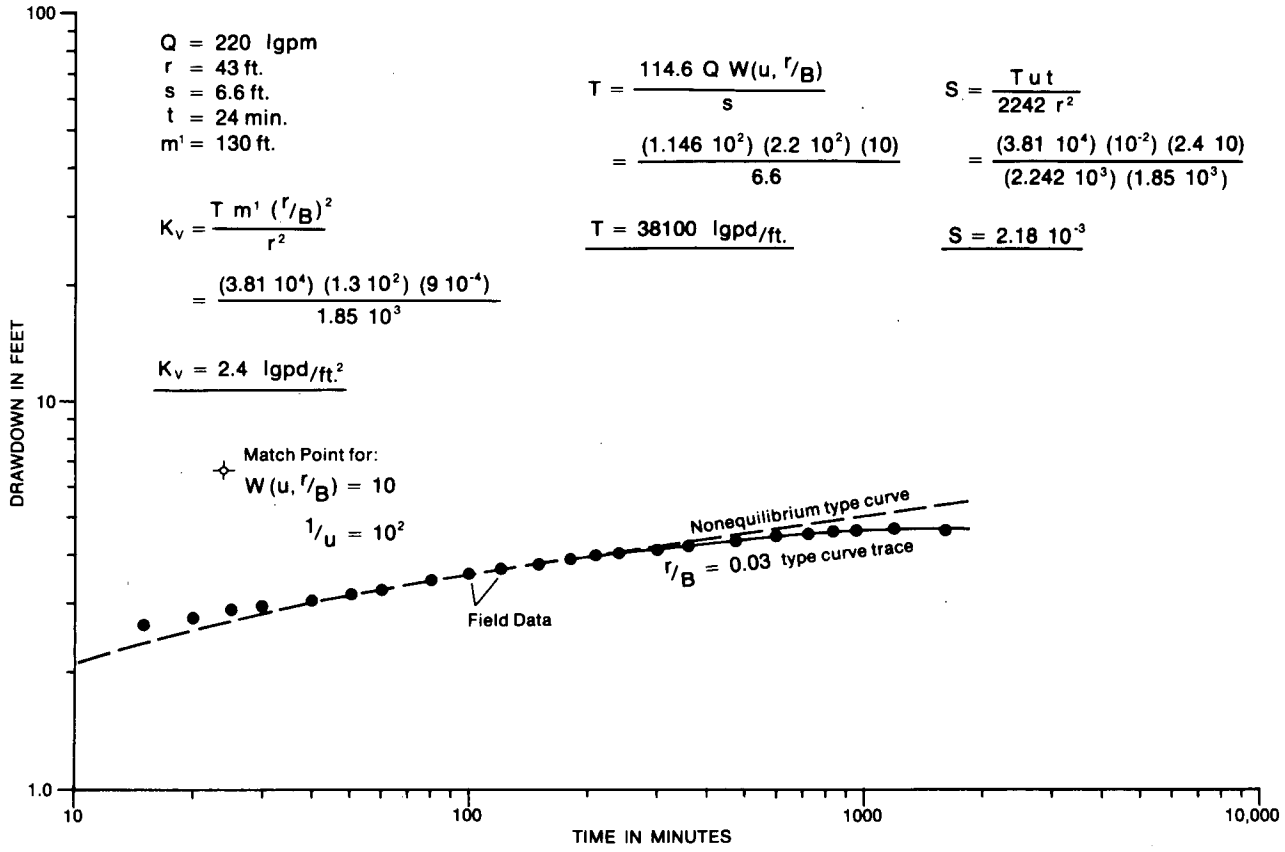

Figure 80. Time/drawdown curve of an observation well at Uxbridge, October 1963.

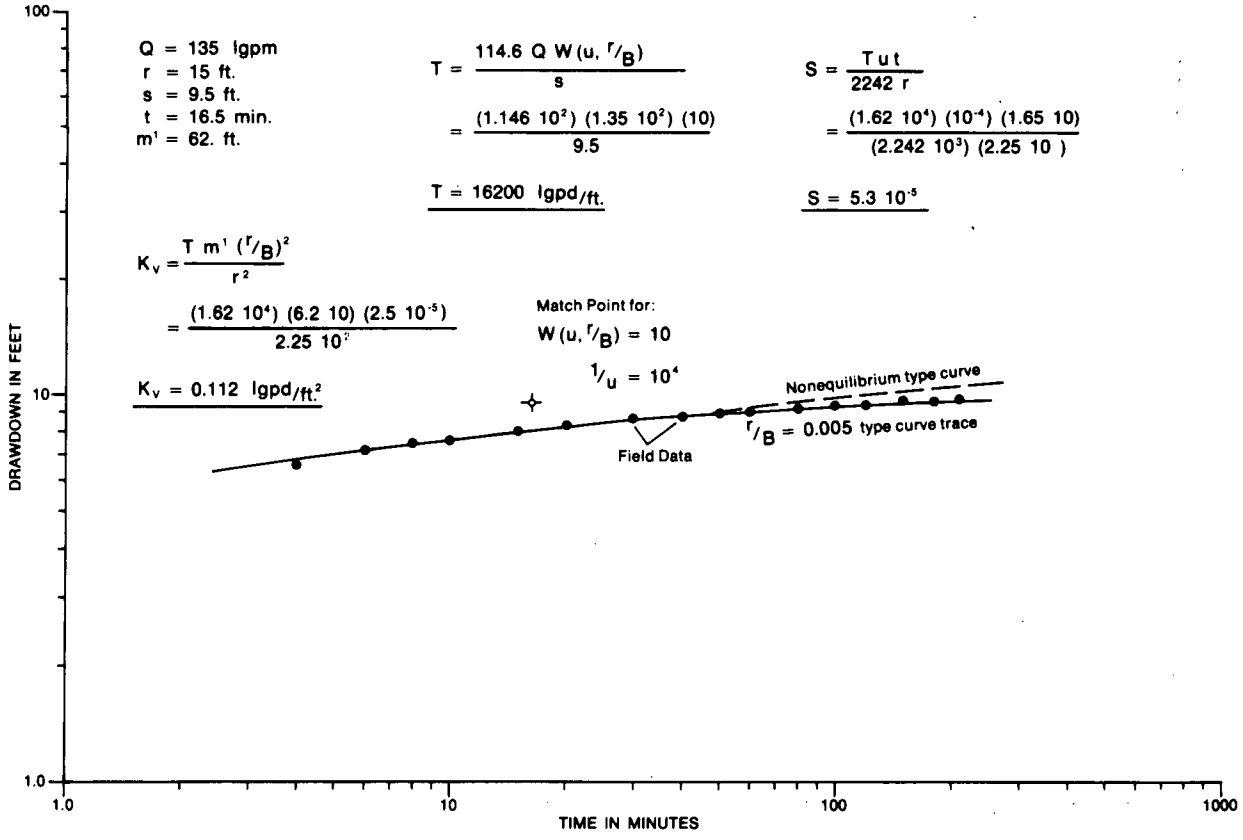

Figure 81. Time/drawdown curve of an observation well at Preston, February 1968.

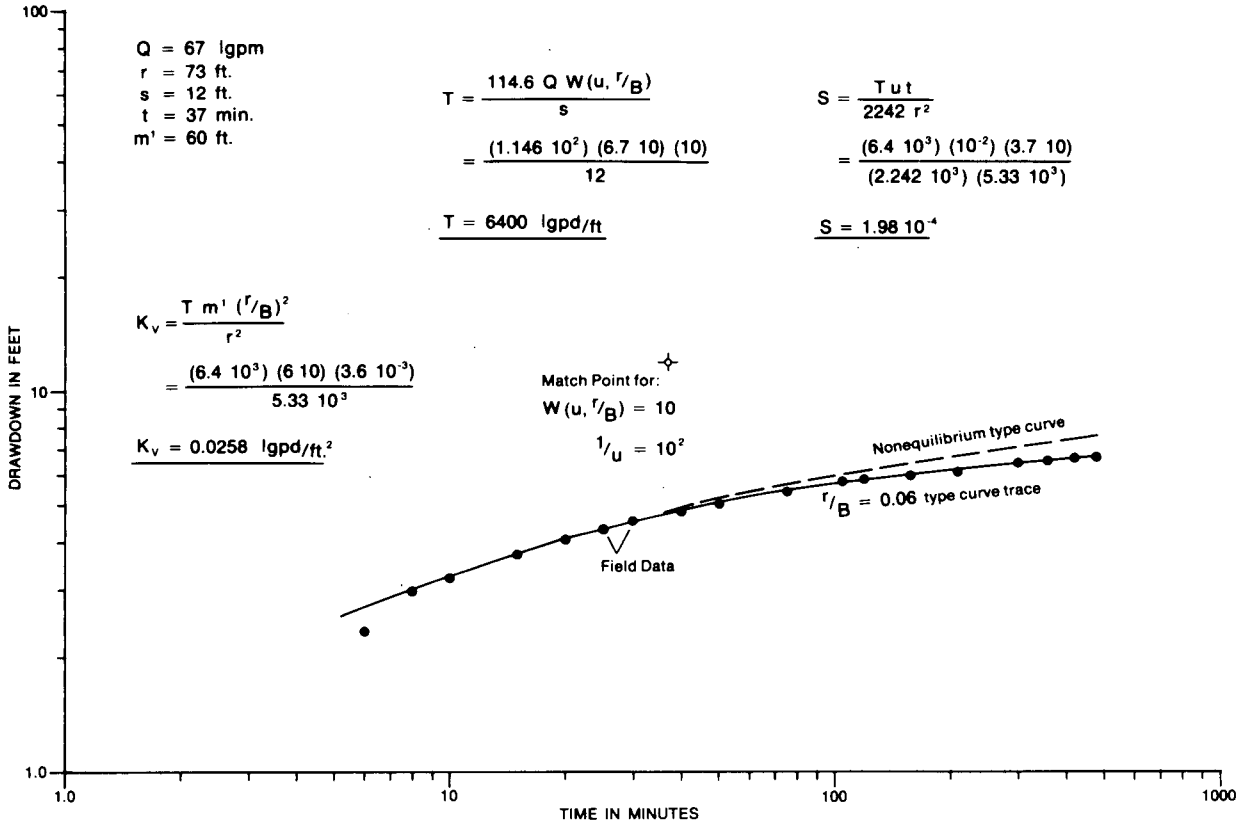

Figure 82. Time/drawdown curve of an observation well at St. Mary's, June 1965.

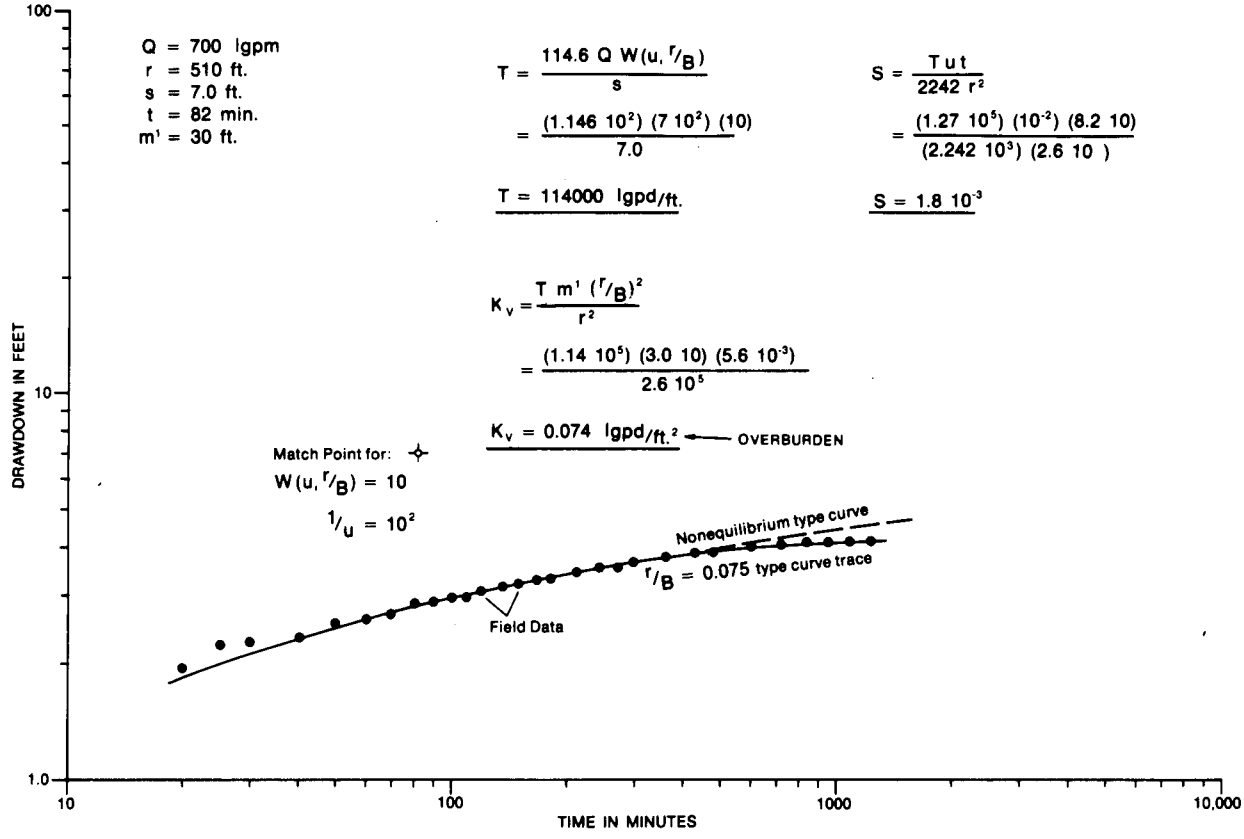

Figure 83. Time/drawdown curve of an observation well at Guelph, June 1963.

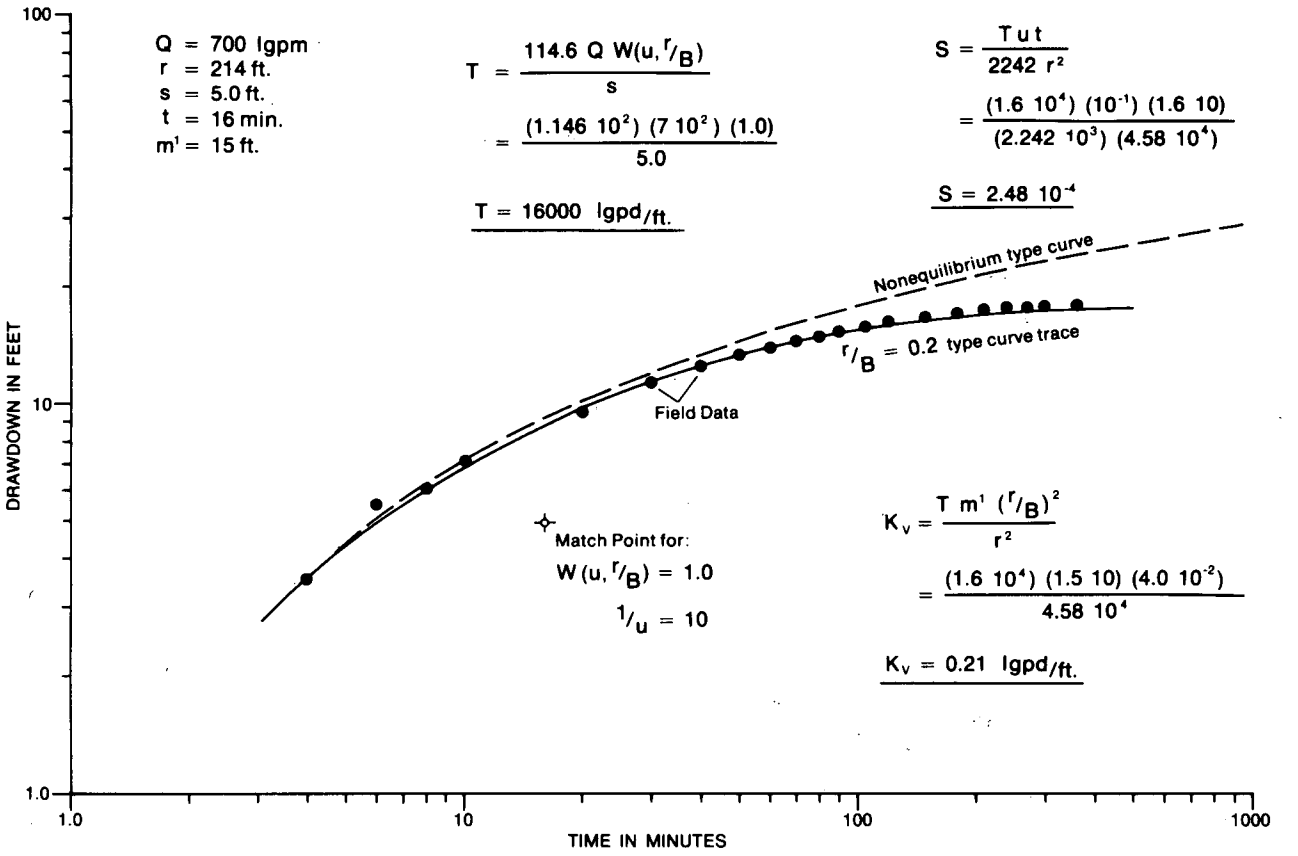

Figure 84. Time/drawdown curve of an observation well at St. Mary's, June 1963.

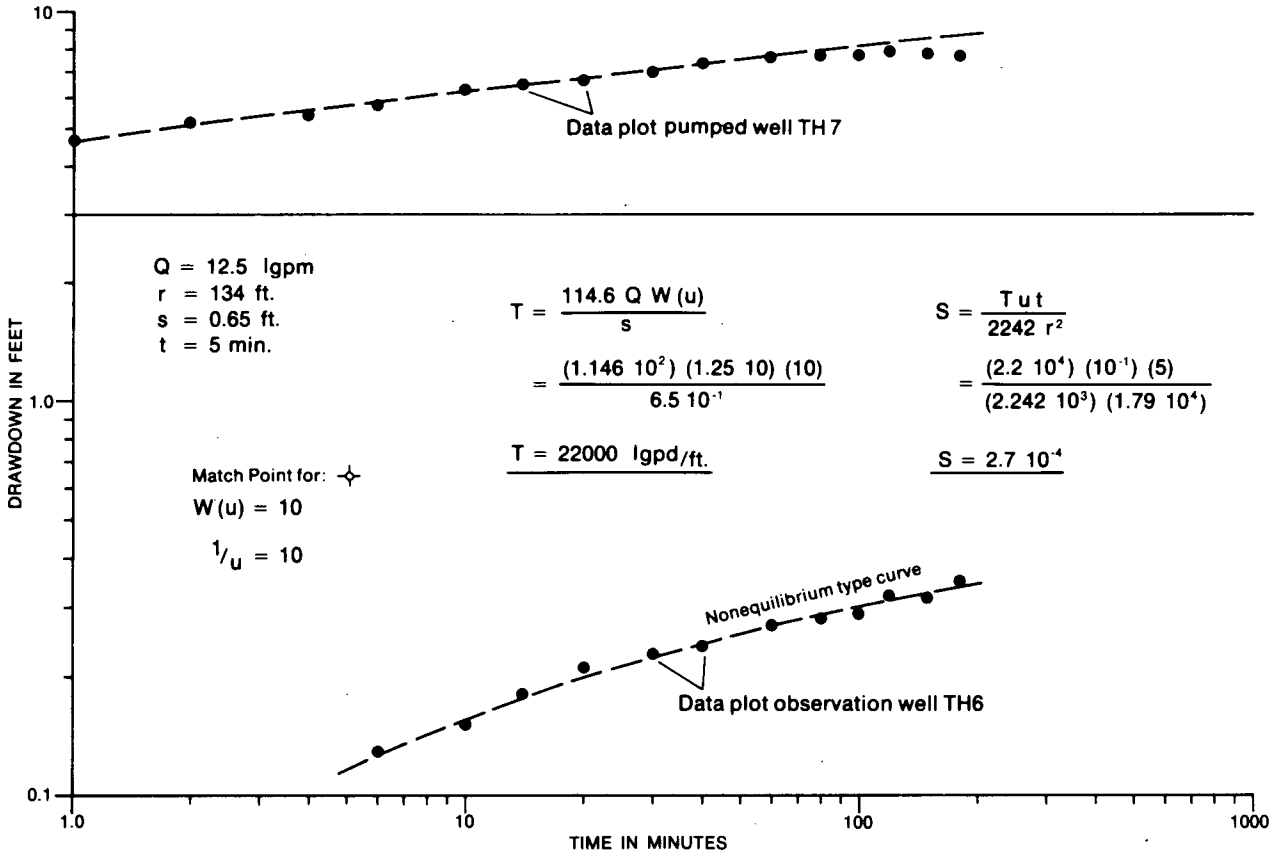

Figure 85. Time/drawdown curve of pumped well TH-7 and observation well TH-6, Don Valley, Toronto, September 1969.

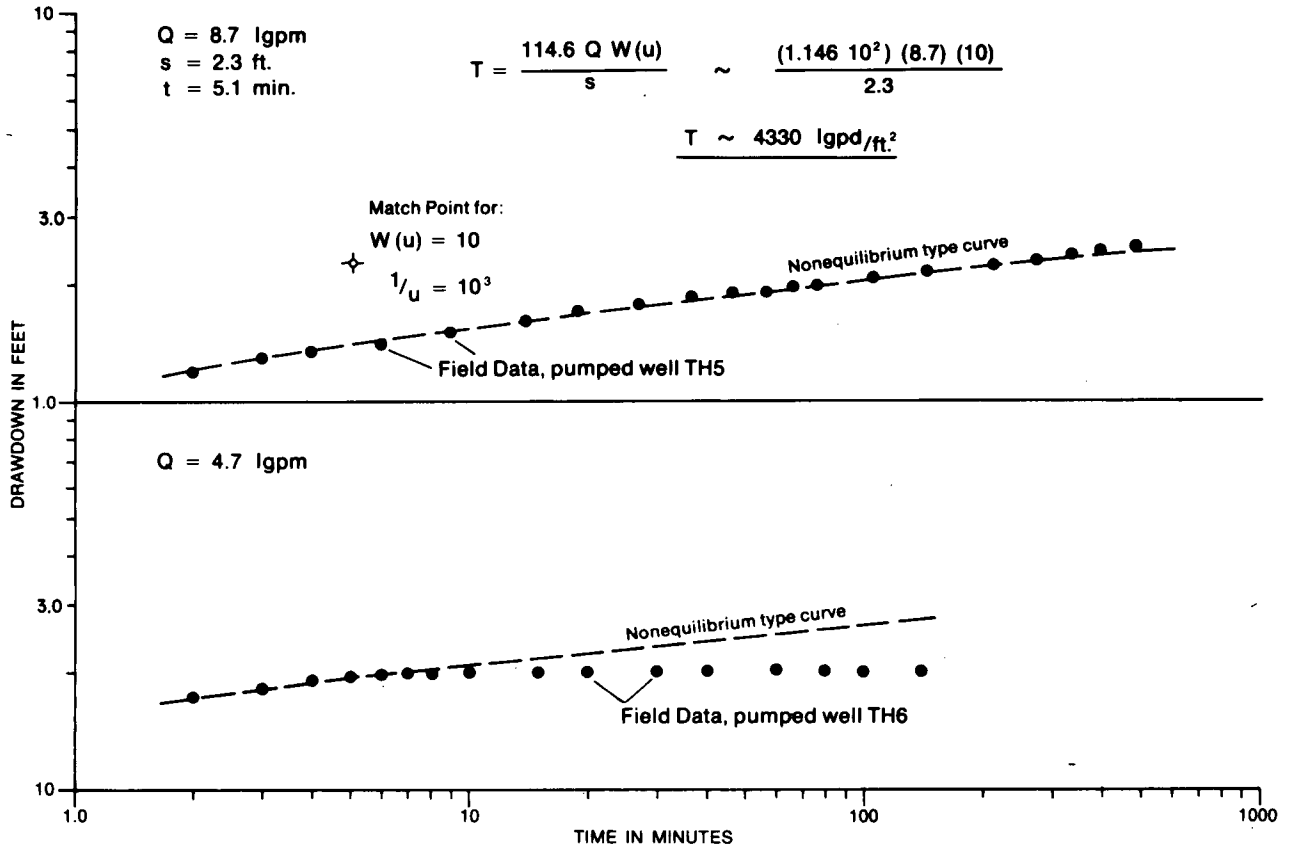

Figure 86. Time/drawdown curve of pumped well TH-5 and time/drawdown plot of pumped well TH-6, Toronto, September 1969.

COMPUTER PROGRAM FREQ

APPENDIX B

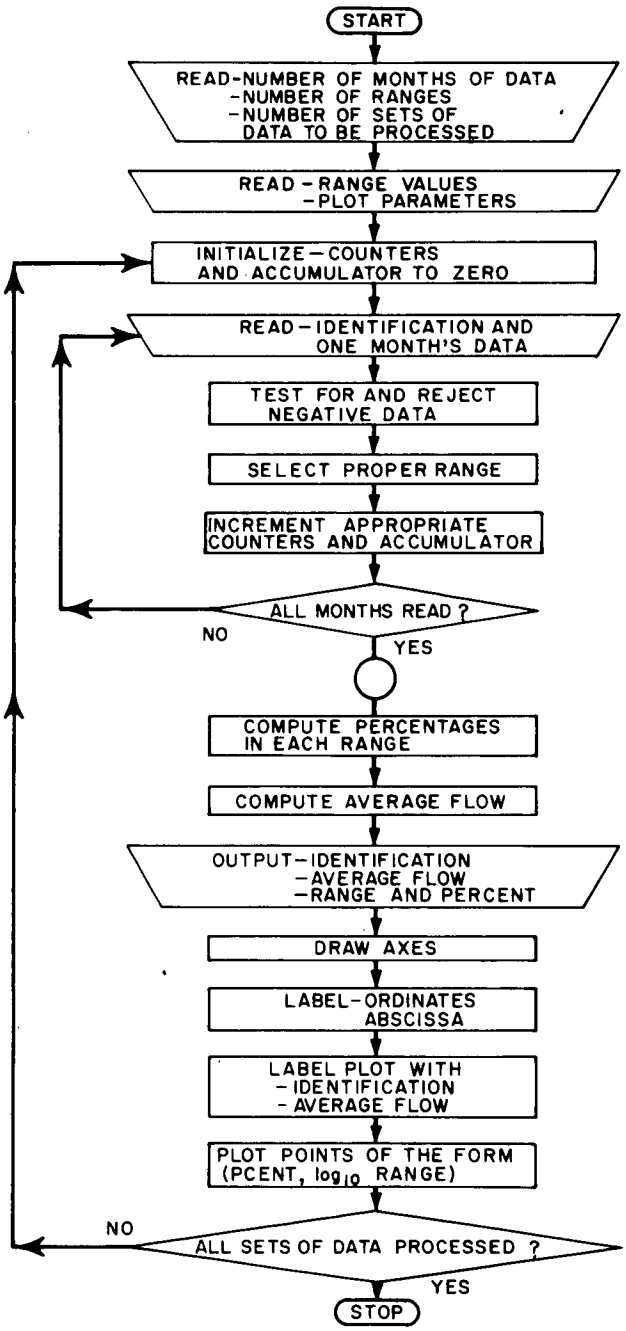

Figure 87. Flowchart Program FREQ.

```
                                3200  FORTRAN    (2.1)          21/04/69
      PROGRAM FREQ
C
C     ************************************************
C     * FREQ READS DAILY DISCHARGE VALUES FOR A      *
C     * GIVEN NUMBER OF MONTHS AND CLASSIFIES THEM   *
C     * INTO GIVEN RANGES.  THESE RANGES ARE NOT GEN-*
C     * ERATED BY THE PROGRAM BUT ARE READ FROM DATA *
C     * CARDS.  UP TO FIFTY RANGES MAY BE USED.  ANY *
C     * NUMBER OF MONTHS OF DISCHARGE DATA IS ACCEPT-*
C     * ABLE.  A COUNT OF THE NUMBER OF DATA VALUES  *
C     * WHICH LIE IN EACH RANGE IS KEPT AS WELL AS A *
C     * COUNT OF THE TOTAL NUMBER OF DATA.  ALSO THE *
C     * SUM OF THE DATA IS CALCULATED TO DETERMINE   *
C     * AVERAGE FLOW.  THE PROGRAM OUTPUTS THE AVERAGE*
C     * FLOW AS WELL AS THE PERCENTAGE OF DATA WHICH *
C     * FALLS IN EACH RANGE.  THE SECOND PART OF THE *
C     * PROGRAM PLOTS THE DISCHARGE RANGE ON THE VER-*
C     * TICAL, LOGARITHMIC SCALE VERSUS THE CUMULATIVE*
C     * PERCENTAGE ON THE HORIZONTAL, LINEAR SCALE.  *
C     * THE RESULTING CURVE IS THE CUMULATIVE DISTRI-*
C     * BUTION OF DISCHARGE.                         *
C     ************************************************
C
      DIMENSION A(31),PCENT(50),RANGE(50),COUNT(50),K(10)
      INTEGER EXPUT
      INPUT=60
      EXPUT=61
C
C     READ NUMBER OF RANGES AND NUMBER OF MONTHS OF
C     DATA
C     NPLOT IS THE NUMBER OF PLOTS TO BE DONE AND HENCE THE NUMBER OF
C     STATIONS BEING PROCESSED IN THIS RUN.
C
      READ(INPUT,1)NRANGE,NMONTH,NPLOT
 1    FORMAT(3I6)
C
C     READ RANGE VALUES
C
      READ(INPUT,4)(RANGE(M),M=1,NRANGE)
 4    FORMAT(12F6.0)
C
C     PLOT ROUTINE INPUT
C
      READ(INPUT,41)(LUN,XL,YL,XTIC,XLNG,YLNG,XMIN,YMIN,XORG,YORG,YTIC)
 41   FORMAT(I6,10F6.2)
      DO 345 IJKLM=1,NPLOT
C
C     THIS LOOP GOVERNS THE NUMBER OF STATIONS TO BE
C     ANALYSED.  ALL STATIONS MUST COVER THE SAME
C     TIME PERIOD AND USE THE SAME RANGES.
C
      DO 101 KI=1,NRANGE
      COUNT(KI)=0
 101  CONTINUE
      SUM=0
      FLWSUM=0.0
      DO 2 I=1,NMONTH
C
C     READ ONE MONTH'S DATA
C
      READ(INPUT,3)NU,NUM,NUMB,JR,MONTH,INTER,(A(IJ),IJ=1,31)
 3    FORMAT(X,A2,A2,A3,I3,I2,I1,10F6.0/14X,10F6.0/14X,11F6.0)
      DO 5 N=1,31
C
C     TEST FOR NEGATIVE DATA. NEGATIVE VALUES ARE
C     REJECTED AS INCORRECT.  THE ALGORITHM DOES
C     NOT BREAK DOWN
C
      IF(A(N))5,6,6
 6    DO 7 M=1,NRANGE
      IF(A(N)-RANGE(M))8,7,7
```

Figure 88. Computer Program FREQ.

```
 7      CONTINUE
 8     COUNT(M)=COUNT(M)+1
       SUM=SUM+1
       FLWSUM=FLWSUM+A(N)
   5   CONTINUE
 2     CONTINUE
       DO9 J=1,NRANGE
C
C      COMPUTE PERCENTAGES
C
       PCENT(J)=(100.0*COUNT(J))/SUM
 9     CONTINUE
C
C      COMPUTE AVERAGE FLOW
C
       AVGFLW=FLWSUM/SUM
C
C      OUTPUT STATION NUMBER, AVERAGE FLOW, PERCENT-
C      AGES FOR EACH RANGE
C
       WRITE(EXPUT,11)NU,NUM,NUMB
 11    FORMAT(1X,10X,6HNUMBER,3X,A2,A2,A3)
       WRITE(EXPUT,12)SUM
 12     FORMAT(//10X,3HSUM,F5.0)
       WRITE(EXPUT,13)AVGFLW
 13    FORMAT(//10X,12HAVERAGE FLOW,2X,F5.1)
       DO 92 MI=1,NRANGE
       WRITE(EXPUT,14)MI,RANGE(MI),PCENT(MI)
   14 FORMAT(//10X,I2,3X,F6.1,5X,F6.1)
 92    CONTINUE
C
C      PLOT ROUTINE
C
C
C      DRAW AXES
C
       CALL AXISXY(LUN,XL,YL,XTIC,XLNG,YLNG,XMIN,YMIN,XORG,YORG,YTIC)
       X1=XORG-1.0*XTIC
       DO 77 IA=0,4
       XIA=IA
       Y1=YORG+(XIA/4.0)*YLNG
       CALL PLOTXY(X1,Y1,0,0)
       ENCODE(5,42,K(1))IA
 42    FORMAT(4H10**,I1)
C
C      DRAW AND LABLE LOG CYCLES
C
       CALL LABEL(5,2,0,K(1))
       CALL PLOTXY(XORG,Y1,0,0)
       CALL PLOTXY(XLNG,Y1,1,0)
 77    CONTINUE
       X2=XORG
       Y2=YORG-0.5*XTIC
       CALL PLOTXY(X2,Y2,0,0)
       ENCODE(1,43,K(2))
 43    FORMAT(1H0)
C
C      LABLE PERCENT SCALE
C
       CALL LABEL(1,2,0,K(2))
       DO 88 IB=10,90,10
       X2 =X2+XTIC
       CALL PLOTXY(X2,Y2,0,0)
       ENCODE(2,44,K(3))IB
 44    FORMAT(I2)
       CALL LABEL(2,2,0,K(3))
 88    CONTINUE
       X2=XORG+10*XTIC
       CALL PLOTXY(X2,Y2,0,0)
```

Figure 88 (Cont'd). Computer Program FREQ.

```
 45   FORMAT(3H100)
      CALL LABEL(3,2,0,K(4))
      CALL PLOTXY(X2,YORG,0,0)
      CALL PLOTXY(X2,YLNG,1,0)
      X3=XORG+.25*XTIC
      Y4=YORG+.25*XTIC
      CALL PLOTXY(X3,Y4,0,0)
      ENCODE(17,201,K(6))AVGFLW
 201  FORMAT(12HMEAN FLOW - ,F5.1)
C
C     WRITE AVERAGE FLOW IN LOWER LEFT CORNER
C
      CALL LABEL(17,2,0,K(6))
      X4=XORG+0.5*XLNG
      Y3=YORG+0.95*YLNG
      CALL PLOTXY(X4,Y3,0,0)
      ENCODE(14,200,K(5))NU,NUM,NUMB
 200  FORMAT(7HST.NO.-,A2,A2,A3)
C
C     LABLE PLOT WITH WELL NUMBER IN UPPER, RIGHT
C     CORNER
C
      CALL LABEL(14,3,0,K(5))
      XNEW=0.0
      DO 234 IPLOT=1,NRANGE
      JYP=NRANGE-IPLOT+1
C
C     PREPARE DATA POINTS
C
      XNEW=XORG+XNEW+PCENT(JYP)
      YNEW=YORG+25.0*ALOG10(RANGE(JYP))
C
C     PLOT CUMULATIVE PERCENT VERSUS LOG OF RANGE
C     PLOTS FROM LEFT TO RIGHT
C
      CALL PLOTXY(XNEW,YNEW,0,15)
 234  CONTINUE
      CALL ENDPLOT(LUN)
 345  CONTINUE
C
C     FINISH PLOT
C
      CALL AXISXY(LUN,XL,YL,XTIC,XLNG,YLNG,XMIN,YMIN,XORG,YORG)
      CALL ENDPLOT(LUN)
      REWIND 01
      STOP
C
C    ************************************************************************
C    * SPECIFICATIONS FOR DATA CARDS                                        *
C    * DATA CARDS ARE READ IN GROUPS CONSISTING OF ONE OR MORE CARDS.       *
C    * EACH RUN REQUIRES THREE GROUPS OF CARDS TO INITIALIZE PARAME-        *
C    * TERS PLUS ONE MORE GROUP FOR EACH STATION TO BE ANALYSED.  THE       *
C    * FOLLOWING TABLE GIVES MORE EXACT INFORMATION AS TO THE MAKE-UP       *
C    * OF THE INDIVIDUAL GROUPS.                                            *
C    *                                                                      *
C    * GROUP NO.    NO. OF CARDS         INFORMATION          FORMAT NO.*
C    *  ONE          ONE            NUMBER OF RANGES,MONTHS        1     *
C    *  TWO          VARIABLE       RANGE VALUES                   4     *
C    *  THREE        ONE            PLOTTER PARAMETERS             41    *
C    *  FOUR,ETC.    VARIABLE       DISCHARGE DATA FROM STA-               *
C    *                              TIONS.  ONE GROUP PER          3     *
C    *                              STATION.  ALL GROUPS OF              *
C    *                              SAME SIZE.                           *
C    ************************************************************************
C
      END

        3200 FORTRAN DIAGNOSTIC RESULTS - FOR   FREQ


NO ERRORS
LOAD,56
RUN
```

Figure 88 (Cont'd). Computer Program FREQ.

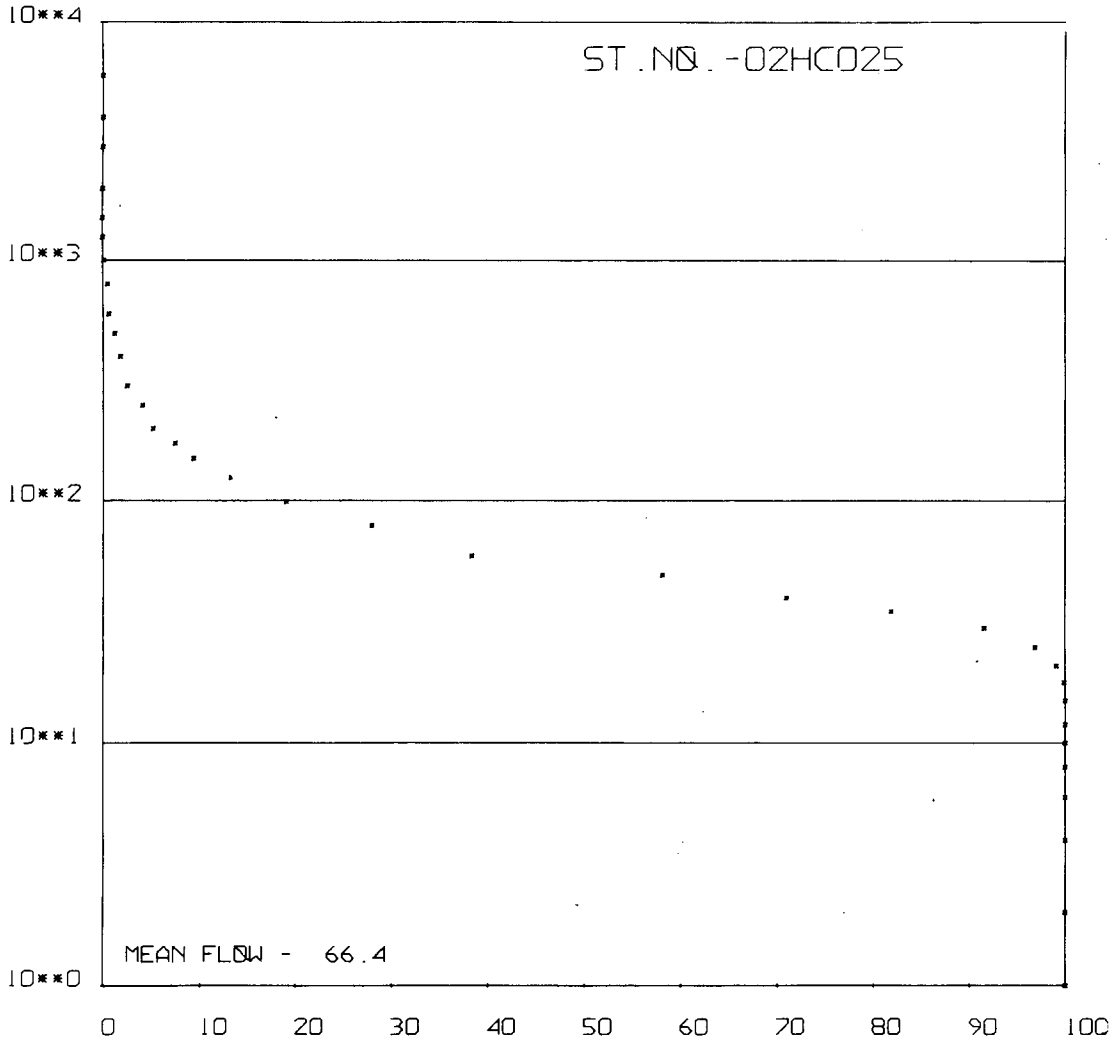

Figure 89. Sample plotted output.

TEST WELL LOGS

APPENDIX C

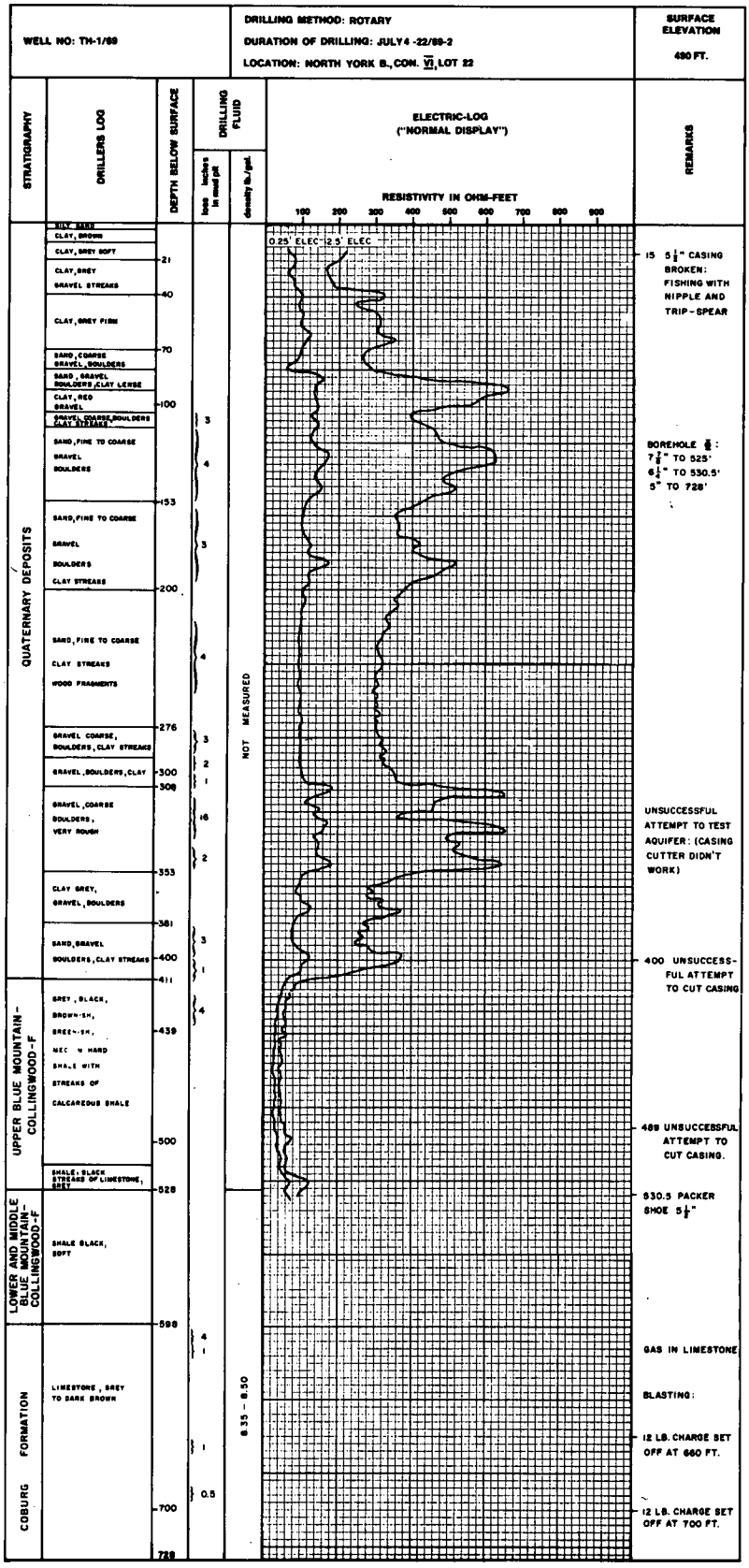

Figure 90. Well log TH-1.

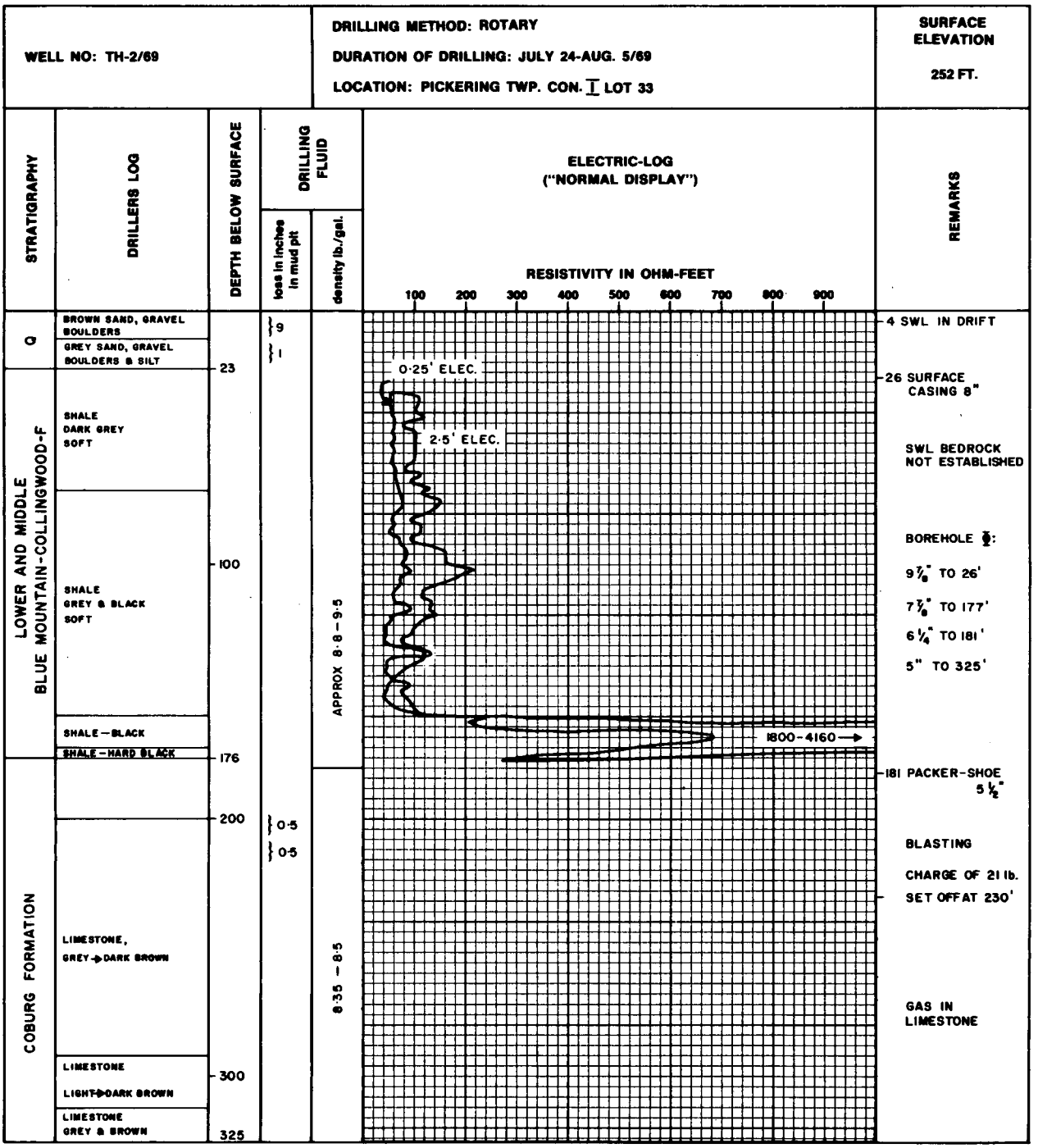

Figure 91. Well log TH-2.

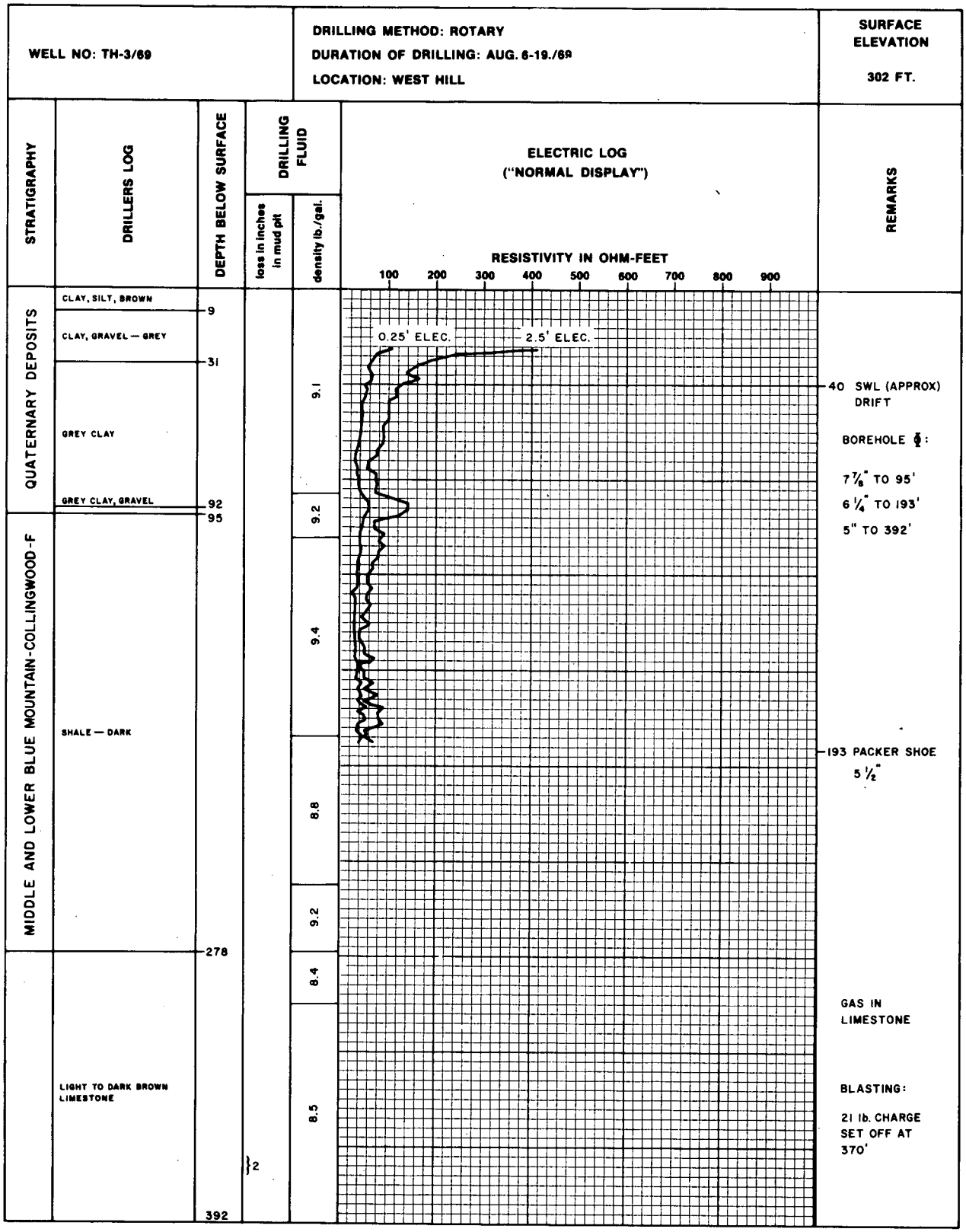

Figure 92. Well log TH-3.

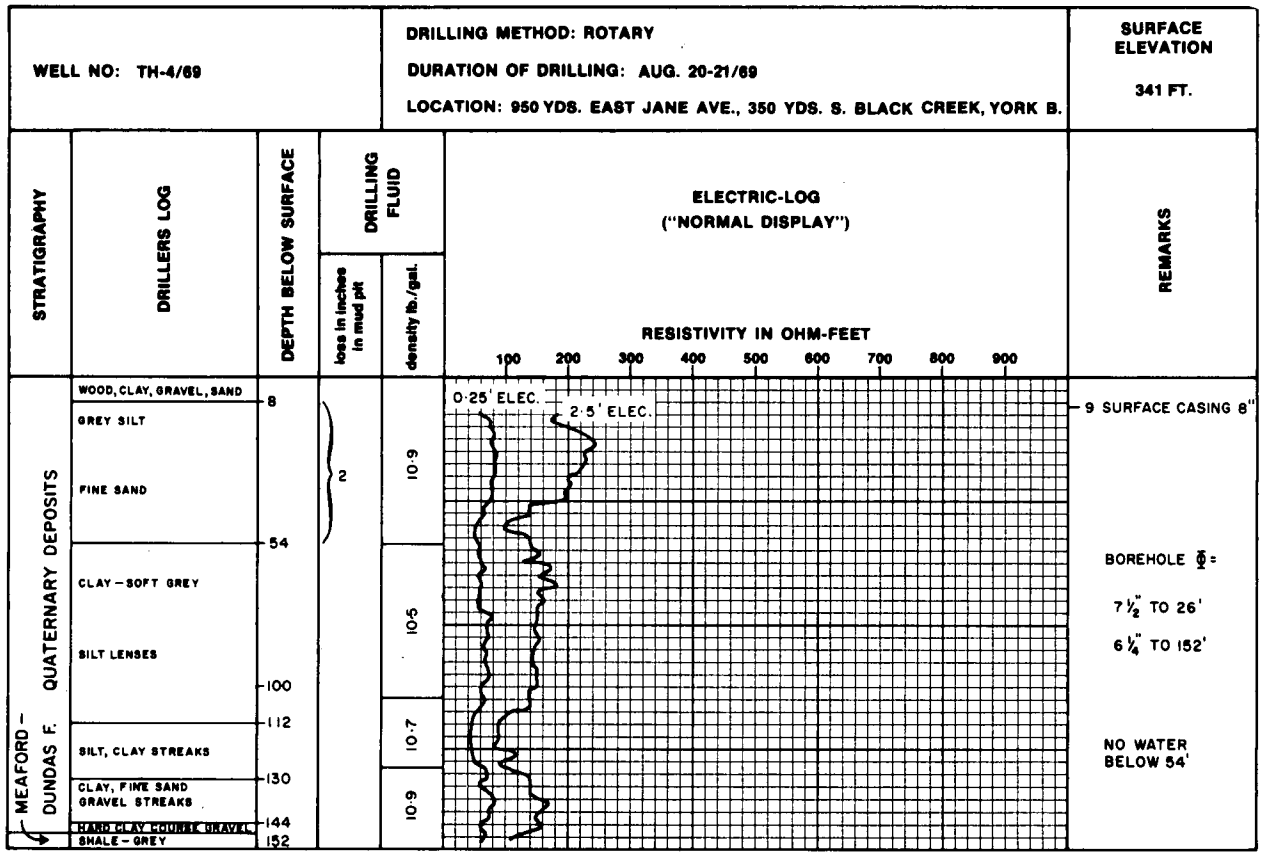

Figure 93. Well log TH-4.

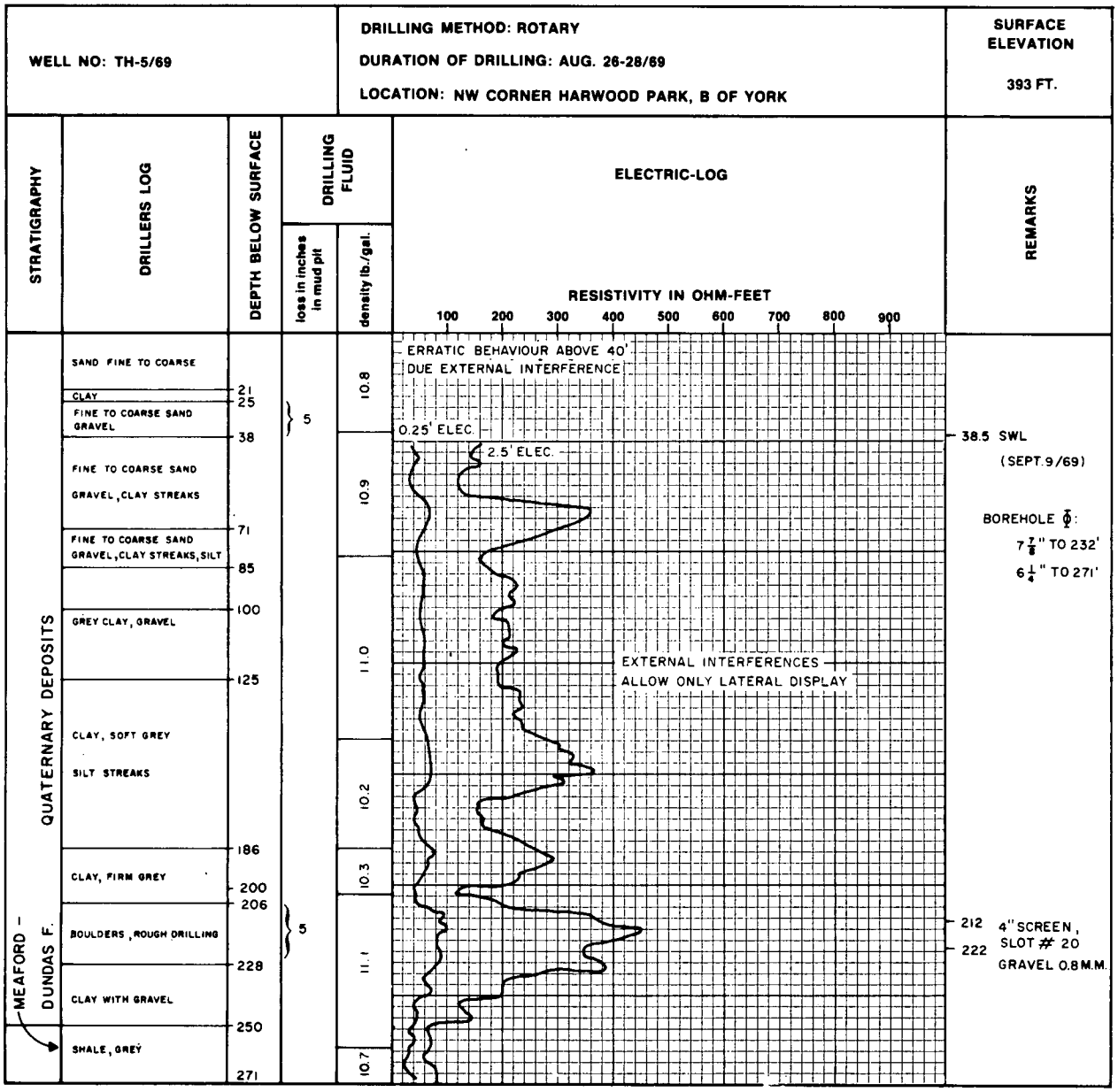

Figure 94. Well log TH-5.

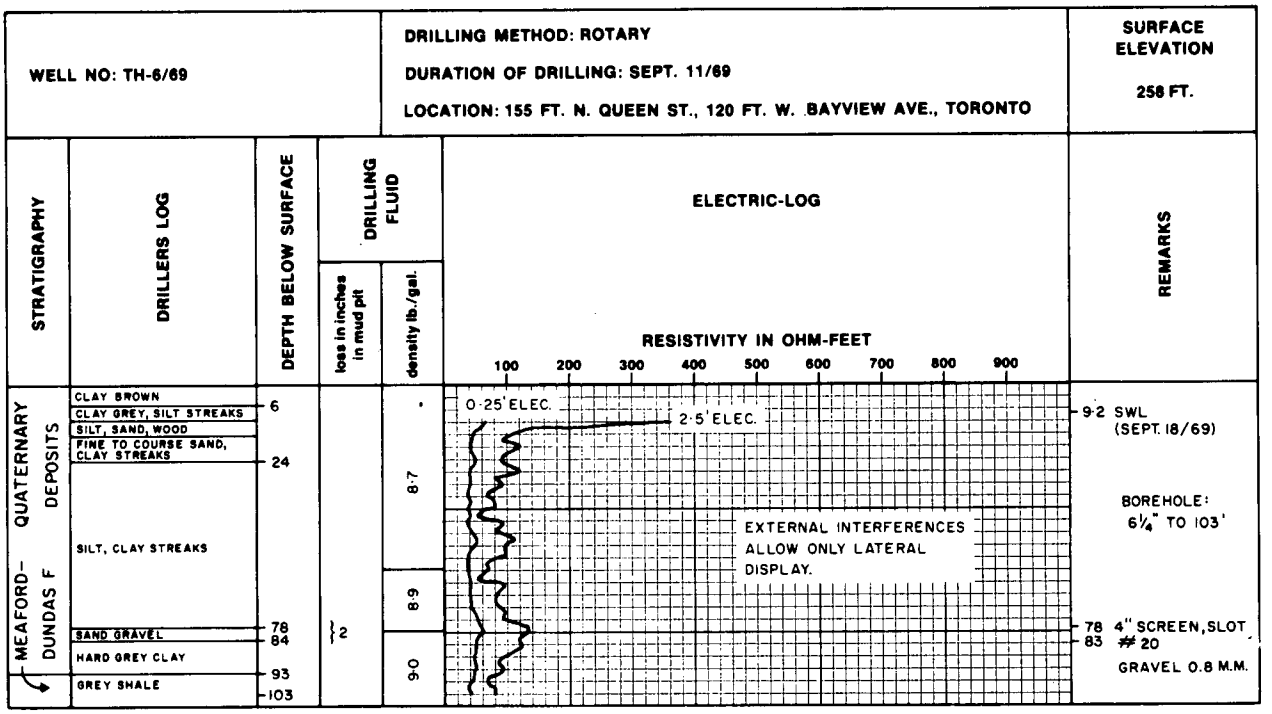

Figure 95. Well log TH-6.

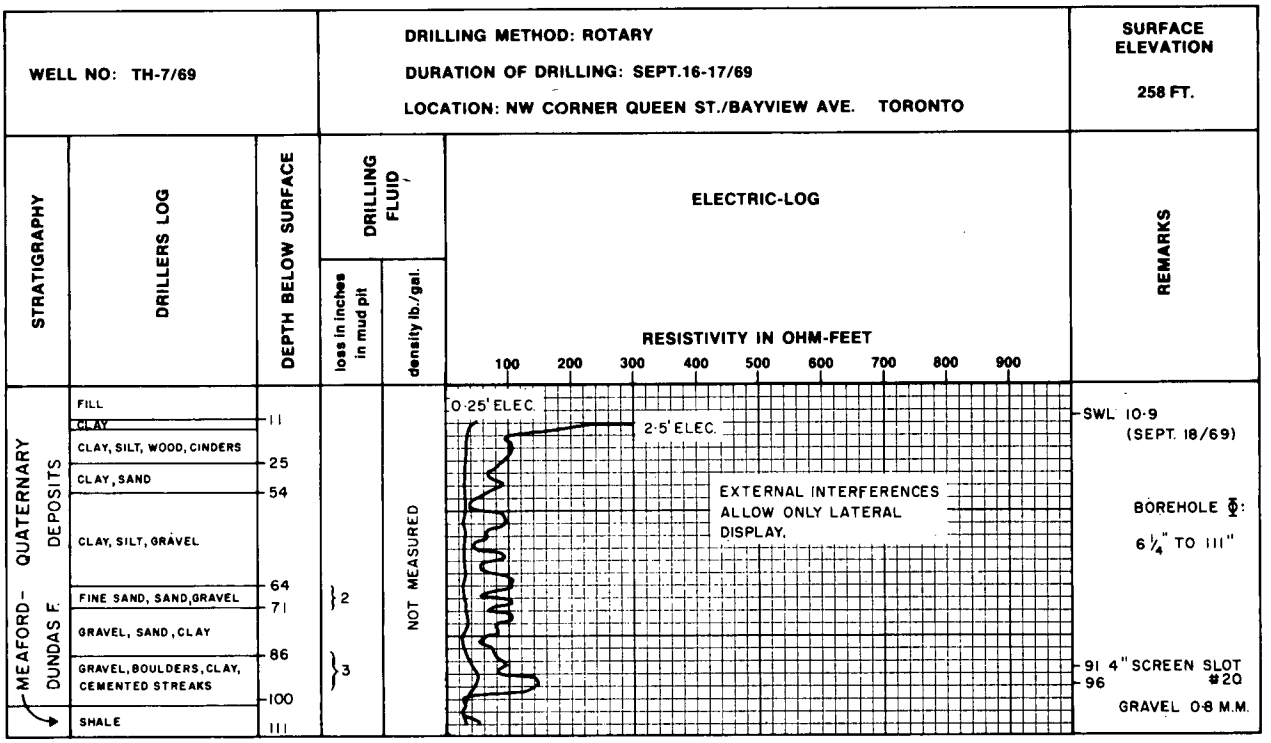

Figure 96. Well log TH-7.

INSERT

LARGE

FORMAT

PROJECT : ENVCAN 1-850

BOX : 2

FOLDER : SERIES No. 9

OF DRWGS : 5

PLATE VIII

PROFILE ALONG BURIED DUNDAS VALLEY

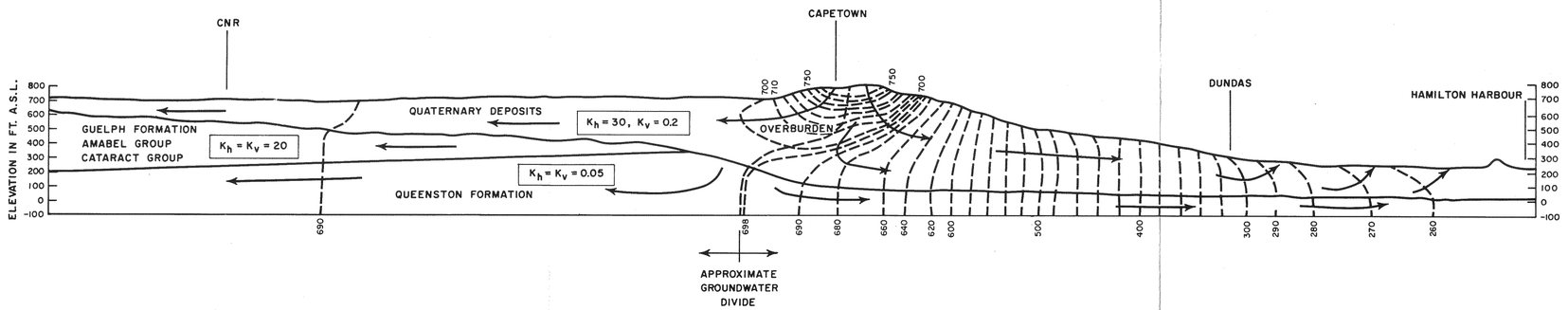

K_h, K_v = ASSUMED HORIZONTAL AND VERTICAL PERMEABILITY ($1 gpd/ft^2$)

EQUIPOTENTCIAL LINE

GENERAL DIRECTION OF FLOW

SCALE

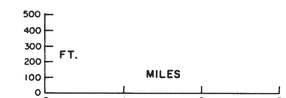

(VERTICAL EXAGGERATION = APPROX. 10x)

PROFILE ACROSS NIAGARA PENINSULA, GRIMSBY - GRANT POINT

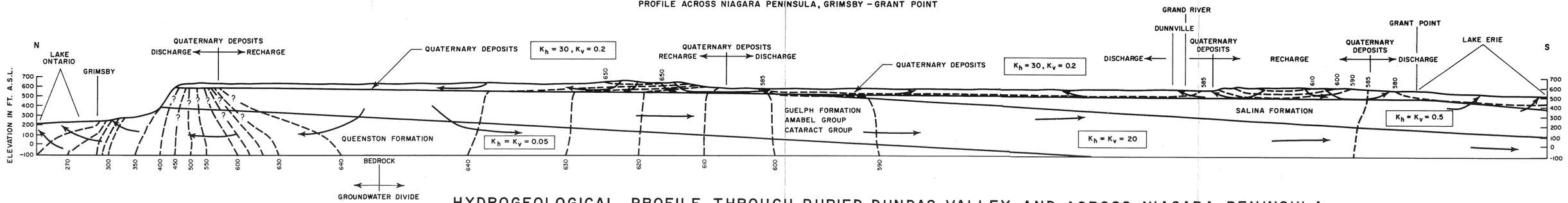

HYDROGEOLOGICAL PROFILE THROUGH BURIED DUNDAS VALLEY AND ACROSS NIAGARA PENINSULA.

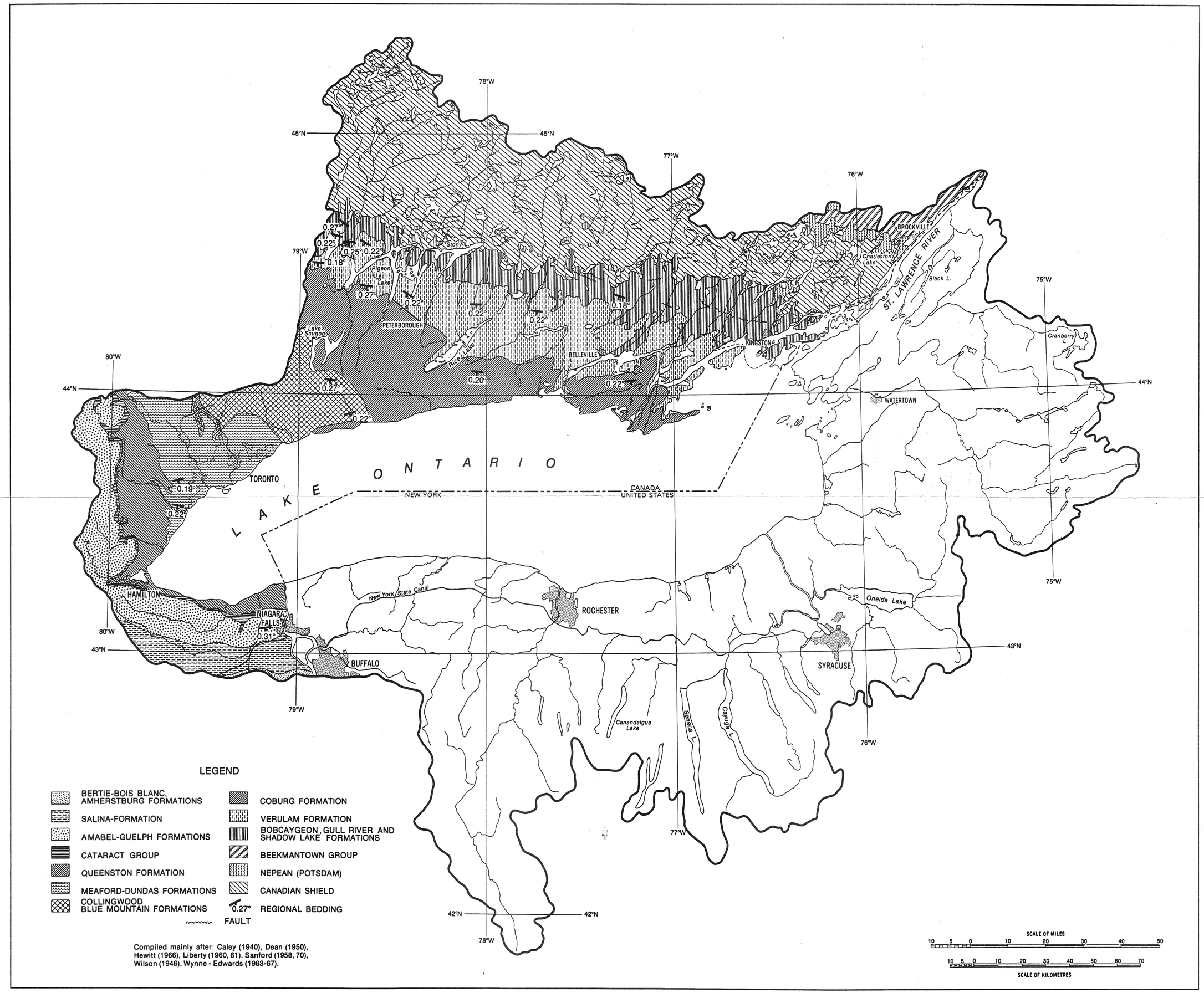

GEOLOGICAL MAP OF THE LAKE ONTARIO DRAINAGE BASIN (CANADIAN SIDE).

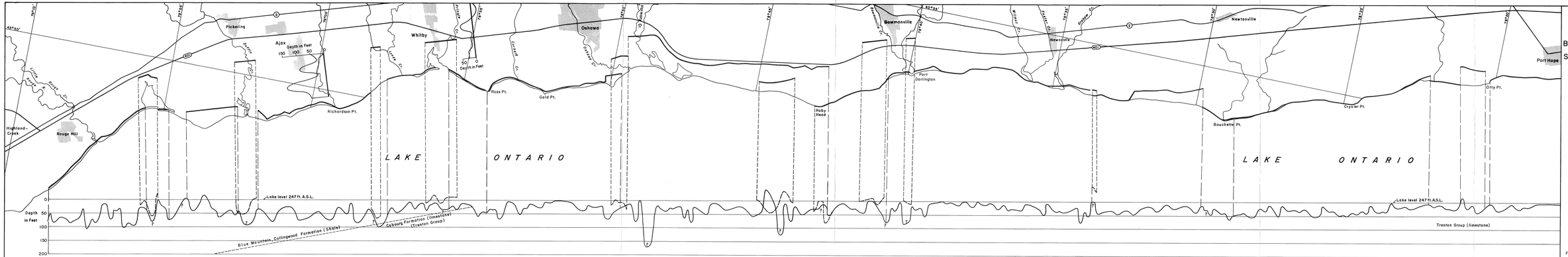

PLATE IV

BEDROCK SURFACE PROFILE SCARBOROUGH - PORT HOPE

0 1 2 3 4 Km.

0 1 2 Miles

From Hammer Seismic Surveys by G.D. Hobson and H.A. Mac Auley, Geol. Survey of Canada 1969

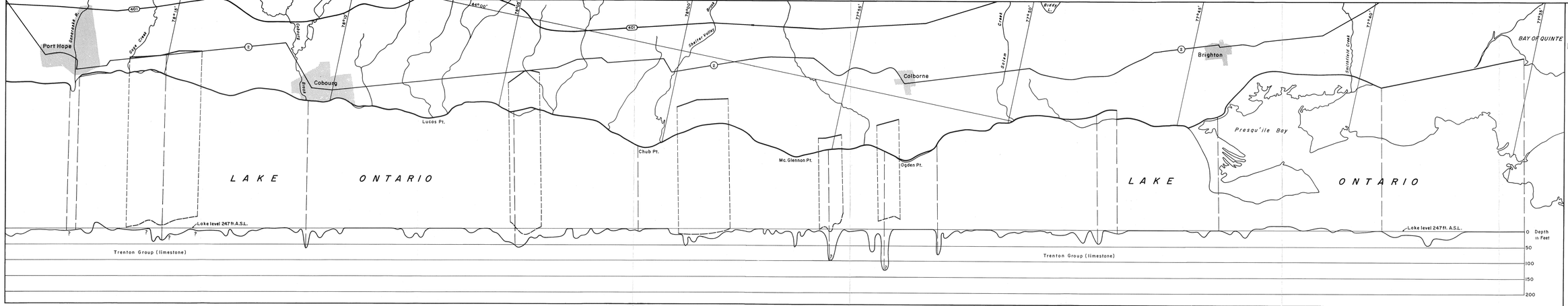

PLATE V

BEDROCK SURFACE PROFILE PORT HOPE - TRENTON

From Hammer Seismic Surveys by G.D. Hobson and H.A. Mac Aulay, Geol. Survey of Canada 1969

PLATE VI

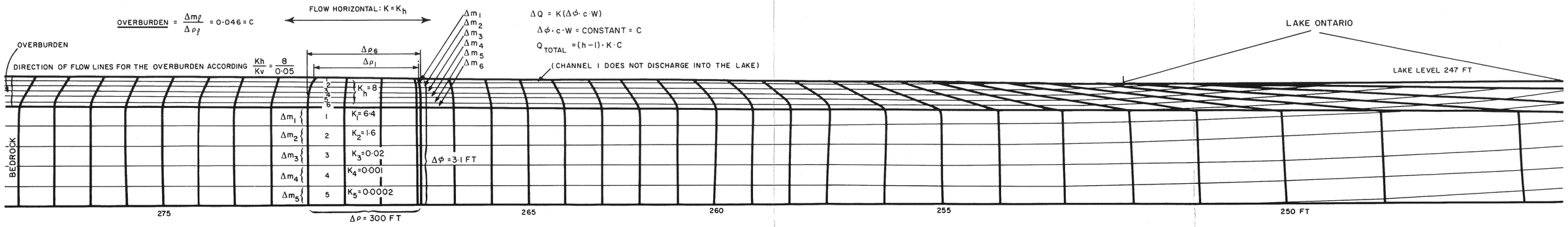

BEDROCK :

$\Delta\rho_\ell$ = 300 FT

Δm_ℓ = 50 FT

$\frac{\Delta m_\ell}{\Delta \rho_\ell}$ = 0·167 = c

$K_h = K_v = K$

$\Delta Q = K(\Delta\phi \cdot c \cdot w)$

$\Delta\phi \cdot c \cdot w$ = CONSTANT = C

$Q_{TOTAL} = \Sigma K_h \cdot C$

(FLOW CHANNEL BOUNDARY = PERMEABILITY BOUNDARY UNDER HORIZONTAL FLOW CONDITIONS)

BASIC FORMULA : $Q = K \frac{\Delta\phi}{\Delta\rho} \Delta m \cdot w$

SCALE

(NO VERTICAL EXAGGERATION)

150 0 150 300 ft.

K_h, K_v	HORIZONTAL AND VERTICAL PERMEABILITY
ΔQ	DISCHARGE THROUGH ONE FLOW CHANNEL IN SEGMENT
ϕ	DROP IN HYDRAULIC HEAD IN SEGMENT
$\Delta\rho$	LENGTH OF SEGMENT
Δm	WIDTH OF CHANNEL IN SEGMENT
w	THICKNESS OF FLOW SYSTEM PERPENDICULAR TO THE PROFILE (SHORELINE LENGTH)
ℓ	ANY FLOW CHANNEL

FLOW NET ANALYSES; COMPUTATION OF DISCHARGE THROUGH REPRESENTATIVE PROFILE PERPENTICULAR TO THE SHORE

PLATE II

BEDROCK SURFACE PROFILE
TORONTO HARBOUR

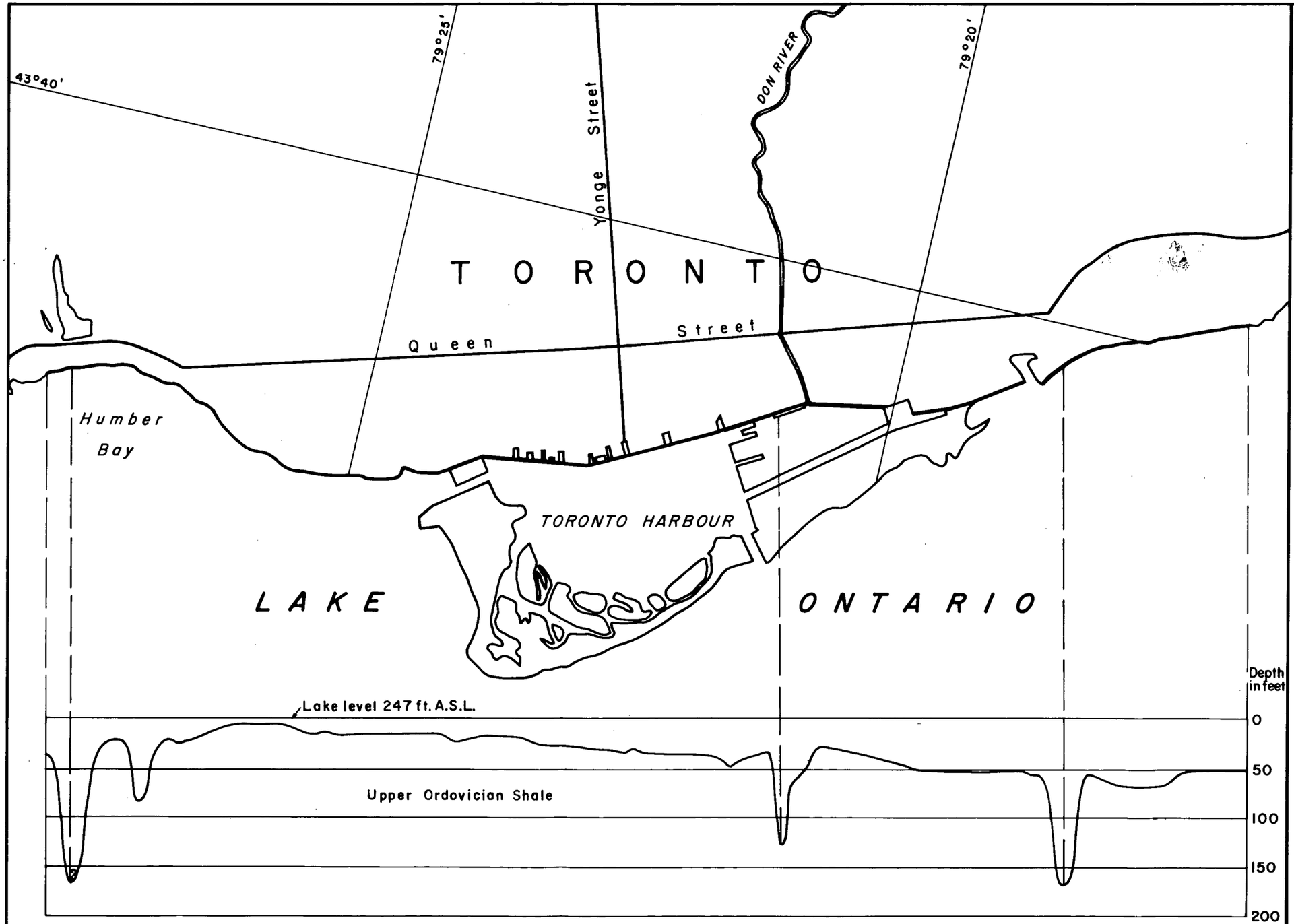

0 1 2 3 4 Km.

0 1 2 Miles

After D.P. Rogers, R.C. Ostry and P.F. Karrow, 1961

PLATE III

BEDROCK SURFACE PROFILE
SCARBOROUGH

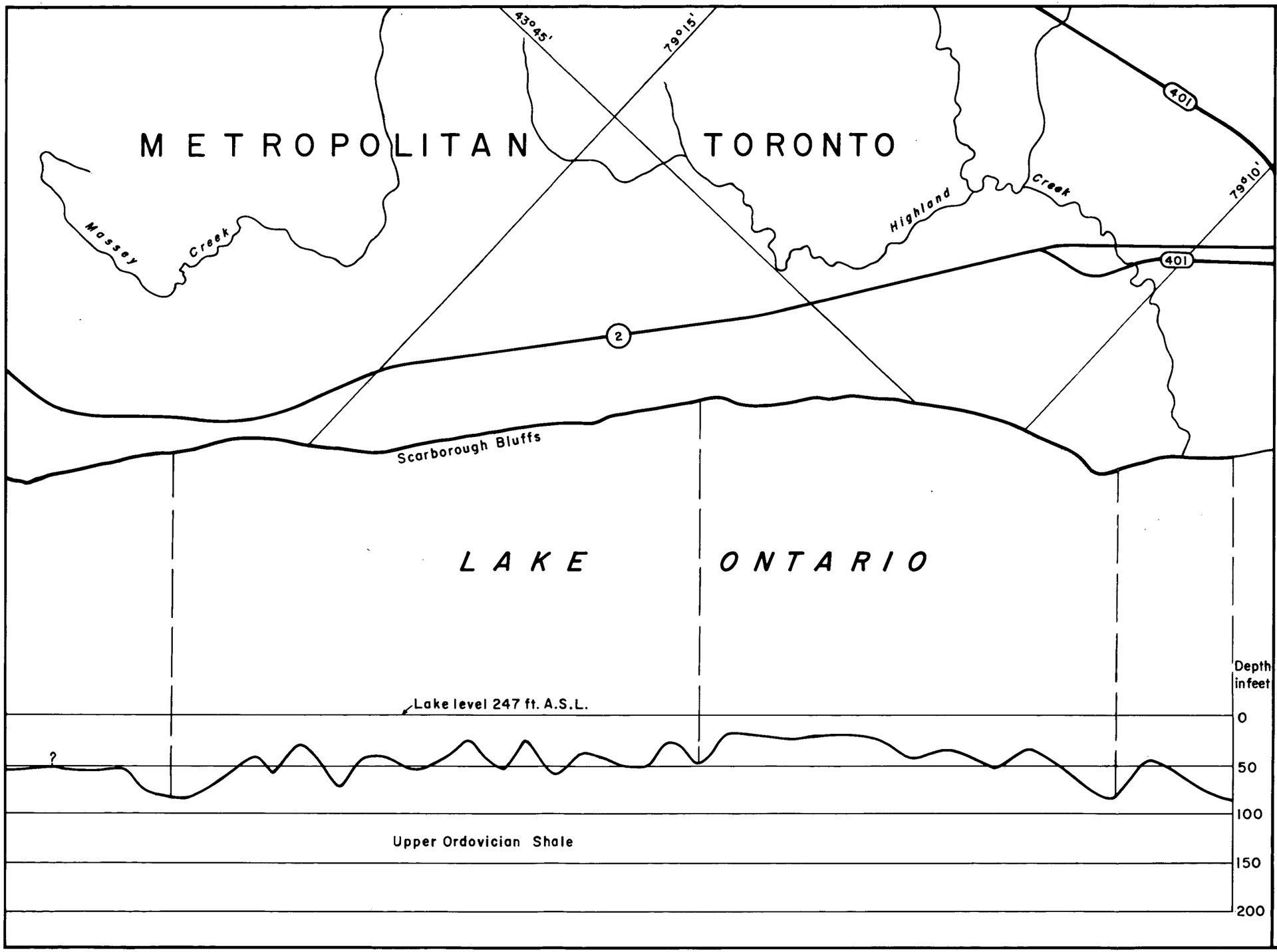

After G.D. Hobson, 1970

PLATE VII

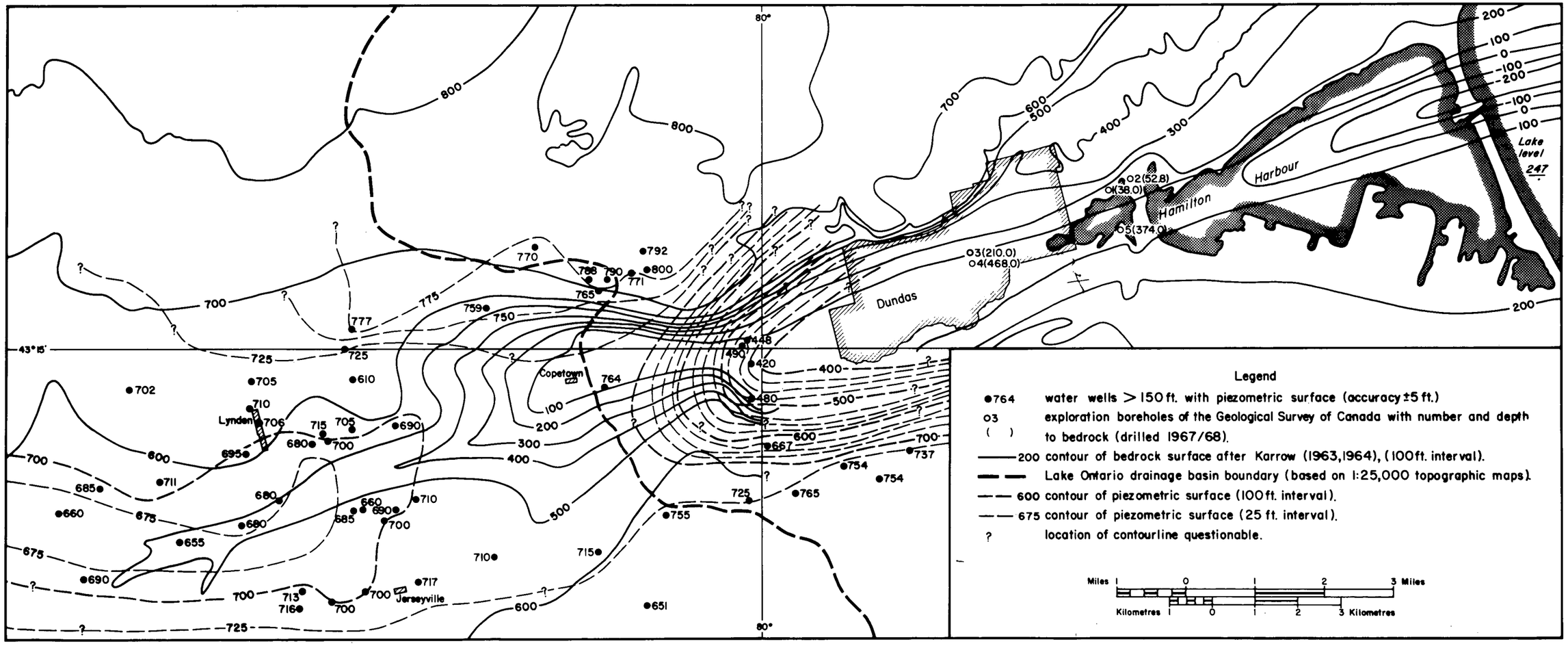

PIEZOMETRIC SURFACE AND BEDROCK CONTOURS OF BURIED DUNDAS VALLEY.